VU Research Portal

Detection and treatment of pulmonary vascular disease

Botros, Liza

2022

document version
Publisher's PDF, also known as Version of record

Link to publication in VU Research Portal

citation for published version (APA)
Botros, L. (2022). *Detection and treatment of pulmonary vascular disease.* Ridderprint.

Detection and treatment of pulmonary vascular disease

Liza Botros

VRIJE UNIVERSITEIT

Detection and treatment of pulmonary vascular disease

ACADEMISCH PROEFSCHRIFT

ter verkrijging van de graad Doctor of Philosophy aan
de Vrije Universiteit Amsterdam,
op gezag van de rector magnificus
prof.dr. C.M. van Praag,
in het openbaar te verdedigen
ten overstaan van de promotiecommissie
van de Faculteit der Geneeskunde
op vrijdag 4 maart 2022 om 13.45 uur
in een bijeenkomst van de universiteit,
De Boelelaan 1105

door

Liza Botros

geboren te Amsterdam

Aut viam inveniam, aut faciam

Ik zal een weg vinden, of er één maken

Contents of Thesis

1

General introduction and scope of thesis

Liza Botros

The pulmonary vasculature

The lung is the most vascularized organ in the body due to its primary and essential function to exchange oxygen and carbon dioxide from the blood into the tissue. The lungs also regulate body acid-base balance and protect against inhaled pathogens through the respiratory epithelium. Respiration can be divided into four essential processes: 1) Exchange of air between the atmosphere and the lungs. 2) Exchange of oxygen and carbon dioxide between the lungs and the blood. 3) Transport of oxygen and carbon dioxide by the blood. 4) Exchange of gases between the blood and cells. It is already made clear here, that the respiratory system has a close interdependence with the circulatory system and that the respiratory system consists of structures involved in both ventilation and circulation. The air-blood barrier forms a very thin membrane of 0.1 µm that is built up by only one layer of alveolar epithelium and one layer of capillary endothelium (1) making it very sensitive to changes in flow and pressure. The high compliance of pulmonary precapillary arterioles and the capacity to recruit available vessels facilitate an increase in blood flow when cardiac output rises. Indeed, this circulatory system can accommodate flow rates ranging from approximately 6 L/min at rest to 25 L/min during exercise, with minimal increases in pulmonary pressure (2, 3). The pulmonary vasculature regulates blood flow away from capillary beds with low oxygen concentrations, a process called pulmonary hypoxic vasoconstriction. Hypoxic vasoconstriction prevents the pulmonary blood flow from shunting and hypoxemia. Adaptation to hypoxia involves transcriptional regulation of a variety of genes, including hypoxia inducible factors that are expressed in pulmonary endothelial cells (4).

Endothelial cells (ECs) form the inner monolayer of all blood vessels throughout the body and regulate several critical physiological processes in the body, such as the transport of proteins and fluids across the vessel wall, regulation of vascular tone, hemostasis, angiogenesis and immunity (5). ECs form the central orchestrator in vascular permeability as they facilitate their permeation for the exchange of gases and osmolytes, the replenishment of metabolic circuitries and communication and coordination among compartments (6). Indeed, endothelial cell phenotypes display remarkable heterogeneity across the body to serve the specific demands of the underlying tissues in health and disease (7).

Pulmonary vascular development and stability

During normal intrauterine development, there is a close crosstalk between the pulmonary vasculature and the bronchial tree and distal airways. At this time, the pulmonary vasculature receives less than 10% of the cardiac output (1). After birth, the pulmonary vascular bed has developed to such an extent that all alveoli are richly endowed with a dense capillary network so that the vascular bed can accept the entire cardiac output that arises from the systemic circulation once the ductus arteriosus closes. This sudden transition from its low flow, high pressure and high resistance to high flow, low pressure and low resistance makes the pulmonary vasculature unique from other parts of the body (1).

Coordinated development of the pulmonary vascular system with the airways is critical for the final structure and function of the lung (8). Morphogenesis of the pulmonary vasculature occurs mainly through angiogenesis (branching of existing blood vessels), and to a lesser extent through vasculogenesis (de novo formation of blood vessels). Both processes require precise regulation which is mediated by vascular endothelial growth factor (VEGF) (8). VEGF is the central regulator of angiogenesis in the lung and both VEGF and its receptors are robustly expressed in lung epithelial cells and vascular endothelial cells during development (9) and in the adult lung (10). Impaired development or injury to the pulmonary endothelium later in life, leads to vascular defects and dysfunction as seen in several chronic and acute lung diseases such as lung hypoplasia, emphysema, exercise intolerance and pulmonary hypertension (8, 11-13). Thus, impaired pulmonary vascular development or reduced vascular stability results in a broad spectrum of pulmonary diseases, including pulmonary arterial hypertension and pulmonary edema, conditions that will be discussed in this thesis.
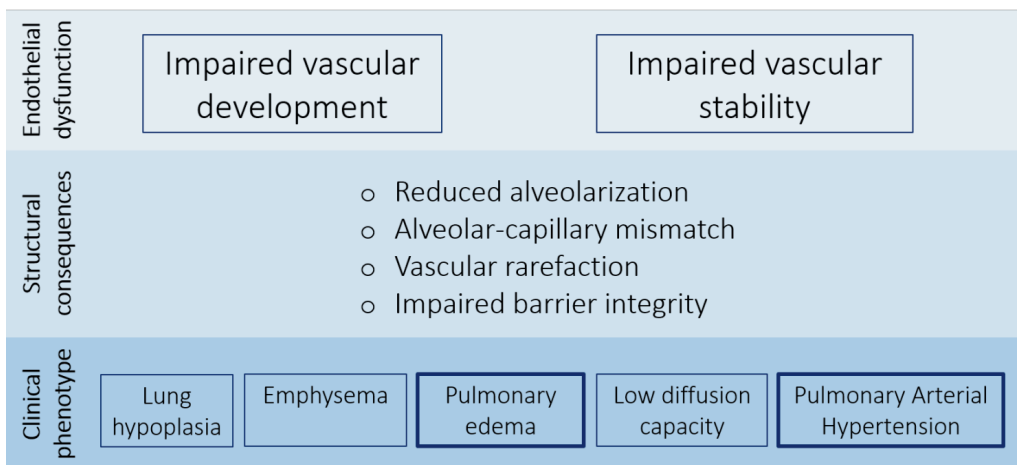
Figure 1: Endothelial dysfunction leads to impaired vascular development and maintenance. Structural consequences include reduced alveolarisation, impaired alveolocapillary interface, a loss of vessels and impaired integrity of the endothelial monolayer. This gives rise to a number of clinical phenotypes including lung hypoplasia, emphysema, pulmonary edema, low diffusing capacity of the lung for carbon monoxide and pulmonary arterial hypertension.

Part I - Pulmonary arterial hypertension

Normally, the pressure in the pulmonary artery is about 14+/-3 mmHg whereas systemic arterial pressures rise to 100+/-20 mmHg (3). When the resting mean pulmonary artery pressure exceeds 20 mmHg, we speak of pulmonary hypertension (PH) (14). PH is divided in pre-and post capillary causes and can arise from various etiologies including chronic hypoxia, as seen with several lung diseases, and left heart disease. Despite the various causes, a common denominator in all forms of PH seems to be endothelial cell dysfunction (15). A

specific subtype of PH is pulmonary arterial hypertension (PAH, group 1 PH), a rare condition with a prevalence of 15-20 per million (16). Features of PAH include excessive pulmonary vasoconstriction and abnormal pulmonary vascular remodeling. The increase in pulmonary vascular resistance eventually leads to an increased right ventricular afterload and right heart failure (17). Histological findings in the pulmonary vasculature of PAH patients show large heterogeneity, but the key components in typical plexiform lesions found in PAH are endothelial cell proliferation, intimal fibrosis, smooth muscle cell hypertrophy and luminal obstruction (18-20).

The diagnosis of PAH is complex and time consuming and uses invasive right heart catheterization as gold standard for defining PH subtype. Thus, there is an urgent need for non-invasive techniques that help in early disease detection. These techniques preferably also assist in identifying factors that determine risk of mortality and prognosis and gauge therapeutic effects on right ventricular (RV) function (21). In **chapter 2**, we performed a meta-analysis on available studies that searched for circulating blood and urine biomarkers which discriminate patients with PAH from healthy controls and non-PH diseased. N-terminal prohormone of brain natriuretic peptide (NT-proBNP) appeared an excellent marker for both right and left ventricular dysfunction (22, 23), and decreased significantly after initiation of vasodilatory treatment (24-26). However, NTproBNP appeared not specific for idiopathic or hereditary PAH. We observed that almost all studies that investigated circulating biomarkers in PAH, focused one single biomarker. Based on the lack of specificity of all these single biomarkers, we conclude that the combination of a number of strong biomarkers is the best way to improve specificity and perhaps replace invasive diagnostic tools in the future.

The pathobiology of PAH features phenomena that are also encountered in cancer, such as enhanced proliferation and apoptosis-resistance (27-29). As secondary alternative approach for diagnosing PAH, we tried to quantify vascular remodeling in **chapter 3** by using 3'-deoxy-3'-[18F]-fluorothymidine ([18]FLT) positron emission tomography (PET) scan. [18]FLT is a thymidine analogue that is retained in proliferating cells and therefore a possible tracer for imaging lung vascular proliferation in PAH. Thus, this imaging multimodality does not only provide anatomical information, but also additional metabolic information. One of the most important risk factors for the development of PAH is a mutation in the gene coding for the bone morphogenic protein receptor type 2 (BMPR2) (30). Subjects carrying this pathogenic variant have an increased risk to develop PAH, but currently there are no methods to predict which unaffected mutation carriers will develop PAH. We compared [18]FLT uptake in the lungs of PAH patients with that in unaffected BMPR2 mutation carriers, prone to develop PAH, and matched healthy controls. Although we could confirm the heterogeneity in the lung [18]FLT signal in PAH patients we could not detect significant differences in lung [18]FLT uptake expressed by phosphorylation rate k3 in PAH patients in comparison to matched healthy controls, nor in unaffected BMPR2 mutation carriers.

Current therapies only target vascular tone through nitric oxide, endothelin and prostacyclin pathways. Thus, targeting the underlying structural changes in the pulmonary vasculature remains an unmet need, carrying high morbidity and mortality (31). We previously showed in a preclinical study that mercaptopurine (MP) prevented and reversed abnormal vascular remodeling and right ventricle hypertrophy in the Sugen-hypoxia rat model of severe angioproliferative PAH (32). In addition, pharmacological activation of Nur77 by MP augmented BMP signaling as measured by BMPR2 expression (32). In **chapter 4** we evaluated the efficacy and safety of antiproliferative treatment with MP in group 1 PAH patients. We found that the mean pulmonary artery pressure and pulmonary vascular resistance were significantly decreased in 11 patients that finished treatment. BMPR2 expression in circulating mononuclear cells increased significantly after treatment. However, frequency and severity of side effects were higher than expected and reported, indicating that MP in this dosing scheme is effective but not safe as add-on treatment for PAH.

Part II - Pulmonary vascular leakage

The pulmonary endothelium forms a monolayer of tightly connected cells. Under basal conditions, integrity of the endothelial barrier is maintained by adherens junctions (AJ) with neighboring cells and through focal adhesions (FA) to the extracellular matrix (ECM) (33-35). FA proteins, such as integrins, are dimeric transmembrane receptors that form a physical link between the ECM and the intracellular milieu, but also facilitate bidirectional signaling across the plasma membrane. By allowing dynamic cell adhesion and by probing the extracellular environment, integrins are pivotal for endothelial barrier stability (36, 37). Regulation of junctional bindings and reorganization of the F-actin cytoskeleton occurs through activation of small G-proteins (38, 39), protein kinases (40) and other factors such as calcium ions and nitric oxide. During inflammation, the primary function of the endothelium to transport fluids and proteins across the monolayer, is disturbed. Intracellular signalling pathways become activated that internalize AJ components like vascular endothelial (VE)-cadherin. In parallel, activation and phosphorylation of myosin light chain (MLC) results in contraction of stress fibres, retracting the cell membrane and rounding of cells (33, 34). Detachment of cell-matrix adhesions, dissociation of adherens junctions and formation of contractile stress fibers are all important hallmarks of vascular leakage syndromes like sepsis and acute respiratory distress syndrome (ARDS) (36, 37). Despite increased understanding of endothelial barrier regulation at the molecular level, no therapeutic options against vascular leakage are available to date, yielding high morbidity and mortality.

Members of the Abl family of tyrosine kinases, phosphorylate several cytoskeletal effectors that mediate vascular permeability and regulate cell-cell and cell-matrix junction dynamics (41). It was already established that the Abl kinase inhibitor (AKI) imatinib reverses pulmonary edema (42) and protects against endothelial barrier disruption by inhibition of Abl-related gene (Arg) (43). We hypothesized that a favorable combination of kinases

inhibited by next generation tyrosine kinase inhibitors provides novel potential for the treatment of vascular leakage syndromes. In **chapter 5,** we demonstrated that the second generation tyrosine kinase inhibitor bosutinib provides strongest protection against inflammation-induced endothelial barrier disruption *in vitro* and in an animal model of pulmonary vascular leakage. By using silencing RNA, we proved that bosutinib exerts its protective effect via inhibition of mitogen-activated protein kinase kinase kinase kinase (MAP4K4) in addition to Arg (Abl2). Inhibition of these kinases improved cell matrix adhesion through focal adhesion reinforcement. The protective effects of bosutinib were further evaluated in an acute-lung injury mice model. We found decreased pulmonary edema and protein extravasation in the alveoli of mice treated with bosutinib. In **chapter 6** we validated the protective effects of bosutinib in a multi-trauma shock model. Bosutinib as additional therapy to a balanced blood component resuscitation reduced trauma-induced endothelial permeability as measured by transfusion need, pulmonary edema and circulating markers of endothelial dysfunction.

As indicated above, imatinib has been linked to protect and reverse inflammatory-induced vascular leak and thereby mitigating pulmonary capillary leak both *in vitro*, *in vivo* and in the clinic (42, 43). In **chapter 7**, we were the first to perform a randomised, double-blind, placebo-controlled clinical trial evaluating imatinib in hospitalised patients with coronavirus disease 2019 (COVID-19). Histopathological and biochemical studies suggest that the entry of SARS-CoV-2 into the pulmonary endothelial cells (44) play a central role in the pathogenesis of COVID-19, including endothelial barrier dysfunction, coagulopathy and hyperinflammation with cytokine storm (see figure 2). As the sudden COVID-19 primarily affects the lungs, the major complication of COVID-19 is hypoxemic respiratory failure from vascular leakage and alveolar edema. We therefore tested imatinib in patients hospitalized with polymerase chain reaction (PCR)-proven SARS-CoV2 infection and requiring supplemental oxygen to maintain a peripheral oxygen saturation of greater than 94%. Four hundred patients were included and started on imatinib for nine days and were followed for 28 days in total. Imatinib did not reduce the time to liberation from ventilation and supplemental oxygen, however improved survival and reduced duration of mechanical ventilation.

Summary

Pulmonary vascular stability is essential for normal lung function and health. Unfortunately, both pulmonary vascular proliferative disorders such as PAH, and pulmonary vascular leakage syndromes still have high morbidity and mortality as no treatment is available. This thesis aimed to investigate novel, less invasive detection techniques for PAH (**chapter 2&3**), and tried to reverse pulmonary vascular remodeling by using an anti-proliferative agent (**chapter 4**). Next, we evaluated the use of two tyrosine kinase inhibitors in both pre-clinical and clinical studies for vascular leakage (**chapter 5-7**).

Figure 2

Healthy state | **SARS-CoV-2 infection**

Alveolar space

Circulation

Hyperinflammation & cytokine storm

Vascular leakage & alveolar edema

Coagulopathy

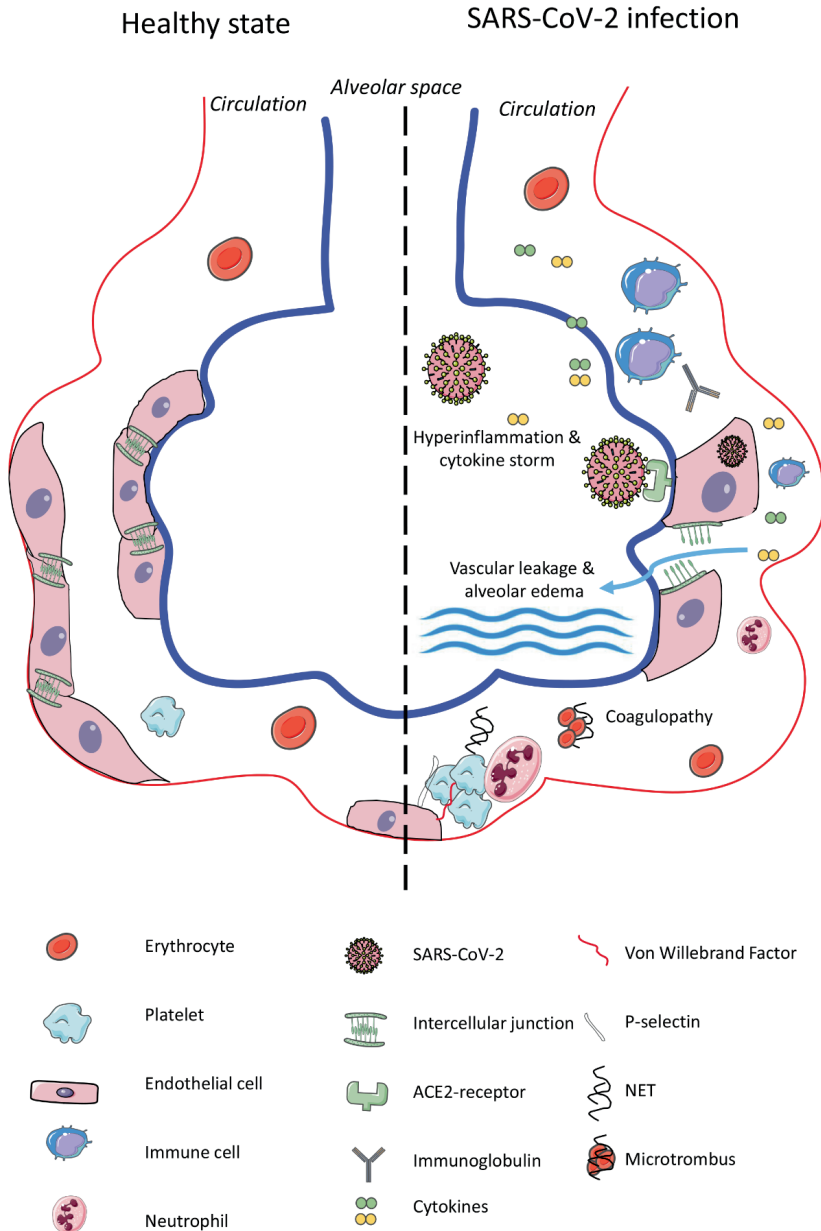| Erythrocyte | SARS-CoV-2 | Von Willebrand Factor |
Platelet	Intercellular junction	P-selectin
Endothelial cell	ACE2-receptor	NET
Immune cell	Immunoglobulin	Microtrombus
Neutrophil	Cytokines	

Figure 2: After viral invasion of endothelial cells, three main pathological pathways simultaneously develop: endothelial barrier dysfunction leading to vascular leakge and alveolar edema, coagulopathy and hyperinflammation with cytokine storm. *Chen et al. AMSj 2021*

References

1.   Aird WC. Phenotypic heterogeneity of the endothelium: II. Representative vascular beds. Circ Res. 2007;100(2):174-90.
2.   West JB. Blood flow to the lung and gas exchange. Anesthesiology. 1974;41(2):124-38.
3.   Huertas A, Guignabert C, Barbera JA, Bartsch P, Bhattacharya J, Bhattacharya S, et al. Pulmonary vascular endothelium: the orchestra conductor in respiratory diseases: Highlights from basic research to therapy. Eur Respir J. 2018;51(4).
4.   Shimoda LA, Laurie SS. HIF and pulmonary vascular responses to hypoxia. J Appl Physiol (1985). 2014;116(7):867-74.
5.   Aird WC. Phenotypic heterogeneity of the endothelium: I. Structure, function, and mechanisms. Circ Res. 2007;100(2):158-73.
6.   Lopez-Otin C, Kroemer G. Hallmarks of Health. Cell. 2021;184(1):33-63.
7.   Regan ER, Aird WC. Dynamical systems approach to endothelial heterogeneity. Circ Res. 2012;111(1):110-30.
8.   Abman SH. Bronchopulmonary dysplasia: "a vascular hypothesis". Am J Respir Crit Care Med. 2001;164(10 Pt 1):1755-6.
9.   Kaipainen A, Korhonen J, Pajusola K, Aprelikova O, Persico MG, Terman BI, et al. The Related Flt4, Flt1, and Kdr Receptor Tyrosine Kinases Show Distinct Expression Patterns in Human Fetal Endothelial-Cells. Journal of Experimental Medicine. 1993;178(6):2077-88.
10.   Voelkel NF, Vandivier RW, Tuder RM. Vascular endothelial growth factor in the lung. Am J Physiol-Lung C. 2006;290(2):L209-L21.
11.   Jakkula M, Le Cras TD, Gebb S, Hirth KP, Tuder RM, Voelkel NF, et al. Inhibition of angiogenesis decreases alveolarization in the developing rat lung. Am J Physiol-Lung C. 2000;279(3):L600-L7.
12.   Kasahara Y, Tuder RM, Taraseviciene-Stewart L, Le Cras TD, Abman S, Hirth PK, et al. Inhibition of VEGF receptors causes lung cell apoptosis and emphysema. Journal of Clinical Investigation. 2000;106(11):1311-9.
13.   Hoeper MM, Vonk-Noordegraaf A. Is there a vanishing pulmonary capillary syndrome? Lancet Respir Med. 2017;5(9):676-8.
14.   Simonneau G, Montani D, Celermajer DS, Denton CP, Gatzoulis MA, Krowka M, et al. Haemodynamic definitions and updated clinical classification of pulmonary hypertension. Eur Respir J. 2019;53(1).
15.   Guignabert C, Tu L, Girerd B, Ricard N, Huertas A, Montani D, et al. New molecular targets of pulmonary vascular remodeling in pulmonary arterial hypertension: importance of endothelial communication. Chest. 2015;147(2):529-37.
16.   Galie N, Humbert M, Vachiery JL, Gibbs S, Lang I, Torbicki A, et al. 2015 ESC/ERS Guidelines for the Diagnosis and Treatment of Pulmonary Hypertension. Rev Esp Cardiol (Engl Ed). 2016;69(2):177.
17.   Voelkel NF, Gomez-Arroyo J, Abbate A, Bogaard HJ, Nicolls MR. Pathobiology of pulmonary arterial hypertension and right ventricular failure. Eur Respir J. 2012;40(6):1555-65.
18.   Schermuly RT, Ghofrani HA, Wilkins MR, Grimminger F. Mechanisms of disease: pulmonary arterial hypertension. Nat Rev Cardiol. 2011;8(8):443-55.
19.   Lee SD, Shroyer KR, Markham NE, Cool CD, Voelkel NF, Tuder RM. Monoclonal endothelial cell proliferation is present in primary but not secondary pulmonary hypertension. J Clin Invest. 1998;101(5):927-34.
20.   Tuder RM, Groves B, Badesch DB, Voelkel NF. Exuberant endothelial cell growth and elements of inflammation are present in plexiform lesions of pulmonary hypertension. Am J Pathol. 1994;144(2):275-85.
21.   Vonk Noordegraaf A, Haddad F, Bogaard HJ, Hassoun PM. Noninvasive imaging in the assessment of the cardiopulmonary vascular unit. Circulation. 2015;131(10):899-913.
22.   Januzzi JL, Jr., Rehman SU, Mohammed AA, Bhardwaj A, Barajas L, Barajas J, et al. Use of amino-terminal pro-B-type natriuretic peptide to guide outpatient therapy of patients with chronic left

ventricular systolic dysfunction. J Am Coll Cardiol. 2011;58(18):1881-9.

23. Nagaya N, Nishikimi T, Okano Y, Uematsu M, Satoh T, Kyotani S, et al. Plasma brain natriuretic peptide levels increase in proportion to the extent of right ventricular dysfunction in pulmonary hypertension. J Am Coll Cardiol. 1998;31(1):202-8.

24. Andreassen AK, Wergeland R, Simonsen S, Geiran O, Guevara C, Ueland T. N-terminal pro-B-type natriuretic peptide as an indicator of disease severity in a heterogeneous group of patients with chronic precapillary pulmonary hypertension. The American journal of cardiology. 2006;98(4):525-9.

25. Calvier L, Legchenko E, Grimm L, Sallmon H, Hatch A, Plouffe BD, et al. Galectin-3 and aldosterone as potential tandem biomarkers in pulmonary arterial hypertension. Heart. 2016;102(5):390-6.

26. Nickel NP, Lichtinghagen R, Golpon H, Olsson KM, Brand K, Welte T, et al. Circulating levels of copeptin predict outcome in patients with pulmonary arterial hypertension. Respir Res. 2013;14:130.

27. Sakao S, Taraseviciene-Stewart L, Lee JD, Wood K, Cool CD, Voelkel NF. Initial apoptosis is followed by increased proliferation of apoptosis-resistant endothelial cells. FASEB J. 2005;19(9):1178-80.

28. Happe CM, Szulcek R, Voelkel NF, Bogaard HJ. Reconciling paradigms of abnormal pulmonary blood flow and quasi-malignant cellular alterations in pulmonary arterial hypertension. Vascul Pharmacol. 2016;83:17-25.

29. Boucherat O, Vitry G, Trinh I, Paulin R, Provencher S, Bonnet S. The cancer theory of pulmonary arterial hypertension. Pulm Circ. 2017;7(2):285-99.

30. Austin ED, Loyd JE. The genetics of pulmonary arterial hypertension. Circ Res. 2014;115(1):189-202.

31. McGoon MD, Benza RL, Escribano-Subias P, Jiang X, Miller DP, Peacock AJ, et al. Pulmonary arterial hypertension: epidemiology and registries. J Am Coll Cardiol. 2013;62(25 Suppl):D51-D9.

32. Kurakula K, Sun XQ, Happe C, da Silva Goncalves Bos D, Szulcek R, Schalij I, et al. 6-mercaptopurine, an agonist of Nur77, reduces progression of pulmonary hypertension by enhancing BMP signalling. Eur Respir J. 2019.

33. Giannotta M, Trani M, Dejana E. VE-cadherin and endothelial adherens junctions: active guardians of vascular integrity. Dev Cell. 2013;26(5):441-54.

34. Mehta D, Malik AB. Signaling mechanisms regulating endothelial permeability. Physiol Rev. 2006;86(1):279-367.

35. Huveneers S, Oldenburg J, Spanjaard E, van der Krogt G, Grigoriev I, Akhmanova A, et al. Vinculin associates with endothelial VE-cadherin junctions to control force-dependent remodeling. J Cell Biol. 2012;196(5):641-52.

36. Shattil SJ, Kim C, Ginsberg MH. The final steps of integrin activation: the end game. Nat Rev Mol Cell Biol. 2010;11(4):288-300.

37. Yamamoto H, Ehling M, Kato K, Kanai K, van Lessen M, Frye M, et al. Integrin beta1 controls VE-cadherin localization and blood vessel stability. Nat Commun. 2015;6:6429.

38. Pierce RW, Merola J, Lavik JP, Kluger MS, Huttner A, Khokha MK, et al. A p190BRhoGAP mutation and prolonged RhoB activation in fatal systemic capillary leak syndrome. J Exp Med. 2017;214(12):3497-505.

39. Rho SS, Ando K, Fukuhara S. Dynamic Regulation of Vascular Permeability by Vascular Endothelial Cadherin-Mediated Endothelial Cell-Cell Junctions. J Nippon Med Sch. 2017;84(4):148-59.

40. Bogatcheva NV, Garcia JG, Verin AD. Role of tyrosine kinase signaling in endothelial cell barrier regulation. Vascul Pharmacol. 2002;39(4-5):201-12.

41. Rizzo AN, Aman J, van Nieuw Amerongen GP, Dudek SM. Targeting Abl kinases to regulate vascular leak during sepsis and acute respiratory distress syndrome. Arterioscler Thromb Vasc Biol. 2015;35(5):1071-9.

42. Aman J, Peters MJ, Weenink C, van Nieuw Amerongen GP, Vonk Noordegraaf A. Reversal of vascular leak with imatinib. Am J Respir Crit Care Med. 2013;188(9):1171-3.

43. Aman J, van Bezu J, Damanafshan A, Huveneers S, Eringa EC, Vogel SM, et al. Effective treatment of edema and endothelial barrier dysfunction with imatinib. Circulation. 2012;126(23):2728-38.

1

44.   Ackermann M, Verleden SE, Kuehnel M, Haverich A, Welte T, Laenger F, et al. Pulmonary Vascular Endothelialitis, Thrombosis, and Angiogenesis in Covid-19. N Engl J Med. 2020.

Pulmonary Arterial Hypertension
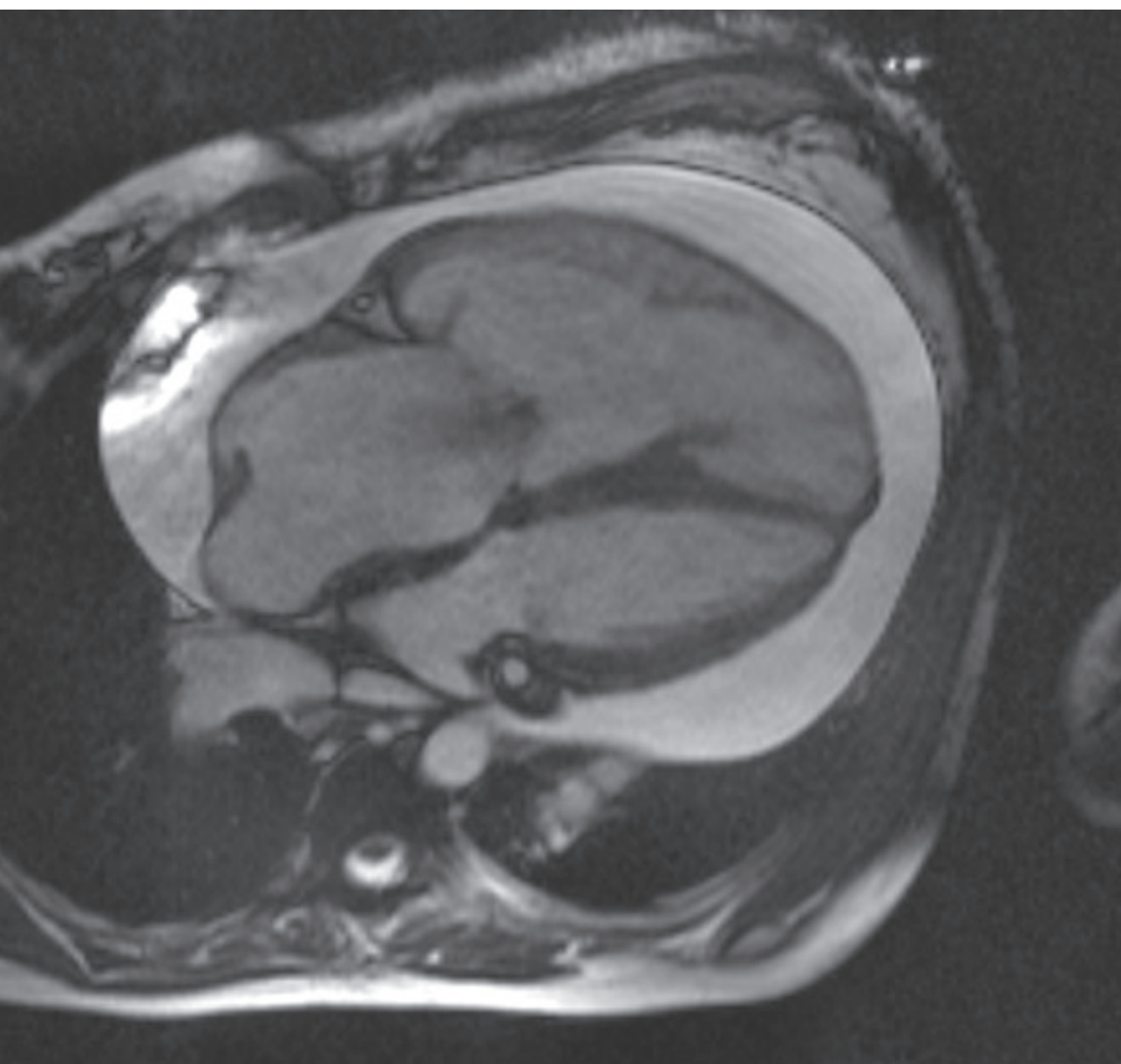
2

Blood biomarkers for the detection of idiopathic and hereditary pulmonary arterial hypertension; a meta-analysis

A. Josien Smits, Liza Botros, Mariska Mol, Kirsten A. Ziesemer,

Martin R. Wilkins, Anton Vonk Noordegraaf, Harm Jan Bogaard &
Jurjan Aman

Abstract

Objective: The blood is a rich source of potential biomarkers for the diagnosis and monitoring of idiopathic and hereditary pulmonary arterial hypertension (IPAH and hPAH, referred to as "PAH"). However, the clinical utility of these biomarkers outside their discovery cohorts often remains unclear. Here we provide a systematic literature review of blood biomarkers for the diagnosis of PAH and evaluate their implementation in clinical practice.

Data sources: A literature search (in PubMed, Embase.com, Clarivate Analytics/Web of Science Core Collection and Wiley/Cochrane Library) was performed up to January 28, 2021 in collaboration with a medical information specialist. Primary end points were biomarker levels in PAH versus asymptomatic controls or patients suspected of pulmonary hypertension (PH) with proven normal hemodynamic profiles.

Results: 149 articles were included. Meta-analysis yielded 26 biomarkers that were differentially expressed in PAH and non-PH control subjects. These biomarkers could be categorized in six domains: haematological, metabolic, coagulation, inflammatory, cardiac and renal. Red cell distribution width, LDL-c, d-dimer, NT-proBNP, IL-6 and uric acid were biomarkers with the largest observed differences and largest sample sizes and with a low risk of publication bias. NT-proBNP was most accurate, but still lacked specificity for PAH. Other markers lacked determination of diagnostic accuracy with receiver operating curve analyses.

Discussion: This meta-analysis provides an overview of blood biomarkers for the detection of PAH. The majority of biomarkers lacked either diagnostic accuracy or sufficient supporting evidence. For this reason, further validation studies are required, as well as studies that test combinations of biomarkers to improve specificity.

Introduction

Pulmonary arterial hypertension (PAH) is a cardiovascular condition in which progressive occlusive remodelling leads to increased pulmonary vascular resistance and ultimately right ventricular failure. PAH can be hereditary (hPAH) or idiopathic (IPAH) after exclusion of significant co-morbidity (1), referred to as "PAH" throughout this study. The diagnosis of PAH is a complex, specialist process, attributing to a mean time to diagnosis of 17-24 months (2). The availability of non-invasive biomarkers for faster diagnosis and initiation of treatment prior to the development of right heart failure may improve survival and quality of life (3).

Until now, NT-proBNP remains the most useful clinical marker of myocardial strain and is employed for risk stratification of patients in guidelines and clinical practice(1). However, improved understanding of the pathways leading to PAH, which include endothelial dysfunction, immunity and altered cellular metabolism, may result in the emergence of novel biomarkers that can detect proliferation and occlusive remodelling of the vascular wall.

We conducted a systematic review and meta-analysis of the literature on published biomarkers of PAH in blood or urine. Here we show: 1) biomarkers differentially expressed in IPAH and hPAH compared to non-pulmonary hypertension (PH) controls; and 2) evidence supporting the suitability of these biomarkers for clinical implementation, including calculation of diagnostic accuracy employing receiver operating curve analyses.

Materials and methods

Search strategy

The conduct and reporting of this review adhere to the Preferred Reporting Items for Systematic Reviews and Meta-analyses (PRISMA)-statement (www.prismastatement.org)(4) and is registered in PROSPERO (CRD42020215820).

Four bibliographic databases (PubMed, Embase.com, Clarivate Analytics/Web of Science Core Collection, Wiley/Cochrane Library) were searched for relevant literature from inception to January 28, 2021. Searches were constructed in collaboration with a medical information specialist (KAZ). Search terms including synonyms, closely related words and keywords were used as index terms or free-text words. The searches contained no methodological search filter, date or language restrictions that would limit results to specific study designs, date or language. The full search strategy used for each database is detailed in supplementary table 1. Duplicate articles were excluded using Endnote (X9.3.3), Amsterdam Efficient Deduplication-method and Bramer-method(5)).

Two reviewers (JS and LB) independently screened all potentially relevant titles and abstracts for eligibility using Rayyan. If necessary, the full text article was checked for the eligibility criteria. Differences in judgement were resolved through; 1) discussion among

reviewers (JS and LB), 2) arbitration of a third reviewer (JA), or 3) contacting the author. Studies were included if they met the following criteria: 1) analysis of potential blood and urine biomarkers in any form, including growth factors, inflammatory mediators, circulating cells, protein, (micro)RNA, or microvesicles; and 2) involved group 1 PAH, provided that IPAH or hPAH patients were included. The following studies were excluded: 1) animal studies; 2) studies involving subjects < 18 years of age; 3) studies that did not report biomarker levels for group 1 PAH, or lacked inclusion of IPAH or hPAH patients; 3) studies that lacked a control group, or included a control group suspected of PH without measurement of hemodynamics; 4) certain publication types: editorials, letters, legal cases, interviews etc. The full text of the selected articles was obtained for further review. Two reviewers (JS and LB) independently evaluated the methodological quality of the full text papers using QUADAS-2(6). Articles were scored as low, unclear or high on domains 'patients inclusion (P)', 'index test (I)', 'reference test (R)' and 'flow and timing (T)'(6). Criteria and rubix were optimized by JS and LB from a pilot of 10 studies and are presented in table S2.

A similar search strategy was adopted in identical databases to identify 'omics' studies performed in patients with IPAH and hPAH, compared to non-PH control subjects. Studies were included if they met the following criteria; 1) adopted an 'omics' technology, including transcriptomics, proteomics, metabolomics, glycomics or lipidomics in blood or urine; and 2) involved patients with group 1 PAH, including IPAH or hPAH. Similar exclusion criteria applied as described above.

Statistics

Primary outcomes were biomarker concentrations in PAH and asymptomatic controls. Meta-analyses were performed when original data (expressed in mean with standard deviation (SD) were available from a minimum of three publications using Review Manager 5.3.5 software, The Nordic Cochrane Center, Copenhagen, Denmark. A randomized model for continuous data was adopted, due to possibile risk of bias. Based on population size, mean and SD, the standardized mean difference, mean difference and odds ratio (OR) of biomarker levels in patients with PAH and non-PH controls were calculated. Mean and standardized mean differences are represented as mean with 95% confidence intervals (95% CI), or OR with 95% CI. Biomarkers were ranked according to effect size and statistical significance. I^2 and Tau^2 statistics were performed to assess heterogeneity among studies, and explainable heterogeneity was solved by exclusion of the aberrant publication.

Publication bias was assessed in Comprehensive Meta-Analysis software V3, Biostat, Englewood, NJ) using funnel plots, Egger's regression test ($p < 0.10$), Duval and Tweedie's trim and fill and Orwin's Fail safe N-test. The failsafe number estimates the number of unpublished studies required to turn the meta-analysis result in a clinically insignificant value. The clinically irrelevant value was arbitrarily set at a standardized mean difference of less than -0.25 or 0.25.

Selection of biomarkers for clinical implementation

We made a selection of differentially expressed biomarkers based on the largest observed difference, sample size, sensitivity and specificity values based on ROC analyses. In addition, we selected for a negligible risk op publication bias, defined by Egger's regression $p > 0.10$, Duval & Tweedie's trim and fill ($p < 0.05$), and a minimum of five publications predicted to bring the result to a clinically insignificant value (standardized mean difference – 0.25, 0.25). All biomarkers were grouped in six pathobiological domains: haematological, metabolic, coagulation, inflammatory, cardiac and renal. In each domain, we selected one preferred biomarker on the basis of clinical and analytic validity.

2

Results

Inclusion and selection of publications

The biomarker literature search generated a total of 3456 references: 887 in PubMed, 1506 in Embase.com, 976 in Clarivate Analytics/Web of Science Core Collection and 87 in Wiley/Cochrane Library. After removal of duplicates 1356 remained. 1207 full-text articles were excluded for not fulfilling inclusion criteria (fig. 1a). 149 publications remained eligible for data extraction. 45 publications were identified that describe biomarkers meeting criteria for meta-analysis and risk of bias assessment. A detailed overview of biomarker origin (whole blood, plasma or serum), location of blood draw (peripheral or central (RHC) blood draw), demographic criteria, treatment and concerns regarding inclusion procedure of these publications is provided in table S3. Risk of bias assessment using QUADAS-2(6) is reported in fig. S1.

Exclusion of urine and non-protein blood biomarkers

In several publications, biomarker expression was studied on circulating platelets(7, 8), immune cells (9-12) and progenitor cells(13-16). Heterogeneity in measurement methods, characterization and FACS gating precluded meta-analysis of these publications.

Three publications were dedicated to different types of extracellular vesicles as biomarker (17, 18) and three to different types of miRNA as biomarker (19-22). A single publication was dedicated to a urine biomarker(23). These publications did not meet the criteria for meta-analysis.

Figure 1
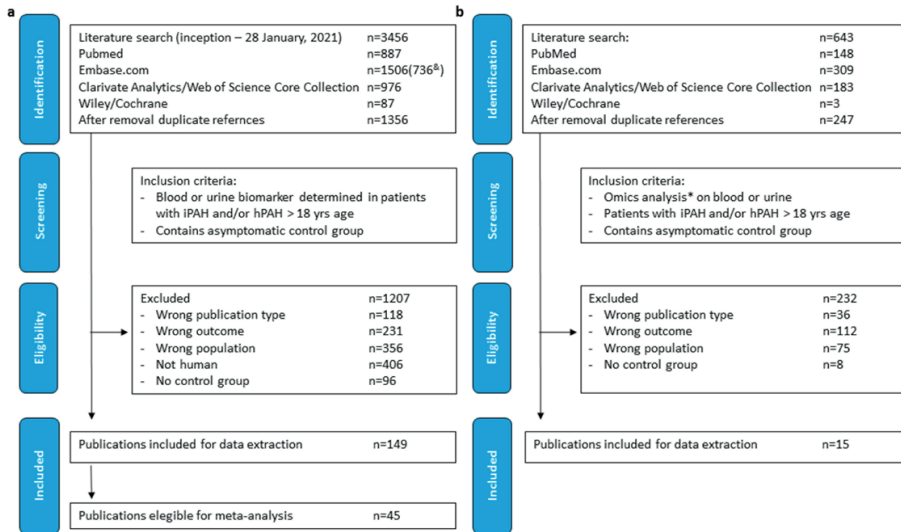
Figure 1: Flow chart visualizing identification of publications, in- and exclusion criteria, and selection of publications eligible for meta-analysis & excluding conference abstracts. a) biomarker search, b) omics search. * transcript-, protein-, metabol-, glyc- or lipidomics

Selection of eligible biomarkers

26 biomarkers were eligible for meta-analysis (table 1). A significant difference in expression was detected for 17 biomarkers in six pathobiological domains. In the haematological domain, these were red blood cell distribution width (RDW), platelet distribution width (PDW), mean platelet volume (MPV) and thrombocytes. In the metabolic domain, total cholesterol, low density lipid-cholesterol (LDL-c), triglycerides and fasting glucose. In the coagulation domain, d-dimer was differentially expressed. In the inflammatory domain, interleukin-6 (IL-6), c-reactive protein (CRP), soluble vascular adhesion molecule-1 (sVCAM-1), C-X-C motif chemokine ligand-10 (CXCL-10) and tissue inhibitor metalloproteinase-1 (TIMP1) were differentially expressed. In the cardiac domain, N-terminal prohormone of brain natriuretic protein (NT-proBNP), and in the renal domain, uric acid (UA) and blood urea nitrogen (BUN) were differentially expressed. Biomarkers described in fewer than three publications or as median with IQRI are summarized in table S4 and S5.

Selected biomarkers are shown in fig. 2 (see MM). These included RDW, LDL-c, d-dimer, IL-6, NT-proBNP and UA. Forest plots for PDW, MPV, thrombocytes, total cholesterol, triglycerides, fasting glucose, CRP, sVCAM-1, CXCL-10, TIMP1, BUN are provided in the supplement (fig. S2-7, table S6).

2

Table 1: Summary of 26 meta-analyses

	Studies (n)	Partici-pants (n)	Mean difference	St. mean difference	Overall effect (p)	Tau²	I² (%)	Heterogeneity (p)	Forest plot
Hematological									
RDW, %	4	427	1.83 [1.39, 2.26]	0.98 [0.61, 2.17]	<0.00001	0.07	51	0.11	Fig. 2a
PDW, %	3	245	1.42 [0.16, 2.67]	0.81 [0.50, 1.12]	<0.00001	0.02	19	0.29	Fig. S2a
MPV, fL	5	361	0.95 [0.76, 1.13]	1.0 [0.81, 1.25]	<0.00001	0.00	0	0.68	Fig. S2b
	6*	395	0.66 [0.24, 1.09]	0.72 [0.24, 1.19]	0.003	0.27	78	0.0003	
Thrombocytes, 10^9/L	7	334	-23.9 [-38.6, -9.2]	-0.38 [-0.62, -0.15]	0.001	0.01	5	0.39	Fig. S2c
Hb, g/dL	9	400	-0.59 [-1.23, 0.06]	-0.18 [-0.43, 0.07]	0.15	0.04	29	0.19	Fig. S2d
Hct, %	5	229	-1.07 [-3.91, 1.76]	-0.21 [-0.76, 0.34]	0.46	0.29	74	0.004	Fig. S2e
Leukocytes, 10^9/L	7	294	-0.23 [-0.70,0.24]	-0.10 [-0.41, 0.21]	0.52	0.07	39	0.13	Fig. S2f
Metabolic									
LDL-c, mg/dL	6	3035	-15.82 [-26.18, -5.46]	-0.44 [-0.65, -0.22]	<0.00001	0.03	46	0.10	Fig. 2b
Total cholesterol, mg/dL	4	368	-17.70 [-24.15, -11.26]	-0.52 [-0.73, -0.32]	<0.00001	0.00	67	0.67	Fig. S3a
TG, mg/dL	4	198	-32.56 [-54.17, -10.94]	-0.52 [-0.87, -0.17]	0.004	0.04	34	0.21	Fig. S3b
Glucose (fasted), mg/dL	3	103	24.06 [0.54, 7.58]	0.48 [0.08, 0.87]	0.02	0.00	0	0.85	Fig. S3c
HDL-c, mg/dL	6	577	-6.15 [-2.11, 14.40]	-0.53 [-1.20, 0.15]	0.13	0.63	91	<0.00001	Fig. S3d
Coagulation									
D-dimer, ng/mL	3	142	245.99 [148.55, 343.43]	0.69 [0.27, 1.11]	0.001	0.04	27	0.26	Fig. 2c
Fibrinogen, mg/mL	4	227	73.75 [-2.58, 150.08]	0.84 [-0.14, 1.81]	0.09	0.88	90	<0.00001	Fig. S4
Inflammatory									
IL-6, pg/mL	5	389	5.01 [2.06, 7.96]	0.64 [0.28, 0.99]	0.0005	0.08	47	0.11	Fig. 2d
CRP, mg/L	8	387	0.74 [0.13, 1.6]	0.25 [0.04, 0.47]	0.02	0.02	0	0.98	Fig. S5a
	9*	493	0.13 [0.10, 0.17]	0.77 [-0.08, 1.61]	0.08	1.57	94	<0.00001	
sVCAM-1, ng/mL	3	150	626.72 [29.38, 1224.07]	1.03 [0.53, 1.52]	<0.00001	0.08	40	0.19	Fig. S5b
CXCL-10, pg/mL	3	171	99.77 [54.53, 145.01]	0.82 [0.49, 1.16]	<0.00001	0.00	0	0.46	Fig. S5c
TIMP-1, ng/mL	3	224	15.58 [-2.56, 33.72]	0.40 [0.13, 0.67]	0.003	0.00	0	0.54	Fig. S5d
	4*	329	40.15 [1.02, 79.29]	0.67 [0.14, 1.21]	0.01	0.24	82	0.0009	
sP-selectin, ng/mL	4	180	0.52 [-11.10, 12.14]	-0.04 [0.35, 0.28]	0.82	0.00	0	0.72	Fig. S5e
Cardiac									
NT-proBNP, pg/mL	10	1152	1684 [1035, 2330]	1.13 [0.93, 1.33]	<0.00001	0.03	30	0.17	Fig. 2e
	11*	1258	1004 [787, 1221]	1.37 [0.96, 1.79]	<0.00001	0.39	85	<0.00001	
Renal markers									
UA, mg/dL	5	441	1.77 [1.06, 2.48]	0.89 [0.58, 1.12]	<0.00001	0.06	51	0.09	Fig. 2f
	6*	531	1.52 [0.77, 2.27]	0.81 [0.53, 1.09]	<0.00001	0.09	59	0.03	

2

BUN, mg/dL	5	891	1.76 [0.51, 3.01]	<0.00001	0.00	0	0.48	Fig. S6a
Creatinine, mg/dL	10	475	0.03 [-0.04, 0.10]	0.23	0.02	20	0.26	Fig. S6b
eGFR, mL−/1.73 m^2	4	189	1.70 [5.98, 9.37]	0.67	0.08	47	0.13	Fig. S6c
Hepatic								
ALT, U/L	3	115	3.57 [-4.18, 11.31]	0.37	0.30	71	0.03	Fig. S7

Table 1: Per biomarker the number of studies included, total sample size, mean difference, and the standardized difference between IPAH and non-PH control with 95% confidence interval (95% CI), p-value of the difference, and heterogeneity of the result (I^2, Tau^2 and p-heterogeneity) are shown. PDW; platelet distribution width, RDW; red cell distribution width, MPV; mean platelet volume, Hb; hemoglobin, Hct; hematocrit, TG; triglycerides, LDL-c; low density lipoprotein, HDL-c; high density lipoprotein, sVCAM-1; circulating vascular cell adhesion molecule-1, CXCL-10; C-X-C motif chemokine ligand-10, IL-6; interleukin-6, TIMP-1; tissue inhibitors of metalloproteinases-1, CRP; c-reactive protein, NT-proBNP; N-terminal prohormone of brain natriuretic peptide, UA; uric acid, eGFR; estimated glomerular filtration rate, ALT; alanine transaminase. St. mean difference; standardized mean difference. *publication excluded due to heterogeneity.

Evaluation of publication bias

Egger's regression analysis revealed a significant association (p < 0.10) between effect size and standard error for MPV and thrombocytes. After correction for possible publication bias by Duval & Tweedie's trim and fill, the mean difference between PAH and control groups remained significant. The failsafe test calculated a minimum of five publications were necessary to bring the differences to a clinically trivial value, defined as a standardized mean difference of less than -0.25 or 0.25. This suggests that the chance that the observed difference relies on publication bias is small (table S7). Funnel plots of all meta-analyses are given in fig. S8a-z.

Haematological markers: RDW

All five publications on RDW were eligible for meta-analysis. RDW was determined in treatment naive IPAH(24) and PAH(25) patients, and in PAH patients receiving vasodilatory treatment(11, 26). As a reference, asymptomatic controls(11, 24-26) and patients suspected of PH(26) or common disease controls(24) were included (fig. 2a). Meta-analysis confirmed a positive mean difference of 1.67% [1.45, 1.89], p<0.00001 between PAH and non-PH control; (table 1). No sensitivity or specificity for the diagnosis could be extracted.

Increased RDW is caused by iron deficiency(27-29), hemolysis, chronic inflammation(30), or ischemia(31). A rise in RDW is predictive for the presence of PH in patients with acute pulmonary embolism (32) or systemic sclerosis(26, 33). RDW was positively associated with pulmonary artery pressure(11, 24), right atrial pressure(24), pulmonary vascular resistance(24), BNP(26) and NT-proBNP(34), and inversely with six minute walking distance(24, 26, 34). Remarkably, RDW outperformed NT-proBNP and IL-6 as prognostic markers for PAH patients(32).

Other markers in the haematological domain are summarized in table 1. PDW was increased with a mean difference of 1.42% [0.16, 2.67], p<0.00001, fig. S2a), as well as MPV (0.95 fL [0.76, 1.13], p < 0.00001, fig. S2b), while thrombocyte count was decreased by a mean of -23.9 x 10^9 cells/L [-38.6, -9.2], p 0.001, fig. S2c. Eligible for meta-analysis but without significant differences were haemoglobin, haematocrit and leukocytes (fig. S2d-f).

Figure 2: Forest plots of selected biomarkers, including; RDW;red cell distribution width, LDL-c; low density lipid-cholesterol; IL-6; interleukin-6, NT-proBNP; N-ter-al prohormone of brain natriuretic peptide, UA; uric acid. Risk of bias (QUADAS-2), P: patient inclusion, I; index-test (biomarker), R; refence standard (diagnosis), T; flow and timing. Publications pressed in bold measured biomarker levels in IPAH and/or hPAH uniquely.

Figure 2

a   Hematological

RDW Study	PAH Type	Mean	n	Control Mean	n	Weight	Std. Mean Difference Random, 95%-CI	Risk of Bias P I R T
Petrauskas, L.A. et al., (2019).	PAH	15.9±2.8	181	14.2±1.1	101	28%	0.7 [0.5, 1.0]	
Decker, I. et al., (2011).	iPAH	14.9±2.1	30	13.2±1.0	12	10%	0.9 [0.2, 1.6]	
Yildiz, A. et al., (2013).	PAH	17.3±2.2	25	15.6±0.8	22	12%	1.0 [0.4, 1.6]	
Yaylali, Y.T. et al., (2019).	PAH	16.3±2.6	21	13.4±1.2	35	12%	1.6 [0.9, 2.2]	
Total effect PAH	p<0.00001		257		170		1.0 [0.6, 1.34]	

b   Metabolic

LDL-c Study	PAH Type	Mean	n	Control Mean	n	Weight	Std. Mean Difference Random, 95%-CI	Risk of Bias P I R T
Jasciewicz, M. et al., (2014).	PAH	105±37	26	140±36	30	11%	-1.0 [-1.5, -0.4]	
Yildiz, A. et al., (2013).	PAH	98±20	25	114±35	22	10%	-0.6 [-1.1, 0.0]	
Kopec, G. et al., (2017).	iPAH	101±31	140	124±46	2431	33%	-0.5 [-0.7, -0.3]	
Varol, E. et al., (2011).	PAH	96±31	22	111±34	25	10%	-0.5 [-1.0, 0.1]	
Wang, G.F. et al., (2020).	iPAH	79±27	177	84±23	103	27%	-0.2 [-0.4, 0.1]	
Yaoita, N. et al., (2014).	PAH	96±26	19	100±31	15	8%	-0.1 [-0.8, 0.6]	
Total effect PAH	p<0.0001		409		2626		-0.4 [-0.7, -0.2]	
Total effect iPAH	**p=0.03**		**217**		**1534**		**-0.4 [-0.7, 0.0]**	

c   Coagulation

D-dimer Study	PAH Type	Mean	n	Control Mean	n	Weight	Std. Mean Difference Random, 95%-CI	Risk of Bias P I R T
Yaoita, N. et al., (2014).	PAH	1630±3280	19	880±500	15	29%	0.3 [-0.4, 1.0]	
Vrigkou, E. et al., (2019).	PAH	657±547	30	355±175	10	26%	0.6 [-0.1, 1.3]	
Can, M.M., et al., (2010).	PAH	420±310	34	190±90	34	45%	1.0 [0.5, 1.5]	
Totall effect PAH	p=0.001		83		59		0.7 [0.3, 1.1]	

d   Inflammatory

IL-6 Study	PAH Type	Mean	n	Control Mean	n	Weight	Std. Mean Difference Random, 95%-CI	Risk of Bias P I R T
Soon, E. et al., (2010).	iPAH	18.9±49	70	5.7±1.8	21	24%	0.3 [-0.2, 0.8]	
Rhodes, C.J. et al., (2011).	iPAH	8.6±18.7	139	1.4±1.4	40	31%	0.4 [0.1, 0.8]	
Prins, K.W. et al., (2018).	PAH	15.1±21	40	2.5±5.5	10	16%	0.7 [-0.1, 1.4]	
Heresi, G.A. et al., (2017).	iPAH	4.5±3.6	14	2.4±1.7	14	14%	0.7 [0.0, 1.5]	
Itoh, T. et al., (2006).	iPAH	2.6±1.6	28	0.6±0.4	13	15%	1.5 [0.7, 2.2]	
Total effect PAH	p=0.0005		291		98		0.6 [0.3, 1.0]	
Total effect iPAH	**p=0.004**		**251**		**88**		**0.7 [0.2, 1.1]**	

e   Cardiac

NT-proBNP Study	PAH Type	Mean	n	Control Mean	n	Weight	Std. Mean Difference Random, 95%-CI	Risk of Bias P I R T
Hennings, J.K. et al., (2014).	PAH	0.5±0.2	25	0.5±0.2	22	8%	0.7 [0.0, 1.3]	
Calvier, L. et al., (2016).	iPAH	0.1±0.5	25	0.1±0.1	25	5%	0.8 [0.0, 1.5]	
Fares, W.H. et al., (2012).	PAH	1.2±3.0	52	0.6±0.3	11	10%	0.8 [0.3, 1.4]	
Renard, S. et al., (2013).	iPAH	0.2±1.0	14	0.1±1.4	30	15%	0.9 [0.5, 1.3]	
Fijalkowska, A. et al., (2006)	iPAH	0.5±0.6	25	0.3±0.6	33	5%	1.0 [0.3, 1.8]	
Lu, G.H. et al., (2020)	iPAH	0.4±0.1	338	0.3±0.1	338	30%	1.2 [1.0, 1.4]	
Zhu, T. et al., (2019)	iPAH	2.5±1.9	14	1.8±1.8	14	8%	1.4 [0.7, 2.0]	
Andreassen, A.K. et al, (2006)	iPAH	0.4±0.6	21	0.2±0.2	27	5%	1.4 [0.5, 2.3]	
Wang, K.Y. et al., (2015).	iPAH	0.7±1.0	41	0.3±0.5	8	8%	1.5 [0.8, 2.1]	
Yang, D. et al., (2013).	iPAH	0.6±0.2	26	0.4±0.1	30	6%	2.0 [1.2, 2.8]	
Total effect PAH	p<0.00001		626		526		1.1 [0.9, 1.3]	
Total effect iPAH	**p<0.00001**		**549**		**482**		**1.2 [1.0, 1.4]**	
* Malhotra, R. et al.(2013), excluded (method)								

f   Renal

UA Study	PAH Type	Mean	n	Control Mean	n	Weight	Std. Mean Difference Random, 95%-CI	Risk of Bias P I R T
Suzuki, S. et al., (2016).	PAH	6.3±1.7	18	6.0±1.8	30	17%	0.2 [-0.4, 0.8]	
Jasciewicz, M. et al., (2014).	PAH	6.3±2.4	26	4.5±1.5	24	17%	0.9 [0.3, 1.4]	
Jiang, X. et al., (2008).	iPAH	6.3±2.0	78	4.5±1.4	98	28%	1.0 [0.7, 1.3]	
Zhu, T. et al., (2019).	iPAH	7.6±2.4	27	5.3±1.4	20	15%	1.1 [0.5, 1.7]	
Nagaya, N. et al., (1999).	iPAH	7.5±2.5	90	4.9±1.2	30	23%	1.2 [0.7, 1.6]	
Total effect PAH	p<0.00001		239		202		0.9	
Total effect iPAH	**p<0.00001**		**214**		**163**		**0.9**	
*Yaoita, N. et al., (2014) excluded (control group severe CVD)								

Metabolic markers: LDL-c

LDL-c was reported in six publications eligible for meta-analysis and determined in patients with PAH receiving vasodilatory treatment. Asymptomatic controls(11, 35-37) or patients with cardiovascular disease or patients suspected of PH(8) were included for reference (fig. 2b). All measurements were performed in blood obtained after >8 hours of fasting. LDL-c was lower in patients with PAH, with a mean difference of -15.82 mg/dL [-26.18, -5.46], p < 0.00001 (table 1). No sensitivity or specificity was calculated.

Decreased insulin sensitivity and altered lipid metabolism in IPAH are a possible consequence of chronic inflammation, malnourishment and alterations in liver function(38, 39). LDL-c was not related to haemodynamic parameters, NT-proBNP, six minute walking distance or BMI. LDL-c was negatively associated with 3-year survival in PAH (hazard-ratio 0.18/mmol/L (0.07-0.47), p<0.01, corrected for statin use)(35). A similar relationship has been described in chronic heart failure(40, 41).

A lower LDL-c in patients with PAH was accompanied by a lower mean total cholesterol of -17.70 mg/dL [-24.15, -11.26], p < 0.00001 (fig. S3a) and lower mean triglycerides of -32.56 mg /dL [-54.17, -10.94], p 0.004, fig. S3b). Despite inclusion of six publications, meta-analysis did not reveal a significant difference in HDL-c (mean difference -6.15 mg/dL [-2.11, 14.40], p 0.13, fig. S3d) or fasting glucose (fig. S3c).

Coagulation markers: D-dimer

From the available markers representing coagulation pathways, fibrinogen and D-dimer levels were eligible for meta-analysis. D-dimer is the degradation product of fibrin(42). D-dimer was studied in treatment naive IPAH patients (43) and in PAH patients receiving vasodilatory treatment(8, 44) and results were compared to asymptomatic controls (fig. 2c). Meta-analysis revealed a significantly higher D-dimer level in patients with PAH compared to asymptomatic controls, with a mean difference of 245.99 ng/mL [148.55, 343.43], p 0.001, table 1, in contrast to fibrinogen (73.75 [-2.58, 150.08], p 0.09, fig. S4); all consistent with the hypothesis that hypercoagulability and in situ thrombosis may contribute to disease pathobiology in PAH(45).

Inflammatory markers: IL-6

Ten publications measured IL-6, five were eligible for meta-analysis. All studies detected elevated levels of circulating IL-6 in treatment naïve IPAH(46), or IPAH receiving vasodilatory treatment(32, 47-51) and naïve PAH(52, 53) or PAH patients receiving treatment(54). Findings were compared to asymptomatic controls (fig. 2d). A significant rise in IL-6 levels was observed in PAH compared to non-PH controls (mean difference (5.01 [2.06, 7.96] pg/mL, p 0.0005 (table 1).

Il-6 levels were negatively associated with the number of circulating endothelial progenitor cells(47), and were elevated in parallel to several interleukines(50), CXCL-10(48), MCP-1(53, 54) and TNF-a(46, 52-54), PlGF(46), sVEGFR-1(46), VEGF-A(46) and VEGF-D(46) and markers related to thrombogenesis(51). IL-6 was negatively associated with RV function(53),

6MWD(32, 46), while positively to WHO-functional class(32), NT-proBNP(32, 46) and mean right atrial pressure(46). IL-6 levels were predictive for all-cause mortality(32, 50) in PAH. No diagnostic accuracy was calculated by calculation of ROC and AUC curves.

Another inflammatory marker in PH is CRP. Eight publications detected a subtle elevation in CRP levels in PAH(11, 47, 55-63) (fig. S5a), (mean difference 0.74 mg/L [0.13, 1,6], p 0.02 (table 1). However, only one study was predicted to bring the difference to an clinically insignificant value, indicating a risk of significant bias. Additionaly, Wang et al. (56) aimed to determine the diagnostic accuracy of CRP for detection of IPAH among asymptomatic controls. A cut-off of 2.7 mg/L yielded an area-under-the-curve (AUC) of 0.51 (p 0.899) with a 85% specificity but low (39%) sensitivity(56). CRP is commonly attributed to other cardiovascular or inflammatory disease(64), and these data indicate that an elevated and may not be suitable for detection of PAH among non-PH controls.

Other inflammatory markers that were eligible for meta-analysis and significantly increased in patients with IPAH compared to non-PH controls included: sVCAM-1 (mean difference of 626.72 ng/mL [29.38, 1224.07], p 0.003, fig. S5b), CXCL-10 (mean difference 99.77 pg/mL [54.53, 145.01], p<0.00001, fig. S5c) and TIMP-1 (mean difference of 15.58 ng/mL [-2.56, 33.72], p 0.003 ,fig. S5d). No significant difference was observed for sP-selectin (fig. S5e).

Cardiac markers: NT-proBNP

11 publications reporting on NT-proBNP met the inclusion criteria, ten of which were eligible for meta-analysis. NT-proBNP was measured in treatment naïve IPAH patients (37, 65-69), as well as in IPAH(56-58, 68-70) and PAH patients receiving vasodilatory treatment(61, 62, 71, 72). Data were compared to asymptomatic controls(37, 63, 65-69, 72) or subjects suspected of PH(61, 62, 71) (fig. 2e). The overall mean difference was 1684 pg/mL [1035, 2330], p <0.00001 (table 1).

Wang et al.(56) determined the diagnostic accuracy of NTproBNP in patients with IPAH among asymptomatic controls employing a cut-off >89.25 pg/mL (AUC 0.87, p<0.0001) with a sensitivity of 89%, and 78% specificity. Similarly, Malhotra et al.(58) detected PAH patients receiving vasodilatory treatment among asymptomatic controls with an AUC of 0.714.

NT-proBNP was positively associated with markers of right ventricular function, including pulmonary vascular resistance(66, 71), right atrial pressure(66), right ventricular dimensions(65, 67, 72), and exercise tolerance (WHO functional class(57, 66, 71). NTproBNP was inversely related to six minute walking distance(57, 71)), cardiac index(66, 71) and mixed venous oxygen concentration(66, 71). In addition, NT-proBNP decreased significantly after initiation of treatment, in line with decreased pulmonary vascular resistance(66, 71). NT-proBNP was not dependent on the location of blood draw or pulmonary capillary wedge procedure(61).

Renal markers: Uric acid

Six publications reporting on uric acid (UA) levels were included in this review, five of which were eligible for meta-analysis. UA levels were measured in treatment naive IPAH

patients(37, 68, 73), IPAH patients receiving treatment(8, 74) and PAH patients on treatment (60, 75), and compared to asymptomatic controls (8, 37, 60, 68, 73-75) (fig. 2f). Meta-analyses detected a significantly higher UA level in PAH compared to control with a mean difference of 1.77 mg/dL [1.06, 2.48], p<0.00001 (table 1). No diagnostic sensitivity or specificity could be extracted.

Ischemia depletes ATP resulting in hyperuricemia through UA overproduction in heart failure, chronic obstructive lung- and cardiovascular disease(76). UA levels in PAH patients were positively associated with right ventricular volume(74), pulmonary vascular resistance(73, 74) and WHO functional class(73, 74), and negatively correlated with cardiac output(73, 74) and mixed venous saturation(74). UA decreased significantly after initiation of vasodilatory treatment, proportional to the decrease in pulmonary vascular resistance(73, 74). UA is an independent predictor of 3-year mortality in IPAH(73) and heart failure(77).

BUN was the second renal marker that was analysed. We observed a significant increase of 1.76 mg/dL [0.51, 3.01], p < 0.0001, (fig. S6a). Creatinine and eGFR were eligible but not significantly altered (fig. S6b-c).

Hepatic markers

In three individual studies reporting on alanine aminotransferase (ALT) in treatment naive IPAH patients(68), IPAH patients receiving vasodilatory treatment(55) and treatment naive PAH patients(43), no significant difference was observed in our meta-analysis (fig. S7). No other hepatic marker was eligible for meta-analysis.

Omics studies

The omics search strategy generated at total of 643 articles: 148 in PubMed, 309 in Embase.com, 183 in Clarivate Analytics/Web of Science Core Collection, and 3 in Wiley/Cochrane Library. After removal of duplicates, 247 remained (represented in figure 1b). We identified 15 publications that analysed metabolomic(78-87) and proteomic profiles (88-92) in IPAH and PAH patients in plasma(78-83, 85, 86, 88, 90, 92, 93) and serum (84, 87, 91, 92, 94). 14 studies compared signatures to asymptomatic controls, while two studies used common disease controls(79, 81). Liquid and gas chromatography coupled with mass spectrometry (LC-MS) or multiplex assays were the most frequently used methods to detect altered metabolites, proteins or antigens. Targeting component analysis was performed employing a variety of statistical tests (table S1). Metabolomic studies mainly described glycolytic shift and increased fatty-acid metabolism in patients with PAH, implicating an enhanced glycolytic catabolic state (79-81, 83-86, 95), which Rhodes et al.(79), and He et al.(82) validated in independent cohorts. Proteomic studies describe induced growth factors (89), including erythropoietin(92), hepatic growth factor(89), and inflammatory or immune-response pathways, including complement C4a(88) and several interleukins(92). Outcomes are summarized in table S8.

Discussion

Biomarkers may contribute to early non-invasive detection and monitoring of disease. This is the first systematic review combined with meta-analyses to evaluate the performance of blood markers in patients with group 1 PAH, to our knowledge. We selected RDW, LDL-c, d-dimer, NT-proBNP, IL-6 and UA as biomarkers with highest clinical and analytical validity. Plasma NT-proBNP levels showed the largest difference between PAH and non-PH controls but lacked specificity for PAH. Other markers lacked diagnostic validation.

Our study confirms the value of plasma NT-proBNP as an excellent cardiac marker(96, 97) with 89% sensitive for the detection of PAH from healthy controls(56) in data from independent sources. However, with a specificity of 78%(56), NT-proBNP is not suitable for identifying PAH amongst patients with left heart disease. NT-proBNP correlated with markers of disease severity(57, 66, 71) and predicted survival(65, 66, 71).

The role of inflammation in IPAH and hPAH is established by many studies(64). CRP is an easily accessible inflammatory marker, however meta-analysis indicated a high risk of bias, while diagnostic validity was low (e.g. Wang et al. (56) AUC 0.51, p 0.899, 85% specificity 39%). IL-6 was significantly increased in patients PAH, while correlating to markers of disease severity, although the diagnostic potential remains invalidated. Diagnostic sensitivity and specificity of RDW, UA, LDL-c and d-dimer remains unclear, despite being markers routinely measured in clinical practice. Clinical adoption and implementation of new biomarkers has to satisfy strict performance metrics (98) as a high level of confidence is necessary before clinical implementation. This in turn mandates robust validation studies. The U.S. Food and Drug Administration states clinical validation of the biomarker consists of: 1) an evidence-based relation between a biomarker and disease, 2) statistical quantification of the predictive strength of biomarker level for the presence of disease, employing calculation of clinical sensitivity and specificity or evaluating ROC curves in diagnostic studies, 3) availability of multiple independent data sources with sufficient sample sizes and power, and 4) identification and correction for possible sources of bias.

The largest drawback of most biomarkers included in this review is lack of clinical validation and a low sample size. This calls for a systematic approach to biomarker studies, the importance of collaborative biobanks, concomitant analysis of biomarkers in clinical trials and registries directed to improve translation to a clinical setting. External validation cohorts should include patients suspected of PH, and a thoroughly characterized control cohort that contains clinically similar and common diseases. The phenotype of PAH originates from multiple altered pathobiologic domains. Therefore, the second drawback of most selected biomarkers is a lack of specificity to detect PAH. The current meta-analysis suggest all single biomarkers fail to combine high sensitivity to high specificity. We propose implementing a quantitative risk-assessment using a panel of circulating biomarkers from several domains,

2

weighed by importance to improve biomarker specificity. An example of such an approach is provided by Rhodes et al. (99), in which a set of nine proteins was selected to accurately predict disease outcome in IPAH and hPAH patients. Alternatively, the biomarkers may be combined with the strength of non-invasive radiological or hemodynamic measurements, as has been done in the OPTICS study(100) or DETECT study(101) to exclude IPAH. Based on our meta-analyses, a set of readily available biomarkers may be proposed: a panel including NT-proBNP, IL-6, RDW, UA and LDL-c could potentially be used to score the risk of PAH among clinically similar diseases. Alternatively, proteomics, transcriptomics and metabolomics use an integrated and unbiased approach to measure multiple diagnostic biomarkers representative for multiple disease domains in PAH(102). After identification of a set of powerful and accurate biomarkers in omics, a PAH-like signature can be used to distinguish IPAH from other diseases. However, clinical validation is currently lacking.

Limitations
The meta-analyses were hampered by the limited number of publications addressing IPAH uniquely. Handling IPAH and hPAH patients together as one group, and extracting data of group 1 PAH as second best, meant inclusion of patients with PAH associated with connective tissue disease, congenital heart disease and drug or toxin use, which may have introduced bias. Next, due to the limitation of studies, we chose not to exclude publications based on QUADAS-2 risk of bias scores, which may have led to inclusion of unreliable data and may have attributed to heterogeneity. However, correction of the most evident sources of bias (treatment status, diagnosis) indicated that bias was negligible.

Conclusion
This study summarizes a large number of biomarker studies performed in PAH during the last three decades. Most of the described studies investigated the performance of one single blood biomarker. Based on the performance of these individual biomarkers, we conclude that none of these biomarkers are accurate enough to predict the presence of PAH and replace invasive diagnostics. All single biomarkers lacked specificity. Using a combination of multiple strong biomarkers may improve specificity, and this can be achieved by either combining a number of routinely available blood tests as well as via an unbiased omics approach.

References

1. Galie N, Humbert M, Vachiery JL, Gibbs S, Lang I, Torbicki A, et al. 2015 ESC/ERS Guidelines for the diagnosis and treatment of pulmonary hypertension: The Joint Task Force for the Diagnosis and Treatment of Pulmonary Hypertension of the European Society of Cardiology (ESC) and the European Respiratory Society (ERS)Endorsed by: Association for European Paediatric and Congenital Cardiology (AEPC), International Society for Heart and Lung Transplantation (ISHLT). Eur Heart J. 2015.

2. Swinnen K, Quarck R, Godinas L, Belge C, Delcroix M. Learning from registries in pulmonary arterial hypertension: pitfalls and recommendations. Eur Respir Rev. 2019;28(154).

3. Veerdonk vd, Kind T, Marcus JT, Mauritz GJ, Heymans MW, Bogaard HJ, et al. Progressive right ventricular dysfunction in patients with pulmonary arterial hypertension responding to therapy. J Am Coll Cardiol. 2011;58(24):2511-9.

4. Moher D, Liberati A, Tetzlaff J, Altman DG, Group P. Preferred reporting items for systematic reviews and meta-analyses: the PRISMA statement. BMJ. 2009;339:b2535.

5. Bramer WM, Giustini D, de Jonge GB, Holland L, Bekhuis T. De-duplication of database search results for systematic reviews in EndNote. J Med Libr Assoc. 2016;104(3):240-3.

6. Whiting PF, Rutjes AW, Westwood ME, Mallett S, Deeks JJ, Reitsma JB, et al. QUADAS-2: a revised tool for the quality assessment of diagnostic accuracy studies. Ann Intern Med. 2011;155(8):529-36.

7. Kereveur A, Callebert J, Humbert M, Herve P, Simonneau G, Launay JM, et al. High plasma serotonin levels in primary pulmonary hypertension. Effect of long-term epoprostenol (prostacyclin) therapy. Arterioscler Thromb Vasc Biol. 2000;20(10):2233-9.

8. Yaoita N, Shirakawa R, Fukumoto Y, Sugimura K, Miyata S, Miura Y, et al. Platelets are highly activated in patients of chronic thromboembolic pulmonary hypertension. Arterioscler Thromb Vasc Biol. 2014;34(11):2486-94.

9. Edwards AL, Gunningham SP, Clare GC, Hayman MW, Smith M, Frampton CMA, et al. Professional killer cell deficiencies and decreased survival in pulmonary arterial hypertension. Respirology. 2013;18(8):1271-7.

10. Sada Y, Dohi Y, Uga S, Higashi A, Kinoshita H, Kihara Y. Non-suppressive regulatory T cell subset expansion in pulmonary arterial hypertension. Heart Vessels. 2016;31(8):1319-26.

11. Yildiz A, Kaya H, Ertas F, Oylumlu M, Bilik MZ, Yuksel M, et al. Association between neutrophil to lymphocyte ratio and pulmonary arterial hypertension. Turk Kardiyoloji Dernegi arsivi : Turk Kardiyoloji Derneginin yayin organidir. 2013;41(7):604-9.

12. Hautefort A, Girerd B, Montani D, Cohen-Kaminsky S, Price L, Lambrecht BN, et al. T-helper 17 cell polarization in pulmonary arterial hypertension. Chest. 2015;147(6):1610-20.

13. Toshner M, Voswinckel R, Southwood M, Al-Lamki R, Howard LS, Marchesan D, et al. Evidence of dysfunction of endothelial progenitors in pulmonary arterial hypertension. Am J Respir Crit Care Med. 2009;180(8):780-7.

14. Smadja DM, Mauge L, Sanchez O, Silvestre JS, Guerin C, Godier A, et al. Distinct patterns of circulating endothelial cells in pulmonary hypertension. European Respiratory Journal. 2010;36(6):1284-93.

15. Farha S, Asosingh K, Xu W, Sharp J, George D, Comhair S, et al. Hypoxia-inducible factors in human pulmonary arterial hypertension: a link to the intrinsic myeloid abnormalities. Blood. 2011.

16. Foris V, Kovacs G, Marsh LM, Balint Z, Totsch M, Avian A, et al. CD133+ cells in pulmonary arterial hypertension. The European respiratory journal. 2016;48(2):459-69.

17. Visovatti SH, Hyman MC, Bouis D, Neubig R, McLaughlin VV, Pinsky DJ. Increased CD39 nucleotidase activity on microparticles from patients with idiopathic pulmonary arterial hypertension. PLoS One. 2012;7(7):e40829.

18. Khandagale A, Aberg M, Wikstrom G, Bergstrom Lind S, Shevchenko G, Bjorklund E,

et al. Role of Extracellular Vesicles in Pulmonary Arterial Hypertension: Modulation of Pulmonary Endothelial Function and Angiogenesis. Arterioscler Thromb Vasc Biol. 2020;40(9):2293-309.

19. Estephan LE, Genuardi MV, Kosanovich CM, Risbano MG, Zhang Y, Petro N, et al. Distinct plasma gradients of microRNA-204 in the pulmonary circulation of patients suffering from WHO Groups I and II pulmonary hypertension. Pulm Circ. 2019;9(2):2045894019840646.

20. Baptista R, Marques C, Catarino S, Enguita FJ, Costa MC, Matafome P, et al. MicroRNA-424(322) as a new marker of disease progression in pulmonary arterial hypertension and its role in right ventricular hypertrophy by targeting SMURF1. Cardiovasc Res. 2018;114(1):53-64.

21. Qian Z, Li Y, Chen J, Li X, Gou D. miR-4632 mediates PDGF-BB-induced proliferation and antiapoptosis of human pulmonary artery smooth muscle cells via targeting cJUN. American Journal of Physiology - Cell Physiology. 2017;313(4):C380-C91.

22. Han Y, Liu Y, Yang C, Gao C, Guo X, Cheng J. LncRNA CASC2 inhibits hypoxia-induced pulmonary artery smooth muscle cell proliferation and migration by regulating the miR-222/ING5 axis. Cell Mol Biol Lett. 2020;25:21.

23. Bogdan M, Humbert M, Francoual J, Claise C, Duroux P, Simonneau G, et al. Urinary cGMP concentrations in severe primary pulmonary hypertension. Thorax. 1998;53(12):1059-62.

24. Decker I, Ghosh S, Comhair SA, Farha S, Tang WH, Park M, et al. High levels of zinc-protoporphyrin identify iron metabolic abnormalities in pulmonary arterial hypertension. Clin Transl Sci. 2011;4(4):253-8.

25. Yaylali YT, Kilic-Toprak E, Ozdemir Y, Senol H, Bor-Kucukatay M. Impaired Blood Rheology in Pulmonary Arterial Hypertension. Heart, lung & circulation. 2019;28(7):1067-73.

26. Petrauskas LA, Saketkoo LA, Kazecki T, Saito S, Jaligam V, deBoisblanc BP, et al. Use of red cell distribution width in a population at high risk for pulmonary hypertension. Respiratory Medicine. 2019;150:131-5.

27. Forhecz Z, Gombos T, Borgulya G, Pozsonyi Z, Prohaszka Z, Janoskuti L. Red cell distribution width in heart failure: prediction of clinical events and relationship with markers of ineffective erythropoiesis, inflammation, renal function, and nutritional state. Am Heart J. 2009;158(4):659-66.

28. Smith TG, Talbot NP, Privat C, Rivera-Ch M, Nickol AH, Ratcliffe PJ, et al. Effects of iron supplementation and depletion on hypoxic pulmonary hypertension: two randomized controlled trials. JAMA. 2009;302(13):1444-50.

29. Rhodes CJ, Wharton J, Howard L, Gibbs JS, Vonk-Noordegraaf A, Wilkins MR. Iron deficiency in pulmonary arterial hypertension: a potential therapeutic target. Eur Respir J. 2011;38(6):1453-60.

30. Lippi G, Targher G, Montagnana M, Salvagno GL, Zoppini G, Guidi GC. Relation between red blood cell distribution width and inflammatory biomarkers in a large cohort of unselected outpatients. Arch Pathol Lab Med. 2009;133(4):628-32.

31. Rhodes CJ, Howard LS, Busbridge M, Ashby D, Kondili E, Gibbs JS, et al. Iron deficiency and raised hepcidin in idiopathic pulmonary arterial hypertension: clinical prevalence, outcomes, and mechanistic insights. J Am Coll Cardiol. 2011;58(3):300-9.

32. Rhodes CJ, Wharton J, Howard LS, Gibbs JS, Wilkins MR. Red cell distribution width outperforms other potential circulating biomarkers in predicting survival in idiopathic pulmonary arterial hypertension. Heart. 2011;97(13):1054-60.

33. Zhao J, Mo H, Guo X, Wang Q, Xu D, Hou Y, et al. Red blood cell distribution width as a related factor of pulmonary arterial hypertension in patients with systemic sclerosis. Clin Rheumatol. 2018;37(4):979-85.

34. Liu J, Yang J, Xu S, Zhu Y, Xu S, Wei L, et al. Prognostic impact of red blood cell distribution width in pulmonary hypertension patients: A systematic review and meta-analysis. Medicine (Baltimore). 2020;99(16):e19089.

35. Kopeć G, Waligóra M, Tyrka A, Jonas K, Pencina MJ, Zdrojewski T, et al. Low-density lipoprotein cholesterol and survival in pulmonary arterial hypertension. Scientific reports. 2017;7:41650.

36. Varol E, Uysal BA, Ozaydin M. Platelet indices in patients with pulmonary arterial

hypertension. Clin Appl Thromb Hemost. 2011;17(6):E171-4.

37. Wang GF, Guan LH, Zhou DX, Chen DD, Zhang XC, Ge JB. Serum High-Density Lipoprotein Cholesterol is Significantly Associated with the Presence and Severity of Pulmonary Arterial Hypertension: A Retrospective Cross-Sectional Study. Adv Ther. 2020;37(5):2199-209.

38. Zamanian RT, Hansmann G, Snook S, Lilienfeld D, Rappaport KM, Reaven GM, et al. Insulin resistance in pulmonary arterial hypertension. The European respiratory journal. 2009;33(2):318-24.

39. Brunner NW, Skhiri M, Fortenko O, Hsi A, Haddad F, Khazeni N, et al. Impact of insulin resistance on ventricular function in pulmonary arterial hypertension. The Journal of heart and lung transplantation : the official publication of the International Society for Heart Transplantation. 2014;33(7):721-6.

40. Charach G, George J, Roth A, Rogowski O, Wexler D, Sheps D, et al. Baseline low-density lipoprotein cholesterol levels and outcome in patients with heart failure. The American journal of cardiology. 2010;105(1):100-4.

41. Gombos T, Forhecz Z, Pozsonyi Z, Janoskuti L, Prohaszka Z, Karadi I. Long-Term Survival and Apolipoprotein A1 Level in Chronic Heart Failure: Interaction With Tumor Necrosis Factor alpha -308 G/A Polymorphism. J Card Fail. 2017;23(2):113-20.

42. Adam SS, Key NS, Greenberg CS. D-dimer antigen: current concepts and future prospects. Blood. 2009;113(13):2878-87.

43. Vrigkou E, Tsangaris I, Bonovas S, Kopterides P, Kyriakou E, Konstantonis D, et al. Platelet and coagulation disorders in newly diagnosed patients with pulmonary arterial hypertension. Platelets. 2019;30(5):646-51.

44. Can MM, Tanboga IH, Demircan HC, Ozkan A, Koca F, Keles N, et al. Enhanced hemostatic indices in patients with pulmonary arterial hypertension: an observational study. Thromb Res. 2010;126(4):280-2.

45. Herve P, Humbert M, Sitbon O, Parent F, Nunes H, Legal C, et al. Pathobiology of pulmonary hypertension. The role of platelets and thrombosis. Clin Chest Med. 2001;22(3):451-8.

46. Kylhammar D, Hesselstrand R, Nielsen S, Scheele C, Rådegran G. Angiogenic and inflammatory biomarkers for screening and follow-up in patients with pulmonary arterial hypertension. Scandinavian Journal of Rheumatology. 2018;47(4):319-24.

47. Diller GP, van Eijl S, Okonko DO, Howard LS, Ali O, Thum T, et al. Circulating endothelial progenitor cells in patients with Eisenmenger syndrome and idiopathic pulmonary arterial hypertension. Circulation. 2008;117(23):3020-30.

48. Heresi GA, Malin SK, Barnes JW, Tian L, Kirwan JP, Dweik RA. Abnormal glucose metabolism and high-energy expenditure in idiopathic pulmonary arterial hypertension. Annals of the American Thoracic Society. 2017;14(2):190-9.

49. Itoh T, Nagaya N, Ishibashi-Ueda H, Kyotani S, Oya H, Sakamaki F, et al. Increased plasma monocyte chemoattractant protein-1 level in idiopathic pulmonary arterial hypertension. Respirology. 2006;11(2):158-63.

50. Soon E, Holmes AM, Treacy CM, Doughty NJ, Southgate L, Machado RD, et al. Elevated levels of inflammatory cytokines predict survival in idiopathic and familial pulmonary arterial hypertension. Circulation. 2010;122(9):920-7.

51. Kopec G, Moertl D, Steiner S, Stepien E, Mikolajczyk T, Podolec J, et al. Markers of thrombogenesis and fibrinolysis and their relation to inflammation and endothelial activation in patients with idiopathic pulmonary arterial hypertension. PLoS One. 2013;8(12):e82628.

52. Säleby J, Bouzina H, Lundgren J, Rådegran G. Angiogenic and inflammatory biomarkers in the differentiation of pulmonary hypertension. Scandinavian Cardiovascular Journal. 2017;51(5):261-70.

53. Prins KW, Archer SL, Pritzker M, Rose L, Weir EK, Sharma A, et al. Interleukin-6 is independently associated with right ventricular function in pulmonary arterial hypertension. Journal of Heart and Lung Transplantation. 2018;37(3):376-84.

54. Schlosser K, Taha M, Deng Y, Jiang B, McIntyre LA, Mei SH, et al. Lack of elevation in plasma levels of pro-inflammatory cytokines in common rodent models of pulmonary arterial hypertension: questions of construct validity

for human patients. Pulm Circ. 2017;7(2):476-85.

55. Gabrielli LA, Castro PF, Godoy I, Mellado R, Bourge RC, Alcaino H, et al. Systemic oxidative stress and endothelial dysfunction is associated with an attenuated acute vascular response to inhaled prostanoid in pulmonary artery hypertension patients. J Card Fail. 2011;17(12):1012-7.

56. Wang KY, Lee MF, Ho HC, Liang KW, Liu CC, Tsai WJ, et al. Serum Caveolin-1 as a Novel Biomarker in Idiopathic Pulmonary Artery Hypertension. Biomed Res Int. 2015;2015:173970.

57. Calvier L, Legchenko E, Grimm L, Sallmon H, Hatch A, Plouffe BD, et al. Galectin-3 and aldosterone as potential tandem biomarkers in pulmonary arterial hypertension. Heart. 2016;102(5):390-6.

58. Malhotra R, Paskin-Flerlage S, Zamanian RT, Zimmerman P, Schmidt JW, Deng DY, et al. Circulating angiogenic modulatory factors predict survival and functional class in pulmonary arterial hypertension. Pulm Circ. 2013;3(2):369-80.

59. Santos M, Reis A, Goncalves F, Ferreira-Pinto MJ, Cabral S, Torres S, et al. Adiponectin levels are elevated in patients with pulmonary arterial hypertension. Clinical cardiology. 2014;37(1):21-5.

60. Suzuki S, Nakazato K, Sugimoto K, Yoshihisa A, Yamaki T, Kunii H, et al. Plasma Levels of Receptor for Advanced Glycation End-Products and High-Mobility Group Box 1 in Patients With Pulmonary Hypertension. International heart journal. 2016;57(2):234-40.

61. Fares WH, Ford HJ, Ghio AJ, Aris RM. Safety and feasibility of obtaining wedged pulmonary artery samples and differential distribution of biomarkers in pulmonary hypertension. Pulm Circ. 2012;2(4):477-82.

62. Hennigs JK, Baumann HJ, Lüneburg N, Quast G, Harbaum L, Heyckendorf J, et al. Fibrinogen plasma concentration is an independent marker of haemodynamic impairment in chronic thromboembolic pulmonary hypertension. Scientific reports. 2014;4:4808.

63. Quarck R, Nawrot T, Meyns B, Delcroix M. C-reactive protein: a new predictor of adverse outcome in pulmonary arterial hypertension. J Am Coll Cardiol. 2009;53(14):1211-8.

64. Smith CL. C-reactive protein and asymmetric dimethylarginine: markers or mediators in cardiovascular disorders? Curr Pharm Des. 2007;13(16):1619-29.

65. Fijalkowska A, Kurzyna M, Torbicki A, Szewczyk G, Florczyk M, Pruszczyk P, et al. Serum N-terminal brain natriuretic peptide as a prognostic parameter in patients with pulmonary hypertension. Chest. 2006;129(5):1313-21.

66. Andreassen AK, Wergeland R, Simonsen S, Geiran O, Guevara C, Ueland T. N-terminal pro-B-type natriuretic peptide as an indicator of disease severity in a heterogeneous group of patients with chronic precapillary pulmonary hypertension. The American journal of cardiology. 2006;98(4):525-9.

67. Yang D, Liu Z, Yang Z. Ghrelin and its relation with N-terminal brain natriuretic peptide, Endothelin-1 and nitric oxide in patients with idiopathic pulmonary hypertension. Cardiology (Switzerland). 2013;124(4):241-5.

68. Zhu T, Luo J, Wang Y, Xiong X, Sheng B, Yang X, et al. Elevated plasma Pim-1 and its clinical significance in patients with pulmonary arterial hypertension. Clinical and experimental pharmacology & physiology. 2019;46(8):752-60.

69. Lu GH, Gong SG, Li C, Zhao QH, Jiang R, Luo CJ, et al. Prognostic Value of Gamma-Glutamyltransferase in Male Patients With Idiopathic Pulmonary Arterial Hypertension. Frontiers in cardiovascular medicine. 2020;7:580908.

70. Renard S, Paulin R, Breuils-Bonnet S, Simard S, Pibarot P, Bonnet S, et al. Pim-1: A new biomarker in pulmonary arterial hypertension. Pulm Circ. 2013;3(1):74-81.

71. Nickel NP, Lichtinghagen R, Golpon H, Olsson KM, Brand K, Welte T, et al. Circulating levels of copeptin predict outcome in patients with pulmonary arterial hypertension. Respir Res. 2013;14:130.

72. Fenster BE, Lasalvia L, Schroeder JD, Smyser J, Silveira LJ, Buckner JK, et al. Cystatin C: A potential biomarker for pulmonary arterial hypertension. Respirology. 2014;19(4):583-9.

73.   Nagaya N, Uematsu M, Satoh T, Kyotani S, Sakamaki F, Nakanishi N, et al. Serum uric acid levels correlate with the severity and the mortality of primary pulmonary hypertension. Am J Respir Crit Care Med. 1999;160(2):487-92.

74.   Jiang X, Han ZY, Wang Y, Xu XQ, Ma CR, Wu Y, et al. Hemodynamic variables and clinical features correlated with serum uric acid in patients with pulmonary arterial hypertension. Chinese medical journal. 2008;121(24):2497-503.

75.   Jasiewicz M, Kowal K, Kowal-Bielecka O, Knapp M, Skiepko R, Bodzenta-Lukaszyk A, et al. Serum levels of CD163 and TWEAK in patients with pulmonary arterial hypertension. Cytokine. 2014;66(1):40-5.

76.   Maiuolo J, Oppedisano F, Gratteri S, Muscoli C, Mollace V. Regulation of uric acid metabolism and excretion. Int J Cardiol. 2016;213:8-14.

77.   Huang H, Huang B, Li Y, Huang Y, Li J, Yao H, et al. Uric acid and risk of heart failure: a systematic review and meta-analysis. Eur J Heart Fail. 2014;16(1):15-24.

78.   Bujak R, Mateo J, Blanco I, Izquierdo-Garcia JL, Dudzik D, Markuszewski MJ, et al. New Biochemical Insights into the Mechanisms of Pulmonary Arterial Hypertension in Humans. PLoS One. 2016;11(8):e0160505.

79.   Rhodes CJ, Ghataorhe P, Wharton J, Rue-Albrecht KC, Hadinnapola C, Watson G, et al. Plasma Metabolomics Implicates Modified Transfer RNAs and Altered Bioenergetics in the Outcomes of Pulmonary Arterial Hypertension. Circulation. 2017;135(5):460-75.

80.   Sanders JL, Han Y, Urbina MF, Systrom DM, Waxman AB. Metabolomics of exercise pulmonary hypertension are intermediate between controls and patients with pulmonary arterial hypertension. Pulm Circ. 2019;9(4):2045894019882623.

81.   Rafikov R, Coletta DK, Mandarino LJ, Rafikova O. Pulmonary Arterial Hypertension Induces a Distinct Signature of Circulating Metabolites. J Clin Med. 2020;9(1).

82.   He YY, Yan Y, Jiang X, Zhao JH, Wang Z, Wu T, et al. Spermine promotes pulmonary vascular remodelling and its synthase is a therapeutic target for pulmonary arterial hypertension. The European respiratory journal. 2020;56(5).

83.   Hemnes AR, Luther JM, Rhodes CJ, Burgess JP, Carlson J, Fan R, et al. Human PAH is characterized by a pattern of lipid-related insulin resistance. JCI Insight. 2019;4(1).

84.   Chen C, Luo F, Wu P, Huang Y, Das A, Chen S, et al. Metabolomics reveals metabolite changes of patients with pulmonary arterial hypertension in China. J Cell Mol Med. 2020;24(4):2484-96.

85.   Heresi GA, Mey JT, Bartholomew JR, Haddadin IS, Tonelli AR, Dweik RA, et al. Plasma metabolomic profile in chronic thromboembolic pulmonary hypertension. Pulm Circ. 2020;10(1):2045894019890553.

86.   Mey JT, Hari A, Axelrod CL, Fealy CE, Erickson ML, Kirwan JP, et al. Lipids and ketones dominate metabolism at the expense of glucose control in pulmonary arterial hypertension: a hyperglycaemic clamp and metabolomics study. The European respiratory journal. 2020;55(4).

87.   Yu M, Wang XX, Zhang FR, Shang YP, Du YX, Chen HJ, et al. Proteomic analysis of the serum in patients with idiopathic pulmonary arterial hypertension. Journal of Zhejiang University Science B. 2007;8(4):221-7.

88.   Abdul-Salam VB, Paul GA, Ali JO, Gibbs SR, Rahman D, Taylor GW, et al. Identification of plasma protein biomarkers associated with idiopathic pulmonary arterial hypertension. Proteomics. 2006;6(7):2286-94.

89.   Amsallem M, Sweatt AJ, Arthur Ataam J, Guihaire J, Lecerf F, Lambert M, et al. Targeted proteomics of right heart adaptation to pulmonary arterial hypertension. The European respiratory journal. 2021;57(4).

90.   Al-Naamani N, Sagliani KD, Dolnikowski GG, Warburton RR, Toksoz D, Kayyali U, et al. Plasma 12- and 15-hydroxyeicosanoids are predictors of survival in pulmonary arterial hypertension. Pulm Circ. 2016;6(2):224-33.

91.   Zhang J, Zhang Y, Li N, Liu Z, Xiong C, Ni X, et al. Potential diagnostic biomarkers in serum of idiopathic pulmonary arterial hypertension. Respiratory Medicine. 2009;103(12):1801-6.

92.   Karamanian VA, Harhay M, Grant GR, Palevsky HI, Grizzle WE, Zamanian RT, et al.

2

Erythropoietin upregulation in pulmonary arterial hypertension. Pulm Circ. 2014;4(2):269-79.

93.   Bouzina H, Hesselstrand R, Radegran G. Higher plasma fibroblast growth factor 23 levels are associated with a higher risk profile in pulmonary arterial hypertension. Pulm Circ. 2019;9(4):2045894019895446.

94.   Terrier B, Tamby MC, Camoin L, Guilpain P, Broussard C, Bussone G, et al. Identification of target antigens of antifibroblast antibodies in pulmonary arterial hypertension. Am J Respir Crit Care Med. 2008;177(10):1128-34.

95.   Bujak R, Mateo J, Blanco I, Izquierdo-García JL, Dudzik D, Markuszewski MJ, et al. New biochemical insights into the mechanisms of pulmonary arterial hypertension in humans. PLoS ONE. 2016;11(8).

96.   Januzzi JL, Jr., Rehman SU, Mohammed AA, Bhardwaj A, Barajas L, Barajas J, et al. Use of amino-terminal pro-B-type natriuretic peptide to guide outpatient therapy of patients with chronic left ventricular systolic dysfunction. J Am Coll Cardiol. 2011;58(18):1881-9.

97.   Nagaya N, Nishikimi T, Okano Y, Uematsu M, Satoh T, Kyotani S, et al. Plasma brain natriuretic peptide levels increase in proportion to the extent of right ventricular dysfunction in pulmonary hypertension. J Am Coll Cardiol. 1998;31(1):202-8.

98.   Ahmad T, Fiuzat M, Pencina MJ, Geller NL, Zannad F, Cleland JG, et al. Charting a roadmap for heart failure biomarker studies. JACC Heart Fail. 2014;2(5):477-88.

99.   Rhodes CJ, Wharton J, Ghataorhe P, Watson G, Girerd B, Howard LS, et al. Plasma proteome analysis in patients with pulmonary arterial hypertension: an observational cohort study. Lancet Respir Med. 2017;5(9):717-26.

100.   Jansen SMA, Huis In 't Veld AE, Jacobs W, Grotjohan HP, Waskowsky M, van der Maten J, et al. Noninvasive Prediction of Elevated Wedge Pressure in Pulmonary Hypertension Patients Without Clear Signs of Left-Sided Heart Disease: External Validation of the OPTICS Risk Score. J Am Heart Assoc. 2020;9(15):e015992.

101.   Coghlan JG, Denton CP, Grunig E, Bonderman D, Distler O, Khanna D, et al. Evidence-based detection of pulmonary arterial hypertension in systemic sclerosis: the DETECT study. Ann Rheum Dis. 2014;73(7):1340-9.

102.   Oldham WM, Hemnes AR, Aldred MA, Barnard J, Brittain EL, Chan SY, et al. NHLBI-CMREF Workshop Report on Pulmonary Vascular Disease Classification: JACC State-of-the-Art Review. J Am Coll Cardiol. 2021;77(16):2040-52.
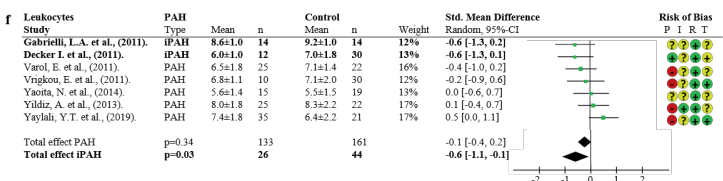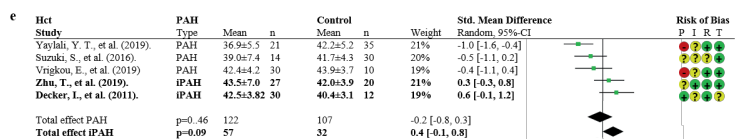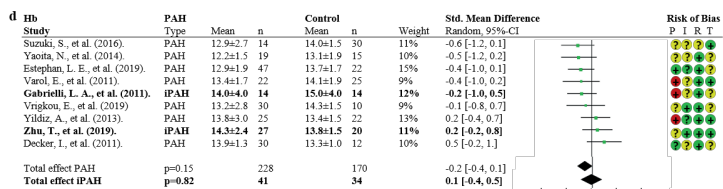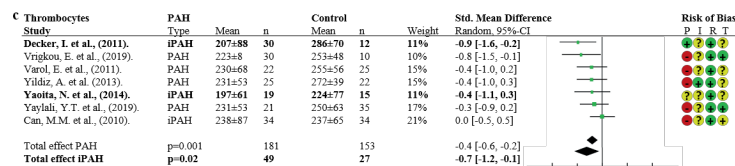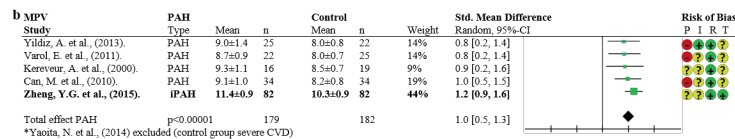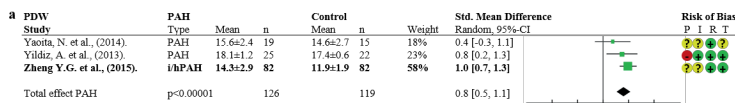
SUPPLEMENTAL INFORMATION

Supplemental figure 1
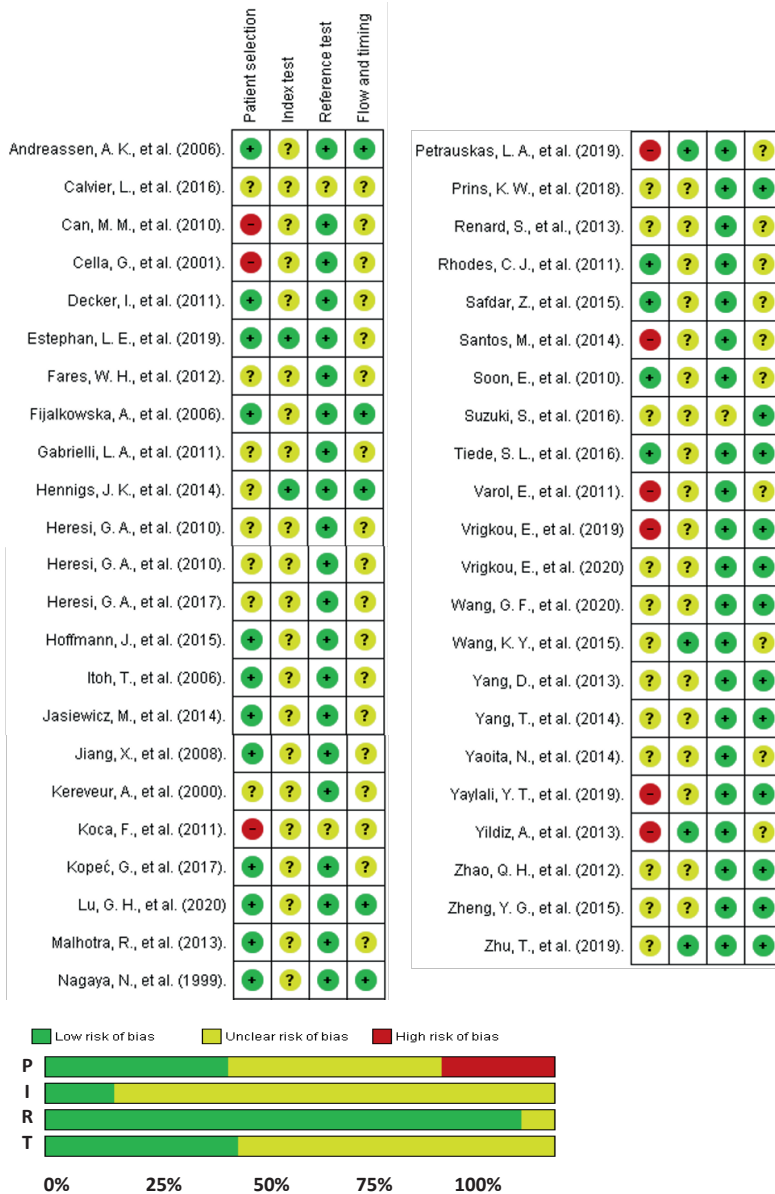
Supplemental figure 1: Risk of bias (QUADAS-2), P: patient inclusion, I; index-test (biomarker), R; reference standard (diagnosis), T; flow and timing. Publications pressed in bold measured biomarker levels in IPAH and/or hPAH uniquely. Green; low risk of bias, orange; unclear risk of bias, red; high risk of bias.

Supplemental figure 2

Supplemental figure 2: Forest plots of non-selected hematologic biomarkers, including; PDW; platelet distribution width, MPV; mean platelet volume, thrombocytes, Hb; hemoglobin, Hct; hematocrit, leukocytes. Risk of bias (QUADAS-2), P: patient inclusion, I; index-test (biomarker), R; refence standard (diagnosis), T; flow and timing. Publications pressed in bold measured biomarker levels in IPAH and/or hPAH uniquely.

Supplemental figure 3
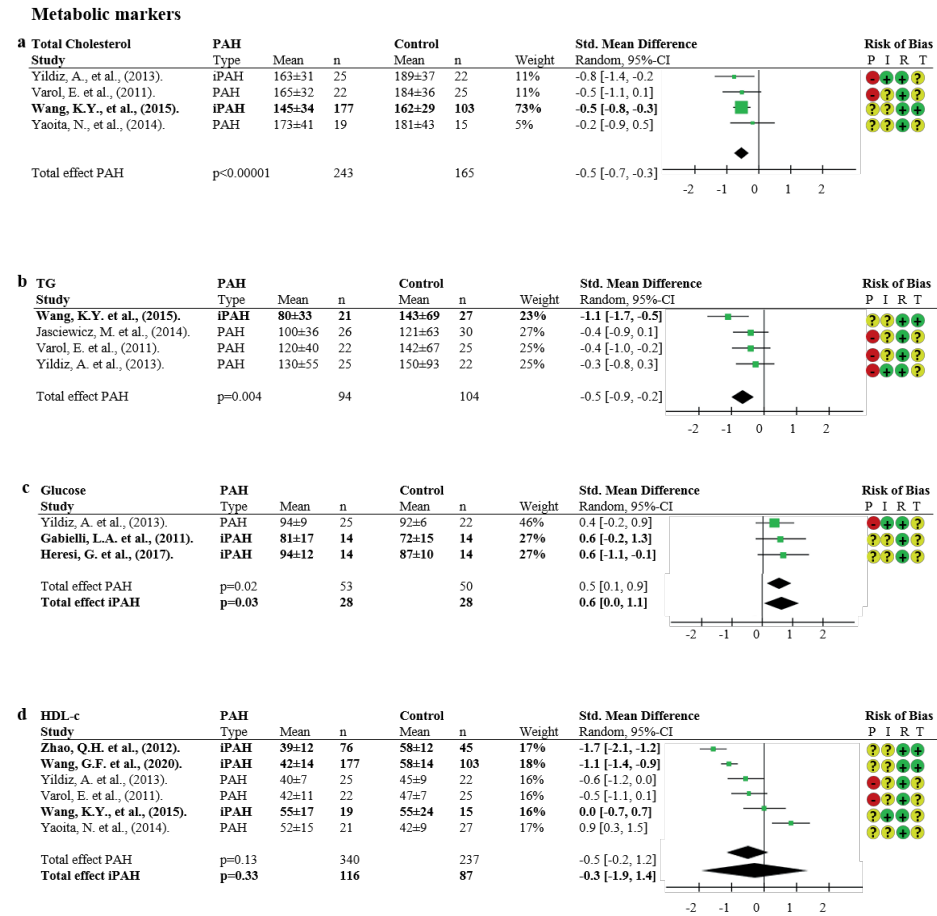
Supplemental figure 3: Forest plots of non-selected metabolic biomarkers, including total cholesterol, TG; triglycerides, glucose, HDL-c; high density lipid-cholesterol. risk of bias (QUADAS-2), P: patient inclusion, I; index-test (biomarker), R; reference standard (diagnosis), T; flow and timing. Publications pressed in bold measured biomarker levels in IPAH and/or hPAH uniquely.

Supplemental figure 4

Coagulation markers

Fibrinogen Study	PAH Type	Mean	n	Control Mean	n	Weight	Std. Mean Difference Random, 95%-CI	Risk of Bias P I R T
Vrigkou, E., et al. (2019)	PAH	306±97	30	290±95	10	24%	0.2 [-0.6, 0.9]	
Yaylali, Y. T., et al. (2019).	PAH	341±85	21	311±88	35	25%	0.4 [-0.2, 0.9]	
Hennigs, J. K., et al. (2014).	PAH	410±140	52	340±50	11	25%	0.5 [-0.1, 1.2]	
Can, M. M., et al. (2010).	PAH	357±98	34	188±31	34	25%	2.3 [1.7, 2.9]	
Total effect PAH	p=0.09		137		90		0.8 [-0.1, 1.8]	

Supplemental figure 4: Forest plots of non-selected coagulation biomarkers, including fibrinogen. Risk of bias (QUADAS-2), P: patient inclusion, I; index-test (biomarker), R; refenrece standard (diagnosis), T; flow and timing. Publications pressed in bold measured biomarker levels in IPAH and/or hPAH uniquely.
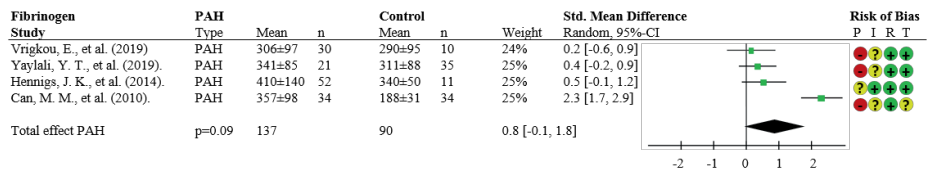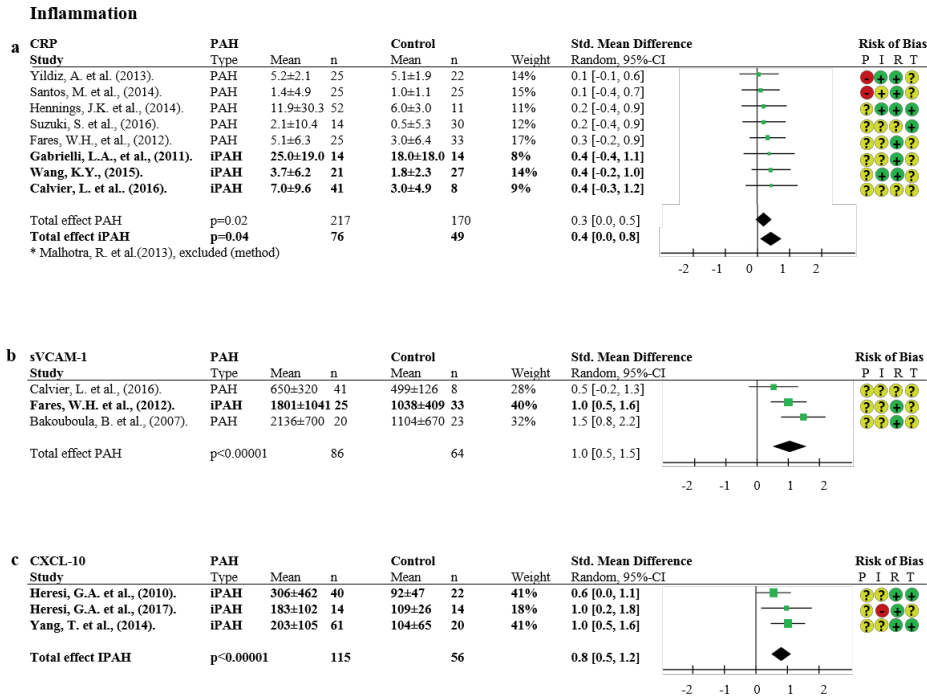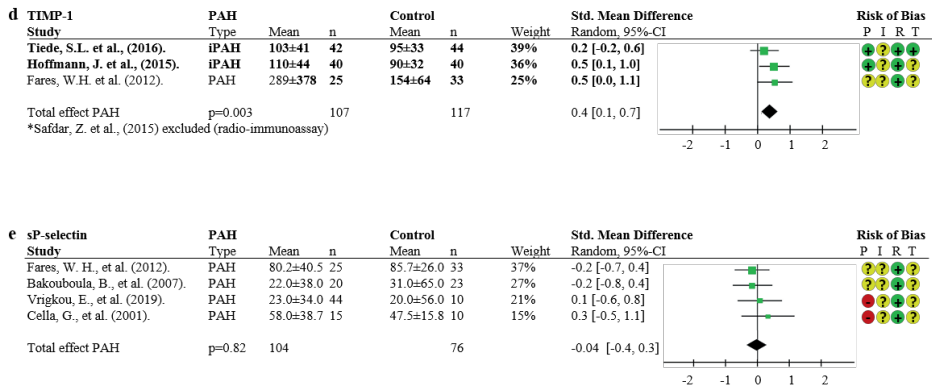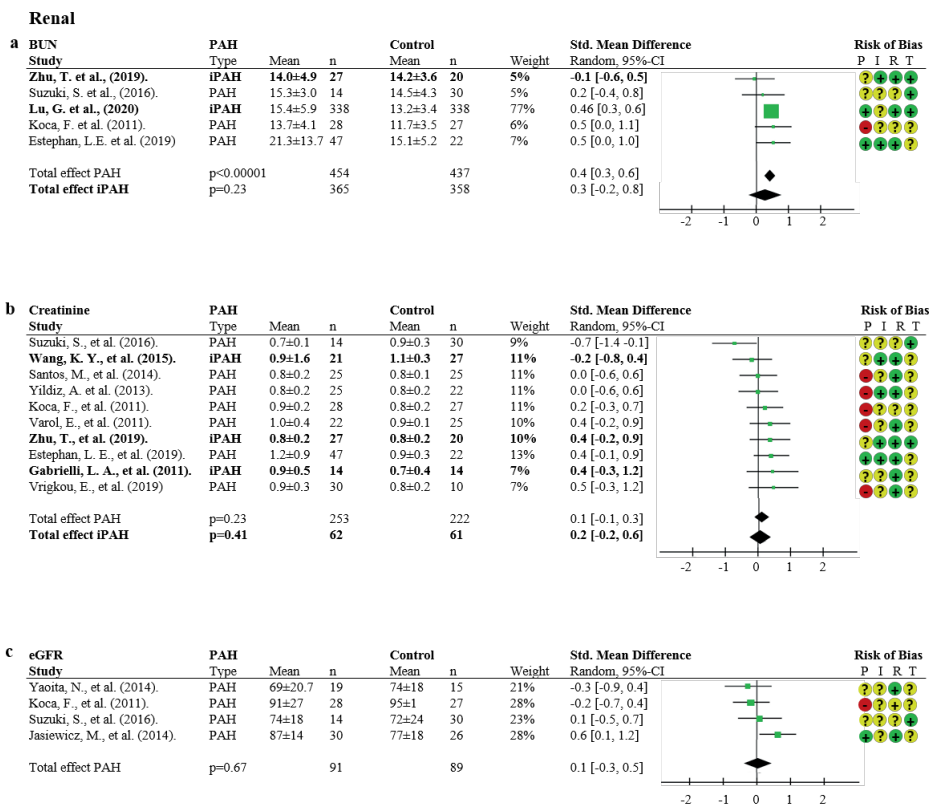
Supplemental figure 5

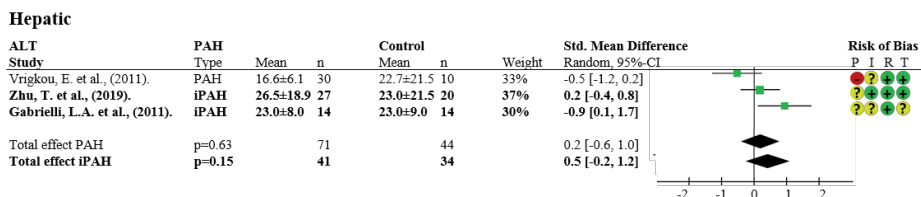**Inflammation**

a **CRP**

Study	PAH Type	Mean	n	Control Mean	n	Weight	Std. Mean Difference Random, 95%-CI	Risk of Bias P I R T
Yildiz, A. et al. (2013).	PAH	5.2±2.1	25	5.1±1.9	22	14%	0.1 [-0.1, 0.6]	
Santos, M. et al., (2014).	PAH	1.4±4.9	25	1.0±1.1	25	15%	0.1 [-0.4, 0.7]	
Hennings, J.K. et al., (2014).	PAH	11.9±30.3	52	6.0±3.0	11	11%	0.2 [-0.4, 0.9]	
Suzuki, S. et al., (2016).	PAH	2.1±10.4	14	0.5±5.3	30	12%	0.2 [-0.4, 0.9]	
Fares, W.H., et al., (2012).	PAH	5.1±6.3	25	3.0±6.4	33	17%	0.3 [-0.2, 0.9]	
Gabrielli, L.A., et al., (2011).	**iPAH**	**25.0±19.0**	**14**	**18.0±18.0**	**14**	**8%**	**0.4 [-0.4, 1.1]**	
Wang, K.Y., (2015).	**iPAH**	**3.7±6.2**	**21**	**1.8±2.3**	**27**	**14%**	**0.4 [-0.2, 1.0]**	
Calvier, L. et al.. (2016).	**iPAH**	**7.0±9.6**	**41**	**3.0±4.9**	**8**	**9%**	**0.4 [-0.3, 1.2]**	
Total effect PAH	p=0.02		217		170		0.3 [0.0, 0.5]	
Total effect iPAH	**p=0.04**		**76**		**49**		**0.4 [0.0, 0.8]**	

* Malhotra, R. et al.(2013), excluded (method)

b **sVCAM-1**

Study	PAH Type	Mean	n	Control Mean	n	Weight	Std. Mean Difference Random, 95%-CI	Risk of Bias P I R T
Calvier, L. et al., (2016).	PAH	650±320	41	499±126	8	28%	0.5 [-0.2, 1.3]	
Fares, W.H. et al., (2012).	**iPAH**	**1801±1041**	**25**	**1038±409**	**33**	**40%**	**1.0 [0.5, 1.6]**	
Bakouboula, B. et al., (2007).	PAH	2136±700	20	1104±670	23	32%	1.5 [0.8, 2.2]	
Total effect PAH	p<0.00001		86		64		1.0 [0.5, 1.5]	

c **CXCL-10**

Study	PAH Type	Mean	n	Control Mean	n	Weight	Std. Mean Difference Random, 95%-CI	Risk of Bias P I R T
Heresi, G.A. et al., (2010).	**iPAH**	**306±462**	**40**	**92±47**	**22**	**41%**	**0.6 [0.0, 1.1]**	
Heresi, G.A. et al., (2017).	**iPAH**	**183±102**	**14**	**109±26**	**14**	**18%**	**1.0 [0.2, 1.8]**	
Yang, T. et al., (2014).	**iPAH**	**203±105**	**61**	**104±65**	**20**	**41%**	**1.0 [0.5, 1.6]**	
Total effect IPAH	**p<0.00001**		**115**		**56**		**0.8 [0.5, 1.2]**	

d TIMP-1

Study	Type	Mean	n	Mean	n	Weight	Std. Mean Difference Random, 95%-CI	P I R T
	PAH			Control				Risk of Bias
Tiede, S.L. et al., (2016).	iPAH	103±41	42	95±33	44	39%	0.2 [-0.2, 0.6]	
Hoffmann, J. et al., (2015).	iPAH	110±44	40	90±32	40	36%	0.5 [0.1, 1.0]	
Fares, W.H. et al. (2012).	PAH	289±378	25	154±64	33	25%	0.5 [0.0, 1.1]	
Total effect PAH	p=0.003		107		117		0.4 [0.1, 0.7]	

*Safdar, Z. et al., (2015) excluded (radio-immunoassay)

e sP-selectin

Study	Type	Mean	n	Mean	n	Weight	Std. Mean Difference Random, 95%-CI	P I R T
	PAH			Control				Risk of Bias
Fares, W. H., et al. (2012).	PAH	80.2±40.5	25	85.7±26.0	33	37%	-0.2 [-0.7, 0.4]	
Bakouboula, B., et al. (2007).	PAH	22.0±38.0	20	31.0±65.0	23	27%	-0.2 [-0.8, 0.4]	
Vrigkou, E., et al. (2019).	PAH	23.0±34.0	44	20.0±56.0	10	21%	0.1 [-0.6, 0.8]	
Cella, G., et al. (2001).	PAH	58.0±38.7	15	47.5±15.8	10	15%	0.3 [-0.5, 1.1]	
Total effect PAH	p=0.82		104		76		-0.04 [-0.4, 0.3]	

Supplemental figure 5: Forest plots of non-selected inflammatory biomarkers, including; sVCAM-1; circulating vascular cell adhesion molecule-1, CXCL-10; C-X-C motif chemokine ligand-10, CRP; C-reactive protein, TIMP-1; tissue inhibitors of metalloproteinases-1, sP-selectin; soluble P-selectin. Risk of bias (QUADAS-2), P: patient inclusion, I; index-test (biomarker), R; reference standard (diagnosis), T; flow and timing. Publications pressed in bold measured biomarker levels in IPAH and/or hPAH uniquely.

Supplemental figure 6

Renal

a

BUN Study	PAH Type	Mean	n	Control Mean	n	Weight	Std. Mean Difference Random, 95%-CI	Risk of Bias P I R T
Zhu, T. et al., (2019).	iPAH	14.0±4.9	27	14.2±3.6	20	5%	-0.1 [-0.6, 0.5]	
Suzuki, S. et al., (2016).	PAH	15.3±3.0	14	14.5±4.3	30	5%	0.2 [-0.4, 0.8]	
Lu, G. et al., (2020)	iPAH	15.4±5.9	338	13.2±3.4	338	77%	0.46 [0.3, 0.6]	
Koca, F. et al. (2011).	PAH	13.7±4.1	28	11.7±3.5	27	6%	0.5 [0.0, 1.1]	
Estephan, L.E. et al. (2019)	PAH	21.3±13.7	47	15.1±5.2	22	7%	0.5 [0.0, 1.0]	
Total effect PAH	p<0.00001		454		437		0.4 [0.3, 0.6]	
Total effect iPAH	p=0.23		365		358		0.3 [-0.2, 0.8]	

b

Creatinine Study	PAH Type	Mean	n	Control Mean	n	Weight	Std. Mean Difference Random, 95%-CI	Risk of Bias P I R T
Suzuki, S., et al. (2016).	PAH	0.7±0.1	14	0.9±0.3	30	9%	-0.7 [-1.4 -0.1]	
Wang, K. Y., et al. (2015).	iPAH	0.9±1.6	21	1.1±0.3	27	11%	-0.2 [-0.8, 0.4]	
Santos, M., et al. (2014).	PAH	0.8±0.2	25	0.8±0.1	25	11%	0.0 [-0.6, 0.6]	
Yildiz, A. et al. (2013).	PAH	0.8±0.2	25	0.8±0.2	22	11%	0.0 [-0.6, 0.6]	
Koca, F., et al. (2011).	PAH	0.9±0.2	28	0.8±0.2	27	11%	0.2 [-0.3, 0.7]	
Varol, E., et al. (2011).	PAH	1.0±0.4	22	0.9±0.1	25	10%	0.4 [-0.2, 0.9]	
Zhu, T., et al. (2019).	iPAH	0.8±0.2	27	0.8±0.2	20	10%	0.4 [-0.2, 0.9]	
Estephan, L. E., et al. (2019).	PAH	1.2±0.9	47	0.9±0.3	22	13%	0.4 [-0.1, 0.9]	
Gabrielli, L. A., et al. (2011).	iPAH	0.9±0.5	14	0.7±0.4	14	7%	0.4 [-0.3, 1.2]	
Vrigkou, E., et al. (2019)	PAH	0.9±0.3	30	0.8±0.2	10	7%	0.5 [-0.3, 1.2]	
Total effect PAH	p=0.23		253		222		0.1 [-0.1, 0.3]	
Total effect iPAH	p=0.41		62		61		0.2 [-0.2, 0.6]	

c

eGFR Study	PAH Type	Mean	n	Control Mean	n	Weight	Std. Mean Difference Random, 95%-CI	Risk of Bias P I R T
Yaoita, N., et al. (2014).	PAH	69±20.7	19	74±18	15	21%	-0.3 [-0.9, 0.4]	
Koca, F., et al. (2011).	PAH	91±27	28	95±1	27	28%	-0.2 [-0.7, 0.4]	
Suzuki, S., et al. (2016).	PAH	74±18	14	72±24	30	23%	0.1 [-0.5, 0.7]	
Jasiewicz, M., et al. (2014).	PAH	87±14	30	77±18	26	28%	0.6 [0.1, 1.2]	
Total effect PAH	p=0.67		91		89		0.1 [-0.3, 0.5]	

Supplemental figure 6: Forest plots of non-selected renal biomarkers, including; BUN; brain urea nitrogen, creatinine, eGFR; estimated glomerular filtration rate. Risk of bias (QUADAS-2), P: patient inclusion, I; index-test (biomarker), R; reference standard (diagnosis), T; flow and timing. Publications pressed in bold measured biomarker levels in IPAH and/or hPAH uniquely.

Supplemental figure 7

Hepatic

ALT Study	PAH Type	Mean	n	Control Mean	n	Weight	Std. Mean Difference Random, 95%-CI	Risk of Bias P I R T
Vrigkou, E. et al., (2011).	PAH	16.6±6.1	30	22.7±21.5	10	33%	-0.5 [-1.2, 0.2]	
Zhu, T. et al., (2019).	iPAH	26.5±18.9	27	23.0±21.5	20	37%	0.2 [-0.4, 0.8]	
Gabrielli, L.A. et al., (2011).	iPAH	23.0±8.0	14	23.0±9.0	14	30%	-0.9 [0.1, 1.7]	
Total effect PAH	p=0.63		71		44		0.2 [-0.6, 1.0]	
Total effect iPAH	p=0.15		41		34		0.5 [-0.2, 1.2]	

Supplemental figure 7: Forest plots of non-selected hepatic biomarkers, including; ALT; alanine transaminase. Risk of bias (QUADAS-2), P: patient inclusion, I; index-test (biomarker), R; reference standard (diagnosis), T; flow and timing. Publications pressed in bold measured biomarker levels in IPAH and/or hPAH uniquely.

Supplemental figure 8
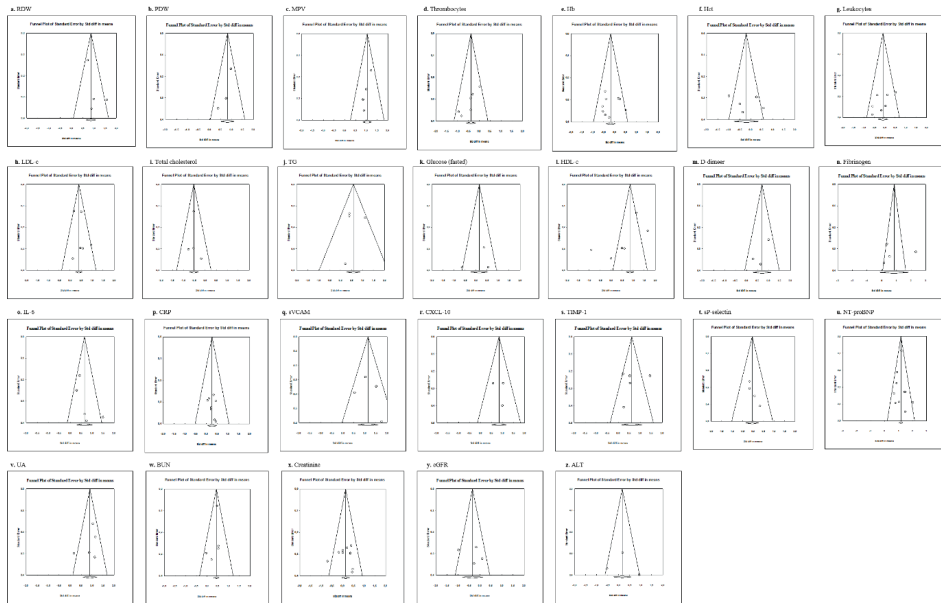
Supplemental figure 8: Funel plots of all meta-analysis indicating publication bias. X-axis; standardized difference in means, y-axis; standard error. Each dot represents one publication.
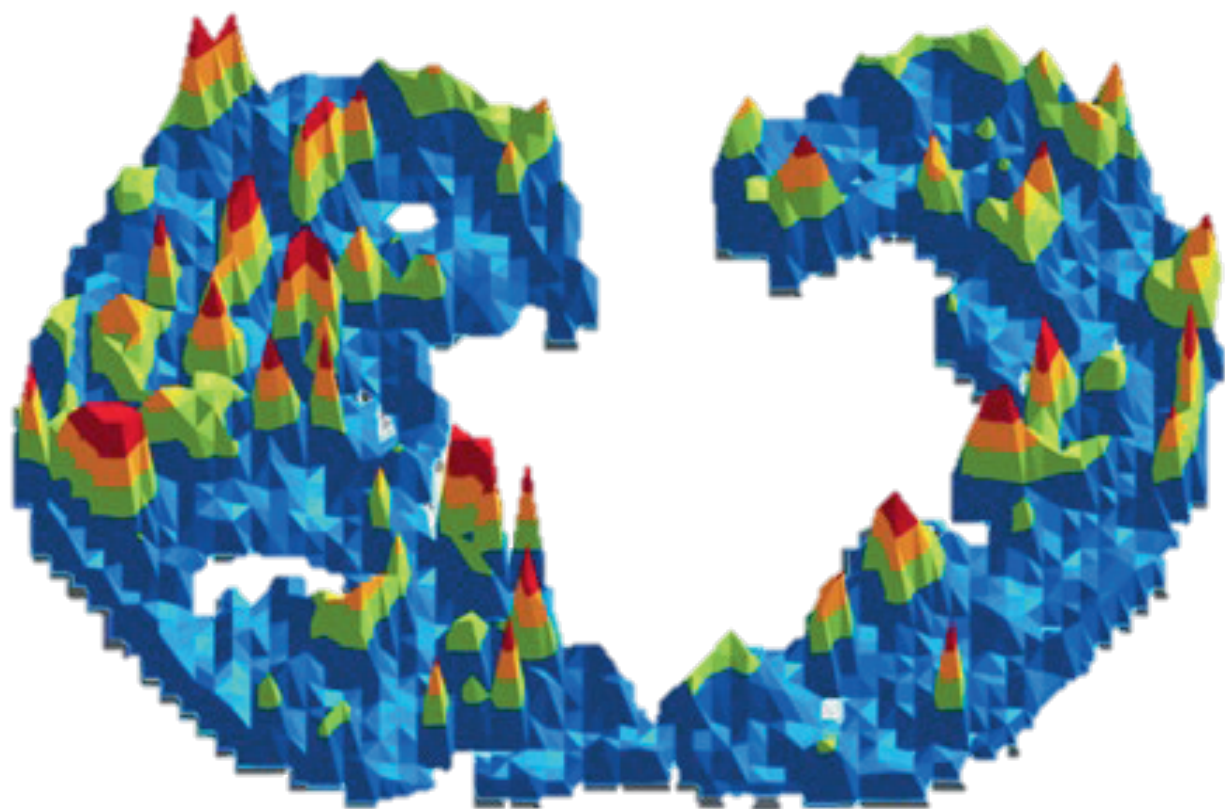
3

Application of [18F]FLT-PET in Pulmonary Arterial Hypertension (PAH): A clinical study in PAH patients and unaffected BMPR2 mutation carriers

Liza Botros*, Samara M.A. Jansen*, Ali Ashek, Jelco Tramper, Onno A. Spruijt, Anton Vonk Noordegraaf, Jurjan Aman, Hans Harms, Frances S. de Man, Marc C. Huisman, Lan Zhao & Harm Jan Bogaard

*Equal contribution

Abstract

Background: Pulmonary arterial hypertension (PAH) is a heterogeneous, incurable group of diseases characterized by exuberant vascular cell proliferation leading to pulmonary vascular remodelling and ultimately right heart failure. Previous data indicated that 3'-deoxy-3'-[18F]-fluorothymidine ([18]FLT) positron emission tomography (PET) scanning was increased in PAH patients, hence providing a possible biomarker for PAH as it reflects vascular cell hyperproliferation in the lung. This study validates [18]FLT-PET in an expanded cohort of PAH patients in comparison to matched healthy controls and bone morphogenetic protein receptor type 2 (BMPR2) mutation carriers who are unaffected by PAH. We aimed to establish [18]FLT-PET as biomarker for PAH severity and assessed the subclinical pulmonary vascular remodeling.

Methods and Results: Dynamic [18]FLT-PET scanning was performed in 21 PAH patients (15 hereditary PAH and 6 idiopathic PAH), 11 unaffected mutation carriers and 9 matched healthy control subjects. In-depth kinetic analysis with a reversible 2-compartment 4k model indicated that there were no differences in lung [18]FLT k3 phosphorylation among PAH patients, unaffected BMPR2 mutation carriers and matched healthy controls. Lung [18]FLT uptake did not correlate with hemodynamic or clinical parameters in PAH patients. Sequential [18]FLT-PET scanning in three patients demonstrated uneven regional distribution and heterogeneity in [18]FLT uptake by 3D parametric mapping of the lung, although this did not follow the clinical course of the patient.

Conclusion: We did not detect significantly increased lung [18]FLT uptake in PAH patients, nor in the unaffected BMPR2 mutation carriers, as compared to healthy subjects. The conflicting results with our preliminary human [18]FLT report may be explained by a small sample size previously and we observed large variation of lung [18]FLT signals between patients, challenging the application of [18]FLT-PET as a biomarker in the PAH clinic.

Introduction

Pulmonary arterial hypertension (PAH) is a heterogeneous group of diseases that is characterized by obliteration and narrowing of the vascular lumen, leading to increased pulmonary vascular resistance and ultimately right heart failure (1-3). Featuring in the pathobiology of PAH are phenomena also encountered in cancer, such as enhanced proliferation, apoptosis-resistance (4-6), altered mitochondrial metabolism (7) and chronic inflammation (8), although it is still unclear whether this is true in all PAH patients and at all stages of the disease. One of the most important risk factors for the development of PAH is a mutation in the gene coding for the bone morphogenetic protein receptor type 2 (BMPR2) (9). Subjects carrying this pathogenic variant have an increased risk to develop PAH, but currently there are no methods to predict which unaffected mutation carriers will develop PAH. To date, screening and monitoring of disease progression rely on indicators of right ventricular dysfunction (10) and no biomarkers of pulmonary vascular remodeling in PAH are available. Thus, there is an urgent need for non-invasive quantification of vascular remodeling in patients with PAH or in subjects at risk (11).

Recently, several studies used positron emission tomography (PET) to provide anatomical and metabolic information in the PAH lung (7, 12-15). In animal models of PAH, uptake of fluorine-18-labelled 2-fluoro-2-deoxyglucose FDG ([18]FDG), a marker of glucose metabolism, correlated with disease severity (13). Increased mean lung parenchymal uptake was also observed in a cohort of 20 patients with PAH (18 with idiopathic PAH (IPAH)) (13). In another recent study, cardiac and lung standardized uptake value (SUV) of [18]FDG was found higher in 30 PH patients (9 IPAH, the rest of various PH groups) compared to healthy controls (16). As [18]FDG measures glucose metabolism, it represents proliferative vascular cells as well as inflammatory cell accumulation, limiting its potential in measuring vascular remodelling in humans directly (13, 17). It is recognised that [18]FDG PET lacks specificity as a clinical tool for the diagnosis of PAH, furthermore, lung [18]FDG uptake did not correlate with any clinical marker in PH patients (13, 16). 3'-deoxy-3'-[18F]-fluorothymidine ([18]FLT), a thymidine analogue, has recently emerged as a more sensible tracer for imaging lung vascular proliferation in PAH (12). [18]FLT is routinely used in clinical oncology (18) as it depicts tumour growth in a variety of malignancies (19), and correlates with histological proliferation markers such as Ki-67 and proliferating cell nuclear antigen (20, 21). [18]FLT phosphorylation by thymidine kinase 1 leads to [18]FLT retention within the cell, thereby providing a quantitative measurement of proliferating tissue (20).

We previously showed increased [18]FLT uptake in pre-clinical models of PAH and in preliminary clinical data with a small group (n=8) of IPAH patients (12). We compared [18]FLT uptake from the contralateral lung of patients with one-sided pulmonary malignancies as control subjects. Herein, we conducted an expanded clinical [18]FLT-PET study a) to include a larger group of PAH patients and an appropriate control group of healthy subjects, aiming to validate the clinical application of [18]FLT-PET as a biomarker for PAH severity; b) to include a

group of unaffected BMPR2 mutation carriers, aiming to assess if [18]FLT-PET can discriminate carriers that may be at risk of developing the subclinical pulmonary vascular remodeling.

Methods

Patient population

This study was conducted in accordance with the principles of the Declaration of Helsinki. Approval was obtained from the Medical Ethical Review Committee of the VU University Medical Centre (2017.334) and informed consent was obtained from all subjects. All subjects were recruited between 2015 and 2019 and all PAH patients were diagnosed according to current guidelines (3). Our expanded cohort consisted of eight PAH patients (five heritable PAH (HPAH) and three IPAH) from previous published study (12) with 13 newly scanned PAH patients (10 HPAH and three IPAH). We also studied 11 unaffected BMPR2 mutation carriers and nine matched healthy controls (siblings without a BMPR2 pathogenic variant). Three PAH patients were scanned twice during their clinical course. The most recent [18]FLT-PET scan was used in the expanded cohort.

Right Heart Catheterizations and Cardiac Magnetic Resonance Imaging

All patients underwent right heart catheterization (RHC) and cardiac magnetic resonance (CMR) imaging within 6 weeks of the [18]FLT-PET scan as previously described (22). In short, a 7F balloon-tipped flow-directed triple-lumen Swan-Ganz catheter (Edwards Lifesciences LLC, Irvine, CA) was inserted in the pulmonary artery via the jugular vein under local anaesthesia and constant electrocardiography (ECG) monitoring, and measurements were performed according to the guidelines (3). With RHC mean pulmonary artery pressure (mPAP), pulmonary vascular resistance (PVR), mean right atrial pressure (mRAP), pulmonary arterial wedge pressure (PAWP) and cardiac output (CO) were measured. CO was measured using the thermodilution method. PVR was calculated as 80x(mPAP-PAWP)/CO. CO was indexed to body surface area (BSA) and shown as cardiac index (CI). CMR imaging scans were performed on a Siemens 1.5T Sonato or Avanto scanner (Siemens Medical Solutions, Erlangen, Germany). Right ventricular end-diastolic volume index (RVEDVI), right ventricular end-systolic volume index (RVESVI) and right ventricular ejection fraction (RVEF) from CMR imaging were collected. The load on the right ventricle was calculated, i.e. arterial elastance (Ea) = mPAP / stroke volume. Stroke volume was measured by CMR. Acquisition and post processing was performed following our standard protocol as described previously (22).

FLT-PET scanning

Dynamic 60-minutes [18]FLT-PET scanning was performed after a fasting period of 6 hours following the scanning protocol that was previously described (12). All participants were positioned supine with lungs and the aortic branch in the field of view of the Philips Ingenuity TF PET/CT (Philips healthcare, Best, Netherlands). A cannula was placed in the arm vein for injection of radioisotope. First, a low-dose computed tomography (CT) scan was performed in all subjects to correct for photon attenuation, scatter and lung densities. [18]FLT

was synthesized as described previously (23). After a bolus injection of 370MBq of [18]FLT in 5 ml saline at 0.8ml/s, blood samples were drawn at 5, 10, 20, 30, 40 and 60 minutes to correct the image derived plasma input function for radiolabelled metabolites (^{18}F-glucuronide) (12). Dynamic PET imaging was started at the time of [18]FLT intravenous injection for 1 hour and emission data was reconstructed into a 36-frame format (1x10, 8x5, 4x10, 3x20, 5x30, 5x60, 4x150, 4x300 and 2x600s) using the 3-Dimensional Row-Action Maximum Likelihood Algorithm (3D-RAMBLA), applying all appropriate corrections for dead time, decay, scatter, attenuation and normalization.

Kinetic Modelling and Data Analysis

Plasma kinetic modelling was performed using Inveon Research Workplace software (Siemens Healthcare Molecular Imaging) which was fitted with a Matlab-based in-house kinetic analysis software package (CLICKFIT). Since the Philips Ingenuity TF PET/CT scanner and software was updated during the conduction of patient recruitment of our expanded cohort, the plasma kinetic model calculated via MATLAB 5.3 software, which was used in the preliminary results, was not compatible anymore and all data from the expanded cohort was reconstructed and analysed using CLICKFIT. Whole-lung tissue time-activity curve (TAC) was calculated from lung PET images co-registered with region of interest (ROI) drawn on lung CT images, covering the lung volume with clearly visible boundaries adjusted by CT density thresholding. The ROI was finalized with 1-cm automated erosion from the edge to prevent partial volume effects. To obtain arterial input function, ROI was drawn on the pulmonary artery (PA) at the level of the pulmonary trunk using early frames. Metabolite corrected PA blood TAC was used as input function and whole lung TAC was used as output function to fit in the software package CLICKFIT. Per voxel, the K3 rate derived from a reversible 2-compartment 4k model was considered as proliferation rate and used as total lung [18]FLT uptake. Typically, we have generated k3 value of 25000 voxels (2mm3 per voxel) from each human lung. Voxels with k3 ≤0 or k3 ≥1 were considered as noise and excluded less than 1% of total voxels). For mid-lung [18]FLT uptake, a 2-cm region at the level of the bifurcation of the PA was used for analysis. For the correction of lung density (air-correction) a CT-generated lung segmentation was generated and used following Patlaks reversible model formula: Air correction = (1-Vb)/(1-Vb-Vair) (24). Further analysis by 3-dimensional (3D) parametric mapping of computed per-voxel [18]FLT uptake, such as Texture Analysis, Heterogeneity Index and Metabolic Tumour Volume measurement were developed to measure the heterogeneity in tracer uptake per voxel level in the lung.

Statistical Analysis

Data were described as either mean (± standard deviation) for continuous variables and as absolute numbers (%) for categorical variables. Between-group differences were compared using one-way ANOVA with Bonferroni post-hoc correction. Differences between control groups were tested using the Student t-tests or chi-square tests, after visually checking for normal distributions. Non-normal distributed variables were LOG-transformed or tested

using Wilcoxon signed rank test. Correlations between [18]FLT uptake (k3) and clinical variables were determined by linear regression analyses. Throughout the analyses a p-value of <0.05 was considered statistically significant. All statistical analyses were performed with R (R Core Team 2019 R version 3.6.1) and Graphpad Prism for Windows version 8 (Graphpad Software, La Jolla, CA).

Results

Characteristics of the subjects

21 PAH patients, 11 unaffected BMPR2 mutation carriers and 9 controls were studied. The baseline characteristics of all subjects are summarized in table 1. The female to male ratio was 2:1. The control group was comparable in age, BMI and gender. As expected, NYHA class, NT-proBNP concentration and right ventricle (RV) volumes differed between the groups (all p-values <0.001). The patients that were scanned in our preliminary report were similar in clinical characteristics (supplementary table 1).

[18]FLT k3 phosphorylation rate

For Kinetic modelling and data analysis, CLICKFIT was used. This method gave similar results in [18]FLT-uptake, expressed as k3 phosphorylation, in the PAH patients from the preliminary results for which MATLAB 5.3 software was used previously (supplemental figure S1). Comparing to lung [18]FLT uptake in control subjects, the mean [18]FLT phosphorylation k3 was not significantly different in PAH patients (fig. 1A), so as in the unaffected BMPR2 mutation carriers. This unsignificant statistics of lung [18]FLT uptake remained among the three groups after correction for lung density measured by CT (k3 score, fig. 1B). We also analysed the [18]FLT phosphorylation k3 in the mid-region of the lungs (12) and no significant differences were observed among the PAH patients, unaffected BMPR2 mutation carriers and controls (fig. 1C). Stratification of the PAH patient groups considering age, subtype of PAH, NYHA class, therapy or co-morbidity did not show correlation to lung [18]FLT phosphorylation k3 measurements.

Table 1: Baseline characteristics and hemodynamics

	Healthy controls n = 9	Unaffected mutation carrier n = 11	PAH n = 21	p-value
Age (yr)	47 ± 17	46 ± 18	45 ± 13	0.953
Male, n(%)	4 (44%)	4 (36%)	7 (33%)	0.846
NYHA functional class, I/II/III/IV (n)	9/0/0/0	11/0/0/0	4/12/5/0	**<0.001**
BMI, kg/m^2	28.1 ± 5.7	24.6 ± 4.1	24.8 ± 3.7	0.134
NT-proBNP, ng/ml	-	21 [13-35]	229 [58-667]	0.001
Hb, mmol	8.9 ± 0.9	9.1 ± 0.8	9.3 ± 1.4	0.725
Medical history				
Malignancy	0 (0%)	0 (0%)	0 (0%)	NA
Hypertension	2 (22%)	0 (0%)	2 (10%)	0.249
Diabetes Mellitus	0 (0%)	0 (0%)	1 (5%)	0.614
VTE/pulmonary embolism	1 (11%)	0 (0%)	1 (5%)	0.517
Treatment				
Treatment Naïve, n(%)	9 (100%)	11 (100%)	1 (5%)*	**<0.001**
Monotherapy (ERA or PDE5I), n(%)	-	-	1 (5%)	-
Dual combination therapy (ERA + PDE5I or PDE5i + prostacyclin* 0), n(%)	-	-	13 (62%)	-
Triple combination therapy (ERA + PDE5I + prostacyclin), n(%)	-	-	6 (29%)	-
Hemodynamic characteristics				
Heart rate, beats/min	74 ± 10	72 ± 11	75 ± 12	0.769
mPAP, mmHg	-	15 [14-17]	50 [42-57]	**<0.001**
PAWP, mmHg	-	9 ± 2	10 ± 3	0.291
mRAP, mmHg	-	5 ± 2	8 ± 3	0.039
PVRI, dyn.s/cm^{-5}/m^2	-	47 [41-66]	362 [281-498]	**<0.001**
Cardiac index, l/min/m^2	-	3.0 ± 0.5	2.7 ± 0.7	0.241
Cardiac magnetic resonance imaging				
RVEDVI, ml/m^2	72 [58-81]	56 [54-69]	92 [75-111]*	**<0.001**
RVESVI, ml/m^2	30 [26-35]	22 [20-26]	48 [41-70]*	**<0.001**
RVEF, %	58 ± 6	61 ± 5	44 ± 12*	**<0.001**
LVEF, %	66 ± 5	66 ± 7	62 ± 13	0.444

Table 1: Data are given as mean(SD), median [IQR] or percentages *significant differences depicted in bold in post-hoc analysis. BMI: body mass index, Hb: haemoglobin, VTE: venous thrombo-embolism, ERA: endothelin receptor antagonist, PDE5I: phosphodiesterase type 5 inhibitor, mRAP: mean right atrial pressure, mPAP: mean pulmonary arterial pressure, PVRI: indexed pulmonary vascular resistance, PAWP: pulmonary arterial wedge pressure, RVEDVI: Indexed right ventricular end-diastolic volume; RVESVI: Indexed right ventricular end-systolic volume; RVEF: right ventricular ejection fraction, LVEF: left ventricular ejection fraction

Figure 1
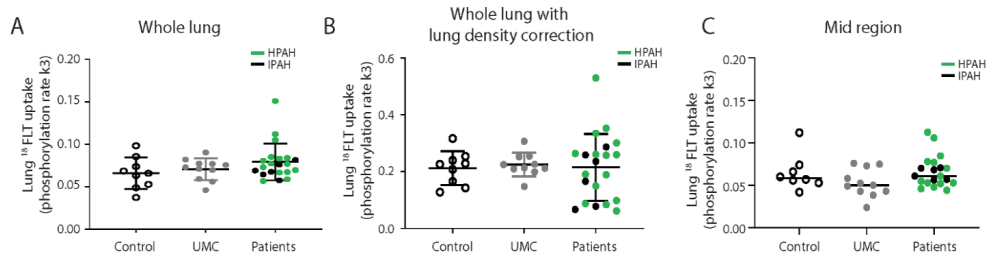
Figure 1: Lung 18FLT uptake was measured (phosphorylation rate k3 of 18FLT). No differences were observed between controls (n=9), unaffected mutation carriers (UMC, n=11) and PAH patients (n=21) in whole lungs (A), whole lungs corrected for lung density measured with CT-scan (B) and in the mid-region of the lungs (C).

Correlation with clinical parameters

We examined the relationship between the lung [18]FLT uptake (k3) and cardiopulmonary hemodynamic parameters in PAH patients and unaffected BMPR2 mutation carriers. No correlation was observed between lung [18]FLT uptake with mPAP and indexed PVR in PAH patients (r^2 =0.05, p=0.317 and r^2 =0.003, p=0.813 respectively) and in unaffected mutation carriers (r^2 =0.15, p=0.265 and r^2 =0.20, p=0.194 respectively). Lung [18]FLT uptake also did not correlate with hemodynamic parameters by CMR, such as RVEDVI, RVESVI, RVEF and the load on the ventricle (arterial elastance; figure 2 C-F).

Figure 2
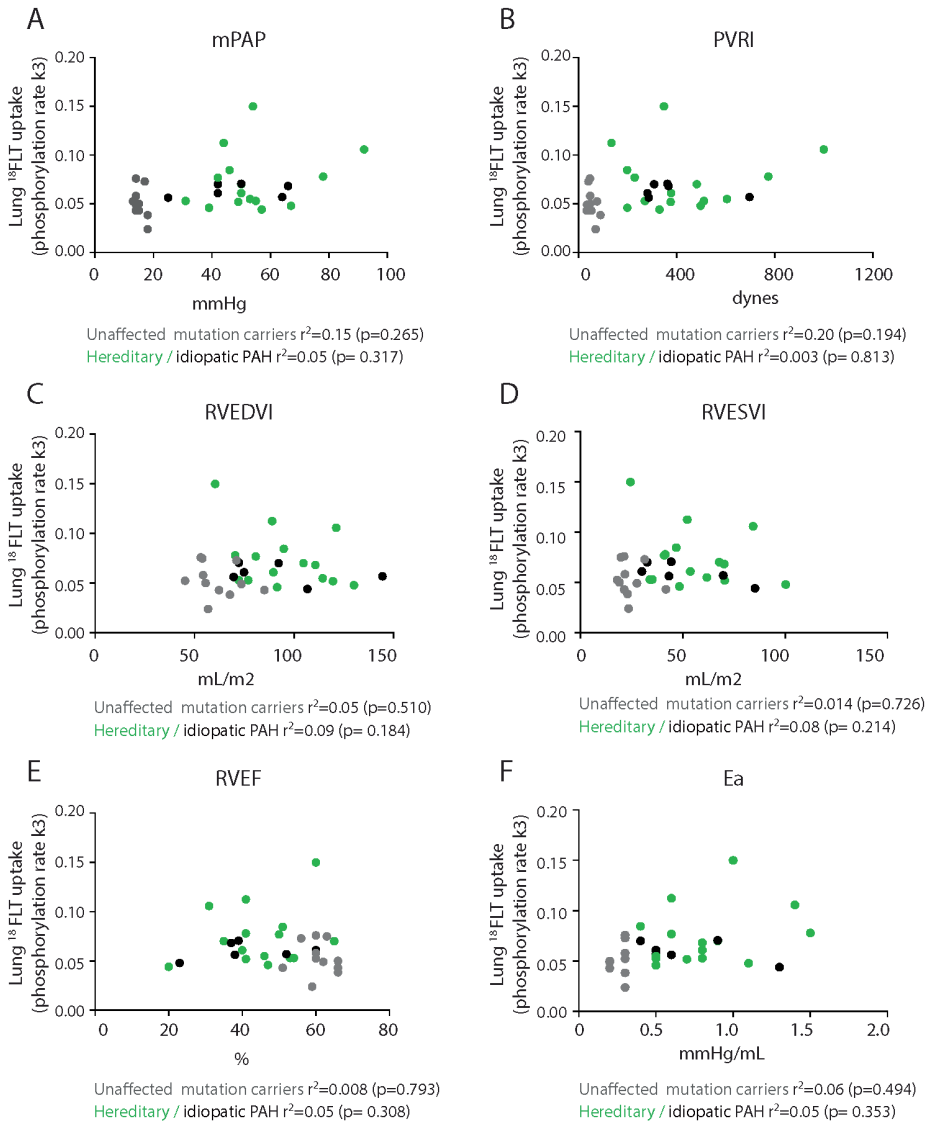
Figure 2. No correlation between [18]FLT uptake (k3) in the mid-region and mean pulmonary artery pressure (mPAP), indexed pulmonary vascular resistance (PVRI), right ventricular dimensions (RVEDVI and RVESVI), right ventricular function (RVEF) and load of the right ventricle (Ea). RVEDVI = Indexed right ventricular end-diastolic volume; RVESVI = Indexed right ventricular end-systolic volume; RVEF = right ventricular ejection fraction; Ea = arterial elastance

Follow up scans

We performed further analysis by 3D parametric mapping in three PAH patients that were scanned sequentially (fig. 3), aiming to define the previous observation of heterogeneous lung [18]FLT uptake within the PAH group (12). Our data demonstrated the uneven regional [18]FLT uptake (patch distribution) in the PAH patient lungs. Further analysis presented the comparative histogram distribution of voxel wise [18]FLT phosphorylation rates of the two sequential [18]FLT PET scans in the three PAH patient (fig. 3). The comparative data indicated no significant differences between the two sequential scans in patients 1 and 2, but a left shift was observed in patient 3, indicating a reduced [18]FLT phosphorylation rate in the second scan. The sequential lung[18]FLT uptake data did not related to the hemodynamic parameters gained from these three PAH patients (fig. 3 and suppl. table 2).
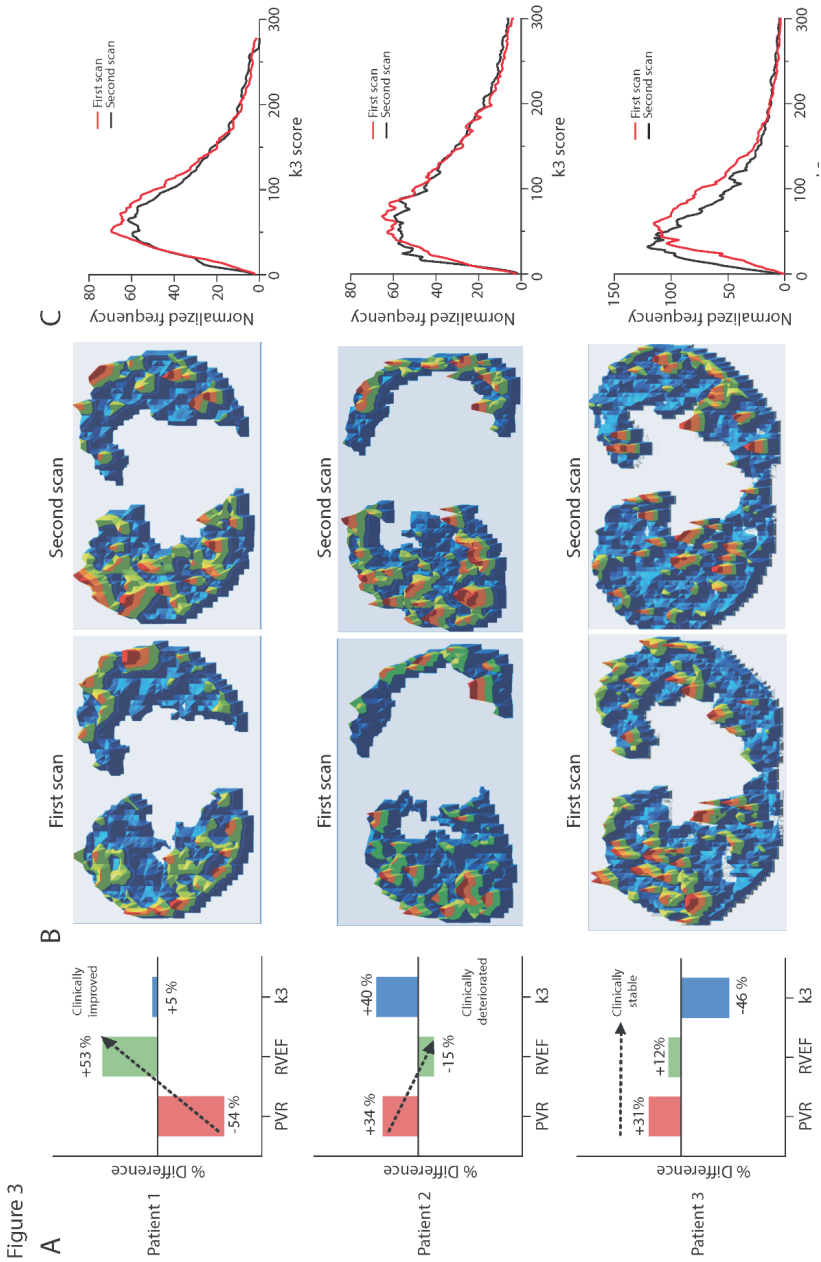
Figure 3: (A) % Difference in pulmonary vascular resistance (PVR), right ventricle ejection fraction (RVEF) and k3 phosphorylaion rate (k3) in follow-up scans from three PAH patients. (B) 3-dimensional parametric map (axial view) generated from computed per-voxel [18F]FLT lung uptake. Uneven regional [18F]FLT uptake was observed in all patients (Blue colour= Base line, Green= low, Yellow=mid and Red= high). (C) Comparative histogram distribution of voxel wise FLT phosphorylation score for first and second scan.

3

Discussion

This study conducted [18]FLT-PET in PAH patients in comparison with a group of healthy control subjects and unaffected BMPR2 mutation carriers. Kinetic modelling of the lung [18]FLT uptake indicated that there were no significant differences of the lung [18]FLT phosphorylation k3 in PAH patients comparing to the healthy control subjects. The lung [18]FLT uptake in PAH patients did not correlate with the clinical and hemodynamical parameters. In depth 3D parametric mapping of the sequential [18]FLT-PET data from three PAH patients during their follow up showed uneven regional lung [18]FLT uptake in these individuals. However, [18]FLT lung uptake did not relate to the hemodynamic clinical parameter changes. We report for the first time that lung [18]FLT uptake in unaffected BMPR2 mutation carriers, who are prone to develop PAH, are similar to the healthy control subjects.

The present study is a carefully designed follow-up study of our previous [18]FLT project, aiming to qualify the clinical application of [18]FLT-PET in the PH clinic. In the previous study, the control [18]FLT lung uptake data was calculated from the contralateral healthy lung lobe of patients with one-sided pulmonary malignancies. Three out of six cancer patients were receiving chemotherapy <1 month before [18]FLT-PET scanning. The current study employed an appropriate group of matched control subjects. These healthy subjects were younger than the previous control projects with cancer (age 47 vs 68 years, p= 0.015). Nevertheless, the present data demonstrated that the [18]FLT lung uptake levels (k3) of these 9 healthy control subjects are comparable to the previous demonstrated control [18]FLT lung uptake levels. The current [8]FLT-PET study has expanded the previous small cohort study to a larger cohort of 21 PAH patients and produced an improved clinical data set. We demonstrated no significant differences in lung [18]FLT uptake between the PAH patients and control healthy subjects, which conflicts with the preliminary human [18]FLT-PET study due to a small sample size previously and large variation of lung [18]FLT signals between patients.

It remains a challenge to develop an appropriate PET tracer that detects, localizes and monitors pulmonary vascular pathology in PAH. [18]FDG-PET and [18]FLT-PET have been used in oncology to stratify patients and assess disease progression and response to treatment and predict clinical outcomes. Increased [18]FDG lung signals with heterogeneous distribution were described in IPAH as well as in PAH patients due to systemic lupus erythematosus (SLE-PAH) (13, 14), consistent with its property in tracking both proliferation and inflammation events. However, there were no significant correlations between lung [18]FDG uptake with hemodynamic and severity parameters in IPAH patients detected (14, 15), whilst data from SLE-PAH patients confirmed that the increased lung [18]FDG uptake reflects an active inflammatory disease status in the lung which impacts remodelling process. In comparison, [18]FLT-PET is a recognised as marker of evaluating whole tumour proliferation heterogeneity. We are challenged by the relatively lower [18]FLT uptake compared to [18]FDG (17) and the large air volume in the lung, although [18]FLT has a low background uptake in the thorax as shown in our previous data that indicated a relatively lower noise threshold than [18]FDG (25). The

present study applied the rate of [18]FLT phosphorylation, k3, calculated from the in-depth kinetic 2T4k modelling of the lung [18]FLT signal for reflecting proliferation events in the lung (12), however, k3 did not discriminate PAH patients from control healthy subjects, contradicting to our original hypothesis. Additionally, the unaffected BMPR2 mutation carriers presented a tighter mean of lung [18]FLT phosphorylation k3 similar to the healthy control subjects.

We found that there is considerable larger variation in the distribution of lung [18]FLT uptake in the PAH patients and there is visually heterogeneity in the lung [18]FLT signal distribution within the lungs of each patient. Further stratification considering PH phenotype, therapy used, age, gender, duration of disease or hemodynamic parameters did not define any significant relevance with lung [18]FLT phosphorylation k3. Comparing k3 phosphorylation of unaffected BMPR2 mutation carriers with healthy controls or PAH patients did not show differences. It remains difficult to state if FLT-PET was unable to detect latent vascular proliferation, or if the lung vasculature of these mutation carriers is indeed unaffected until a second hit occurs. The data from sequential [18]FLT PET scans that follows up three PAH patients under combination treatments (Prostacyclin, ERA, PDE5I) is informative, however, [18]FLT lung uptake did not relate to hemodynamic or clinical parameter changes over time. Patient 3 started with prostacyclin treatment in between the sequential FLT-PET scans, and his k3 value decreased impressively. It may be that a decrease in vessel wall remodelling was due to prostacyclin treatment (26), or that the vascular remodelling simply 'burns out' at a late phase of the disease. We are limited to make a direct correlation between [18]FLT signal with pulmonary pathology in the same human study subjects, the natural history of the pulmonary pathology following clinical presentation is unknown. It may be episodic or particularly active at the start of the disease and reduced in the later phase. Evidence of vascular proliferation that is tracked by FLT imaging might be episodic or more evident in some patients than others irrespective of their clinical impairment at the time of imaging.

In the past decade, several clinical trials have targeted cancer-like features in PAH. Inhibition of endothelial cell-and smooth muscle cell proliferation by for example tacrolimus (27) and mercaptopurine (28) showed some hemodynamic improvement, but in small patient groups and with serious side-effects. As there is still no evidence of structurally abnormal growth factor receptors in the PAH vasculature, clinical trials with growth factor inhibitors such as tyrosine kinase inhibitors have not yet shown an overall clinical benefit (29-31). This indicates that the general consensus of sustained proliferative signalling in PAH might be more nuanced and complex.

In conclusion, the current study with a larger expanded PAH patient cohort established a valuable and critical clinical [18]FLT-PET data set. We could not detect significant differences in lung [18]FLT phosphorylation rate k3 in PAH patients in comparison to the age matched healthy controls, nor in unaffected BMPR2 mutation carriers. Our data informed and challenged the application of [18]FLT-PET as a biomarker in PH clinic. Novel tracers with a

higher sensitivity for tracking PAH disease pathology are needed which may help to improve the detection of PAH and tailoring therapy strategies.

References

1. Tuder RM, Groves B, Badesch DB, Voelkel NF. Exuberant endothelial cell growth and elements of inflammation are present in plexiform lesions of pulmonary hypertension. Am J Pathol. 1994;144(2):275-85.

2. Lee SD, Shroyer KR, Markham NE, Cool CD, Voelkel NF, Tuder RM. Monoclonal endothelial cell proliferation is present in primary but not secondary pulmonary hypertension. J Clin Invest. 1998;101(5):927-34.

3. Galie N, Humbert M, Vachiery JL, Gibbs S, Lang I, Torbicki A, et al. 2015 ESC/ERS Guidelines for the diagnosis and treatment of pulmonary hypertension: The Joint Task Force for the Diagnosis and Treatment of Pulmonary Hypertension of the European Society of Cardiology (ESC) and the European Respiratory Society (ERS): Endorsed by: Association for European Paediatric and Congenital Cardiology (AEPC), International Society for Heart and Lung Transplantation (ISHLT). Eur Heart J. 2016;37(1):67-119.

4. Sakao S, Taraseviciene-Stewart L, Lee JD, Wood K, Cool CD, Voelkel NF. Initial apoptosis is followed by increased proliferation of apoptosis-resistant endothelial cells. FASEB J. 2005;19(9):1178-80.

5. Happe CM, Szulcek R, Voelkel NF, Bogaard HJ. Reconciling paradigms of abnormal pulmonary blood flow and quasi-malignant cellular alterations in pulmonary arterial hypertension. Vascul Pharmacol. 2016;83:17-25.

6. Boucherat O, Vitry G, Trinh I, Paulin R, Provencher S, Bonnet S. The cancer theory of pulmonary arterial hypertension. Pulm Circ. 2017;7(2):285-99.

7. Michelakis ED, Gurtu V, Webster L, Barnes G, Watson G, Howard L, et al. Inhibition of pyruvate dehydrogenase kinase improves pulmonary arterial hypertension in genetically susceptible patients. Sci Transl Med. 2017;9(413).

8. Pullamsetti SS, Savai R, Seeger W, Goncharova EA. Translational Advances in the Field of Pulmonary Hypertension. From Cancer Biology to New Pulmonary Arterial Hypertension Therapeutics. Targeting Cell Growth and Proliferation Signaling Hubs. Am J Respir Crit Care Med. 2017;195(4):425-37.

9. Austin ED, Loyd JE. The genetics of pulmonary arterial hypertension. Circ Res. 2014;115(1):189-202.

10. "2015 ESC/ERS Guidelines for the diagnosis and treatment of pulmonary hypertension. The Joint Task Force for the Diagnosis and Treatment of Pulmonary Hypertension of the European Society of Cardiology (ESC) and the European Respiratory Society (ERS)." Nazzareno Galie, Marc Humbert, Jean-Luc Vachiery, Simon Gibbs, Irene Lang, Adam Torbicki, Gerald Simonneau, Andrew Peacock, Anton Vonk Noordegraaf, Maurice Beghetti, Ardeschir Ghofrani, Miguel Angel Gomez Sanchez, Georg Hansmann, Walter Klepetko, Patrizio Lancellotti, Marco Matucci, Theresa McDonagh, Luc A. Pierard, Pedro T. Trindade, Maurizio Zompatori and Marius Hoeper. Eur Respir J 2015; 46: 903-975. Eur Respir J. 2015;46(6):1855-6.

11. Vonk Noordegraaf A, Haddad F, Bogaard HJ, Hassoun PM. Noninvasive imaging in the assessment of the cardiopulmonary vascular unit. Circulation. 2015;131(10):899-913.

12. Ashek A, Spruijt OA, Harms HJ, Lammertsma AA, Cupitt J, Dubois O, et al. 3'-Deoxy-3'-[18F]Fluorothymidine Positron Emission Tomography Depicts Heterogeneous Proliferation Pathology in Idiopathic Pulmonary Arterial Hypertension Patient Lung. Circ Cardiovasc Imaging. 2018;11(8):e007402.

13. Zhao L, Ashek A, Wang L, Fang W, Dabral S, Dubois O, et al. Heterogeneity in lung (18)FDG uptake in pulmonary arterial hypertension: potential of dynamic (18)FDG positron emission tomography with kinetic analysis as a bridging biomarker for pulmonary vascular remodeling targeted treatments. Circulation. 2013;128(11):1214-24.

14. Wang L, Xiong C, Li M, Zeng X, Wang Q, Fang W, et al. Assessment of lung glucose uptake in patients with systemic lupus erythematosus pulmonary arterial hypertension: a quantitative FDG-PET imaging study. Ann Nucl Med. 2020;34(6):407-14.

15. Ruiter G, Wong YY, Raijmakers P, Huisman MC, Lammertsma AA, Knaapen P, et

al. Pulmonary 2-deoxy-2-[(18F)]-fluoro-d-glucose uptake is low in treated patients with idiopathic pulmonary arterial hypertension. Pulm Circ. 2013;3(3):647-53.

16. Saygin D, Highland KB, Farha S, Park M, Sharp J, Roach EC, et al. Metabolic and Functional Evaluation of the Heart and Lungs in Pulmonary Hypertension by Gated 2-[18F]-Fluoro-2-deoxy-D-glucose Positron Emission Tomography. Pulm Circ. 2017;7(2):428-38.

17. Tehrani OS, Shields AF. PET imaging of proliferation with pyrimidines. J Nucl Med. 2013;54(6):903-12.

18. Shields AF. PET imaging of tumor growth: not as easy as it looks. Clin Cancer Res. 2012;18(5):1189-91.

19. Soloviev D, Lewis D, Honess D, Aboagye E. [(18F)]FLT: an imaging biomarker of tumour proliferation for assessment of tumour response to treatment. Eur J Cancer. 2012;48(4):416-24.

20. Shields AF, Grierson JR, Dohmen BM, Machulla HJ, Stayanoff JC, Lawhorn-Crews JM, et al. Imaging proliferation in vivo with [F-18]FLT and positron emission tomography. Nat Med. 1998;4(11):1334-6.

21. Salskov A, Tammisetti VS, Grierson J, Vesselle H. FLT: measuring tumor cell proliferation in vivo with positron emission tomography and 3'-deoxy-3'-[18F]fluorothymidine. Semin Nucl Med. 2007;37(6):429-39.

22. van de Veerdonk MC, Huis In TVAE, Marcus JT, Westerhof N, Heymans MW, Bogaard HJ, et al. Upfront combination therapy reduces right ventricular volumes in pulmonary arterial hypertension. Eur Respir J. 2017;49(6).

23. Frings V, de Langen AJ, Yaqub M, Schuit RC, van der Veldt AA, Hoekstra OS, et al. Methodological considerations in quantification of 3'-deoxy-3'-[18F]fluorothymidine uptake measured with positron emission tomography in patients with non-small cell lung cancer. Mol Imaging Biol. 2014;16(1):136-45.

24. Lambrou T, Groves AM, Erlandsson K, Screaton N, Endozo R, Win T, et al. The importance of correction for tissue fraction effects in lung PET: preliminary findings. Eur J Nucl Med Mol Imaging. 2011;38(12):2238-46.

25. Thureau S, Chaumet-Riffaud P, Modzelewski R, Fernandez P, Tessonnier L, Vervueren L, et al. Interobserver agreement of qualitative analysis and tumor delineation of 18F-fluoromisonidazole and 3'-deoxy-3'-18F-fluorothymidine PET images in lung cancer. J Nucl Med. 2013;54(9):1543-50.

26. Lambers C, Kornauth C, Oberndorfer F, Boehm PM, Tamm M, Klepetko W, et al. Mechanism of anti-remodelling action of treprostinil in human pulmonary arterial smooth muscle cells. PLoS One. 2018;13(11):e0205195.

27. Spiekerkoetter E, Sung YK, Sudheendra D, Scott V, Del Rosario P, Bill M, et al. Randomised placebo-controlled safety and tolerability trial of FK506 (tacrolimus) for pulmonary arterial hypertension. Eur Respir J. 2017;50(3).

28. Botros L, Szulcek R, Jansen SMA, Kurakula K, Goumans MTH, van Kuilenburg ABP, et al. The Effects of Mercaptopurine on Pulmonary Vascular Resistance and BMPR2 Expression in Pulmonary Arterial Hypertension. Am J Respir Crit Care Med. 2020;202(2):296-9.

29. Rol N, de Raaf MA, Sun XQ, Kuiper VP, da Silva Goncalves Bos D, Happe C, et al. Nintedanib improves cardiac fibrosis but leaves pulmonary vascular remodelling unaltered in experimental pulmonary hypertension. Cardiovasc Res. 2019;115(2):432-9.

30. Hoeper MM, Barst RJ, Bourge RC, Feldman J, Frost AE, Galie N, et al. Imatinib mesylate as add-on therapy for pulmonary arterial hypertension: results of the randomized IMPRES study. Circulation. 2013;127(10):1128-38.

31. Montani D, Bergot E, Gunther S, Savale L, Bergeron A, Bourdin A, et al. Pulmonary arterial hypertension in patients treated by dasatinib. Circulation. 2012;125(17):2128-37.

SUPPLEMENTAL INFORMATION

Supplemental table 1: Comparison between patients in the preliminary study and in the expanded cohort

	Preliminary study n=8	Expanded cohort n=13	p-value
Age (yr)	46 ± 12	44 ± 14	0.732
HPAH, n(%)	5 (63%)	9 (69%)	1.000
Male, n(%)	4 (50%)	3 (23%)	0.427
NYHA functional class, I/II/III/IV (n)	2/4/2/0	2/8/3/0	0.834
BMI, kg/m^2	24.6 ± 3.7	24.9 ± 3.7	0.825
NT-proBNP, ng/ml	190 [30-654]	229 [70-485]	0.943
Medical history			
Malignancy	0	0	NA
Hypertension	2 (25%)	0	0.259
Diabetes Mellitus	1 (13%)	0	0.802
VTE/pulmonary embolism	0	1 (8%)	1.000
Treatment			
Treatment Naïve, n(%)	1 (13%)	0	0.802
Monotherapy (ERA or PDE5I), n(%)	1 (13%)	0	0.802
Dual combination therapy (ERA + PDE5I or PDE5i + prostacyclin* 0), n(%)	3 (38%)	11 (85%)	0.081
Triple combination therapy (ERA + PDE5I + prostacyclin), n(%)	3 (38%)	2 (15%)	0.530
Hemodynamic characteristics			
Heart rate, beats/min	79 ± 8	73 ± 14	0.236
Mean pulmonary artery pressure, mmHg	45 [44-55]	53 [42-57]	0.704
Pulmonary arterial wedge pressure, mmHg	9 [7-10]	12 [10-13]	**0.017**
Mean right atrial pressure, mmHg	6 [3-8]	9 [7-10]	0.117
Pulmonary vascular resistance, dyn.s/cm^{-5}	318 [222-366]	367 [308-511]	0.296
Cardiac index, l/min/m^2	2.9 ± 0.7	2.7 ± 0.7	0.470
Cardiac magnetic resonance imaging			
RVEDVI, ml/m^2	91 [79-101]	92 [75-111]	0.999
RVESVI, ml/m^2	49 [44-63]	48 [34-70]	0.329
RVEF, %	39 ± 11	47 ± 12	0.104
LVEF, %	63 ± 8	60 ± 16	0.565
^{18}FLT PET K3 phosphorylation			
Mid-region	0.081 [0.067-0.107]	0.057 [0.053-0.068]	0.053
Whole lung	0.079 [0.065-0.095]	0.076 [0.067-0.083]	0.828

Table S1: Data are depicted as mean(SD), median [IQR] or percentages. BMI: body mass index, VTE: venous thromboembolism, ERA: endothelin receptor antagonist, PDE5I: phosphodiesterase type 5 inhibitor, mRAP: mean right atrial pressure, RVEDVI: Indexed right ventricular end-diastolic volume, RVESVI: Indexed right ventricular end-systolic volume, RVEF: right ventricular ejection fraction, LVEF: left ventricular ejection fraction

Supplemental table 2: follow-up [18F]FLT-PET scans in three pulmonary arterial hypertension patients

	Baseline characteristics			[18F]FLT-PET 2015 first scan							[18F]FLT-PET 2018 second scan							
	Age	Sex	BMI	mPAP	PVR	RVEDVI	RVESVI	RVEF	k3 mid-region	Medication	mPAP	PVR	RVEDVI	RVESVI	RVEF	k3 mid-region	Change in medication	12-months follow up
Patient 1	54	F	24.5	25	489	69	43	38	0.056	Prostacyclin + PDE5I	26	176	65	27	58	0.059	+ ERA	deteriorated mildly
Patient 2	68	F	18.3	44	548	94	55	41	0.050	ERA + PDE5I	50	732	105	68	35	0.070	none	Severe deterioration and died after stroke
Patient 3	43	M	24.4	69	762	126	105	17	0.150	ERA + PDE5I	67	998	130	100	19	0.081	+ prostacyclin	Severe deterioration, received lung transplantation and died after transplantation

Table S2: mPAP: mean pulmonary artery pressure, PVR: pulmonary vascular resistance, RVESVI: Indexed right ventricular end-systolic volume; RVEDVI: Indexed right ventricular end-diastolic volume, RVEF: right ventricular ejection fraction, ERA: endothelin receptor antagonist, PDE5I: phosphodiesterase type 5 inhibitor

3

Supplemental figure 1
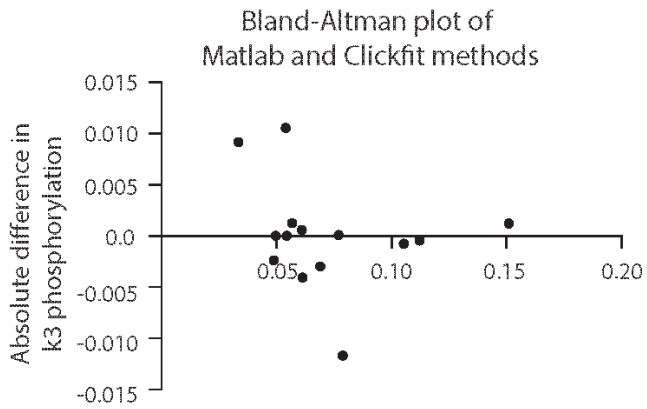
Supplemental figure 1: Bland-Altman plot comparing two differet methods to calculate FLT-uptake in the lung. In PAH patients from the preliminary cohort, kinetic modelling modelling using CLICKFIT gave similar results as the MATLAB 5.3 software.

1
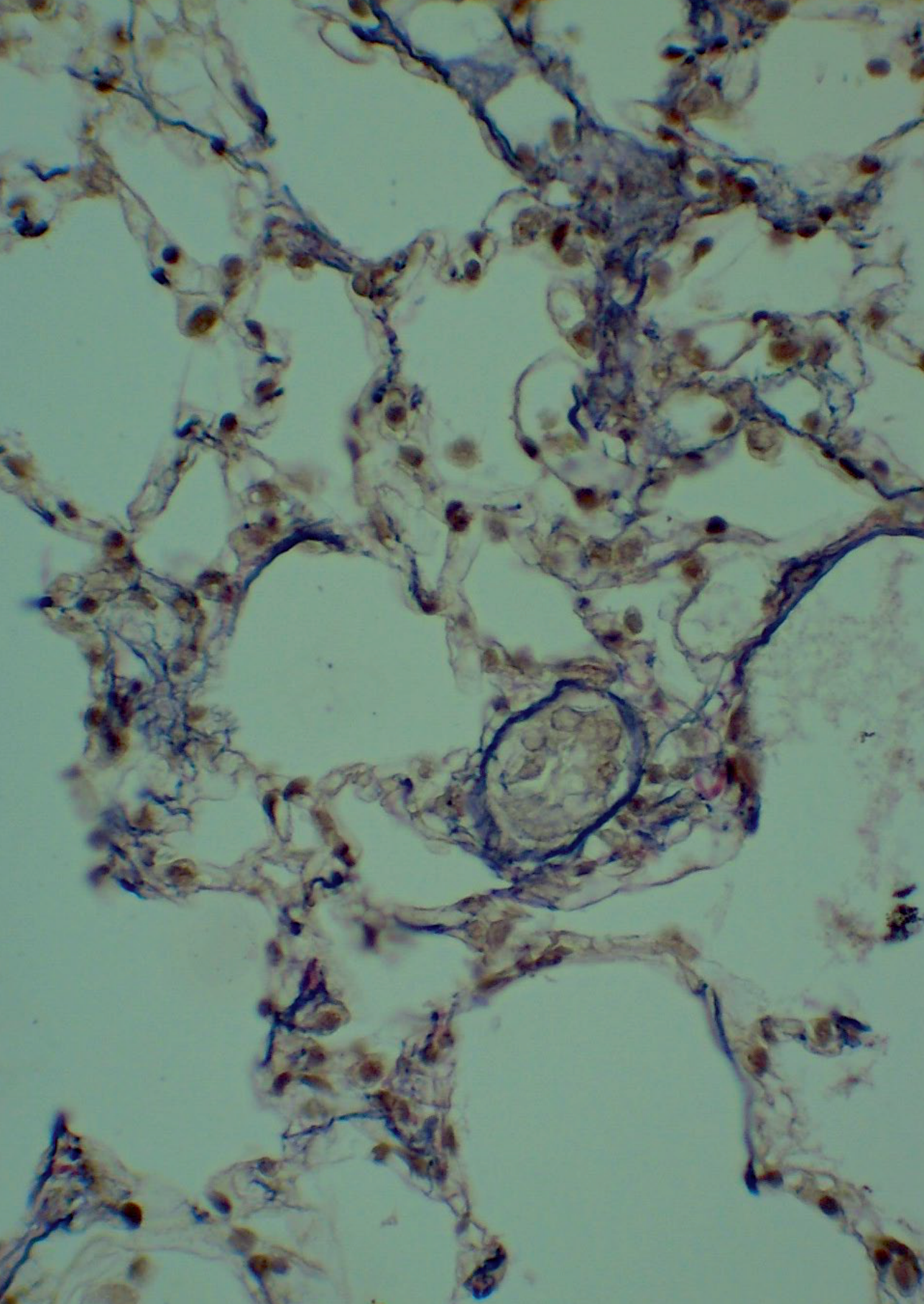
4

The effects of Mercaptopurine on Pulmonary Vascular Resistance and BMPR2 expression in Pulmonary Arterial Hypertension

Liza Botros, Robert Szulcek, Samara M.A. Jansen, Kondababu Kurakula, Marie-José T.H. Goumans, André B.P. van Kuilenburg, Anton Vonk Noordegraaf, Frances S. de Man, Jurjan Aman & Harm Jan Bogaard

Letter to the editor:

Pulmonary arterial hypertension (PAH) is an incurable disease characterized by vascular obliteration and luminal narrowing (1). Current vasodilator therapies have no proven effect on the underlying molecular and cellular changes in the PAH lung, which include the emergence of apoptosis-resistant cell populations (2, 3) and proliferation of endothelial cells (4).

We recently showed that 6-mercaptopurine (MP, Purinethol) augmented BMP (bone morphogenetic protein) signaling and reversed abnormal vascular remodeling and right ventricle (RV) hypertrophy in the Sugen-hypoxia rat model of PAH (5). MP has been used in leukemia and inflammatory bowel disease for decades with an acceptable and manageable toxicity profile (6, 7). MP is an immunosuppressant that reduces inflammation and proliferation of vascular cells, which is one of the pathophysiological hallmarks of PAH (4). Here, we report the results of an open-label, proof-of-concept, single-center study of MP in patients with PAH (EudraCT 2017-000137-31, Dutch Medical Ethical Committee 2017.059). The primary aim was to evaluate the efficacy and safety of MP treatment in patients with PAH, using a dose of 1.2–1.5 mg/kg (80–100%) once daily for 16 weeks, rounded in tablets of 25 mg. The patient population consisted of idiopathic, hereditary, or drug-induced PAH; New York Heart Association (NYHA) functional class II, III, or IV; and stable on current PAH medication (no dose adjustments in PAH-specific therapy for >3 mo or changes in diuretics for 30 d). Eligible patients were required to show precapillary pulmonary hypertension with mean pulmonary artery pressures (mPAPs) >25 mm Hg, pulmonary artery wedge pressure 915 mm Hg, and, to enrich the population under study, a pulmonary vascular resistance (PVR) of >480 dyn $dyn.s^{-1}.cm^{-5}$). Thiopurine methyltransferase activity was tested before enrollment to prevent MP toxicity. Safety assessments included recording of all adverse events and blood sampling at Weeks 1, 2, 4, 6, 8, 12, and 16. The primary study endpoint was a change in PVR, and secondary study endpoints included changes in mPAP and cardiac index, changes in RV volumes measured by cardiac magnetic resonance imaging, NT-proBNP (N-terminal brain natriuretic peptide) levels, 6-minute-walk distance, NYHA functional class, and quality-of-life scores. With a statistical power of 80% ($\alpha = 0.05$), we expected to detect a clinically relevant decrease in PVR of 240 $dyn.s^{-1}.cm^{-5}$ (SD, 400 $dyn.s^{-1}.cm^{-5}$). With an expected responder rate of 50% (8) and a dropout rate of 15%, we estimated the sample size at 50 patients.

Table 1

	Intention to treat Before n=15 mean (SD)	Intention to treat After n=14 mean (SD)	p-value	Per protocol Before n=11 mean (SD)	Per protocol After n=11 mean (SD)	p-value
Patient characteristics						
Age (years)	42 (15)					
NYHA (2/3/4)	8 / 5 / 2					
Diagnosis (HPAH / IPAH / DIPAH)	11 / 3 /1					
BMPR2 mutation	9					
TBX4 mutation	2					
PAH therapy (Mono / duo / triple)	2 / 9 / 4					
Weight (kg)	65.6 (11)	65.3 (11)	0.2589	69.6 (11)	67.4 (10.8)	0.2183
6 minute walking distance (m)	499 (127)	506 (114)	0.4511	510 (116)	513 (107)	0.7130
NTproBNP (pg/mL)	626 [156-169][1]	413 [168-859][1]	0.9999[1]	626 [156 − 782][1]	340 [176-561][1]	>0.999[1]
Quality of Life questionnaire score (0-84)	36 (18)	39 (16)	**0.0432**	29 (17)	35 (15)	**0.0096**
Hemodynamic characteristics						
Mean right atrial pressure (mmHg)	8 (3)	8 (3)	0.2880	8 (3)	8 (3)	0.5024
Mean pulmonary artery pressure (mmHg)	58 (12)	53 (9)	0.1181	59 (14)	53 (9)	**0.0411**
Pulmonary arterial wedge pressure (mmHg)	11 (3)	12 (4)	0.2715	11 (3)	12 (4)	0.2392
Pulmonary vascular resistance (dyn.s^{-1}.cm^{-5})	878 (345)	757 (308)	**0.0273**	879 (354)	759 (342)	**0.0044** **0.0071**[2]
Systemic mean arterial blood pressure (mmHg)	81 (13)	82 (9)	0.3200	78 (13)	81 (10)	0.5316
Heart rate (bpm)	76 (10)	72 (11)	0.2526	72 (7)	69 (11)	0.4068

Peripheral blood cell count	n=11	n=11	
Peripheral blood mononuclear cells (*10^9/L)	10.9 (7.3)	5.7 (2.4)	**0.0390**
Monocytes (*10^9/L)	3.0 (2.2)	1.3 (0.6)	**0.0350**
Neutrophils (*10^9/L)	1.2 (0.9)	0.8 (0.6)	0.1910
Interleukin-6 (pg/mL)	4.5 (3.8)	5.5 (5.9)	0.4420
Tumor necrosis factor-α (pg/mL)	1.3 (1.1)	1.3 (0.9)	0.7595
Relative BMPR2 expression	1.001 (0.59)	2.027 (0.63)	**0.0057**

Table 1: Intention to treat analysis on all patients that started therapy in white, and per protocol analysis on patients that finished 16-week treatment in blue. Data are presented as mean (SD). NYHA: New York Heart Association; HPAH: hereditary pulmonary arterial hypertension; IPAH: idiopathic pulmonary arterial hypertension; DIPAH: drug-induced pulmonary arterial hypertension; BMPR2: Bone morphogenetic protein receptor type II; TBX4: T-box transcription factor; NT-proBNP: N-terminal brain natriuretic peptide; p-value in paired-Test. [1]: non-parameteric data depicted as median [interquartile range] and Wilcoxon non-parametric test. [2]: Generalized Estimation Equation analysis of PVR corrected for decrease in hemoglobin.

Out of 77 patients who were eligible for inclusion in our center, 60 patients (78%) declined to participate, mainly because of high study burden (time, need to travel and undergo procedures, and fear of side effects). A total of 15 patients were enrolled into the study from 2017 to 2019. The mean PVR was 878 $dyn.s^{-1}.cm^{-5}$ and was significantly decreased after treatment (P = 0.0273 intention-to-treat analysis and P = 0.0044 per-protocol analysis in Figure 1). This decrease in PVR remained significant after correcting for confounding effects of Hb (P = 0.0071). mPAP was significantly decreased in the per-protocol analysis (25 mm Hg, P = 0.04) but not in intention-to-treat analysis. Although this decrease in PVR was significant, the magnitude of reduction was relatively small, leading to no improvement in cardiac index, RV function, NYHA functional class, 6-minute-walk distance, or NT-proBNP concentrations.

Although the dosage of MP used in this study is generally well tolerated by patients with inflammatory bowel disease (6), it appeared too burdensome for this PAH population. Two patients stopped the study after 2 (data not shown) and 13 weeks because of nausea, vomiting, and fatigue. Two other patients were excluded after 6 and 8 weeks because of migraine and myelosuppression. Hb and leukocyte counts were decreased in almost all patients (Hb, 20.81 g/dl, P = 0.0399; leukocytes, 22.7 3 109/L, P = 0.0001). Leucopenia was higher than expected (5–25% reported [6] vs. 40% in our study), and quality-of-life scores were significantly worse. Eight out of 15 patients who finished the protocol (53%) received dose reductions, indicating poor tolerability. Interestingly, none of the patients showed liver toxicity. All side effects were dose dependent and resolved after dose adjustments or treatment discontinuation. Low thiopurine methyltransferase enzymatic activity, the best-known and most frequently studied risk factor for thiopurine-induced leukopenia (6), was not present in our patient cohort.

In accordance with our preclinical study (5), this proof-of-concept study provides first evidence that MP decreases PVR coinciding with an increased BMPR2 (bone morphogenetic protein receptor type II) mRNA expression in peripheral blood mononuclear cells of 10/11 patients after MP treatment (p= 0.006 in Figure 1 and BMPR2 expression per patient in Figure 2). Impaired BMP signaling is observed in both hereditary PAH and idiopathic PAH lungs, and pulmonary vascular remodeling can be attenuated by enhancing BMPR2 activity (9). Therefore, targeting the BMPR2 pathway has repeatedly emerged as a novel treatment strategy for PAH (10), and improvement of BMPR2 expression in circulating peripheral blood mononuclear cells could have contributed to the decrease in PVR.

4
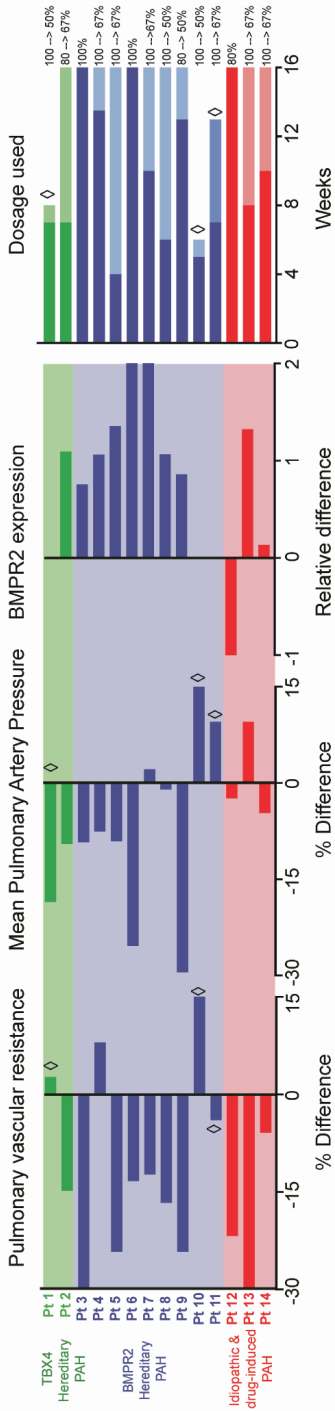
Figure 1:

Figure 1: Percentage difference of pulmonary vascular resistance and mean pulmonary artery pressure depicted per patient. Patients with T-box transcription factor (TBX4) mutations depicted in green. Patients with a bone morphogenetic protein receptor type II (BMPR2) mutation depicted in blue. Idiopathic and drug-induced patients depicted in red. ◊ indicate patients that pre-maturely ended the study. Right panel depicts the used dosage per patient during the time course of the study. Starting dose was 80-100% (1.2-1.5mg/kg rounded to tablets of 25mg), light colour means dose reduction.

In addition to the small inclusion capacity of a single center, this study suffered from patient reluctance to participate after sharing of negative experiences by study participants in the PAH patient community (e.g., social media and patient supportive groups). High toxicity rates together with declining inclusion led us to prematurely end the study. We did not measure thiopurine end-products 6-thioguanine nucleotides or 6-methylmercaptopurine, which are known to generate the cytotoxic and apoptotic effects of thiopurines and give rise to an increased risk for thiopurine-induced leucopenia. Literature shows that alternative thiopurine analogs, such as azathiopurine, thioguanine (Thiosix), or a (metabolite-sensed) step-up dosing, may result in less toxicity (6, 7). This is also shown by the fact that patients who started with 1.2 mg/kg (80%) all completed the study because of lower side effects (Figure 2). As myelosuppression is dose dependent, we hypothesize that a lower starting dosage in a step-up scheme increases the tolerability of MP treatment (6) but at the same time still effectively reduces pulmonary pressures. The observed decrease in PVR confirms that targeting excessive vascular remodeling by inhibiting cell proliferation and inducing apoptosis with MP is of therapeutic interest. As frequency and severity of side effects were higher than reported and expected in the current design, we conclude that antiproliferative therapy with MP as add-on treatment for hereditary and idiopathic PAH has an unfavorable risk/benefit ratio. However, improvements in dosing schemes and/or use of other thiopurine analogs deserve further study.

4

References

1.	Tuder RM, Groves B, Badesch DB, Voelkel NF. Exuberant endothelial cell growth and elements of inflammation are present in plexiform lesions of pulmonary hypertension. Am J Pathol. 1994;144(2):275-85.

2.	Sakao S, Taraseviciene-Stewart L, Lee JD, Wood K, Cool CD, Voelkel NF. Initial apoptosis is followed by increased proliferation of apoptosis-resistant endothelial cells. FASEB J. 2005;19(9):1178-80.

3.	McMurtry MS, Archer SL, Altieri DC, Bonnet S, Haromy A, Harry G, et al. Gene therapy targeting survivin selectively induces pulmonary vascular apoptosis and reverses pulmonary arterial hypertension. J Clin Invest. 2005;115(6):1479-91.

4.	Lee SD, Shroyer KR, Markham NE, Cool CD, Voelkel NF, Tuder RM. Monoclonal endothelial cell proliferation is present in primary but not secondary pulmonary hypertension. J Clin Invest. 1998;101(5):927-34.

5.	Kurakula K, Sun XQ, Happe C, da Silva Goncalves Bos D, Szulcek R, Schalij I, et al. Prevention of progression of pulmonary hypertension by the Nur77 agonist 6-mercaptopurine: role of BMP signalling. Eur Respir J. 2019;54(3).

6.	van Gennep S, Konte K, Meijer B, Heymans MW, D'Haens GR, Lowenberg M, et al. Systematic review with meta-analysis: risk factors for thiopurine-induced leukopenia in IBD. Aliment Pharmacol Ther. 2019;50(5):484-506.

7.	Jharap B, Seinen ML, de Boer NK, van Ginkel JR, Linskens RK, Kneppelhout JC, et al. Thiopurine therapy in inflammatory bowel disease patients: analyses of two 8-year intercept cohorts. Inflamm Bowel Dis. 2010;16(9):1541-9.

8.	Ashek A, Spruijt OA, Harms HJ, Lammertsma AA, Cupitt J, Dubois O, et al. 3'-Deoxy-3'-[18F]Fluorothymidine Positron Emission Tomography Depicts Heterogeneous Proliferation Pathology in Idiopathic Pulmonary Arterial Hypertension Patient Lung. Circ Cardiovasc Imaging. 2018;11(8):e007402.

9.	Long L, Ormiston ML, Yang X, Southwood M, Graf S, Machado RD, et al. Selective enhancement of endothelial BMPR-II with BMP9 reverses pulmonary arterial hypertension. Nat Med. 2015;21(7):777-85.

10.	Spiekerkoetter E, Sung YK, Sudheendra D, Bill M, Aldred MA, van de Veerdonk MC, et al. Low-Dose FK506 (Tacrolimus) in End-Stage Pulmonary Arterial Hypertension. Am J Respir Crit Care Med. 2015;192(2):254-7.

SUPPLEMENTAL INFORMATION

Exclusion criteria

Exclusion criteria consisted of PAH of any cause other than permitted in the entry criteria, contraindication for right heart catheterization or CMR imaging, receipt of investigational medication within 1 month prior to the start of this study, known intolerance to 6MP or with a TPMT enzyme deficiency, active liver disease, porphyria or elevations of serums transaminases >3 x ULN (upper limit of normal) or bilirubin > 1.5 x ULN, history or suspicion of inability to cooperate adequately, cancer or other malignant hematological disease, eGFR <30 ml/min, white blood count <$4.0*10^9$/l, hemoglobin < 6.0mmol/l, thrombocytes < 100 10^9/l, transfer capacity for carbon monoxide (TLCO) <40% of predicted, total lung capacity (TLC) <60% of predicted, use of xanthine oxidase inhibitors, pregnant or breastfeeding female subjects and female subjects unwilling or unable to use a highly effective method of contraception.

Risk classification and safety

Following the Dutch Federation of University Medical Centres (NFU) risk classification and European Medical Association (EMA) Data Monitoring Committee, the risk of participation in this study was intermediate. AEs were scored using Common Terminology Criteria for Adverse Events (CTCAE) and reviews of adverse events and serious AEs and did not identify any issues that required intervention. As MP is used for decades with a well-known safety profile, and risk classification was scored as intermediate, no external independent safety committee had to be appointed. Based on the laboratory results of hemoglobin, leucocytes, thrombocytes, serum transaminases and bilirubin concentration, a patient was eligible for dose reduction of 50-80% when the leukocyte number dropped below $4*10^9$/L, hemoglobin dropped <6.5 mmol/L, thrombocytes decreased below $100*10^9$/L, serum transaminases were elevated >3 x ULN (upper limit of normal) or bilirubin increased > 1.5 x ULN. A dose reduction of >50% or treatment was stopped if the leukocyte number was <$2.5*10^9$/L, hemoglobin concentration <5.0 mmol/L or thrombocyte count < $30*10^9$/L.

Right Heart Catheterizations and Cardiac Magnetic Resonance Imaging

Right-sided heart catheterization was performed as previously described (1). In short, 7F balloon-tipped flow-directed triple-lumen Swan-Ganz catheter (Edwards Lifesciences LLC, Irvine, CA) was inserted in the PA via the jugular vein under local anesthesia and constant ECG monitoring, and measurements were performed according to the guidelines(2). Cardiac output (CO) was measured using the thermodilution method. PVR was calculated as 80x(mPAP-PAWP)/CO. CO was indexed to body surface area (BSA) and shown as cardiac index (CI). Cardiac magnetic resonance (CMR) imaging scans were performed on a Siemens 1.5T Sonato or Avanto scanner (Siemens Medical Solutions, Erlangen, Germany). Acquisition and post processing was performed following our stand protocol as described previously (1).

Cardio-pulmonary exercise test (CPET)

Maximal CPET was performed in the upright position using an electromagnetically braked cycle-ergometer (Ergoline GmbH, Bitz, Germany) according to the American Thoracic Society guidelines and as described previously by our group (3). Breath-by-breath measurements were made of VO2, VCO2, and VECO2 (Vmax229; Sensormedica, Yorba Linda, CA).

Isolation of peripheral blood mononuclear cells (PBMCs)

Blood samples were drawn from all patients during right heart catheterization from the superior vena cava. 50mL of whole blood was collected into BD Vacutainer heparin-coated tubes and transferred into Falcon tubes. Subsequently blood was centrifuged at 500g for 10 minutes at room temperature to initiate plasma separation. Aliquots of plasma were stored at −80°C until further analysis. Isolation of peripheral blood mononuclear cells (PBMCs) following blood collection using a Ficoll density gradient (Corning, New York, USA). Isolated cells were stored in freezing media comprising 10% dimethyl sulfoxide (DMSO), 90% fetal bovine serum (FBS). The mixtures were promptly frozen in liquid nitrogen before RNA extraction.

RNA isolation from PBMCs, cDNA synthesis, PCR procedures

RNA was isolated and cDNA was generated using RNA-isolation Kit (Zymo Research Direct-zol MiniPrep R2050) and iScript cDNA synthesis kit (Bio-Rad, #170-8891) according to manufacturer's instructions. For PCR reactions FAST SYBR Green Master Mix (Thermo Fisher Scientific, 4385612) was used. P0 was used as housekeeping gene to normalize for the amount of total RNA per sample. Primer sequences:

BMPR2: F GTCCTGGATGGCAGCAGTAT R CCAGCGATTCAGTGGAGATGA

P0 F TCGACAATGGCAGCATCTAC R ATCCGTCTCCACAGACAAGG

Cytokine measurements in patient plasma

Peripheral venous blood samples were collected on the same day of RHC and CMR. Blood was centrifuged and plasma was stored at -80°C within 2 hours. Plasma (EDTA) and serum concentrations of Il-6 and TNFα were measured using high-sensitivity ELISA from R&D systems following manufacturer's instructions (TNFα: HSTA00E; IL6: HS600C).

4

Supplemental table 1: Concomitant medications

		Frequency (n=15)
Oral medications	Spironolactone / bumetanide / furosemide	6/2/7
	Amlodipine /verapamil	1/1
	Irbesartan	1
	Bisoprolol / sotalol / metoprolol	2/1/1
	Phenprocoumon	12
	Rivaroxaban	2
	Rosuvastatin	1
	Zolpiclon / temazepam / oxazepam	1/1/1
	Celecoxib	1
	Codeine	1
	Levothyroxine	2
	Pantoprazole / ranitidine	1/1
	Ethinylestradiol-levonorgestrel	1
	Loperamide	1
	Testosterone	1
Inhalation medication	Formoterole-budesonide / tiotropium bromide / salbutamol	3 /1 /1

Supplemental table 2: Living with pulmonary hypertension questionnaire

Holdback in daily activities score 0=no complaints 4=complaints all the time				
	T= 0 Mean	T= 16 Mean	Mean difference in score	P-value
Complaints of swollen feet / fluid retention	0.80	0.62	-0.15	0.427
Need to rest during the day	1.93	2.31	0.46	0.028*
Breathless when walking up stairs or walking	2.33	2.38	0.0	0.759
Breathless when performing household chors	2.40	2.77	0.31	0.139
Feel restricted in outdoor activities	1.87	2.46	0.62	0.069
Problems with sleeping	1.53	1.92	0.46	0.139
Feel restricted in activities with family and friends	1.67	1.85	0.38	0.040*
Problems with maintaining work	1.93	1.69	-0.23	0.436
Feel restricted in performing hobbies and sport activities	2.33	2.15	-0.23	0.866
Hindered in sexual activities	1.53	1.38	0.0	0.999
Decreased appetite	1.87	1.92	0.08	0.337
Breathlessness all the time	2.33	2.46	0.08	0.794
Feelings of fatigue and pithlessness	2.00	2.77	0.62	0.015*
Need for hospital admission	0.47	1.00	0.46	0.151
Incurred additional medical expenses	0.80	0.92	0.15	0.851
Experienced side effects of treatment	1.13	1.92	0.77	0.044*
Feelings of being a burden to family and friends	1.27	2.00	0.54	0.222
Feelings of losing control over your own life	1.93	2.00	0.08	0.656
Increased worrying	2.27	2.46	0.15	0.367
Trouble concentrating and remembering things	2.07	2.08	0.0	0.870
Feelings of depression	1.87	2.08	0.23	0.231

The quality of life was qualitativly assessed by using the living with pulmonary hypertension quostionnaire (LPH) as validated by Bonner et al (4) *P<0.01 in paired-Test

4

Supplemental references:

1. van de Veerdonk MC, Huis In TVAE, Marcus JT, Westerhof N, Heymans MW, Bogaard HJ, Vonk-Noordegraaf A. Upfront combination therapy reduces right ventricular volumes in pulmonary arterial hypertension. *Eur Respir J* 2017; 49.

2. Galie N, Humbert M, Vachiery JL, Gibbs S, Lang I, Torbicki A, Simonneau G, Peacock A, Vonk Noordegraaf A, Beghetti M, Ghofrani A, Gomez Sanchez MA, Hansmann G, Klepetko W, Lancellotti P, Matucci M, McDonagh T, Pierard LA, Trindade PT, Zompatori M, Hoeper M. 2015 ESC/ERS Guidelines for the diagnosis and treatment of pulmonary hypertension: The Joint Task Force for the Diagnosis and Treatment of Pulmonary Hypertension of the European Society of Cardiology (ESC) and the European Respiratory Society (ERS): Endorsed by: Association for European Paediatric and Congenital Cardiology (AEPC), International Society for Heart and Lung Transplantation (ISHLT). *Eur Respir J* 2015; 46: 903-975.

3. Spruijt OA, de Man FS, Groepenhoff H, Oosterveer F, Westerhof N, Vonk-Noordegraaf A, Bogaard HJ. The effects of exercise on right ventricular contractility and right ventricular-arterial coupling in pulmonary hypertension. *Am J Respir Crit Care Med* 2015; 191: 1050-1057.

4. Bonner N, Abetz L, Meunier J, Sikirica M, Mathai SC. Development and validation of the living with pulmonary hypertension questionnaire in pulmonary arterial hypertension patients. *Health Qual Life Outcomes* 2013; 11: 161.

Pulmonary Vascular Leakage

Journal of
Cell Science
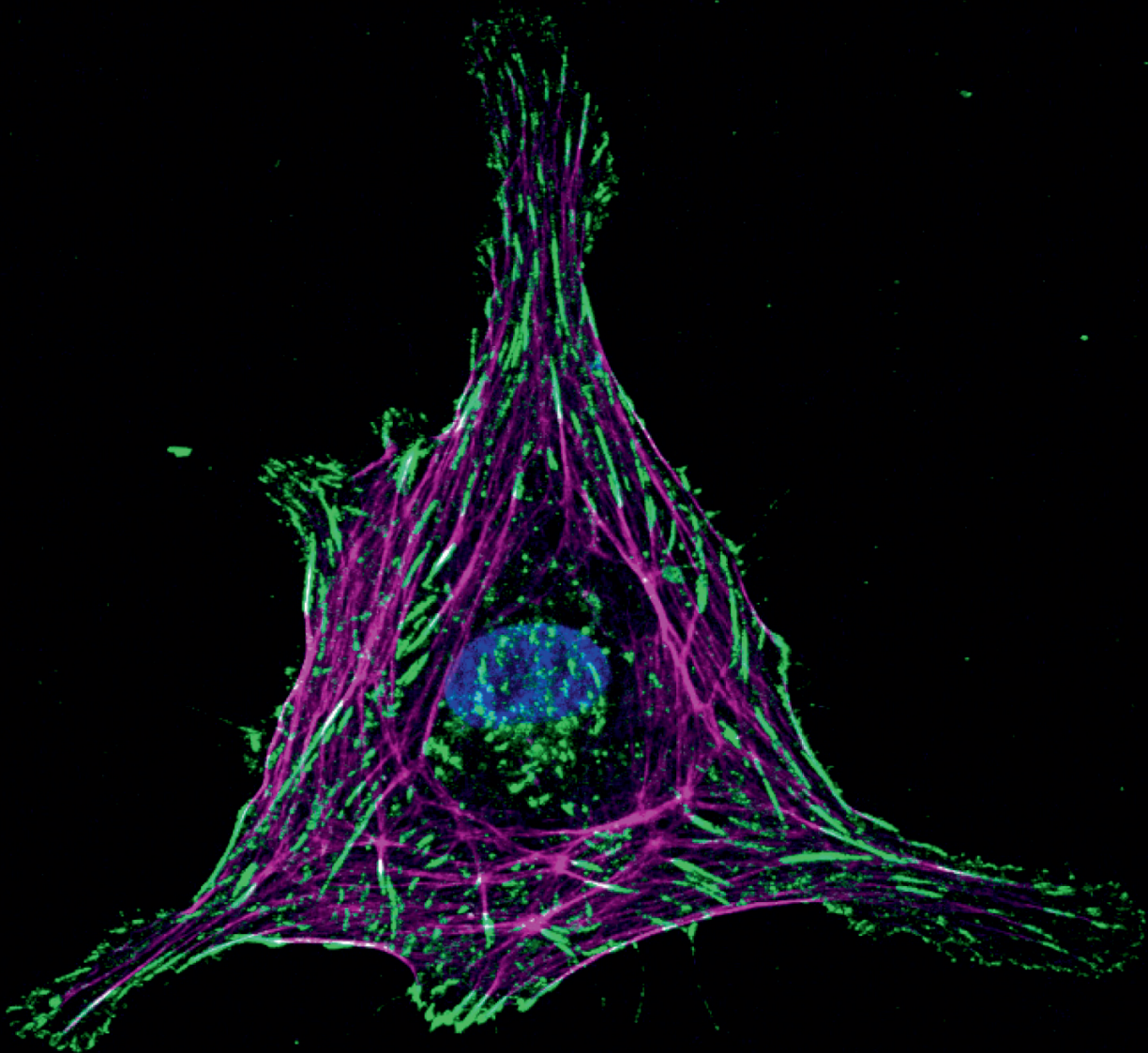
5

Bosutinib prevents vascular leakage by reducing focal adhesion turnover and reinforcing junctional integrity

Liza Botros, Manon C.A. Pronk, Jenny Juschten, John Liddle, Sofia K.S.H Morsing, Jaap D. van Buul, Robert H. Bates, Pieter R. Tuinman, Jan S.M. van Bezu, Stephan Huveneers, Harm Jan Bogaard, Victor W.M. van Hinsbergh, Peter L. Hordijk & Jurjan Aman

Abstract

Aim: Endothelial barrier dysfunction leads to edema and vascular leak, carrying high morbidity and mortality. Previously, Abl kinase inhibition was shown to protect against vascular leak. Using the distinct inhibitory profiles of clinically available Abl kinase inhibitors, we aimed to provide a mechanistic basis for novel treatment strategies against vascular leakage syndromes.

Methods & Results: Bosutinib most potently protected against inflammation-induced endothelial barrier disruption. *In vivo,* bosutinib prevented LPS-induced alveolar protein extravasation in an acute lung injury mice model. Mechanistically, Mitogen-activated Protein 4 Kinase 4 (MAP4K4) was identified as important novel mediator of endothelial permeability, which signals via ezrin, radixin and moesin proteins to increase turnover of integrin-based focal adhesions. The combined inhibition of MAP4K4 and Arg by bosutinib preserved adherens junction integrity and reduced turnover of focal adhesions, which synergistically act to stabilize the endothelial barrier during inflammation.

Conclusion: MAP4K4 was identified as important regulator of endothelial barrier integrity, increasing focal adhesion turnover and disruption of cell-cell junctions during inflammation. Inhibiting both Arg and MAP4K4, the clinically available drug bosutinib may form a viable strategy against vascular leakage syndromes.

Introduction

The vascular endothelium controls the transport of proteins and solutes from the blood to the tissues (1, 2). Dysregulation of the endothelial barrier leads to capillary leakage and edema as seen in pathological conditions such as acute respiratory distress syndrome (ARDS) and sepsis (2, 3). Inflammatory mediators open endothelial cell junctions, enhancing vascular permeability (4). Despite increased understanding of endothelial barrier regulation at the molecular level (5), only supportive care with oxygen supplementation and lung-protective ventilation are available, but do not target the underlying inflammation-induced structural defects in the endothelium (3, 6).

Adherens junctions (AJ) comprise transmembrane proteins that form dynamic interactions between adjacent cells and play an important role in maintaining the integrity of the vascular endothelial monolayer and in the regulation of its barrier function (7, 8). The main AJ protein is vascular-endothelial (VE) cadherin, a single span transmembrane, homotypic adhesion molecule which connects intracellularly to the cortical F-actin cytoskeleton (7). In the presence of pro-inflammatory stimuli, intracellular signalling leads to phosphorylation, destabilization and internalization of VE-cadherin (8). In parallel, activation of RhoGTPases induces acto-myosin based contraction, following the phosphorylation of myosin light chain (MLC), which lead to contractile stress fibres, exertion of force on the junctional complexes and finally retraction of the cell membrane (1, 9).

We have previously demonstrated that the Abl kinase inhibitor (AKI) imatinib reverses pulmonary edema (10) and protects against endothelial barrier disruption by inhibition of Abl-related gene (Arg) (11). The inhibition of Arg resulted both in enhanced cell–cell interactions and enhanced cell–matrix adhesion. Mechanistically, we showed that imatinib-mediated inhibition of Arg increased the activity of Rac1 and the stabilization of peripheral, β1-integrin containing, focal adhesions (FA). FA are multi-protein structures that link the cytoskeleton to the extracellular matrix (ECM) (12). Within FA, integrins play a pivotal role both in cell-matrix adhesion and in bidirectional signaling across the plasma membrane (13). Similar to cadherins, the intracellular domains of integrins are dynamically connected to the actin cytoskeleton through a large variety of adapter and signaling proteins. As a result, integrin stability and adhesive function is subject to regulation by signaling from within the cell ('inside-out' signaling). Conversely, integrins probe the extracellular environment where their adhesive interactions with the ECM trigger subsequent intracellular ('outside-in') signaling (12, 13).

Integrins are essential for endothelial barrier stability, cell migration and proliferation (13-15) and there is growing evidence for a role of FA and β1-integrins in blood vessel stability and barrier function (14, 16, 17). Integrin-containing FA have shown to stabilize and localize VE-cadherin at cell-cell junctions (14, 16), although the underlying mechanism remains unclear. The involvement of integrins in endothelial barrier regulation is diverse and is

dependent on the availability of different integrin subtypes and their cellular distribution (17-19).

Next generation AKIs have been developed to treat imatinib-resistant forms of chronic myeloid leukemia (20) that show different kinase inhibition and safety profiles. We hypothesized that inhibition of a favorable combination of kinases (as provided by next generation AKIs), provides greater potential for the treatment of vascular leakage syndromes. In the current study, we made use of the distinct inhibitory profiles of clinically available AKIs to provide a mechanistic basis for novel treatment strategies against vascular leakage syndromes (21). We identified the clinically available AKI bosutinib as robust protector of vascular permeability both *in vitro* and *in vivo*, which exerts its protective effect through combined inhibition of Arg and Mitogen-activated Protein Kinase 4 (MAP4K4).

Methods and materials

Reagents, antibodies and siRNAs

For all experiments bosutinib was purchased from Selleck chemicals (s104) and dissolved in dimethylsulphoxide (DMSO) in a concentration of 1µM. Imatinib (free base) was purchased from ChemieTek (Indianapolis, IN) and dissolved in DMSO in a concentration of 10µM. All tyrosine kinases used in the screen were provided by GlaxoSmithKline (GSK, Stevenage, UK) and used in their optimal concentration: GNF2 10µM, Nilotinib 10µM, Nintedanib 1µM, Erlotinib 10µM and Dasatinib 0.1µM, as determined by concentration series in ECIS (data not shown). PF-6260933 (Selleckem) was dissolved in sterile water in a concentration of 3µM.

The following antibodies were used: α-MAP4K4(HGK, #3485 1:1000), α-VE-cadherin XP (D87F2,#2500 1:200-1000), α-phospho-Ezrin(Thr567)/Radixin(Thr564) /Moesin(Thr558) (#3141S 1:500-1000), α-Ezrin/Radixin/Moesin (#3142 1:500-1000), pMLC (#3671 1:2000), α-P44/42 MAP Kinase (ERK)(#9102 1:2000) vinculin (#4650 1:5000) all Cell Signaling, α-VE-cadherin (SC-6458, Santa Cruz 1:500-1000), α-integrinβ1 (12G10, ab30394, Abcam 1:200-500), α-ABL2 (M09, clone 5C6, Abnova 1:500-1000). The following small interference RNAs (siRNAs) were purchased: ON-TARGET plus non-targeting pool (siNT), GAG CCA AAU UUC CUA A (siARG #2) GACCAACUCUGGCUUGUUA ON-TARGET plus human MAP4K4 (siMAP4K4 #10, 11, 12, 13 or pool), ON-TARGET plus human MINK1 pool (siMAP4K6), ON-Target plus human TNIK pool (siMAP4K7) (All GE-Healthcare/Dharmacon). Human Moesin siRNA (sc-35955) and Human Ezrin siRNA (sc-35349) both Santa Cruz biotechnology Inc.

Endothelial cell culture

Human Umbilical Vein Endothelial Cells (HUVECs) were purchased from Lonza or freshly isolated from umbilical cords of healthy donors. Cells were isolated and characterized as previously described (48). Human pulmonary microvascular endothelial cells (PMVECs) were isolated and cultured from healthy donors, approved by the institutional review board of the

VU University Medical Center following principles outlined in the Declaration of Helsinki and consent was given. Isolation and culturing of human pulmonary microvascular endothelial cells (PMVECs) from healthy donor lungs was described by our group previously(49). HUVECs were cultured in M199 medium supplemented with penicillin 100U/ml and streptomycin 100µg/mL, L-glutamine 2 mMol/L (all Biowhittaker/Lonza, Verviers, Belgium), heat-inactivated human serum 10% (Sanquin blood supply, Amsterdam, The Netherlands), heat-inactivated new-born calf serum 10% (Gibco, Grand Island, NY), crude endothelial cell growth factor 150µg/mL (prepared from bovine brains) and heparin 5U/mL (Leo pharmaceutical products, Weesp, The Netherlands), cultured at 37°C and 5% CO_2, with a medium change every other day. Cells were used for experiments in passage 1-2.

Transfection with small interfering RNAs

Subconfluent HUVECs (80% confluency) were transfected with 10% NBCS/M199 containing 25nM Dharmafect 1 (Dharmacon/GE-healtcare) and 25nM of siRNA. After 16 hours of transfection, medium was changed to regular culture medium to avoid toxicity. Experiments were done 72 hours after transfection. Efficiency of transfection was evaluated by western blot analysis or PCR of whole cell lysates

Endothelial barrier function assays

Endothelial barrier function was measured by Electrical Cell-substrate Impedance Sensing (ECIS) or macromolecule passage assay. HUVECs were seeded to immediate confluency on gelatin-coated ECIS arrays (Applied Biophysics, Troy, NY). Culture medium was renewed 24 hours after seeding, while experiments were performed 48 hours after seeding. Before thrombin stimulation, cells were incubated with EBM medium containing 1% Human Serum Albumin (HSA, Sanquin CLP) and the compounds in designated concentrations. After 60-90 minutes of pre-incubation, thrombin was added to the wells in a final concentration of 1U/mL (Sigma Aldrich). HUVECs were transfected 24 hours after seeding using Dharmafect 1 and siRNAs for 16 hours, followed by medium change. For analyzing cell-adhesion cells were serum starved and pre-incubated with DMSO or bosutinib (1µM) for 1 hour in m199 containing 1% HSA after which cells were detached by trypsin and counted. A final number of 10.000 cells per well was seeded on gelatin-coated ECIS arrays and resistance was measured during the adhesion-and growth phase for two hours.

After pre-incubation with DMSO (0.01%) or bosutinib (1µM) in 1% HSA for 90 minutes, integrin blocking peptides GRGDNP (AS-62049 AnaSpec) and GRGDSP (AS-22945 AnaSpec) dissolved in 1% HSA were added in increasing concentrations of 0-4mM on primary HUVEC monolayers in ECIS. After 60 minutes a plateau-phase was reached and thrombin 1 U/mL was added. When the concentration of the peptides exceeded 500µM the barrier could not recover over time and we therefore used an optimal concentration of 450µM in subsequent experiments.

Macromolecular passage

HUVECs were seeded to confluency on top of 0.33cm^2 gelatin-coated ThinCerts® cell culture inserts (Greiner Bio-one) with a pore-size of 3.0μm and cultured in EGM-2 medium with a medium change every other day. When a solid barrier was formed, defined as the absence of medium leak, cells were pre-incubated for 1 hour with EBM medium containing 1% HSA and the compounds in designated concentrations. For stimulation, medium in the upper compartment was replaced by 1% HSA/EBM containing horse radish peroxide (HRP) 5μg/ml and thrombin 1U/mL or a vehicle control. Also 1% HSA/EBM was added to the lower compartment. Samples were taken from the lower compartment for HRP quantification at several time points. Cells were transfected 24 hours before transfer to 1% gelatin-coated ThinCerts®. HRP was quantified by measuring absorption after adding tetramethylbenzidine (Upstate/Millipore) and sulfuric acid to stop the reaction.

Kinase Binding Assay

In vitro kinase binding assay was performed by GSK following standard procedures. In short, base reaction buffer was prepared, containing 20 mM Hepes (pH 7.5), 10mM MgCl$_2$, 1mM EGTA, 0.02% Brij35, 0.02 mg/ml BSA, 0.1mM Na$_3$VO$_4$, 2mM DTT and 1% DMSO. The indicated kinase was mixed with substrate solution and compounds were delivered into the kinase reaction mixture by Acoustic technology (Echo550; nanoliter range). To initiate the kinase binding reaction, 33P-ATP was added, incubated for 2 hours at room temperature and reactions were spotted onto P81 ion exchange paper. Kinase activity against 396 kinases was detected by filter-binding method. Thresholds for kinase inhibition of ≥75% at 10nM bosutinib and ≤50% at 10μM imatinib were chosen to select candidate kinases.

Protein analysis

For protein analysis, cells were seeded in 5 or 10 cm^2 culture wells and possibly transfected as described above. When cells reach confluency they were washed with ice-cold PBS and whole-cell lysates were collected by scraping the cells in 2x concentrated SDS sample buffer. Protein samples were separated on 8 or 12.5% SDS page gels or 4-12% precast gels (Biorad) by electrophoresis and transferred to nitrocellulose membranes. Protein analysis was performed by incubation of the nitrocellulose membranes with the designated antibodies. Bands were visualized with enhanced chemiluminescence (Amersham/GE-healthcare) on a AI600 machine (Amersham/GE-healthcare) and intensity was quantified using ImageQuant TL software (GE-healthcare).

Immunofluorescent imaging of cultured endothelial cells

Cells were seeded on 2cm^2 and 12mm glass coverslips (Menzel), coated with 1% gelatin and crosslinked with 0.5% glutaraldehyde (Sigma Aldrich). Transfected cells were seeded approximately 24 hours after the start of transfection. Untransfected cells were seeded and grown to confluence in 48 hours with a medium change the day after seeding. Cells were pre-incubated with 1% HSA/M199 for 1 hour with bosutinib (1μM) or DMSO, thrombin was

added to the wells in a final concentration of 1U/mL. After 2-15 minutes, cells were fixated with warm (37°C) 4% paraformaldehyde (Sigma Aldrich) and put on ice for 15 minutes. Cells were permeabilized with 0,2% triton X-100 in PBS (Sigma Aldrich) and blocked for 30 minutes with 0.1% HSA. Subsequently, coverslips were stained with primary antibodies (in 0.1% HSA/PBS) for 1-2 hours at room temperature. After washing 3 times, the cells were incubated with FITC or Cy5-labeled secondary antibodies (Anti-rabbit or anti-mouse 1:100 in 0.1% HSA/PBS) and F-actin was visualized using labeled phalloidin (in 0,1% HSA/PBS (Tebu bio)) at room temperature for 1-2 hours. After washing, the cells were incubated with DAPI (Thermo Fisher scientific) at room temperature for 30 minutes. Coverslips were mounted with Mowiol4-88/DABCO solution (Calbiochem, Sigma Aldrich). Confocal scanning microscopy was performed on a Nikon A2R confocal microscope (Nikon). Images were analyzed and processed using ImageJ. Gap area was quantified using the freehand selection tool in VE-cadherin staining. The density and number of focal adhesions in total and at the periphery relative to the cell were quantified using ImageJ. In short, images were converted to 8-bit grayscale, foreground/background colors were inverted, and threshold-adjusted. The analyze particles function was used to select and measure focal adhesions. FA were considered peripheral when present at >2/3 of the distance from nucleus to cell membrane. Number of FA was counted and corrected for the number of nuclei. VE-cadherin intensity was quantified using line-measurement from cytosol to cell membrane using ImageJ. Individual peak intensity was divided by individual cytosolic intensity from four positions per pictures, five pictures per condition and averaged in four separate experiments.

Live fluorescence microscopy of FA dynamics

HUVECs were transduced with third generation lentivirus derived from pRRL-Vinculin-GFP plasmid as previously described(9). Cells were plated in a density of 50.000 cells/mL on Lab-Tek chambered 1.0 borosilicated coverglass slides coated with 3 mg/ml fibronectin. The next day, cells were imaged using Total Internal Reflection Fluorescence (TIRF) microscopy. Immunofluorescent VE-cadherin antibody (BD biosciences 647 anti-human CD144 Cat: 561567) was added 30 minutes before imaging in movie 3 to illustrate cell responses in a monolayer. After 60-90 minutes of DMSO or bosutinib treatment, thrombin was added and imaging continued for 30 minutes with intervals of 30 seconds. Cells were imaged using a NIKON Eclipse TI equipped with a 60x Apo TIRF oil objective (NA 1.49) and an Andor Zyla 4.2 plus sCMOS camera. An Okolab cage incubator and humidified CO_2 gas chamber set to 37°C and 5% CO_2 were used during the imaging process. Original data of single cells without VE-cadherin staining in movie 1&2 was uploaded on the FA analysis server (http://faas.bme.unc.edu/)(50, 51) for quantification of FA dynamics. Images were enhanced for display with an unsharp mask filter and by adjusting brightness and contrast settings. In brief, FAs were identified based on GFP-vinculin positivity within thresholded images. Dynamic properties ((dis)assembly rate and longevity) of FA was obtained by the tracking of changes in intensity of the fluorescence from single adhesions through subsequent image frames. 9-16 images per condition were imaged and analyzed out of 2 experiments. Please

5

note that in movie 3 the VE-cadherin intensity was equalized and enhanced against bleaching.

MTT cell viability assay

MTT (3-(4,5-dimethylthiazol-2-yl)-2,5-diphenyl-2Htetrazolium bromide) was purchased from Abcam ab211091 lot number GR3285654-2. HUVECs were grown as previously described on 1% gelatin coated 96-wells flat bottom plates in a density of 50.000cells/ well. After 48 hours, cells were incubated with 0, 0.1µM, 1 µM and 10 µM bosutinib in serum starved medium, or 500uM H_2O_2 as positive control for 120min. MTT reagent and MTT solvent were added following manufacturers protocol. Absorbance was read at 590nm. Percentage cell viability was calculated as (sample-background) / control * 100.

PCR

RNA was isolated and cDNA was generated using RNA-isolation Kit (Zymo Research Direct-zol MiniPrep R2050) and iScript cDNA synthesis kit (Bio-Rad, #170-8891) according to manufacturer's instructions. For PCR reactions FAST SYBR Green Master Mix (Thermo Fisher Scientific, 4385612) was used. qPCR was then performed to quantify the expression of MAP4K4, MAP4K5, MAP4K6 and MAP4K7. GAPDH and TBP were used as housekeeping genes to normalize for the amount of total RNA per sample. Gene expression was determined by the LightCycler 480 Instrument II (Roche Applied Science, Penzberg, Germany), and the reactions were prepared using Light Cycler SYBR Green IMaster (Roche Applied Science).

MAP4K4_F1   AAGATGTACGGCCACCTCAC R1   ATTCCGTTTCACCATTGCTC

MAP4K5 F1   GCAGCCAGCAGTTAGATTCC R1   TCCAGAAAGCCAACACACTG

MAP4K6_F1   GAGAACAGCAAAGGCCAAAG_R1   TGACCACAGAACCCTTCCTC

MAP4K7 F1   TCACCTGCACCAGCATAAAG R1   TGCCATCCAGTAGGGAGTTC

TBP-c472-01F AGTTCTGGGATTGTACCGCA

TBP-c610-01R TCCTCATGATTACCGCAGCA

Animals

The Ethical Committee for Animal Experiments of the Academic Medical Center (Amsterdam, The Netherlands) approved all animal protocols (LEICA-132AE) conform to the guidelines from Directive 2010/63/EU of the European Parliament on the protection of animals used for scientific purposes. Experiments were performed in 42 male C57/Bl6 mice with a mean ± SD bodyweight of 23.5 ± 1.7 gram purchased from Charles River Laboratories (The Netherlands). Animals were handled one week before the experiment to diminish stress activation. Housing took place in a specific-pathogen free facility on a 12/12 hour light/dark cycle and animals were allowed to take food and tap water ad libitum. Animals were

randomized into a control group (NaCl n=6), LPS group (n = 9), and LPS + bosutinib group (n=9). For the additional experiment assessing Evan's blue extravasation, each group consisted out of n=6.

Direct lung injury model

At baseline, mice were weighed and labelled, followed by intranasal administration of lipopolysaccharide (LPS; 5 mg/kg, E. Coli, serotype: 0127:B8, Sigma Aldrich, St. Louis, MO, USA) diluted in 50µl NaCl 0.9 % (NaCl, Braun, Germany) or 50µl NaCl 0.9% (NaCl group) under isoflurane anaesthesia (2–4 %). Concomitantly, mice received either bosutinib (Selleck chemicals s104, 20 mg/kg dissolved in a solution buffer (2% DMSO, 30% PEG, 5% Tween in MQ) or solution buffer only (control and LPS group) in a total volume of 500uL intraperitoneally (i.p.). After six hours, all animals were sacrificed under general anaesthesia (KDA mix: 1.26 mL 100 mg/mL Ketamine (Anesketin, EuroVetAnimal Health B.V., Bladel, The Netherlands) + 0.2 mL 0.5 mg/mL Dexmedetomidine (Pfizer Animal Health, B.V., Capelle a/d Ijssel, The Netherlands) + 1mL 0.5 mg/mL Atropine (Pharmachemie, Haarlem, The Netherlands) in 5mL 0.9 % NaCl by exsanguination via the vena cava inferior. Whole blood was collected a heparin-coated syringe and centrifuged for 10 minutes at 4000 rpm at 4 °C (Eppendorf, microcentrifuge). Plasma was obtained and stored at –80 °C for further analyses. Bronchoalveolar Lavage Fluid (BALF) was obtained from the left lung. The superior and inferior lobe of the right lung were excised for histopathologic examination. The two middle lobes were used for the lung weight / body weight ratio.

Assessment of lung injury

After ligating the hilum of the right lung, the trachea was cannulated and the left lung was washed three times with 0.3mL saline to obtain BALF. BALF was centrifuged for 10 minutes at 2000 rpm at 4 °C (Eppendorf, microcentrifuge) and stored at –80°C for further analyses. The superior and inferior lobe of the right lung were excised, instilled with 4 % paraformaldehyde and embedded in paraffin for histopathological assessment. The two middle lobes were removed and weighed together directly after resection followed by incubation in a 37 °C stove for determination of the dry weight after seven days. Total protein content in BALF was determined using the Lowry method. Total cell counts in BALF were evaluated with the Beckman Coulter (Fullerton, CA, USA). Differential cell counts were performed on cytospin preparations (Shandon CytospinR 4 Cytocentrifuge; Thermo Electron Corporation) and stained with a modified Giemsa stain (DiffQuick, Dade Behring AG, Duedingen, Switzerland). The inflammatory cytokine Interleukin (IL)–6 was assessed in plasma and BALF and tumor necrosis factor (TNF)–α was measured in BALF using a mouse-specific ELISA kit (R&D systems; Minneapolis, MN, USA) according to manufacturer's instructions. Histologic evidence of lung injury was assessed from hematoxylin and eosin-stained lung sections by using an established histopathologic score from 0 (no injury) to 3 (severe injury). This score consists of endothelialitis, bronchitis, edema formation, interstitial inflammation and hemorrhage which was scored by a blinded pathologist.

Evans blue extravasation

Lung permeability was determined by assessing tissue accrual of Evans blue (EB) (Sigma Chemical Co.) as previously described(52). Lung injury was induced and treatment administered as described above. After five hours, mice were anesthetized with isoflurane and 200μL of 0,5% Evans blue was administered via the penile vein. One hour later, animals were anesthetized as described above and sacrificed through blood collection from the heart. 5 ml of 0.9% NaCl was injected in the inferior vena cava to rinse the circulation. The right lung was collected, snapfrozen in liquid nitrogen and stored at -80°C. The left lung, kidneys and heart were placed in 300uL formamide at 55°C to extract the Evan's blue from the tissue. After 48 hours, the organs were placed in an incubator at 90°C for 24 hours to calculate and correct for dry weight. Evans blue concentration in supernatants was quantified by a dual wavelength spectrophotometric method at 620 nm and 740 nm absorbance and corrected for the dry weight.

Neutrophil isolation

Polymorphonuclear neutrophils (PMNs) were isolated from whole-blood derived from healthy donors. All volunteers signed an informed consent, under the rules and legislation in place within the Netherlands and maintained by the Sanquin Medical Ethical Committee. The rules and legislations are based on the Declaration of Helsinki and guidelines for Good Clinical Practice. Whole blood was diluted (1:1) with 5% (v/v) TNC in PBS. Diluted whole blood was pipetted carefully onto 12.5 ml Percoll (room temperature) 1.076 g/ml. Tubes were centrifuged (Rotanta 96R) at 800G, slow start, low brake for 20 min. Bottom fraction containing PMNs was further processed by erythrocyte lysis in ice-cold isotonic lysis buffer (155 mM NH4CL, 10 mM KHCO3, 0.1 mM EDTA, pH7.4 in Milli-Q(Millipore). PMNs were centrifuged at 500G for five minutes at 4 °C and incubated again with lysis buffer for 5 min on ice. After another centrifugation at 500G for 5 min at 4 °C, PMNs were washed once with PBS and centrifuged again at 500G for 5 min at 4 °C before resuspension in HEPES medium (20 mM HEPES, 132 mM NaCl, 6 mM KCl, 1 mM CaCl2, 1 mM MgSO4, 1.2 mM K2HPO4, 5 mM glucose (all from Sigma-Aldrich) and 0.4 % (w/v) human serum albumin (Sanquin Reagents), pH7.4). PMNs count and purity was determined by cell counter (Casy) and cells kept at room temperature for no longer than 4 h before use.

Transendothelial migration of neutrophils

Primairy lung microvascular endothelial cells (PMVECs) were cultured on fibronectin-coated ibidi slides in a density of $0.5*10^5$ per channel (μ-slide VI0.4, Ibidi). After 72 hours, cells were stimulated for 4h with 100 ng/mL of LPS (Sigma-Aldrich) and 1 μM DMSO or bosutinib. Freshly isolated PMNs were suspended in HEPES medium and activated by 30 min incubation at 37°C. Flow channels were connected to a perfusion system and exposed to 0.5 mL/min HEPES medium pH 7.4, shear flow (0.8 dyn/cm2) and $1*10^6$ cells/channel heat-activated PMN were injected. Leukocyte-endothelial interactions were recorded for 20 min at 0.2 frames/s by a Zeiss Observer Z1 microscope. All live imaging was performed at 37°C in the

presence of 5% CO_2. Transmigrated PMNs were distinguished from those adhering to the apical surface of the endothelium by their transition from bright to phase-dark morphology. Number of transmigrated PMNs was manually quantified using ImageJ.

Statistical analysis

Data are represented as mean ± SD. Comparison of 2 conditions were tested by student t-test. Comparison of more than 2 conditions were tested by 1-way ANOVA or repeated measures ANOVA. Dunnet's posthoc test was used when conditions were compared to one control, bonferroni posthoc test was used when multiple conditions were compared to multiple conditions unless indicated otherwise. P-values were considered statistically significant if $p<0.05$. Analysis was performed using Graphpad prism software.

Results

Bosutinib provides full protection against thrombin-induced endothelial barrier disruption

Previously, we identified the kinase inhibitor imatinib as a compound which protects against agonist-induced loss of barrier function (11). In search for novel, more effective barrier-protecting compounds, we tested three generations of Abl-kinase inhibitors on endothelial barrier function in HUVECs (Fig 1A,B, Fig S 1A,B). In these studies, we challenged stable endothelial monolayers with the protease thrombin, which represents a well-established model for inflammation induced loss of endothelial integrity. Similar to other G-protein-coupled receptor agonists, the loss of barrier function induced by thrombin is acute and reversible (Fig S1B). Our screen showed that the synthetic quinolone derivate bosutinib demonstrated the strongest protection to thrombin-challenged loss of endothelial barrier function. This was observed both in macromolecule passage assays (Fig. 1A&S1A) and in transendothelial electrical resistance assays (Fig. 1B&S1B). Validation experiments further confirmed that bosutinib increased basal barrier function, (Fig. S1C), and that bosutinib protected against thrombin and histamine-induced endothelial barrier disruption (Fig. 1C,D&S1D) at an optimal concentration of 1μM (Fig. S1E,F). Cell viability assays showed no cell toxicity at this concentration (Fig. S1G). Similar protective effects were observed in PMVECs (Fig. 1E) showing that barrier protection by bosutinib is neither agonist nor endothelial cell-type specific. These experiments demonstrate a strong protective effect of bosutinib against inflammation-induced endothelial barrier loss.

Subsequent immunofluorescent studies showed that bosutinib in both PMVECs and HUVECs protected against thrombin-induced intercellular gap formation,(Fig. 1F,G; S1H,I) and increased VE-cadherin intensity at cell-cell junctions (Fig. 1F,H; Fig S1H,J). Moreover, bosutinib increased the number of β1-integrin-positive FAs (Fig. 1F, I, Fig S1H,K). Bosutinib did not reduce F-actin stress fiber formation or Ser18/Thr19-phosphorylation of MLC (Fig. S1L), indicating that bosutinib does not inhibit actomyosin contractility. Total, VE-cadherin or

vinculin levels did not change after bosutinib treatment in Western blot (Fig. S1M-N). These results suggest that bosutinib protects against endothelial barrier disruption by enhancing VE-cadherin-containing adherens junctions and reinforcing β1-integrin-containing FAs.

Figure 1: Bosutinib provides robust protection against inflammation-induced endothelial barrier dysfunction. A) Macromolecule passage over HUVEC monolayers after 2 hours of thrombin stimulation with second and third generation tyroinse kinase inhibitors in their optimal concentration (n=5-6). Imatinib 10μM, GNF2 10μM, Nilotinib 10μM, Bosutinib 1μM, Nintedanib 1μM, Erlotinib 10μM and Dasatinib 0.1μM. B) Quantification of the thrombin response by calculating the maximal drop in endothelial resistance (%) as measured by ECIS. * compared to DMSO control and *&* compared to imatinib (n=6-8). C-D) Absolute endothelial resistance in HUVECs and quantification of the thrombin and histamine response by calculating the maximal drop in resistance (%) (n=3-4). E) Absolute endothelial resistance in PMVECs and quantification of the thrombin response by calculating the maximal drop in resistance (%) (n=3). F) Immunofluorescent staining of active integrin β1 (green) and VE-cadherin (red) in control versus bosutinib treated PMVECs counterstained with DAPI (blue). Scale bar represents 50 μm. Representative images of n=3 experiments. G) Gap area in control versus bosutinib treated PMVECs after 15 minutes of thrombin stimulation (n=3). H-I) VE-cadherin intensity (membrane/cytosol ratio) and number of integrin β1-containing FA in control versus bosutinib treated PMVECs stimulated with thrombin (n=3). *P<0.05, **P<0.01***P<0.001, ****P<0.0001. All data is represented as mean ± SD. Comparison of 2 conditions was tested by student t-test. Comparison of more than 2 conditions was tested by 1-way ANOVA or repeated measures ANOVA.

Figure 1
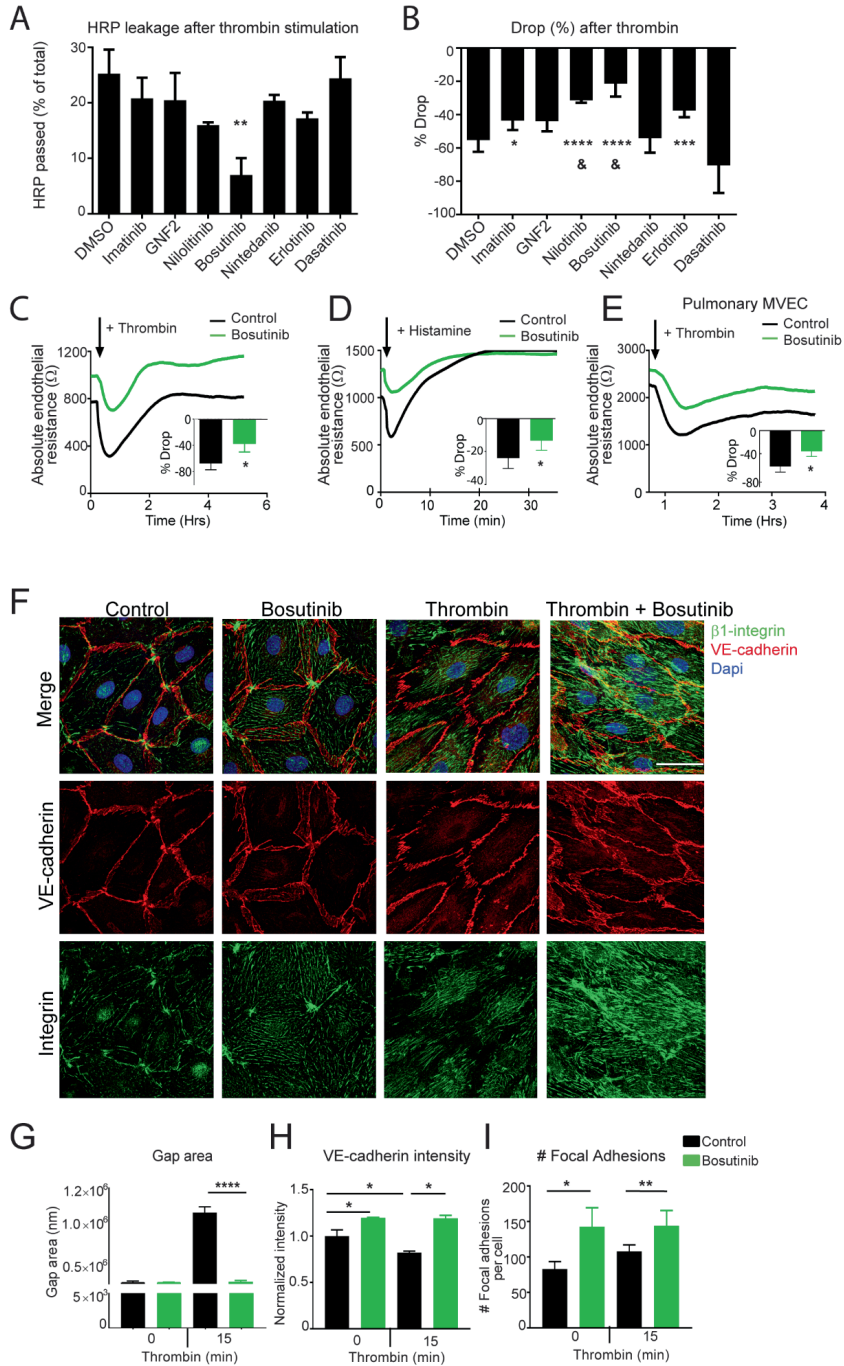
Inhibition of Mitogen-activated protein kinase 4 (MAP4K4) by bosutinib stabilizes endothelial barrier function

Our previous studies showed that imatinib prevents endothelial barrier dysfunction and edema via inhibition of Arg (11). As bosutinib had stronger barrier-protective effects than imatinib (Fig 1A,B), we hypothesized that combined inhibition of multiple kinases favors endothelial barrier preservation under inflammatory conditions. To understand which kinases could be involved, bosutinib and imatinib were profiled by measuring the inhibitory activity against 369 kinases at a single concentration in competition binding assays. Thresholds for kinase inhibition of ≥75% at 10nM bosutinib and ≤50% at 10μM imatinib were chosen to select candidate kinases that may account for the differential effects of these two inhibitors on endothelial barrier function (Fig 2A). Interestingly, bosutinib showed specificity against several mitogen-activated protein family of kinases (MAP4K4, MAP4K5, MAP4K6, MAP4K7). Since bosutinib showed highest specific kinase inhibition against MAP4K5, siRNA-mediated knockdown of MAP4K5 was tested in ECIS and compared to knockdown of MAP4K4, a kinase known to regulate focal adhesion and barrier function (22-24). siRNA-mediated knockdown of MAP4K4 resulted in specific and efficient (>80%) depletion of MAP4K4 (Fig S2A,B). To our surprise, depletion of MAP4K4, but not MAP4K5, significantly attenuated thrombin-induced barrier disruption (Fig. 2B& S2C). Simultaneous knockdown of both MAP4K4 and MAP4K5 did not further improve barrier protection (Fig. 2B,C). Different siRNAs for MAP4K4 displayed a similar degree protective effect during thrombin stimulation (Fig. S2D).

As prolonged knockdown may result in compensatory upregulation of redundant pathways, we evaluated the effect of a pharmacological MAP4K4 inhibitor (PF-6260933) that inhibits the trio of MAP4K4, 6 and 7 (24, 25). Treatment with PF-6260933 increased basal monolayer resistance and significantly attenuated the thrombin-induced loss of barrier function (Fig. 2C). MAP4K4 shares greater than 90% amino acid identity with MINK/MAP4K6 and TNIK/MAP4K7 (26) and redundancy and overlapping functions have been described for these kinases (26, 27). Knockdown of MAP4K6 and 7 did not improve endothelial barrier function and combined knockdown of the trio MAP4K4/6/7 gave similar results compared to siMAP4K4 alone (Fig. 2D, S2E). Knockdown efficiency and specificity is depicted in Fig. S2A&F-H, showing that MAP4K5 had some cross-reactivity with MAP4K6/7.

As Arg is inhibited by both bosutinib and imatinib, we hypothesized that combined inhibition of Arg and MAP4K family of kinases, results in a similar protective effect as bosutinib treatment. To test this, macromolecule passage was measured under basal conditions, showing significant reduction of macromolecule passage in siMAP4K4 (Fig. S2I), in line with the barrier stabilizing effect of bosutinib (Fig. 1C). Knockdown of MAP4K4 either alone or combined with the loss of Arg effectively reduced thrombin-induced HRP passage, although this effect did not mimic the protective effect of bosutinib completely (Fig. S2J). Likely, acute kinase inhibition by bosutinib is more effective in barrier protection as compared to the siRNA-mediated loss of cognate kinase expression quantified only after 72 hrs.

Notably, knockdown of Arg combined with PF-6260933 completely mimicked the positive effect of bosutinib on basal endothelial barrier function as well as thrombin-induced loss of integrity (Fig. 2D&S2K,I). Together, these data show that combined kinase inhibition of Arg and MAP4K4 can account for the protective effects of bosutinib on endothelial barrier function.
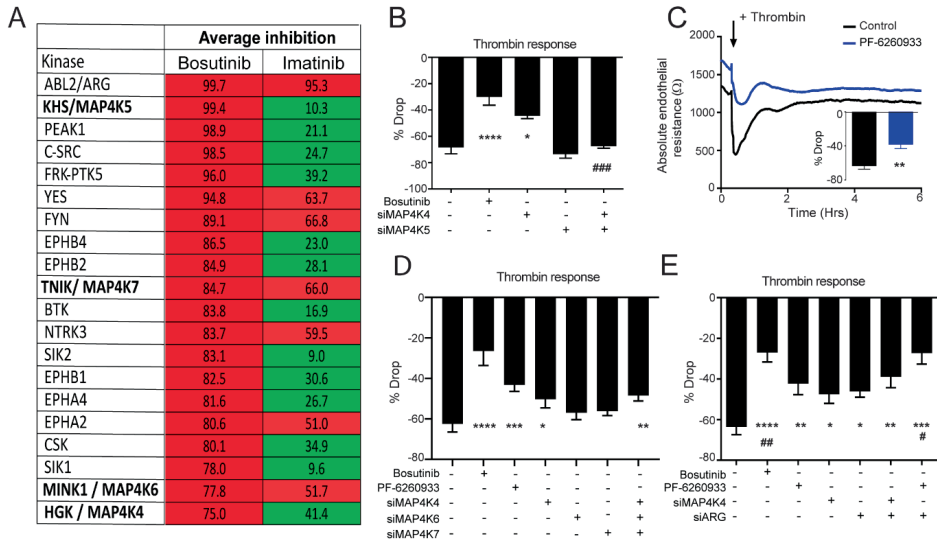
Figure 2

Figure 2: Inhibition of MAP4K4 by bosutinib enhances endothelial barrier function
A) Comparison of the kinase inhibitory activity of Abl-tyrosine kinase inhibitors bosutinib and imatinib. At a threshold of ≥75% inhibition at 10nM bosutinib and ≤50% at 10µM imatinib 13 kinases were identified to be inhibited by 1µM bosutinib but not by 10µM imatinib (shown in green), including mitogen-kinase activated family of kinases (MAP4K4/5/6/7). B) Quantification of the thrombin response by calculating the maximal drop in resistance after siMAP4K4 and siMAP4K5 (%) (n=3-5). C) Absolute endothelial resistance of HUVEC monolayers and percentage drop during thrombin stimulation with 3µM pharmacological MAP4K4 inhibitor PF-6260933 (n=3). D) Quantification of the thrombin response by calculating the maximal drop in resistance after bosutinib treatment, PF-6260933 and the knock down of MAP4K4/6/7 (n=3). Quantification of the thrombin response by calculating the maximal drop in resistance after knock down and inhibition of MAP4K4 with knock down of Arg (%) (n=5). *P<0.05 **P<0.01 ***P<0.001 ****P<0.0001 compared to NT control. #P<0.05 ##P<0.01 ###P<0.0001 compared to siMAP4K4. All data is represented as mean ± SD. Comparison of 2 conditions was tested by student t-test. Comparison of more than 2 conditions was tested by 1-way ANOVA.

To evaluate the effect of MAP4K4 on cell-cell junctions and cell-ECM interaction, immunostaining for VE-cadherin, active β1-integrin and F-actin was performed after treatment with siMAP4K4, siArg and PF-6260933 (Fig. 3A). VE-cadherin intensity was unaltered under basal conditions (Fig S3A,B). After thrombin stimulation, MAP4K4 knockdown or its inhibition completely prevented intercellular gap formation (Fig. 3A,B). In line with this, thrombin-induced loss of VE-cadherin intensity at the cell periphery was fully preserved after PF-6260933 treatment (Fig. 3C). Similar to bosutinib treatment, the number of FAs increased after inhibition or loss of MAP4K4 under basal conditions (Fig S3C) as well as in thrombin stimulated cells (Fig 3D). Peripheral focal adhesions were increased with bosutinib treatment, PF-6260933, siMAP4K4 and siArg with PF-6260933 (Fig 3E). Since the total number of FA also increased, the ratio remained unaltered in all conditions except bosutinib treatment (Fig. 3F).

In line with the effects of bosutinib on the F-actin cytoskeleton (Fig S1H), stress fiber formation was not affected by the loss or inhibition of Arg or MAP4K4 (Fig. S3A), indicating that increased acto-myosin-based contraction is not sufficient for intercellular gap formation. Together, these data provide further evidence that MAP4K4 and Arg both negatively regulate the stabilization of FAs and adherens junctions, and that combined loss or inhibition of these kinases might recapitulate the strong barrier protective effects of bosutinib.

MAP4K4 increases focal adhesion turnover

As recent studies pointed to a role for β1-integrin activation in maintaining VE-cadherin at AJs(14, 16, 17) and bosutinib enhanced β1-integrin localization in peripheral FAs (see Fig.1F,I & Fig.3D-F), we tested if MAP4K4 inhibition may have an additional effect via FA reorganization. The involvement of MAP4K4 in FA dynamics was analyzed using live-cell imaging of primary human endothelial cells expressing GFP-vinculin (Movie 1-3, Online Supplement). Time lapse images of GFP-vinculin expressing endothelial cells show basal FA dynamics after treatment with bosutinib or PF-6260933, followed by thrombin stimulation, in line with the data in Fig. 3B. Both bosutinib and PF-6260933 increased the abundance of FAs in unstimulated and in thrombin-treated cells. (Fig. 4A). We next quantified FA turnover, which showed that FA assembly and disassembly were decreased by bosutinib and PF-6260933 under basal and thrombin-stimulated conditions (Fig. 4B,C). This results in increased FA lifetime (Fig. 4D). In further support of a FA-stabilizing effect, bosutinib increased cell spreading as measured by ECIS (Fig. S3D-E) and by microscopy (Fig. 4E) without changing F-actin levels or MLC phosphorylation (Fig. S1L).

Figure 3
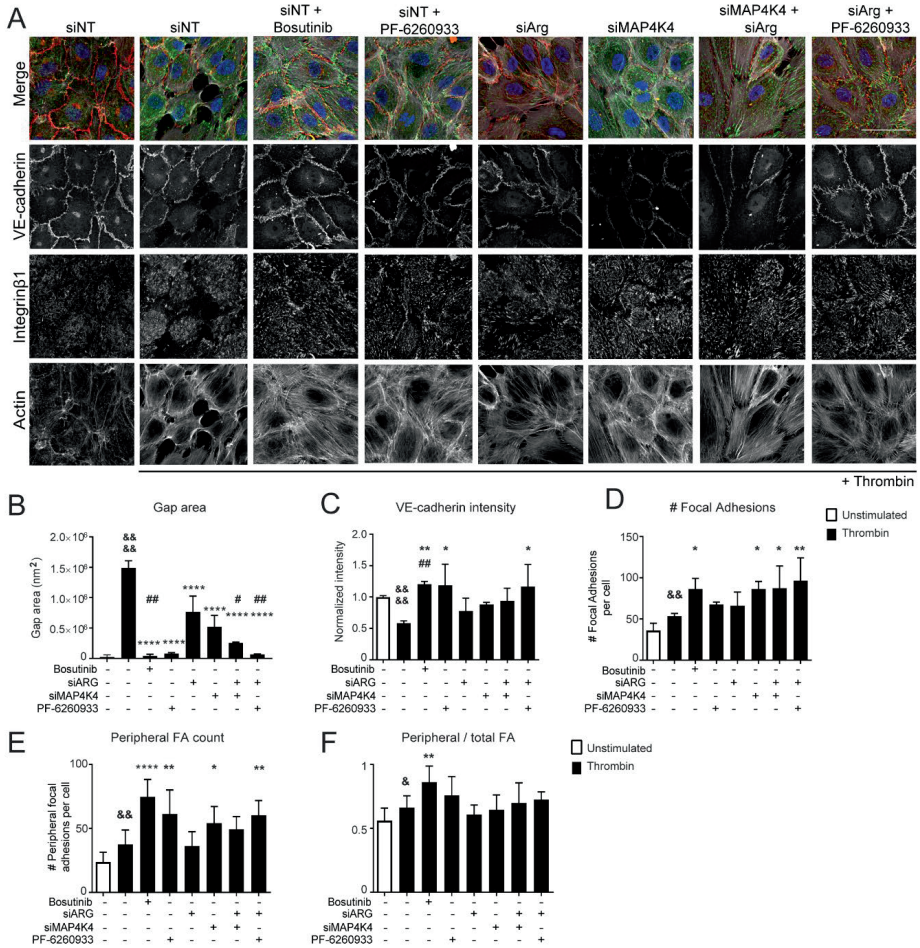
Figure 3: MAP4K4 inhibition increases endothelial barrier integrity

A) Immunofluorescent stainings of active integrinβ1 (green), actin (white) and VE-cadherin (red) under basal and thrombin stimulated conditions and counterstained with DAPI (blue). Treatment with bosutinib was compared with PF-6260933, siMAP4K4 and siArg. Scale bar represents 50μm. Representative images of n=4 experiments. B) Quantification of the gap area after 15 minutes of thrombin stimulation (n=3). C) Quantification of VE-cadherin intensity at the membrane divided by the intensity in the cytosol (n=3) D) Quantification of FA count using active integrinβ1 staining (n=3). E) Quantification of peripheral FA count per cell F) ratio of peripheral / total FA *p<0.05 **P<0.01 ***P<0.001 ****P<0.0001 compared to thrombin response. &P<0.05 &&P<0.01 &&&& P<0.0001 thrombin compared to basal conditions. #P<0.05 ##P<0.01 compared to siMAP4K4. All data is represented as mean ± SD. Comparison of 2 conditions was tested by student t-test. Comparison of more than 2 conditions was tested by 1-way ANOVA.

Figure 4
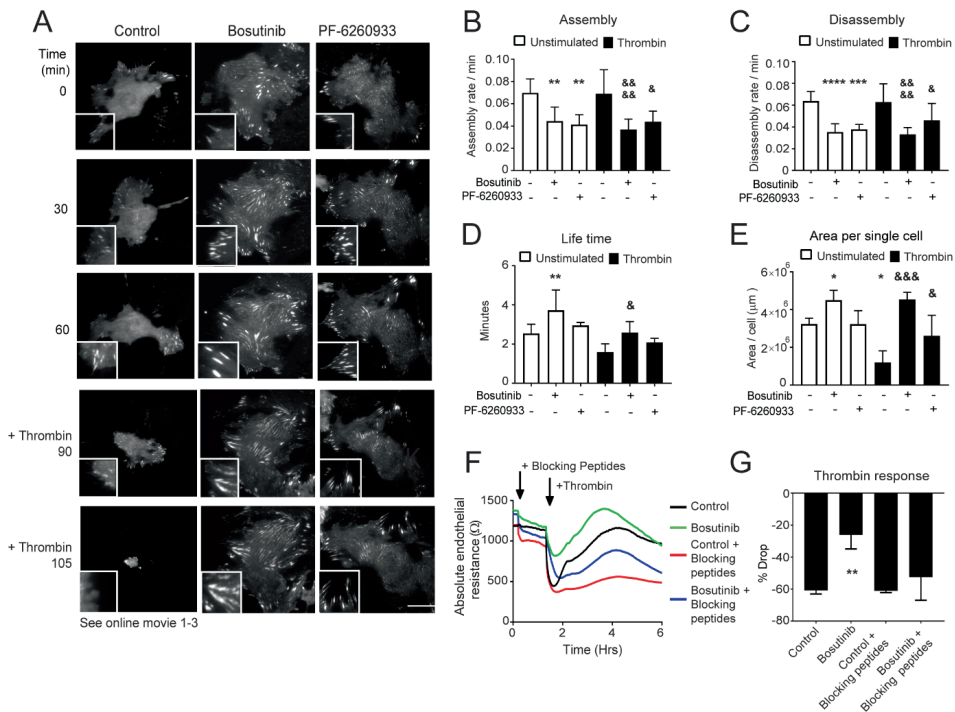
Figure 4: MAP4K4 enhances FA turnover
A) Representative images of movies on vinculin-containing FA imaged by TIRF microscopy every 30 seconds in control (DMSO), bosutinib or PF-6260933 treatment. Thrombin was added after 90 minutes. Scale bar represents 50μm. (B-D) Live-cell imaging analysis of single adhesions, including assembly rate (B), disassembly rate (C) and longevity (D) of GFP-vinculin under control (1 hour imaging) and thrombin stimulated (30-45 minutes imaging) conditions with bosutinib or PF-6260933 treatment (n=9-16 positions in 2 experiments). E) Quantification of single cell area after bosutinib and PF-6260933 under basal conditions and after 90-105 minutes of thrombin stimulation. F) Absolute endothelial resistance of HUVEC monolayers with thrombin stimulation. Control (black), bosutinib treatment (green), control with addition of 450μM peptides that block the adhesive function of integrins αvβ5, α5β1 and αvβ3 (red) and bosutinib treatment with addition of 450μM peptides that block the adhesive function of integrins αvβ5, α5β1 and αvβ3 (blue) (n=3). G) Quantification of maximal drop in resistance (%) after αvβ5, α5β1 and αvβ3 integrin blocking peptides (n=3) *P<0.05 **P<0.01 ***P<0.001 ****P<0.0001 compared to control. & P<0.05 &&& P<0.01 &&&& P<0.001 compared to thrombin stimulation. All data is represented as mean ± SD. Comparison of 2 conditions was tested by student t-test. Comparison of more than 2 conditions was tested by 1-way ANOVA.

Because MAP4K4 inhibition induced stabilization of both FA and AJ, we evaluated whether the observed FA stabilization contributes to AJ stabilization and endothelial barrier protection by bosutinib. We therefore used peptides that block integrin adhesive function (GRGDSP; GRGDNP) to evaluate whether bosutinib still protects the endothelial barrier in the absence of functional integrins and FA. GRGDSP is described to bind αvβ5 and α5β1 but preferential binding to αvβ3. GRGDNP also blocks adhesion by αvβ3 and α5β1 with similar specificity but preferential binding to α5β1 (28). As measured by transendothelial resistance, the simultaneous addition of GRGDSP and/or GRGDNP induced a loss of endothelial integrity in a concentration-dependent manner (Fig. S3F). No differences were observed between the different peptides when tested individually (Fig. S3G-H). Using an integrin-β1 blocking peptides in a low concentration at which the basal barrier function was not compromised (450μM), we found that bosutinib no longer rescued the thrombin-induced drop in barrier function (Fig. 4F,G & S3I). These results indicate that functional integrins are required for the barrier-protective effects of bosutinib and help to stabilize the endothelial barrier during thrombin-induced actomyosin contraction.

The MAP4K4-ERM pathway drives focal adhesion turnover during endothelial barrier disruption

Since MAP4K4 enhances FA turnover via phosphorylation of the ezrin, radixin and moesin (ERM) group of proteins (23), and since MAP4K4 directly binds the N-terminus of moesin (27), we hypothesized that MAP4K4 signals via ERM proteins to stabilize FAs and barrier function. In immunofluorescence studies, siMAP4K4 or PF-6260933 reduced junctional localization and intensity of phosphorylated ERM (Fig. 5A,B). Moreover, bosutinib treatment significantly decreased total phosphorylation of ERM proteins in western blot upon thrombin stimulation at several time points (Fig. 5C). This was not seen in cells treated with siMAP4K4, siArg or PF-6260933 (Fig. 5D&S4A)).

To test whether ERM proteins act downstream MAP4K4 during thrombin-induced barrier disruption, we compared the effect of silencing ezrin and moesin (siEzrin+siMoesin), both expressed in endothelial cells (29) with loss of MAP4K4 on thrombin-induced barrier disruption (see Fig. S4B for knockdown efficiency). Although siMAP4K4 and siEzrin+siMoesin attenuated the thrombin-induced drop in endothelial barrier function to a similar extent, combined siEzrin+siMoesin and siMAP4K4 had an additive protective effect (Fig. 5E&S4C). This can be explained by the fact that we observed restoration of VE-cadherin junctional intensity after thrombin stimulation in siEzrin+siMoesin treated cells, but not in siMAP4K4 treated cells (Fig. 5F,G). Furthermore, siMAP4K4 and siEzrin+siMoesin increased the number of FA to a similar extent, whereas the triple knockdown had no additive effect (Fig. 5H). Together, these data indicate that ERM proteins act downstream of MAP4K4 in stabilization of β1-integrin-based FA, whereas ERM proteins stabilize junctional VE-cadherin in a MAP4K4-independent manner.
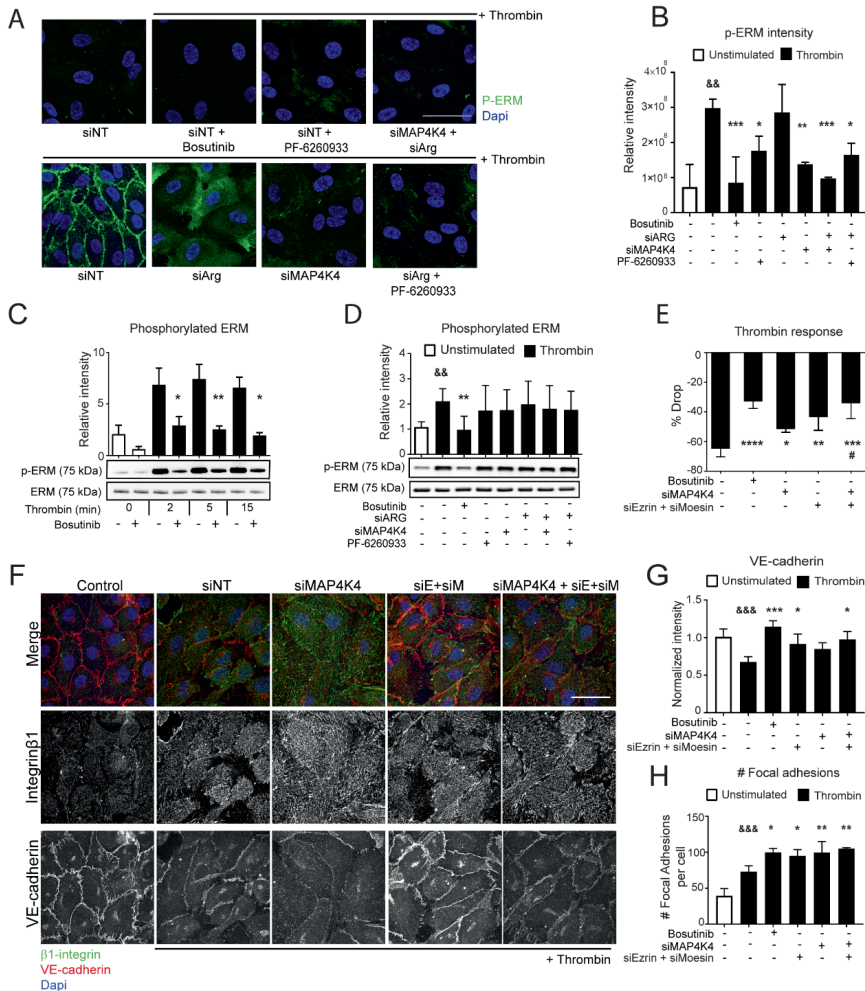
Figure 5

Figure 5: The MAP4K4-ERM pathway drives FA turnover during endothelial barrier disruption

A) Phospho Ezrin (Thr567)/ Radixin (Thr564)/ Moesin (Thr558) (green) counterstained with dapi (blue) in basal conditions and with 5 minutes of thrombin stimulation in siNT, siNT+bosutinib, siNT+PF-6260933nhibitor, siARG, siMAP4K4 and siARG+siMAP4K4 or siArg+ PF-6260933 (representative images of n=3) scale bar represents 50μm. B) Quantification of phospho Ezrin (Thr567)/ Radixin (Thr564)/ Moesin (Thr558) intensity in immunofluorescent stainings (n=3). C) Western blot analysis of phospho Ezrin (Thr567)/ Radixin (Thr564)/ Moesin (Thr558) after thrombin stimulation at 0-2-5-15 minutes compared to total ERM (n=3). D) Western blot analysis of phospho Ezrin (Thr567)/ Radixin (Thr564)/ Moesin (Thr558) after thrombin stimulation for 5 minutes compared to total ERM (n=3) E) Quantification of maximal drop in resistance in ECIS (%) after thrombin with bosutinib treatment, siMAP4K4 and PF-6260933 (n=3-4) F) Immunofluorescent staining for active integrin β1 (green), VE-cadherin (red) and counterstained with DAPI (blue) under basal conditions and with thrombin stimulation for 15 minutes in siNT, siMAP4K4, siE+siM and the

combination. Representative images of n=4 experiments, scale bar represents 50µm. G) Quantification of VE-cadherin intensity (membrane/cytosol ratio) after 15 minutes of thrombin stimulation (n=3-5). H) Quantification of FA number after 15 minutes of thrombin stimulation (n=4-5). *P<0.05 **P<0.01 ***P>0.001 ****P>0.001 compared to control, &&P<0.01 &&&P<0.001 thrombin response compared to unstimulated condition. # compared to siMAP4K4. All data is represented as mean ± SD. Comparison of 2 conditions was tested by student t-test. Comparison of more than 2 conditions was tested by 1-way ANOVA.

Bosutinib treatment attenuates LPS-induced pulmonary vascular leakage

Bosutinib is currently in clinical use for the treatment of chronic myeloid leukemia (20, 30). Repurposing bosutinib for prevention of vascular damage and edema would have large clinical benefit. We therefore tested the vascular barrier protective effects of bosutinib in a clinically relevant mouse model for pulmonary vascular leakage. Lung inflammation and edema were induced via intranasal administration of LPS in mice concomitantly treated with bosutinib (20 mg/kg) or saline (control) injection as previously described (31) (Fig. 6A). Lung vascular leakage, measured by the lung weight/body weight ratio and protein concentration in BALF, was significantly increased in the LPS treated animals and this effect was prevented by bosutinib (Fig. 6B,C). As an additional measure of vascular leakage, 0.5% Evans Blue was administered intravenously five hours after the induction of lung injury, and organs were harvested one hour after Evans Blue administration. Evans Blue extravasation was significantly increased in lungs and kidneys of LPS-treated mice, an effect that was prevented in bosutinib-treated mice (Fig. S5A-C).

Inflammation, measured by total cell count, percentage neutrophils together with IL-6 levels in BALF were markedly increased after LPS administration and significantly attenuated by bosutinib treatment (Fig. 6D-F), although active trans-endothelial neutrophil migration over pulmonary endothelial cells was not affected by bosutinib (Fig. S5F). TNF-α concentration in BALF was increased after LPS exposure, however, no significant reduction was observed with bosutinib treatment (Fig. S5D). A systemic inflammatory cytokine response measured by circulating IL-6 in plasma was not observed (Fig. S5E). As an additional measure of direct lung injury, the LPS-treated mice showed a significantly higher histopathology score in endothelialitis, edema, interstitial inflammation and hemorrhage in the lungs, whereas bosutinib significantly reduced edema and hemorrhage scores (Fig. 6G). These data demonstrate that repurposing the clinically available drug bosutinib, effectively reduces inflammation-induced lung vascular leakage.
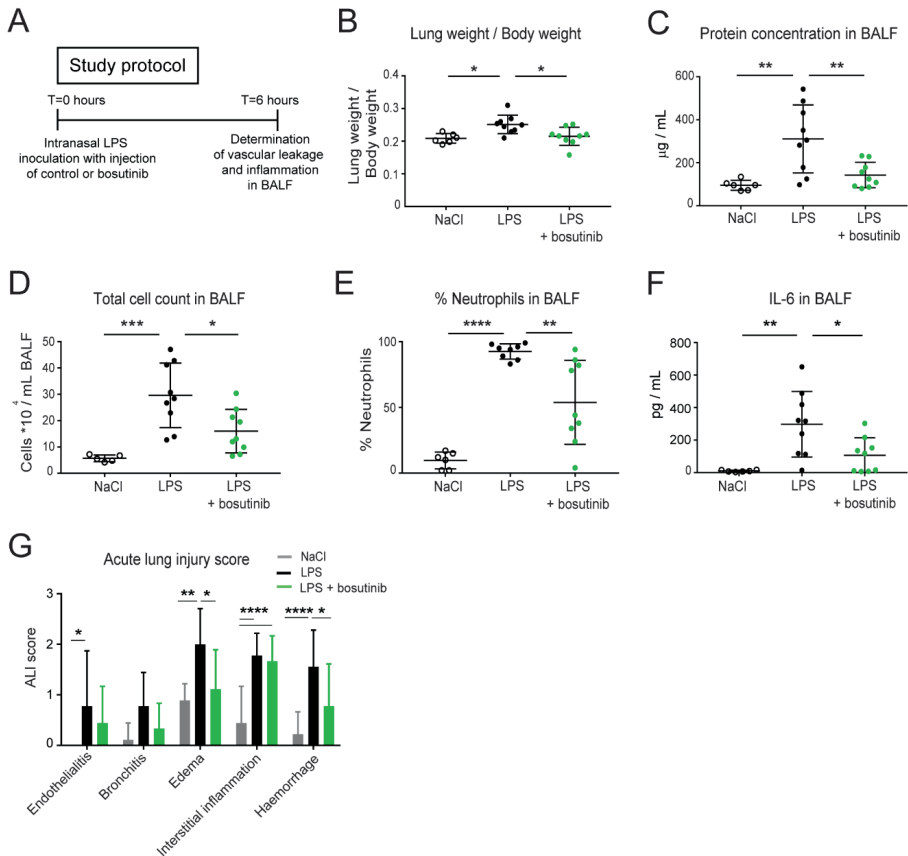
5

Figure 6

Figure 6: Bosutinib treatment attenuates LPS-induced pulmonary vascular leakage
A)Lung injury was induced in 42 male C57/BL6J mice by intranasal inoculation of LPS to assess the effect of bosutinib on direct LPS induced lung-injury. B-C) Vascular leakage was determined by calculating the ratio of lung weight divided by the body weight and by measuring protein concentration in BALF (n=6-9 per group). D-F) Inflammation in BALF measured by total cell count, percentage neutrophils and IL-6 concentrations in BALF (n=6-9 per group). G) Acute lung injury score quantified blind in histological coupes of right lungs (n=6-9 per group).   *P<0.05 **P<0.01 ***P<0.001 ****P<0.0001. All data is represented as mean ± SD.Comparison of 2 conditions was tested by student t-test. Comparison of more than 2 conditions was tested by 1-way ANOVA.
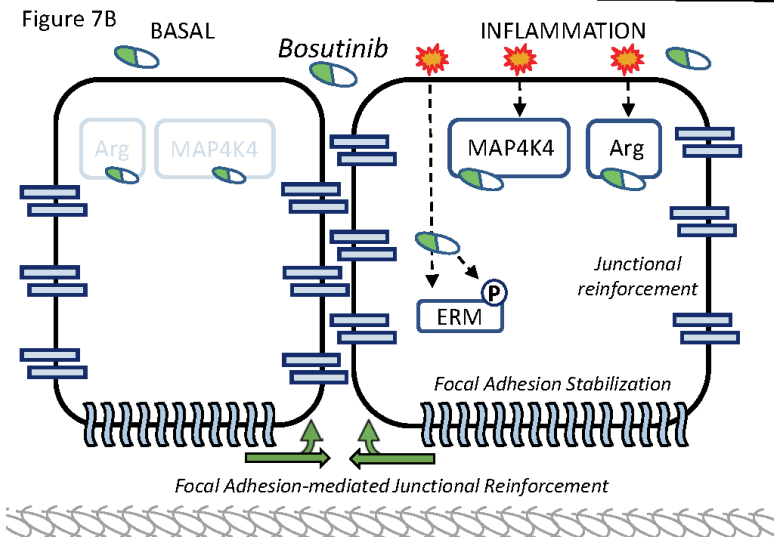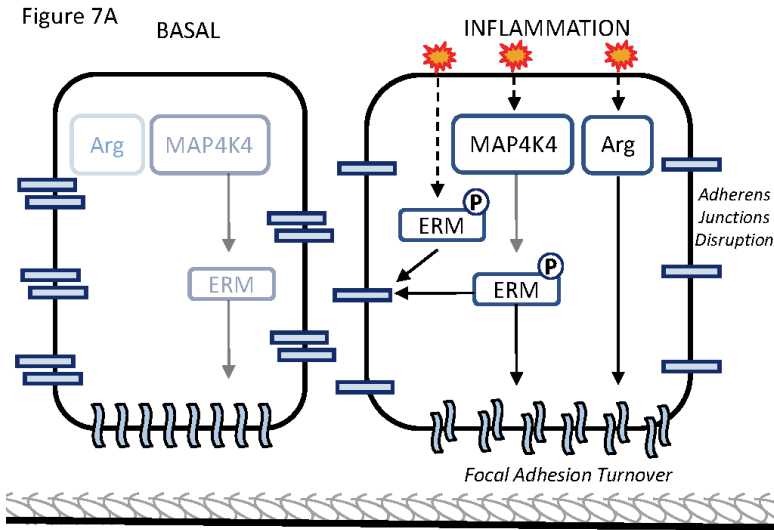
Figure 7: Proposed mechanism

A) Under basal conditions, Arg is not active and minor MAP4K4 activity results in minimal FA turnover. During inflammation, for example in thrombin stimulated conditions, MAP4K4 and Arg signal to increase FA turnover, reducing cell-matrix adhesion. MAP4K4 either phosphorylates part of the ERMs at a specific location in the cell and / or affects the translocation of phosphorylated ERM as indicated by a transparent arrow, disrupting AJs.

B) Bosutinib (indicated as white-green tablet), inhibits several kinases including Arg and MAP4K4, enhancing basal barrier integrity. During inflammation, for example in thrombin stimulated conditions, bosutinib prevents FA turnover through Arg and MAP4K4 inhibition. Bosutinib inhibits ERM activity directly, as through a MAP4K4-inhibiting effect. This results in junctional reinforcement and increased cell-cell contact. Stable FA further signal to AJs, to increase endothelial barrier integrity.

Discussion

While the molecular basis of endothelial integrity is extensively studied, compounds that provide effective protection against vascular leak, strongly associated with inflammatory disease, remain to be identified. Here we show that the AKI bosutinib provides full protection against agonist-induced endothelial- and vascular permeability *in vitro* and *in vivo*. We identified MAP4K4 as an important regulator of endothelial barrier function, contributing to adherens junction dissociation and signaling via ERM to increase FA turnover, with subsequent cell retraction and barrier disruption (Fig. 7). Our data support a model in which the turnover of peripheral, β1-integrin containing FAs contributes to the loss of VE-cadherin mediated cell-cell contact (Fig. 7) (16, 32). While we previously showed that the first generation AKI imatinib provides partial protection from vascular leak by inhibiting Arg, bosutinib is more effective due to its additional effect on MAP4K4, a kinase only moderately targeted by imatinib (Fig 2A).

Identification of MAP4K4 as regulator of endothelial barrier function

The regulation and function of individual serine/threonine MAP4K family of kinases is largely unknown, although MAP4K4 has repeatedly emerged as regulator of cell migration, adhesion and FA stabilization (22, 33-35). MAP4K4 activation by TNFα regulates important inflammatory responses including cytokine production as well as atherosclerosis and insulin resistance (24, 25, 36). Divergent findings regarding a role for MAP4K4 in endothelial barrier function have been reported. Vitorino et al found no role for MAP4K4 in basal endothelial permeability using siRNA-mediated knockdown. On the other hand, others report that depletion of MAP4K4 increased basal barrier resistance (37) and macromolecule permeability reduced in MAP4K4-silenced monolayers basally, and after TNF-α-mediated inflammation *in vitro* (24). A role for MAP4K4 for barrier function has been suggested by the observations that inhibition of MAP4K4 reduces cholesterol accumulation in aorta of mice and knockdown of MAP4K4 increased basal endothelial barrier function (24, 37). Family members of the serine/threonine MAP4K4 kinase family MAP4K6 and MAP4K7 share a common function in regulating cell shape and migration and show greater than 90% amino acid identity (27). Despite this structural similarity only knockdown of MAP4K4, but not 6 and 7 protected against endothelial barrier disruption during inflammation.

Focal adhesion distribution by bosutinib and MAP4K4 is mediated by ERM

We observed that bosutinib and MAP4K4 inhibition stabilized FA dynamics, leading to increased spreading of endothelial cells to the ECM. Since we found imatinib to increase predominantly peripheral FA through Arg inhibition (11, 38), we propose that bosutinib exerts an additional effect on FA dynamics by increasing β1 integrin and FA stability and longevity through MAP4K4 inhibition. Indeed, loss of MAP4K4 and moesin increased the number of both central and peripheral FA (23). Moesin is the most abundant ERM protein in endothelial cells and the individual ERM proteins show functional redundancy (29, 39). ERM

proteins control cell shape through crosslinking the actin cytoskeleton to the plasma membrane (27, 29, 40) and phosphorylation of ERM after thrombin stimulation induces its translocation to the cell periphery, modulating AJ integrity and promoting gap formation (29, 41). pERM were previously also detected in endothelial retraction fibers, linking ERM-phosphorylation to the induction of contraction (23). In line with these observations, the present study demonstrates that ERM proteins act downstream of MAP4K4 to regulate β1 integrin activity and FA turnover during inflammation. As MAP4K4 inhibition increased cell adhesion and spreading, the MAP4K4/ERM pathway appears as an important mediator of decreased cell-ECM binding of endothelial cells under inflammatory conditions, although we cannot exclude a role for ERM protein in endothelial barrier regulation independent from MAP4K4.

Interaction between focal adhesions and adherens junctions in endothelial barrier regulation

The protective effects of bosutinib were paralleled by improvement of AJ integrity and FA stability. Whereas the contribution of the AJ to endothelial barrier integrity is undisputed, the functional role of FA, and specifically integrins, is more controversial. We showed that peptides blocking the adhesive function of integrins αvβ5, α5β1 and αvβ3 counteracted the protective effect of bosutinib, indicating that FAs are functionally involved in endothelial barrier regulation and required for a functional barrier. It is known that β1-integrin interacts directly with talin (42) and that β1-integrins stabilize cell-cell contacts (14-16). Although it is reported that integrin engagement leads to disruption of VE-cadherin containing AJ via the activation of Src kinase (43) and that β1-integrin-inhibiting antibodies decrease LPS-induced vascular leakage in murine endotoxemia (17), our data demonstrate that bosutinib decreases FA turnover and enhance cell adhesion to impair cell retraction, even in the presence of intact acto-myosin contraction. Although previous studies have shown that intact FA are essential for a mature endothelial barrier (14-16) the present study is the first to demonstrate that active regulation of FA turnover contributes to the hyperpermeability response *in vitro* and *in vivo*. Inhibition of Arg and MAP4K4 simultaneously with ERM-mediated reinforcement of the AJ, leads to barrier stabilization. This mechanism aligns well with the suggestion in previous studies that peripheral FA reinforce AJ integrity (16, 17).

Perspective

Bosutinib attenuated vascular leakage, protein extravasation and inflammation in a murine acute lung injury model, in line with previous research on virus induced vascular leakage in human pulmonary endothelial cells (44) and recovery of lung inflammation in an animal model for silicosis (45). In addition, in our study LPS and bosutinib were administered simultaneously preventing the development of lung edema. Active neutrophil migration remained unchanged *in vitro*, therefore we could not exclude a direct effect of bosutinib on neutrophil migration. As a clinically available drug, bosutinib is orally administered and well tolerated (46), with milder cardiac hypertrophy and fewer vascular adverse events compared

to several other AKIs (21, 47). Moreover, only low-grade gastrointestinal toxicity is reported after bosutinib treatment (30). Based on these drug characteristics, the fact that bosutinib inhibits endothelial MAP4K4 during inflammation, and the protective effects of bosutinib on vascular endothelial integrity identified in this study, repurposing bosutinib as novel treatment for clinical syndromes associated with vascular leak is a suitable option.

Conclusion

During inflammation, Arg and MAP4K4 signal to increase turnover of integrin-based peripheral FAs, which is required for the loss of VE-cadherin mediated cell-cell contact. This study identifies MAP4K4/ERM signaling as important pathway that mediates stimulus induced FA dissolution and adherens junction dissociation. Since the clinically available drug bosutinib inhibits both Arg and MAP4K4/ERM signaling, bosutinib may be a viable strategy against vascular leakage.

References

1. Mehta D, Malik AB. Signaling mechanisms regulating endothelial permeability. Physiol Rev. 2006;86(1):279-367.
2. Komarova YA, Kruse K, Mehta D, Malik AB. Protein Interactions at Endothelial Junctions and Signaling Mechanisms Regulating Endothelial Permeability. Circ Res. 2017;120(1):179-206.
3. Lee WL, Slutsky AS. Sepsis and endothelial permeability. N Engl J Med. 2010;363(7):689-91.
4. Wessel F, Winderlich M, Holm M, Frye M, Rivera-Galdos R, Vockel M, et al. Leukocyte extravasation and vascular permeability are each controlled in vivo by different tyrosine residues of VE-cadherin. Nat Immunol. 2014;15(3):223-30.
5. Filewod NC, Lee WL. Inflammation without Vascular Leakage Science Fiction No Longer? Am J Resp Crit Care. 2019;200(12):1472-6.
6. Matthay MA, Zemans RL, Zimmerman GA, Arabi YM, Beitler JR, Mercat A, et al. Acute respiratory distress syndrome. Nat Rev Dis Primers. 2019;5(1):18.
7. Dejana E, Giampietro C. Vascular endothelial-cadherin and vascular stability. Curr Opin Hematol. 2012;19(3):218-23.
8. Gavard J. Endothelial permeability and VE-cadherin: a wacky comradeship. Cell Adh Migr. 2013;7(6):455-61.
9. Huveneers S, Oldenburg J, Spanjaard E, van der Krogt G, Grigoriev I, Akhmanova A, et al. Vinculin associates with endothelial VE-cadherin junctions to control force-dependent remodeling. J Cell Biol. 2012;196(5):641-52.
10. Aman J, Peters MJ, Weenink C, van Nieuw Amerongen GP, Vonk Noordegraaf A. Reversal of vascular leak with imatinib. Am J Respir Crit Care Med. 2013;188(9):1171-3.
11. Aman J, van Bezu J, Damanafshan A, Huveneers S, Eringa EC, Vogel SM, et al. Effective treatment of edema and endothelial barrier dysfunction with imatinib. Circulation. 2012;126(23):2728-38.
12. Hynes RO. Integrins: bidirectional, allosteric signaling machines. Cell. 2002;110(6):673-87.
13. Shattil SJ, Kim C, Ginsberg MH. The final steps of integrin activation: the end game. Nat Rev Mol Cell Biol. 2010;11(4):288-300.
14. Yamamoto H, Ehling M, Kato K, Kanai K, van Lessen M, Frye M, et al. Integrin beta1 controls VE-cadherin localization and blood vessel stability. Nat Commun. 2015;6:6429.
15. Song J, Zhang X, Buscher K, Wang Y, Wang H, Di Russo J, et al. Endothelial Basement Membrane Laminin 511 Contributes to Endothelial Junctional Tightness and Thereby Inhibits Leukocyte Transmigration. Cell Rep. 2017;18(5):1256-69.
16. Pulous FE, Grimsley-Myers CM, Kansal S, Kowalczyk AP, Petrich BG. Talin-Dependent Integrin Activation Regulates VE-Cadherin Localization and Endothelial Cell Barrier Function. Circ Res. 2019.
17. Hakanpaa L, Kiss EA, Jacquemet G, Miinalainen I, Lerche M, Guzman C, et al. Targeting beta1-integrin inhibits vascular leakage in endotoxemia. Proc Natl Acad Sci U S A. 2018.
18. Su G, Atakilit A, Li JT, Wu N, Bhattacharya M, Zhu J, et al. Absence of integrin alphavbeta3 enhances vascular leak in mice by inhibiting endothelial cortical actin formation. Am J Respir Crit Care Med. 2012;185(1):58-66.
19. Su G, Hodnett M, Wu N, Atakilit A, Kosinski C, Godzich M, et al. Integrin alphavbeta5 regulates lung vascular permeability and pulmonary endothelial barrier function. Am J Respir Cell Mol Biol. 2007;36(3):377-86.
20. Khoury HJ, Cortes JE, Kantarjian HM, Gambacorti-Passerini C, Baccarani M, Kim DW, et al. Bosutinib is active in chronic phase chronic myeloid leukemia after imatinib and dasatinib and/or nilotinib therapy failure. Blood. 2012;119(15):3403-12.
21. Gover-Proaktor A, Granot G, Pasmanik-Chor M, Pasvolsky O, Shapira S, Raz O, et al. Bosutinib, dasatinib, imatinib, nilotinib, and ponatinib differentially affect the vascular molecular pathways and functionality of human endothelial cells. Leuk Lymphoma. 2018:1-11.

5

22.   Yue J, Xie M, Gou X, Lee P, Schneider MD, Wu X. Microtubules regulate focal adhesion dynamics through MAP4K4. Dev Cell. 2014;31(5):572-85.

23.   Vitorino P, Yeung S, Crow A, Bakke J, Smyczek T, West K, et al. MAP4K4 regulates integrin-FERM binding to control endothelial cell motility. Nature. 2015;519(7544):425-30.

24.   Roth Flach RJ, Skoura A, Matevossian A, Danai LV, Zheng W, Cortes C, et al. Endothelial protein kinase MAP4K4 promotes vascular inflammation and atherosclerosis. Nat Commun. 2015;6:8995.

25.   Ammirati M, Bagley SW, Bhattacharya SK, Buckbinder L, Carlo AA, Conrad R, et al. Discovery of an in Vivo Tool to Establish Proof-of-Concept for MAP4K4-Based Antidiabetic Treatment. ACS Med Chem Lett. 2015;6(11):1128-33.

26.   Chuang HC, Wang X, Tan TH. MAP4K Family Kinases in Immunity and Inflammation. Adv Immunol. 2016;129:277-314.

27.   Baumgartner M, Sillman AL, Blackwood EM, Srivastava J, Madson N, Schilling JW, et al. The Nck-interacting kinase phosphorylates ERM proteins for formation of lamellipodium by growth factors. Proc Natl Acad Sci U S A. 2006;103(36):13391-6.

28.   Kapp TG, Rechenmacher F, Neubauer S, Maltsev OV, Cavalcanti-Adam EA, Zarka R, et al. A Comprehensive Evaluation of the Activity and Selectivity Profile of Ligands for RGD-binding Integrins. Sci Rep. 2017;7:39805.

29.   Adyshev DM, Dudek SM, Moldobaeva N, Kim KM, Ma SF, Kasa A, et al. Ezrin/radixin/moesin proteins differentially regulate endothelial hyperpermeability after thrombin. Am J Physiol Lung Cell Mol Physiol. 2013;305(3):L240-55.

30.   Kong JH, Khoury HJ, Kim AS, Hill BG, Kota V. The safety of Bosutinib for the treatment of chronic myeloid leukemia. Expert Opin Drug Saf. 2017;16(10):1203-9.

31.   Tuinman PR, Muller MC, Jongsma G, Hegeman MA, Juffermans NP. High-dose acetylsalicylic acid is superior to low-dose as well as to clopidogrel in preventing lipopolysaccharide-induced lung injury in mice. Shock. 2013;40(4):334-8.

32.   Pulous FE, Petrich BG. Integrin-dependent regulation of the endothelial barrier. Tissue Barriers. 2019;7(4):1685844.

33.   Huang C, Jacobson K, Schaller MD. MAP kinases and cell migration. J Cell Sci. 2004;117(Pt 20):4619-28.

34.   Tripolitsioti D, Kumar KS, Neve A, Migliavacca J, Capdeville C, Rushing EJ, et al. MAP4K4 controlled integrin beta1 activation and c-Met endocytosis are associated with invasive behavior of medulloblastoma cells. Oncotarget. 2018;9(33):23220-36.

35.   Machida N, Umikawa M, Takei K, Sakima N, Myagmar BE, Taira K, et al. Mitogen-activated protein kinase kinase kinase kinase 4 as a putative effector of Rap2 to activate the c-Jun N-terminal kinase. J Biol Chem. 2004;279(16):15711-4.

36.   Huang H, Tang Q, Chu H, Jiang J, Zhang H, Hao W, et al. MAP4K4 deletion inhibits proliferation and activation of CD4(+) T cell and promotes T regulatory cell generation in vitro. Cell Immunol. 2014;289(1-2):15-20.

37.   Pannekoek WJ, Linnemann JR, Brouwer PM, Bos JL, Rehmann H. Rap1 and Rap2 antagonistically control endothelial barrier resistance. PLoS One. 2013;8(2):e57903.

38.   Rizzo AN, Aman J, van Nieuw Amerongen GP, Dudek SM. Targeting Abl kinases to regulate vascular leak during sepsis and acute respiratory distress syndrome. Arterioscler Thromb Vasc Biol. 2015;35(5):1071-9.

39.   Fehon RG, McClatchey AI, Bretscher A. Organizing the cell cortex: the role of ERM proteins. Nat Rev Mol Cell Biol. 2010;11(4):276-87.

40.   Tachibana K, Haghparast SM, Miyake J. Inhibition of cell adhesion by phosphorylated Ezrin/Radixin/Moesin. Cell Adh Migr. 2015;9(6):502-12.

41.   Amsellem V, Dryden NH, Martinelli R, Gavins F, Almagro LO, Birdsey GM, et al. ICAM-2 regulates vascular permeability and N-cadherin localization through ezrin-radixin-moesin (ERM) proteins and Rac-1 signalling. Cell Commun Signal. 2014;12:12.

42.   Giancotti FG. Complexity and specificity of integrin signalling. Nat Cell Biol. 2000;2(1):E13-4.

43.   Wang Y, Jin G, Miao H, Li JY, Usami S, Chien S. Integrins regulate VE-cadherin and catenins: dependence of this regulation on

Src, but not on Ras. Proc Natl Acad Sci U S A. 2006;103(6):1774-9.

44. Gorbunova EE, Gavrilovskaya IN, Pepini T, Mackow ER. VEGFR2 and Src kinase inhibitors suppress Andes virus-induced endothelial cell permeability. J Virol. 2011;85(5):2296-303.

45. Carneiro PJ, Clevelario AL, Padilha GA, Silva JD, Kitoko JZ, Olsen PC, et al. Bosutinib Therapy Ameliorates Lung Inflammation and Fibrosis in Experimental Silicosis. Front Physiol. 2017;8:159.

46. Cortes JE, Gambacorti-Passerini C, Deininger MW, Mauro MJ, Chuah C, Kim D-W, et al. Bosutinib Versus Imatinib for Newly Diagnosed Chronic Myeloid Leukemia: Results From the Randomized BFORE Trial. Journal of Clinical Oncology.0(0):JCO.2017.74.7162.

47. Heyen JR, Hu W, Jamieson J, Thibault S, Batugo M, Loi C-M, et al. Cardiovascular differentiation of imatinib and bosutinib in the rat. International Journal of Hematology. 2013;98(5):597-607.

48. Jaffe EA, Nachman RL, Becker CG, Minick CR. Culture of Human Endothelial cells derived from Umbilical veins. j Clin Invest. 1973;52(11):2745-56.

49. Szulcek R, Happe CM, Rol N, Fontijn RD, Dickhoff C, Hartemink KJ, et al. Delayed Microvascular Shear Adaptation in Pulmonary Arterial Hypertension. Role of Platelet Endothelial Cell Adhesion Molecule-1 Cleavage. American journal of respiratory and critical care medicine. 2016;193(12):1410-20.

50. Berginski ME, Vitriol EA, Hahn KM, Gomez SM. High-resolution quantification of focal adhesion spatiotemporal dynamics in living cells. PLoS One. 2011;6(7):e22025.

51. Berginski ME, Gomez SM. The Focal Adhesion Analysis Server: a web tool for analyzing focal adhesion dynamics. F1000Res. 2013;2:68.

52. Green TP, E. JD, Marchessault RP, Gatto CW. Transvascular flux and tissue accrual of Evans blue: effects of endotoxin and histamine. J Lab Clin Med. 1988;111(2):173-83.

5

SUPPLEMENTAL INFORMATION
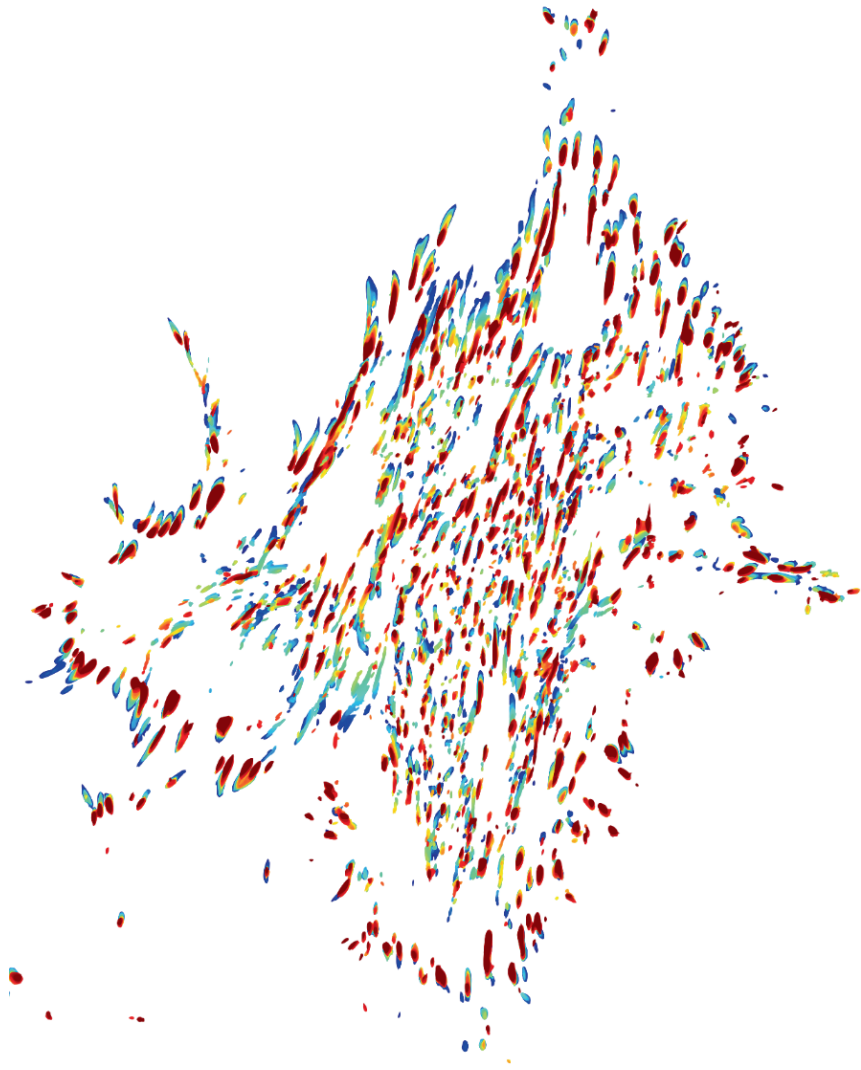
Supplemental figure 1
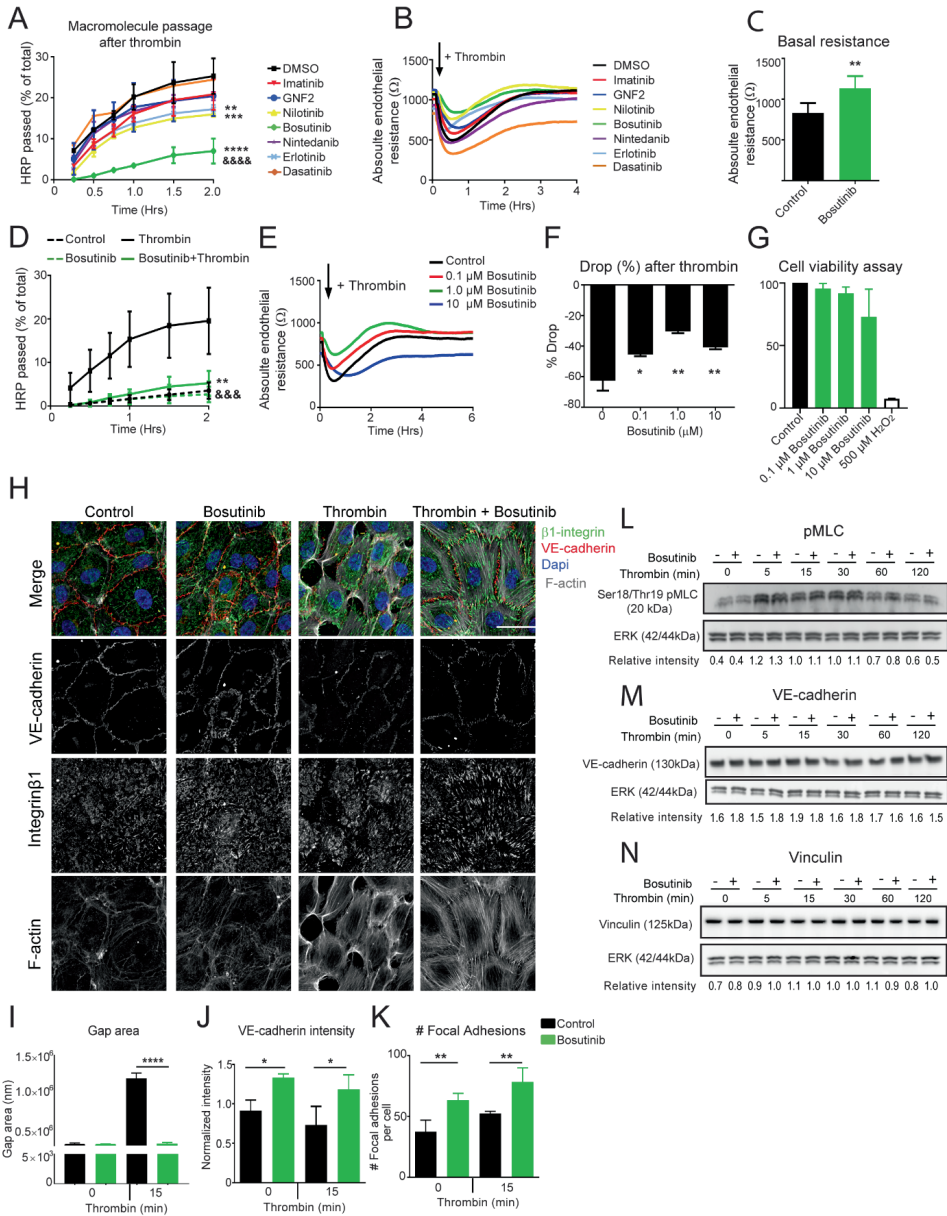
Supplemental figure 1: A) Macromolecule passage over HUVEC monolayers after 90 minutes of pre-incubations during thrombin stimulation (n=5-6) with second and third generation tyroinse kinase inhibitors in their optimal concentration (n=5-6). Imatinib 10µM, GNF2 10µM, Nilotinib 10µM, Bosutinib 1µM, Nintedanib 1µM, Erlotinib 10µM and Dasatinib 0.1µM B) Absolute endothelial resistance of HUVEC monolayers in ECIS after 90 minutes of pre-incubations with several AKIs (n=3). C) Absolute endothelial resistance of HUVEC monolayers under basal conditions after 90 minutes of bosutinib treatment (n=4). D) HRP passage over HUVEC monolayers with bosutinib compared to control conditions. Dotted line unstimulated condition, continuous line for thrombin treatment (n=3). E) Absolute endothelial resistance of HUVEC monolayers after increasing concentrations of bosutinib incubation (0.1-1.0-10µM) and thrombin stimulation (n=3). F) Quantification of the thrombin response (%) by calculating the maximal drop in resistance after increasing concentrations of bosutinib incubation (0.1-1.0-10µM) (n=3). G) Cell viability assay as measured by conversion of MTT (3-(4,5-dimethylthiazol-2-yl)-2,5-diphenyltetrazolium bromide). The number of viable cells was measured at an absorbance of OD 590 nm (background corrected) and calculated as OD sample / control * 100. H) Immunofluorescent staining of active integrin β1 and VE-cadherin and F-actin in control versus bosutinib treated HUVECs counterstained with dapi (blue). Scale bar represents 50 µm. (Representative images of n=4 experiments). I) Gap area in control versus bosutinib treated HUVECs after 15 minutes of thrombin stimulation (n=4). J-K) VE-cadherin intensity (membrane/cytosol ratio) and number of integrin β1-containing FA in control versus bosutinib treated HUVECs stimulated with thrombin (n=4) L-N) Western blot analysis of Ser18/Thr19 myosin light chain (MLC) phosphorylation, total VE-cadherin and vinculin after thrombin stimulation (n=3). Represenative blots of n=3*P<0.05 **P<0.01 ***P<0.001 ****P<0.0001 compared to control. &&&&P<0.0001 compared to imatinib. &&&P<0.001 compared to thrombin. All data is represented as mean ± SD. Comparison of 2 conditions was tested by student t-test. Comparison of more than 2 conditions was tested by 1-way ANOVA or repeated measures ANOVA.
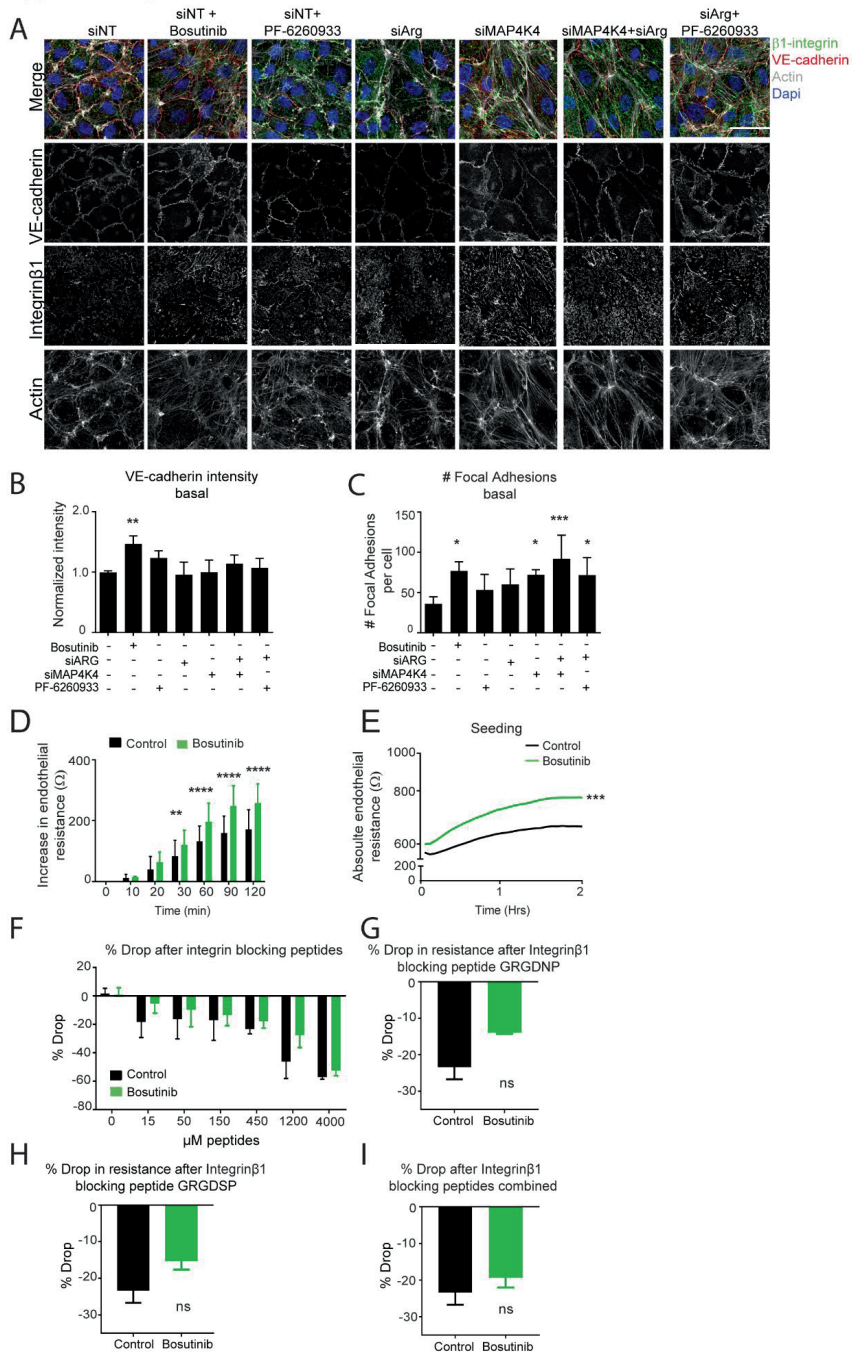
5

Supplemental figure 2
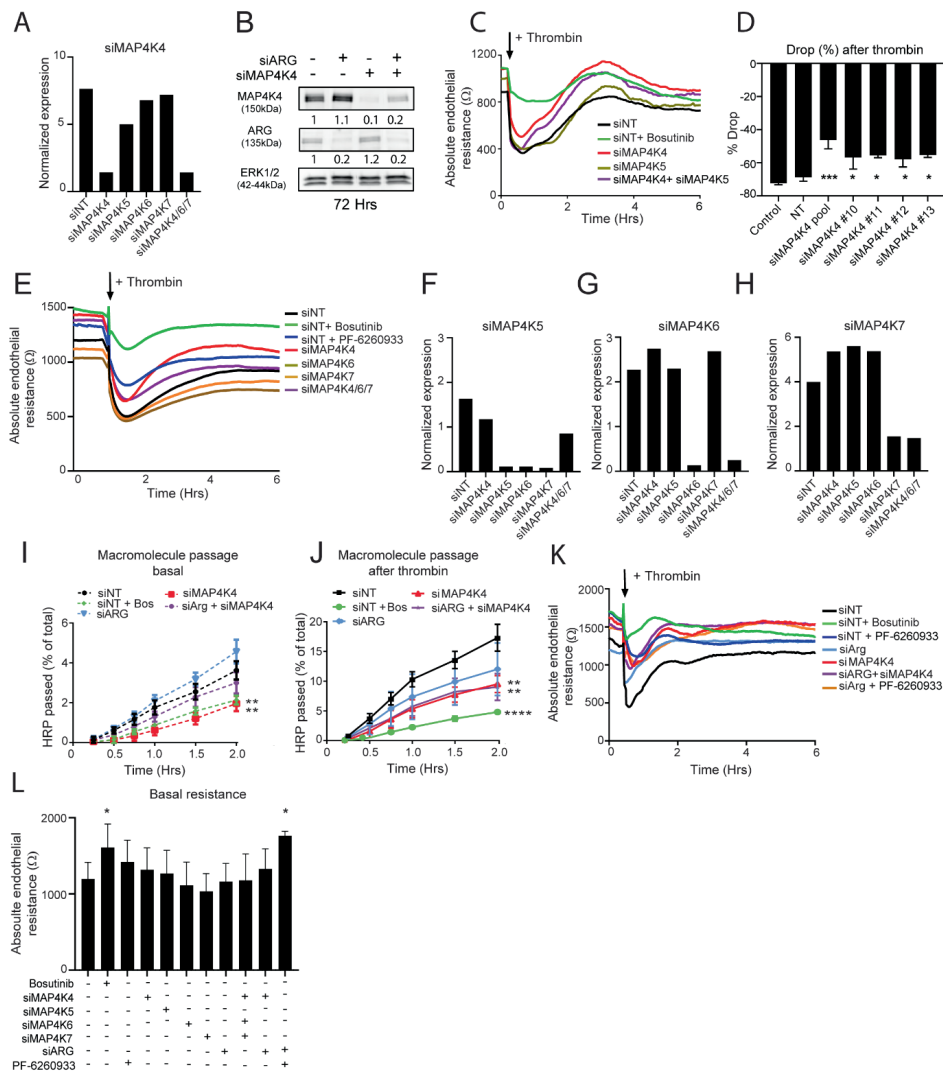
Supplemental figure 2: A) mRNA quantity of MAP4K4 measured by qPCR. B) Western blot analysis of Arg and MAP4K4 expression after 72 hours of knockdown. ERK was used as loading control. Representative image of n=3. C) Absolute endothelial resistance of HUVEC monolayers during thrombin stimulation after knockdown of MAP4K4 and MAP4K5 (n=3-5). D) Quantification of the thrombin response by calculating the maximal drop in resistance (%) after different siRNAs for MAP4K4. E) Absolute endothelial resistance in HUVECs after bosutinib treatment, PF-6260933 and knockdown of MAP4K4/6/7 and thrombin stimulation (n=3-4). F-H) mRNA quantity of MAP4K5/6/7 measured by qPCR. I) Macromolecule passage over HUVEC monolayers with siMAP4K4, siArg or the combination or 90 minutes of pre-incubation with bosutinib (n=3-4). J) Macromolecule passage over HUVEC monolayers with siMAP4K4, siArg or the combination or 90 minutes of pre-incubation with bosutinib during 2 hours of thrombin stimulation (n=3-4). K) Absolute endothelial resistance of

HUVEC monolayers after bosutinib treatment, PF-6260933 and knockdown of MAP4K4 and Arg and thrombin stimulation (n=4-5). L) Absolute endothelial resistance of HUVEC monolayers under basal conditions with bosutinib treatment, PF-6260933 and knockdown of MAP4K4/5/6/7 or Arg (n=4) *P<0.05 **P<0.01 ***P<0.001 ****P<0.0001 compared to siNT. All data is represented as mean ± SD. Comparison of 2 conditions was tested by student t-test. Comparison of more than 2 conditions was tested by 1-way ANOVA

5

Supplemental figure 3

Supplemental Figure 3: A) Immunofluorescent stainings of active integrinβ1 (green), actin (white) and VE-cadherin (red) under basal conditions and counterstained with dapi (blue). Scale bar represents 50μM. (Representative images of n=4 experiments). B) Quantification of VE-cadherin intensity at the membrane divided by the intensity in the cytosol under basal conditions (n=4). C) Quantification of number of FA under basal conditions in active integrin β1 staining (n=4). D) Increase in endothelial barrier resistance at several time points after 90 minutes of bosutinib pre-incubation (n=3) E) Absolute endothelial resistance of HUVEC monolayers during barrier formation directly after seeding after 90 minutes of bosutinib pre-incubation (n=3). F) Quantification of drop in resistance (%) after addition of increasing concentrations GRGDNP and GRGDSP peptides. Concentrations below 450μM combined peptides showed no disruptions of the basal barrier, whereas concentrations exceeding 450μM did not show recovery of the barrier over time (n=3). G-H) % Drop in endothelial resistance with Integrinβ1 blocking peptide GRGDNP (blocking the adhesive function of integrins αvβ3 and α5β1) and GRGDSP (blocking the adhesive function of integrins αvβ3, αvβ5 and α5β1) in a total concentration of 450μM (n=3). I) % Drop in endothelial resistance after addition of the combined integrin blocking peptides GRGDNP and GRGDSP in a total concentration of 450 μM (n=3). *P<0.05 **P<0.10 ***P<0.001 ****P<0.0001 compared to control. All data is represented as mean ± SD. Comparison of 2 conditions was tested by student t-test. Comparison of more than 2 conditions was tested by 1-way ANOVA.

Supplemental figure 4
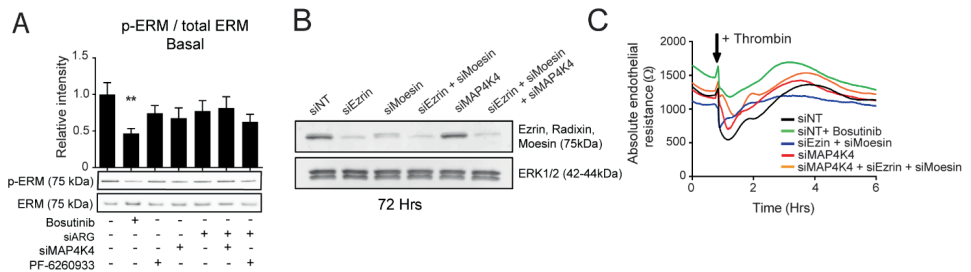
Supplemental Figure 4: A) Western blot analysis of phosphorylated ERM expression over total ERM expression after bosutinib or PF-6260933 treatment, siMAP4K4, siArg or the combination B) Western blot analysis of ezrin and moesin expression after 72 hours of knockdown. ERK was used as loading control. C) Absolute endothelial resistance of HUVEC monolayers transfected with siMAP4K4 and siEzrin+siMoesin or the combination and stimulated with thrombin (n=4).

Supplemental figure 5
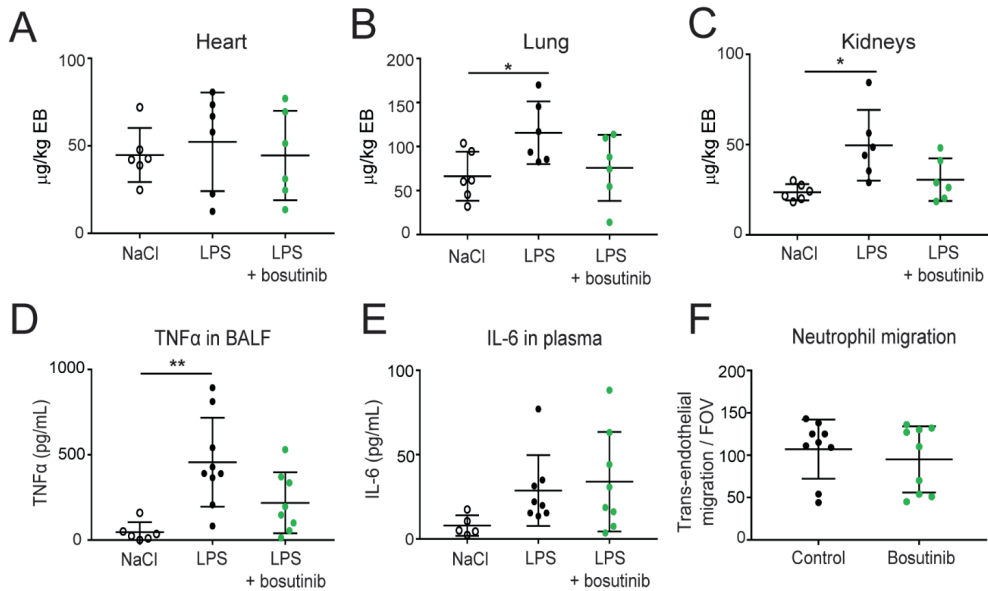
Supplemental Figure 5: A-C) Vascular leakage of 0.5 % Evans Blue into lungs, kidneys and heart was measured by photospectrometry corrected for Evans Blue in plasma compared between NaCl (control group), LPS and LPS + bosutinib treated mice at T=6 hours (n=6 per group). D) TNFα concentration in BALF (n=6-9 per group). E) IL-6 concentration in plasma (n=6-9 per group). F) Migration of neutrophils over pulmonary microvascular endothelium pre-incubated with or without bosutinib per field of view (FOV). *P<0.05 **P<0.01 compared to NaCl control group. All data is represented as mean ± SD and 1-way ANOVA was used.

Video legends:

Video 1: Time-lapse confocal imaging of GFP-vinculin in control- or bosutinib-treated HUVEC under basal conditions for 30 minutes, and after thrombin addition 15 minutes. Frame rate 12 frames/s.

Video 2: Time-lapse confocal imaging of GFP-vinculin in control-or PF-6260933 treated HUVEC under basal conditions 30 minutes, and after thrombin addition 15 minutes. Frame rate 12 frames/s.

Video 3: Time-lapse confocal imaging of GFP-vinculin with immunofluorescent VE-cadherin in control-or bosutinib treated HUVEC under basal conditions 30 minutes, and after thrombin addition 15 minutes. Frame rate 12 frames/s.
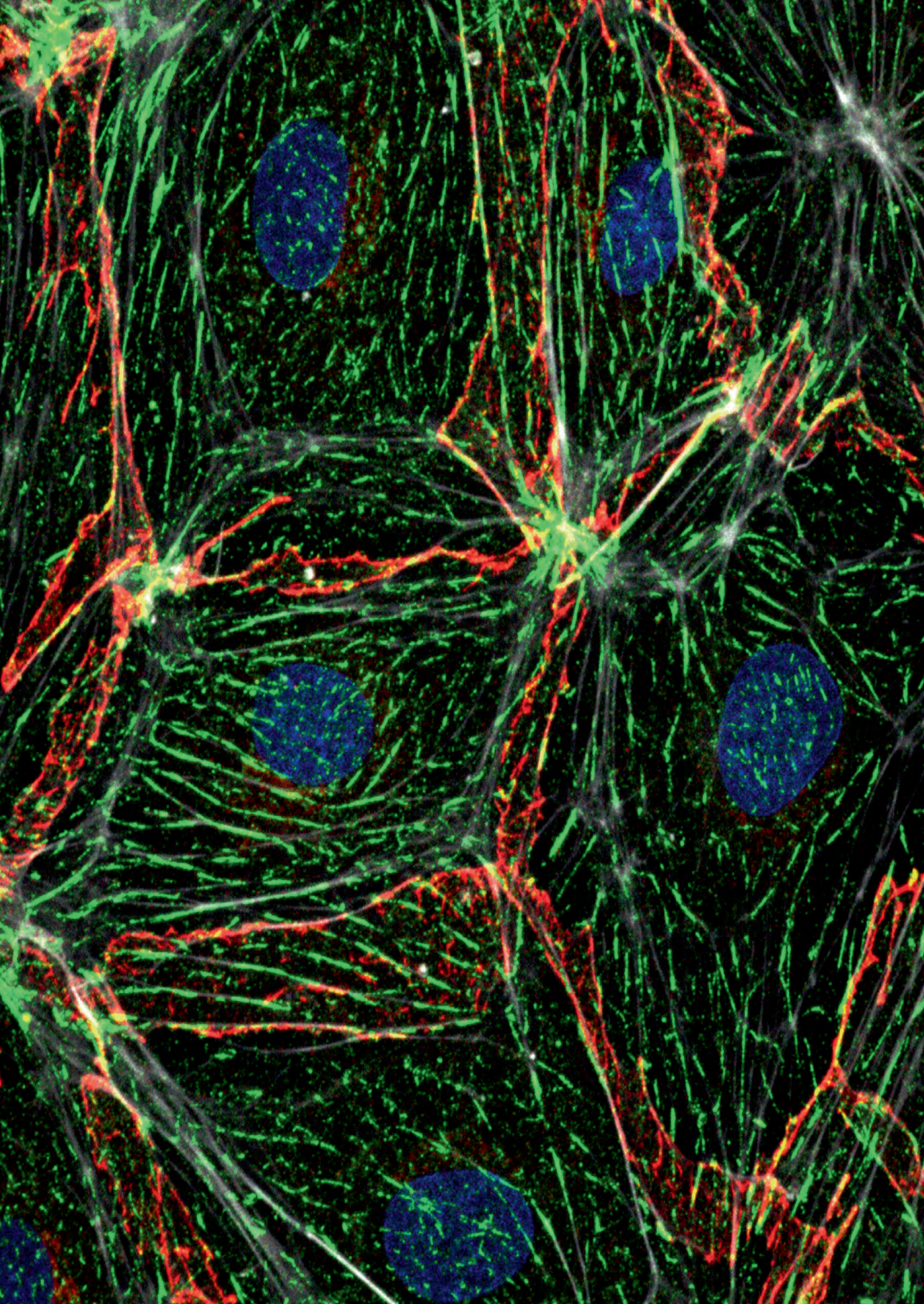
6

Bosutinib reduces endothelial permeability and organ failure in a rat polytrauma transfusion model

Derek J.B. Kleinveld, <u>Liza Botros</u>, M. Adrie W. Maas, Jesper Kers, Jurjan Aman, Markus W. Hollmann & Nicole P. Juffermans

Abstract

Background: Trauma-induced shock is associated with endothelial dysfunction. We examined whether the tyrosine kinase inhibitor bosutinib as an adjunct therapy to a balanced blood component resuscitation strategy reduces trauma-induced endothelial permeability, thereby improving shock reversal and limiting transfusion requirements and organ failure in a rat polytrauma transfusion model.

Methods: Male Sprague Dawley rats (*n*=13 per group) were traumatized and exsanguinated until a mean arterial pressure (MAP) of 40 mmHg was reached and randomized to two groups: red blood cells, plasma and platelets in a 1:1:1 ratio with either bosutinib or vehicle. Controls were randomized to sham (=median laparotomy, no trauma) with bosutinib or vehicle. Organs were harvested for histology and wet/dry (W/D) ratio.

Results: Traumatic injury resulted in shock, depicted by higher lactate levels compared to controls. In trauma-induced shock, the amount of resuscitation volume needed to obtain a MAP of 60 mmHg was lower in the bosutinib treated animals (2.8 [2.7 – 3.2] ml kg^{-1}) when compared to vehicle (6.1 [5.1 – 7.2] ml kg^{-1}, p<0.001). There was a trend towards lower lactate levels in the bosutinib group (2.9 [1.7 – 4.8] mM) compared to the vehicle group (6.2 [3.1 – 14.1] mM, p=0.06). Bosutinib compared to vehicle reduced lung vascular leakage (W/D ratio of 5.1 [4.6 – 5.3] vs 5.7 [5.4 – 6.0] (p=0.046) and lung organ injury scores (p=0.027).

Conclusions: Bosutinib as an adjunct therapy to a balanced transfusion strategy reduces resuscitation volume and improves shock reversal, associated with a reduction in vascular leakage and organ injury.

Introduction

Use of a balanced 1:1:1 red blood cell-to-plasma-to-platelet transfusion ratio has improved outcome of traumatic bleeding.(1) However, morbidity and mortality remain high.(2) Research efforts in trauma have mainly focused on treating or preventing trauma-induced coagulopathy, resulting in shifts towards mortality later in the disease process during Intensive Care stay.(1, 3-5) Whereas early mortality is predominantly attributed to exsanguination and traumatic brain injury, late mortality is caused by organ failure.(6, 7) Organ failure is thought to be mediated by inflammation-induced endothelial activation, resulting in leakage and oedema.(6, 8) To date, adjunctive treatment strategies aimed at limiting organ failure in trauma by minimizing the dysfunctional endothelial barrier function have been scarcely investigated.(9)

Tyrosine kinase inhibitors, such as bosutinib, are used in the treatment of chronic myeloid leukemia.(10-12) Some of these inhibitors have been shown to protect endothelial integrity in a mouse model of vascular leakage.(13) Bosutinib compared to other tyrosine kinase inhibitors was superior in protecting against inflammation-induced vascular leakage.(14) The mechanism of bosutinib-induced reduction of vascular leakage was shown to involve combined inhibition of the kinases Abl-related gene (Arg) and Mitogen Activated Protein 4 Kinase 4 (MAP4K4) which results in reinforcement of endothelial cell-cell junctions and enhanced adhesion to the subcellular matrix.(14, 15) In experimental animal models, other tyrosine kinase inhibitors have shown benefits on endothelial function in settings of acute lung injury(16, 17), in a cardiopulmonary bypass model(18) and in a hemodilution shock model.(19) However, none of these studies evaluated bosutinib in an acute setting next to a balanced transfusion resuscitation strategy.

6

The aim of this study was to investigate the effect of bosutinib as an adjunctive therapy to a balanced transfusion strategy on endothelial leakage, on resuscitation volume needed to restore perfusion and on organ failure in a rat model of multiple trauma and transfusion. We hypothesize that bosutinib limits endothelial leakage leading to a reduction of the transfusion requirements to restore perfusion, thereby reducing organ injury.

Materials and Methods

Ethical statement, housing and species

The experiments described in this study were approved by the Institutional Animal Care and Use Committee of the Amsterdam University Medical Centers. The procedures were in accordance with the European Parliament directive (2010/63/EU) and the national law of the Experiments on Animals Act (Wod, 2014).

A total of 52 male Sprague Dawley rats weighing 350 – 400 grams (Envigo, UK) were used in the experiments. Additionally, 40 male rats were used for the preparation of blood products. Animals were group housed with access to water and food *ad libitum* at least seven days before the experiment. Housing of animals was temperature-controlled with a 12/12 h light/dark cycle.

Experimental model

Transfusion products were made from syngeneic donor rats according to national blood bank standards as described before.[20]

Anaesthesia was induced with intraperitoneal ketamine 100 mg kg^{-1} (Alfasan, the Netherlands), 0.25 mg kg^{-1} dexmedetomidine (Orion Pharma, Finland) and 0.1 mg kg^{-1} atropine (Dechra, the Netherlands) and maintained with a combination of 33.3 mg kg^{-1} per hour ketamine and 0.02 mg kg^{-1} per hour dexmedetomidine intravenously. Rats were tracheotomised and mechanically ventilated using a pressure control mode (Babylog 8000, Draeger, Germany) with a respiratory rate of 60min^{-1} (70 min^{-1} during shock), positive end expiratory pressure of 3.5 kPa and inspiratory pressures (Pinsp) of 10 kPa. Tidal volumes were maintained between 6-7 ml kg^{-1} in all groups. Recruitment was performed every hour by increasing Pinsp to 25 kPa for five seconds. Blood pressure was measured continuously via a cannula (fine bore polyethylene tubing, inner diameter 0.58mm) inserted in the right carotid artery. The right jugular vein was cannulated for administration of fluids and the allocated treatment. Maintenance fluids consisted of Ringer's lactate at 4 ml kg^{-1} per hour. The bladder was emptied before trauma and urine output was measured during the experiment. Temperature was kept within range (36.5 – 37.0 ˚C) using a heat table and a heat lamp.

Trauma was induced by a fracture of the right femur using a guillotine, a crush injury to the small intestine and left lateral liver lobe as described before[20](**Supplemental Figure 1**). Then, an initial volume of blood was drawn from the carotid artery according to the following formula (0.30(0.06 x weight + 0.77)) [21], and further adjusted in steps of 0.5 ml to reach a mean arterial pressure (MAP) below 40 mmHg (total initial volume drawn: 30-40% of circulating volume). Different from the previous described model [20]was the duration of shock of 1 hour, after which rats were randomized to two groups: resuscitation with either a balanced 1:1:1 transfusion ratio of red blood cell:plasma:platelet either with bosutinib (selleckchem.com, USA; licensed by Pfizer, USA 5mg kg^{-1} dissolved in 2% DMSO/ 30% PEG/

5% Tween in a volume of 200 µl NaCl 0.9%) or with vehicle initially given in bolus prior to transfusion. The operator was blinded to treatment allocation. Transfusion was administered at a speed of 8 ml/hour (Perfusor fm, B Braun, USA) in the jugular vein. Different from the previous described model was the termination of resuscitation.(20) After an animal reached a MAP of 60 mmHg lasting for at least 5 minutes, transfusion was stopped. The concentration of bosutinib was based on a previous experiment.(22) Due to the half-life of bosutinib, a repeated dose of bosutinib or vehicle was given 5 hours post-trauma or sham.(23) Control groups were randomized separately to sham with bosutinib or vehicle. Sham consisted of a median laparotomy without inflicting traumatic injury. The laparotomy was closed immediately in order to avoid loss of temperature. Bosutinib or vehicle was administered directly following shock or at a similar time in the sham groups.

Measurements

Blood draws were obtained before trauma (T=0), after trauma-induced shock and before initiation of the resuscitation strategy (T=1 hour), 3 hours, 4 hours and 6 hours after trauma (T=3, 4 and 6). Arterial blood gas analyses were done at all time points, rotational thromboelastometry (ROTEM) at two time points (T0, T6), biochemical assessments at two time points (T0, T6). Additionally, plasma was prepared and stored at -80 ˚C after double spinning (20min, 2500G, 18 ˚C, acceleration 9, brake 0, 5804 R, Eppendorf, Germany).

Syndecan-1 (Elabscience, USA), soluble vascular adhesion molecule-1 (VCAM-1) (Elabscience, USA), tumour necrosis factor alpha and interleukin-6 (R&D, USA), were determined with enzyme-linked immunosorbent assays according to the manufacturer guidelines. The lowest detection limit was noted when values were below the detection limit. Aspartate and alanine transaminases, creatinine and total urine protein were measured by standard enzymatic reactions using spectrophotometric, colorimetric or turbidimetric measurement methods. Estimated glomerular filtration rate was calculated according to the formula: (urine creatinine at termination times urine production in 6 hours) divided by plasma creatinine).

To assess vascular leakage, 0.5ml of 12.5mg/ml FITC-labelled 70kDa dextran (Sigma Aldrich, USA) was injected in the jugular vein 30 minutes prior to animal sacrifice. Rats were sacrificed by exsanguination after which organs were flushed with 50ml NaCl 0.9% administered at the left side of the heart while the right jugular catheter was connected to the flushing system. Flushing was done against gravitational force. Before flushing, the hilum of the left lung and left kidney were tied off to assess these organs for wet/dry ratio.

All organs were assessed in haematoxylin and eosin slides by a pathologist, who was blinded for treatment allocation. (20, 24) The scale of each category consisted of a score of 0 (=absent) to 3 (=severe). For the full scoring list see **Supplemental Table 1**.

Immunohistochemical analysis of vascular leakage

Slides of organs were deparaffinised and coloured using a rabbit – anti-FITC/ anti-rabbit HRP and NovaRed colouring method. The staining time was kept constant within each organ system, ranging from 5 min (lung) – 7 min (small intestine) per slide. Five different images of each slide were obtained with a microscope (10x magnification) and a camera (BX51 with UC90, Olympus, Japan). Pictures were inverted using Image J (1.50i, NIH, USA). Five random inverted pictures were used to set a threshold for FITC-70kDa dextran leakage. The median percentage of the area intensity was used as measure of endothelial leakage.

Outcomes

The primary outcome was the amount of transfusion until a MAP of 60 mmHg was reached for 5 minutes. The secondary outcomes were the circulating markers of endothelial damage and inflammation, vascular leakage, organ oedema and organ failure parameters.

Statistical analyses

Based on previous experiments(20), we estimated a treatment effect of 0.6 ml reduction in transfusion volume with a standard deviation of 0.4 ml. In this scenario, 11 rats per group will have a power of 80% to detect a statistical significant difference in transfusion volume needed to reach a MAP of 60mmHg using a Mann-Whitney U test with a two-sided 0.05 significance level. As we previously experienced a mortality of approximately 20% in our model, we added 2 additional rats per group, yielding n=13 per group.

Data were analysed using SPSS (IBM, version 25.0, USA), graphs were made using GraphPad Prism (version 8.0.2, USA). All parameters were checked for normality using a Kolmogorov-Smirnov test and by visual inspection of histograms. Data were presented as mean with standard deviation or median with interquartile range based on their distribution. The amount of transfusion needed to reach a MAP of 60 mmHg was evaluated with a Mann-Whitney U-test. Other outcomes were tested for differences using Kruskal-Wallis. Post-hoc tests were performed between sham and trauma groups and between trauma + vehicle and trauma + bosutinib were performed. A p-value of less than 0.05 was considered statistically significant.

Results

Shock, transfusion needs and mortality

There was no mortality in both the experimental groups as the control groups. Trauma and the shock phase resulted in shock, with increased base deficits compared to the sham groups (Table 1 and Figure 1). No differences in arterial blood gas analysis were found between trauma groups after shock (Table 1). After resuscitation (T=3), the bosutinib group had lower lactate levels (median 1.5 [interquartile range: 1.2 – 2.0]mM) compared to the vehicle group (2.2 [1.6 – 3.9]mM), albeit not statistically significant (p=0.06) (Figure 1). This trend of lower lactate levels in the bosutinib group (2.9 [1.7 – 4.8] mM) compared to the vehicle group (6.2 [3.1 – 14.1]mM, p=0.06) remained until termination (T=6). Animals in the bosutinib treated group required less transfusion volume for shock reversal (2.8 [2.7-3.2]ml kg^{-1} in 7.5 [7.5 – 9.0] min) compared to vehicle (6.1 [5.1 – 7.2]ml kg^{-1} in 15.8 [15.0 – 19.5 min], p<0.001) (Figure 1). Quality assessments of the different products are described in Supplemental Table 2.

Coagulation

During the experiment, normal ROTEM values were observed in sham groups. The EXTEM and FIBTEM maximum clot firmness, however, was significantly different between the sham groups and the trauma + vehicle group. Despite the lower transfusion volume in the trauma + bosutinib compared to vehicle, no differences were found in ROTEM and platelet counts between groups (Table 2).

Systemic organ dysfunction and inflammation

Animals with trauma-induced shock compared to sham animals developed severe organ damage as shown by increased creatinine and liver transaminase levels (**Table 2**), which was not different between trauma groups. Bosutinib resulted in higher urine output compared to vehicle. Moreover, IL-6 levels were lower in the bosutinib treated rats compared to the vehicle treated rats (Table 2).

6

Table 1: Baseline and trauma-induced shock parameters

Parameter	Sham + vehicle		Sham + bosutinib		Trauma + vehicle		Trauma + bosutinib	
	Baseline	1 hour (T1)	Baseline	1 hour (T1)	Before injury	After injury and shock (T=1)	Before injury	After injury and shock (T=1)
Weight (gram)	365 (7)	ND	363 (12)	ND	368 (19)	ND	366 (13)	ND
Total blood volume (ml)	22.7 (0.4)	ND	22.0 (0.7)	ND	22.9 (1.1)	ND	22.7 (0.8)	ND
Temperature (°C)	36.6 (36.5 – 37.0)	36.4 (36.3 – 36.7)	36.7 (36.6 – 36.9)	36.5 (36.4 – 36.7)	36.4 (36.3 – 36.8)	36.5 (36.2 – 36.9)	36.7 (36.4 – 36.9)	36.5 (36.1 – 36.8)
pH	7.43 (7.36 – 7.47)	7.37 (7.33 – 7.43)	7.41 (7.38 – 7.44)	7.38 (7.35 – 7.40)*	7.40 (7.39 – 7.45)	7.34 (7.31 – 7.36)*	7.43 (7.40 – 7.46)	7.34 (7.31 – 7.38)*
pCO$_2$ (kPa)	5.1 (4.6 – 5.9)	5.1 (4.3 – 5.9)	5.3 (4.5 – 6.0)	5.3 (4.7 – 5.8)	4.9 (4.6 – 5.3)	5.1 (4.7 – 5.4)	5.0 (4.3 – 5.2)	4.8 (4.7 – 6.0)
BE (mEq L^{-1})	0.3 (-1.5 – 1.1)	-2.8 (-3.3 – -1.3)	0.6 (0.2 – 2.1)	-1.8 (-3.2 – -0.7)	-0.7 (-2.3 – 0.4)	-5.1 (-7.3 – -4.5)*	-0.3 (-1.2 – 0.5)	-4.1 (-5.2 – -3.6)*
Lactate (mM)	0.7 (0.6 – 0.9)	1.2 (1.0 – 1.2)	0.6 (0.5 – 0.7)	1.3 (0.9 – 1.4)	0.6 (0.5 – 1.0)	2.1 (1.9 – 3.0)*	0.6 (0.6 – 0.8)	2.0 (1.6 – 2.3)*
Hb (mM)	9.1 (8.4 – 9.3)	8.0 (7.6 – 8.4)	9.4 (8.8 – 9.6)	8.0 (7.5 – 8.5)	9.3 (8.9 – 9.6)	7.4 (7.0 – 8.2)	9.1 (8.9 – 9.3)	7.8 (7.0 – 8.2)
Ca^{2+} (mM)	1.2 (1.1 – 1.2)	1.1 (1.0 – 1.2)	1.2 (1.0 – 1.2)	1.3 (1.2 – 1.3)	1.1 (1.0 – 1.2)	1.1 (0.9 – 1.1)*	1.1 (1.0 – 1.2)	1.1 (0.9 – 1.2)*
Glucose (mM)	20.4 (18.6 – 21.4)	27.8 (25.4 – 30.2)	22.7 (21.5 – 23.1)	27.0 (25.4 – 28.2)	23.9 (19.3 – 26.2)	38.2 (34.1 – 40.7)*	22.6 (20.7 – 24.2)	36.5 (34.5 – 38.2)*

Data are presented as mean (SD) or median (IQR). BE=base excess, Hb=haemoglobin. *p<0.05 compared to sham groups. No significant differences were found between the trauma + vehicle and trauma + bosutinib groups.
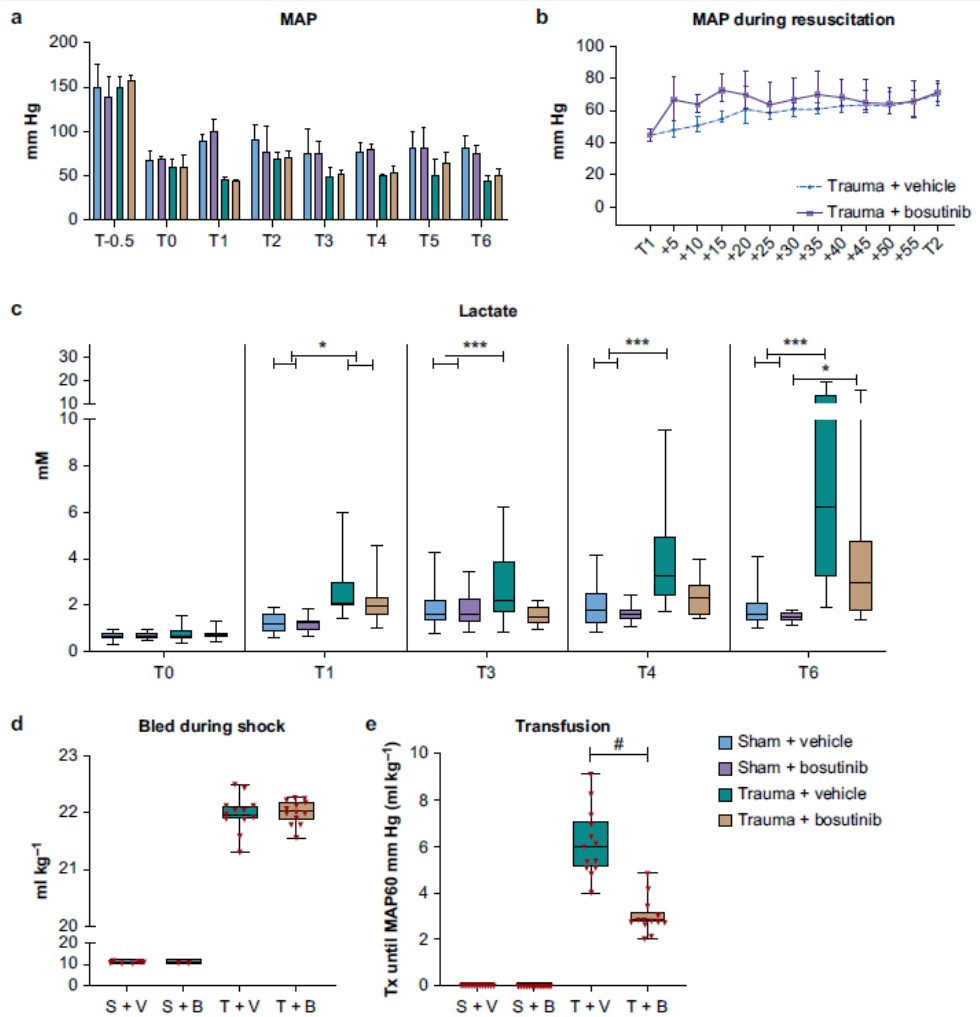
Figure 1

Figure 1: Bosutinib improved shock reversal and reduced resuscitation volume. Data are median (IQR). T-0.5 (before trauma), T0 (Trauma), T1 (start resuscitation), T2 - 6 = 2 to 6 hours after trauma. (a) Mean arterial pressure (MAP). Between T-0.5 and T0 traumatic injury was initiated, the first blood draw was used as baseline sample. Injury and traumatic shock lasted for 1 hour, thereafter rats were randomized to receive allocated transfusion and treatment (Tx), controls were sham with bosutinib or vehicle. (b) Mean arterial pressure for the trauma groups during resuscitation (T1 – T2). (c) Lactate levels. (d) Volume of haemorrhage during shock phase. (e) Volume of transfusion needed to restore a MAP of 60mmHg. In traumatic injury, the vehicle and bosutinib groups were treated with standard transfusion strategy of a 1:1:1 red blood cell-to-plasma-to-platelet ratio. S+V = sham + vehicle, S+B = sham + bosutinib, T+V = trauma + vehicle, T+B= trauma + bosutinib. Sham vs trauma groups: *p<0.05, **<p<0.01. Trauma + vehicle vs trauma + bosutinib: #p<0.05.

Table 2

Parameter	Sham + vehicle		Sham + bosutinib		Trauma + vehicle		Trauma + bosutinib	
	Baseline	After 6 hours	Baseline	After 6 hours	Baseline	After 6 hours	Baseline	After 6 hours
Endotheliopathy								
sVCAM-1 (pg ml^{-1})	283 (265 – 382)	289 (77 – 502)	265 (209 – 307)	200.0 (141 – 285)	244 (204 – 279)	818 (524 – 2183)*	273 (238 – 339)	352 (269 – 650)[#]
Syndecan-1 (ng ml^{-1})	31.0 (27.0 – 35.1)	61.3 (55.0 – 69.0)	31.2 (27.0 – 33.8)	46.6 (30.1 – 74.0)	32.3 (27.5 – 37.4)	110.8 (43.7 – 142.6)*	33.3 (26.7 - 39.3)	51.2 (37.2 – 71.6)
Hepatic								
AST (U L^{-1})	64.0 (60.0 – 68.0)	181.0 (105.0 – 356.0)	65.5 (60.3 – 69.8)	149.0 (121.0 – 195.5)	67.0 (59.5 – 69.0)	2670 (2047.5 – 4806.5)**	66.0 (61.0 – 68.0)	1574.0 (579.5 – 2686.5)**
ALT (U L^{-1})	48.0 (45.5 – 55.5)	63.0 (49.5 – 107.5)	54.0 (50.5 – 57.0)	63.0 (47.5 – 91.5)	57.0 (48.0 – 62.0)	1719.0 (1326.0 – 3034.0)**	52.0 (47.5 – 60.0)	798.5 (254.5 – 1468.5)**
Renal								
Creatinine (µM)	24.0 (22.5 – 26.5)	62.0 (43.0 – 91.5)	23.5 (22.3 – 25.0)	50.0 (41.0 – 62.0)**	25.0 (24.0 – 29.0)	139.5 (115.8 – 163.5)**	26.0 (25.0 – 28.5)	120.5 (93.5 – 141.8)*
Urine protein (g L^{-1})	0.5 (0.2 – 0.9)	1.0 (0.6 – 1.5)	0.6 (0.2 – 0.8)	0.8 (0.7 – 1.4)	0.6 (0.3 – 1.0)	1.7 (1.5 – 2.1)*	0.5 (0.4 – 0.8)	1.6 (0.8 – 2.0)
Urine output (ml kg^{-1})	ND	11.4 (9.5 – 13.3)	ND	14.5 (10.1 – 19.9)	ND	7.4 (4.2 – 9.7)**	ND	10.9 (8.7 – 13.3)[#]
eGFR (ml min^{-1})	ND	1.11 (0.44 – 1.51)	ND	1.16 (0.50 – 1.63)	ND	0.11 (0.04 – 0.21)**	ND	0.25 (0.15 – 0.56)**
Inflammation								
Leukocytes (*10^9 L^{-1})	5.8 (4.8 – 6.5)	7.0 (4.9 – 8.6)	6.6 (5.8 – 8.0)	8.3 (6.5 – 8.9)	6.3 (5.2 – 7.5)	5.2 (4.5 – 7.8)	6.7 (5.0 – 7.6)	6.2 (4.5 – 7.3)
[±]IL-6 (pg ml^{-1})	<12	<12	<12	<12	<12	1639 (707 – 2526)**	<12.0	121 (12 – 1020)*, [#]
[±]TNF-a (pg ml^{-1})	<62.5	<62.5	<62.5	<62.5	<62.5	<62.5	<62.5	<62.5
Coagulation								
Platelets (*10^9 L^{-1})	881 (819 – 916)	564 (504 – 600)	947 (780 – 1014)	582 (552 - 628)	970 (934 – 1019)	479 (345 – 593)	903 (889 – 964)	573 (506 – 650)
EXTEM CT (s)	52 (49 – 55)[#]	51 (45 – 57)	49 (46 – 53)	49 (47 – 58)	47 (46 – 50)	53 (49 – 74)	48 (47 – 51)	45 (43 – 51)
EXTEM MCF (mm)	69 (69 – 72)	71 (69 – 71)	71 (70 – 73)	70 (70 – 73)	71 (70 – 74)	67 (62 – 69)*	71 (70 – 72)	70 (66 – 70)
EXTEM Li30 (%)	100 (100-	100 (100-	100 (100-	100 (100-	100 (100-	100 (100-100)	100 (100-	100 (100-100)

	100)	100)	100)	100)	100)		100)	
FIBTEM CT (s)	49 (48 – 51)	49 (42 – 51)	46 (44 – 50)	46 (43 – 51)	43 (41 – 47)	54 (47 – 69)	42 (39 – 44)	43 (40 – 49)
FIBTEM MCF (mm)	14 (14 – 15)	13 (13 – 14)	15 (14 – 15)	13 (12 – 14)	15 (14 – 19)	10 (6 – 13)*	15 (13 – 15)	11 (9 – 13)

Table 2: Data are presented as median (IQR). Before trauma/sham and at termination, samples were measured for different parameters. ALT, alanine aminotransferase; AST, aspartate aminotransferase; eGFR, estimated glomerular filtration rate determined by urine creatinine times urine production in 6 hours divided by plasma creatinine; IL-6, interleukin 6; ND, not determined; ROTEM EXTEM, rotational thromboelastometry; sVCAM-1, soluble vascular adhesion molecule 1; TNF-α = tumour necrosis factor alpha. ±values below detection limit are depicted as lower than the lowest reference range. *p<0.05, **p<0.01 sham vs trauma groups, #p<0.05, ##p<0.01 trauma group + vehicle vs trauma + bosutinib group.

Endothelial damage and leakage

Endothelial damage was present in all trauma-induced shock groups, as characterized by elevated plasma syndecan-1 and sVCAM-1. Bosutinib treatment resulted in reduced plasma levels of sVCAM-1 compared to vehicle (Table 2). Also, bosutinib treated rats showed lower lung wet/dry (W/D) ratios (5.1 [4.6 – 5.3]) compared to vehicle (5.7 [5.4 – 6.0], p=0.046) (Figure 2) and less dextran leakage in the lung (1 [0 – 3]% vs 6 [2 – 25]%, p=0.01). However, bosutinib did not limit vascular leakage of dextran in the other organs (liver, spleen, small intestine, kidney).

Organ damage and mortality

Bosutinib resulted in lower total lung organ injury (4.0 [2.5 – 5.5] compared to vehicle 6.0 [4.5 – 8.0], p=0.027) (Figure 2, Figure 3), but did not affect organ injury scores of kidney, liver, spleen and small intestine.(Figure 2, Figure 3 and Supplemental Figure 2). The distributions of the individual organ injury scores are shown in Supplemental Figure 3. No mortality was observed in these experiments.
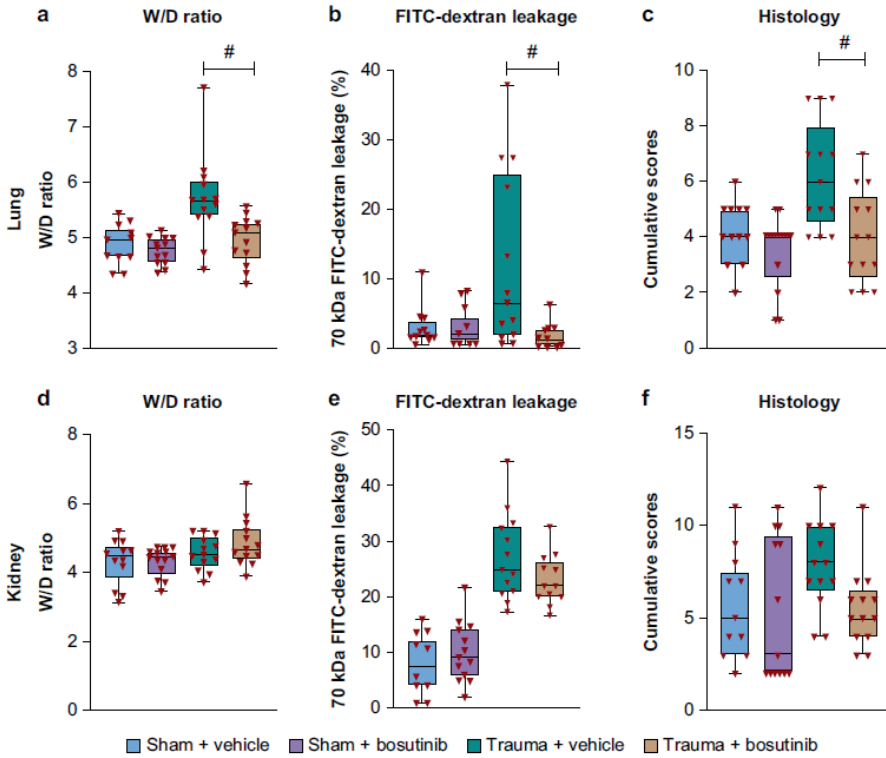
6

Figure 2

Figure 2: Bosutinib reduced organ oedema, vascular leakage and organ injury score in lung and kidney. Data are median (IQR) or boxplot with range. (a-c) Lung WD, lung FITC-70 kDa dextran leakage and total lung score. (d-f) Kidney WD, kidney FITC-70 kDa dextran leakage and total kidney score. Significance is shown for trauma + vehicle vs trauma + bosutinib. #p<0.05. W/D, wet/dry; FITC, fluorescein isothiocyanate.
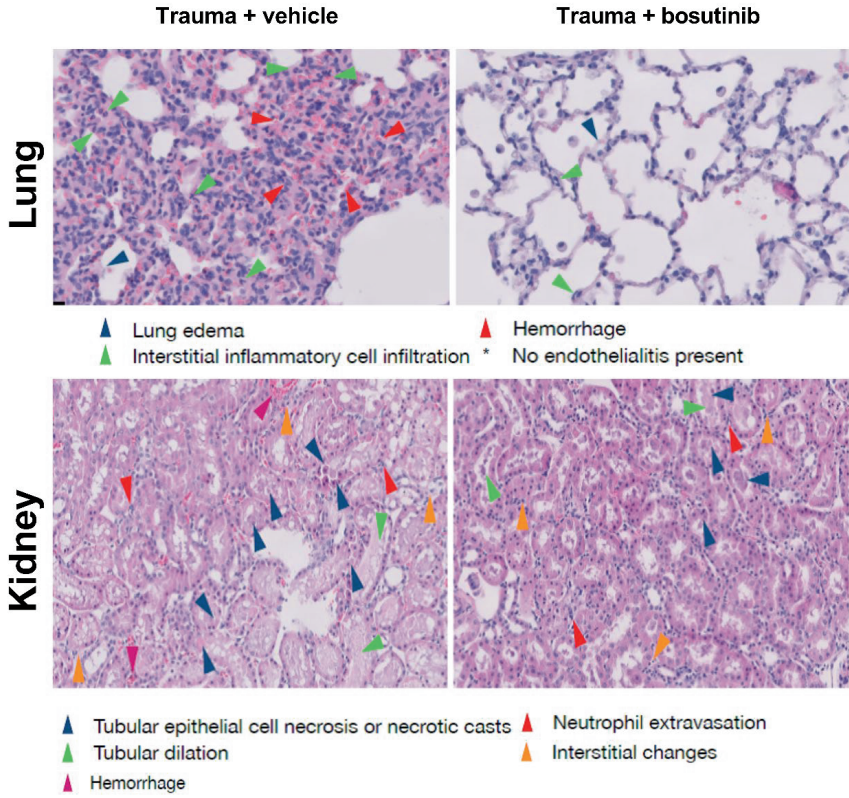
Figure 3

Figure 3: Histology of lung and kidney after trauma-induced shock

Discussion

In this study, bosutinib as an adjunctive therapy to a balanced transfusion strategy was associated with less transfusion need, improved shock reversal and a reduction in endothelial leakage with concomitant reduction in pulmonary edema and lung injury when compared to a vehicle treated group. Also, bosutinib treated rats had less endothelial damage indicated by lower plasma sVCAM-1 levels. Collectively, these data suggest that bosutinib is protecting the endothelial barrier integrity in traumatic bleeding, and can be used to reduce transfusion requirements to restore circulation.

Our findings of an improved shock reversal, endothelial barrier function and organ protective effects of bosutinib are in line with previous studies, in which bosutinib reduced lipopolysaccharide-induced lung permeability[14]. Also, other tyrosine kinase inhibitors such as imatinib resulted in lower organ oedema in several disease models, including acute lung injury, sepsis, cardiopulmonary bypass model and a trauma and hypovolemic shock model.[16, 18, 19, 25, 26] We add to the existing literature by using a polytrauma haemorrhagic shock model with a balanced transfusion resuscitation strategy. Moreover, we use bosutinib instead of imatinib. Bosutinib has a stronger effect on endothelial tight junctions and hence barrier integrity when compared to imatinib, because bosutinib synergistically inhibits both Arg and MAP4K4 kinases while imatinib has a high specificity to inhibit Arg kinase.[14] In this study, the effects of bosutinib on organ injury were most clear for the lung. As lung injury is often the first manifestation of a multiple organ dysfunction syndrome, protection of the lung may result in better outcomes.[27, 28] However, we have only studied the acute effects (6 hours after trauma), therefore long term effects of bosutinib in trauma-induced shock remain to be determined.

IL-6 levels were lower in bosutinib compared to vehicle treated rats with traumatic injury. The immunomodulatory effects of bosutinib were previously studied in mouse-derived macrophages, in which bosutinib reduced IL-6 production.[29] Possibly, less endothelial damage led to a reduction in the inflammatory response as well.

The bosutinib treated group required less transfusion products (and hence less plasma and platelets) than the vehicle group, while coagulation parameters in the ROTEM assays did not differ. Therefore, besides an effect on endothelial barrier function, bosutinib may also reduce endothelial-driven coagulopathy in this model.. Further evaluation is necessary to pinpoint the effects of bosutinib on coagulopathy, such as platelet function and coagulation proteins.

In our model, both a reduction in endothelial leakage as well as a lower transfusion volume needed to restore circulation could have contributed to a reduction of organ failure (6-8), because both endothelial leakage and the use of transfusion products have been associated with organ failure in trauma.[6, 30, 31] We chose a resuscitation strategy targeted at a predetermined blood pressure level. Presumably, adding a model with a fixed transfusion

volume with as primary outcome organ failure could have identified which factor contributed more to a reduction in organ failure: bosutinib-induced reduction of endothelial leakage or bosutinib-induced reduction of transfusion volume needed to restore a fixed blood pressure transfusion target. However, this may not be a relevant question in clinical practice, as a volume fixed approach may induce overtransfusion.

Bosutinib has a rapid bioavailability *in vivo* when administered intravenously.(32) As bosutinib is clinically licensed and has a better safety profile compared to other tyrosine kinase inhibitors (15), administration of bosutinib in a bleeding trauma patient is feasible. With regard to safety, there are concerns about decreasing platelet counts and low-grade liver toxicity in patients on long-term treatment with tyrosine kinase inhibitors.(11, 15, 33, 34) However, in an acute setting, in which only one or two doses are to be administered to the patient, the protective effects of bosutinib may outweigh the potential side-effects. Indeed, we did not observe differences in platelet counts or liver injury when comparing the sham treated with vehicle to sham treated with bosutinib.

This study has some limitations. Despite a prior calculated power analysis, the sample size was probably too small to reveal differences in kidney scores. However, we did find that all effects of bosutinib pointed in the same direction of organ protection. Furthermore, because many secondary outcomes were exploratory we did not correct for multiple testing. Also, rats used in this model were young and male. It remains to be determined whether the endothelial response to bosutinib is influenced by age, sex and/or vascular comorbidities. Furthermore, the coagulation system in rats is different from humans.(35, 36) For example, rats have three to four times as many platelets as humans. Therefore, the effects of bosutinib needs to be further studied in trauma models with longer duration of mechanical ventilation to determine the long term side effects of bosutinib administered in an acute setting.

6

In conclusion, in a trauma and transfusion model, bosutinib reduced resuscitation needs and concomitantly reduced vascular leakage, , and lung injury. Although preliminary due to the experimental set-up, bosutinib may be an appealing therapeutic option to ameliorate organ failure in severe traumatic bleeding patients, thereby improving outcome after trauma.

References

1. Holcomb JB, Tilley BC, Baraniuk S, Fox EE, Wade CE, Podbielski JM, et al. Transfusion of plasma, platelets, and red blood cells in a 1:1:1 vs a 1:1:2 ratio and mortality in patients with severe trauma: the PROPPR randomized clinical trial. JAMA. 2015;313(5):471-82.

2. DiMaggio CJ, Avraham JB, Lee DC, Frangos SG, Wall SP. The Epidemiology of Emergency Department Trauma Discharges in the United States. Acad Emerg Med. 2017;24(10):1244-56.

3. Juffermans NP, Wirtz MR, Balvers K, Baksaas-Aasen K, van Dieren S, Gaarder C, et al. Towards patient-specific management of trauma hemorrhage: the effect of resuscitation therapy on parameters of thromboelastometry. J Thromb Haemost. 2019;17(3):441-8.

4. Balvers K, van Dieren S, Baksaas-Aasen K, Gaarder C, Brohi K, Eaglestone S, et al. Combined effect of therapeutic strategies for bleeding injury on early survival, transfusion needs and correction of coagulopathy. Br J Surg. 2017;104(3):222-9.

5. Sperry JL, Guyette FX, Brown JB, Yazer MH, Triulzi DJ, Early-Young BJ, et al. Prehospital Plasma during Air Medical Transport in Trauma Patients at Risk for Hemorrhagic Shock. N Engl J Med. 2018;379(4):315-26.

6. Naumann DN, Hazeldine J, Davies DJ, Bishop J, Midwinter MJ, Belli A, et al. Endotheliopathy of Trauma is an on-Scene Phenomenon, and is Associated with Multiple Organ Dysfunction Syndrome: A Prospective Observational Study. Shock. 2018;49(4):420-8.

7. Wei S, Gonzalez Rodriguez E, Chang R, Holcomb JB, Kao LS, Wade CE, et al. Elevated Syndecan-1 after Trauma and Risk of Sepsis: A Secondary Analysis of Patients from the Pragmatic, Randomized Optimal Platelet and Plasma Ratios (PROPPR) Trial. J Am Coll Surg. 2018;227(6):587-95.

8. Naumann DN, Hazeldine J, Dinsdale RJ, Bishop JR, Midwinter MJ, Harrison P, et al. Endotheliopathy is associated with higher levels of cell-free DNA following major trauma: A prospective observational study. PLoS One. 2017;12(12):e0189870.

9. Sordi R, Nandra KK, Chiazza F, Johnson FL, Cabrera CP, Torrance HD, et al. Artesunate Protects Against the Organ Injury and Dysfunction Induced by Severe Hemorrhage and Resuscitation. Ann Surg. 2017;265(2):408

10. Khoury HJ, Cortes JE, Kantarjian HM, Gambacorti-Passerini C, Baccarani M, Kim DW, et al. Bosutinib is active in chronic phase chronic myeloid leukemia after imatinib and dasatinib and/or nilotinib therapy failure. Blood. 2012;119(15):3403-12.

11. Gambacorti-Passerini C, Cortes JE, Lipton JH, Kantarjian HM, Kim DW, Schafhausen P, et al. Safety and efficacy of second-line bosutinib for chronic phase chronic myeloid leukemia over a five-year period: final results of a phase I/II study. Haematologica. 2018;103(8):1298-307.

12. Gourd E. Bosutinib more effective than imatinib in CML. Lancet Oncol. 2017;18(12):e716.

13. Aman J, van Bezu J, Damanafshan A, Huveneers S, Eringa EC, Vogel SM, et al. Effective treatment of edema and endothelial barrier dysfunction with imatinib. Circulation. 2012;126(23):2728-38.

14. Botros L, Pronk MCA, Juschten J, Liddle J, Morsing SKH, van Buul JD, et al. Bosutinib prevents vascular leakage by reducing focal adhesion turnover and reinforcing junctional integrity. J Cell Sci. 2020;133(9).

15. Gover-Proaktor A, Granot G, Pasmanik-Chor M, Pasvolsky O, Shapira S, Raz O, et al. Bosutinib, dasatinib, imatinib, nilotinib, and ponatinib differentially affect the vascular molecular pathways and functionality of human endothelial cells. Leuk Lymphoma. 2019;60(1):189-99.

16. Rizzo AN, Sammani S, Esquinca AE, Jacobson JR, Garcia JG, Letsiou E, et al. Imatinib attenuates inflammation and vascular leak in a clinically relevant two-hit model of acute lung injury. Am J Physiol Lung Cell Mol Physiol. 2015;309(11):L1294-304.

17. Letsiou E, Rizzo AN, Sammani S, Naureckas P, Jacobson JR, Garcia JG, et al. Differential and opposing effects of imatinib on LPS- and ventilator-induced lung injury. Am

J Physiol Lung Cell Mol Physiol. 2015;308(3):L259-69.

18. Koning NJ, de Lange F, van Meurs M, Jongman RM, Ahmed Y, Schwarte LA, et al. Reduction of vascular leakage by imatinib is associated with preserved microcirculatory perfusion and reduced renal injury markers in a rat model of cardiopulmonary bypass. Br J Anaesth. 2018;120(6):1165-75.

19. Jarrar D, Wang P, Song GY, Cioffi WG, Bland KI, Chaudry IH. Inhibition of tyrosine kinase signaling after trauma-hemorrhage: a novel approach for improving organ function and decreasing susceptibility to subsequent sepsis. Ann Surg. 2000;231(3):399-407.

20. Kleinveld DJB, Wirtz MR, van den Brink DP, Maas MAW, Roelofs J, Goslings JC, et al. Use of a high platelet-to-RBC ratio of 2:1 is more effective in correcting trauma-induced coagulopathy than a ratio of 1:1 in a rat multiple trauma transfusion model. Intensive Care Med Exp. 2019;7(Suppl 1):42.

21. Lee HB, Blaufox MD. Blood volume in the rat. J Nucl Med. 1985;26(1):72-6.

22. Xu Y, Huang X-c, Dai S, Xiao Y, Zhou M-t. A simple method for the determination of Bosutinib in rat plasma by UPLC-MS/MS. Journal of Chromatography B. 2015;1004:93

23. Tauer JT, Hofbauer LC, Jung R, Erben RG, Suttorp M. Micro-osmotic pumps for continuous release of the tyrosine kinase inhibitor bosutinib in juvenile rats and its impact on bone growth. Med Sci Monit Basic Res. 2013;19:274-8.

24. Wirtz MR, Jurgens J, Zuurbier CJ, Roelofs J, Spinella PC, Muszynski JA, et al. Washing or filtering of blood products does not improve outcome in a rat model of trauma and multiple transfusion. Transfusion. 2019;59(1):134-45.

25. Nadeem A, Ahmad SF, Al-Harbi NO, Al-Harbi MM, Ibrahim KE, Kundu S, et al. Inhibition of spleen tyrosine kinase signaling protects against acute lung injury through blockade of NADPH oxidase and IL-17A in neutrophils and gammadelta T cells respectively in mice. Int Immunopharmacol. 2019;68:39-47.

26. Rizzo AN, Aman J, van Nieuw Amerongen GP, Dudek SM. Targeting Abl kinases to regulate vascular leak during sepsis and acute respiratory distress syndrome.

Arterioscler Thromb Vasc Biol. 2015;35(5):1071-9.

27. Sauaia A, Moore FA, Moore EE. Postinjury Inflammation and Organ Dysfunction. Crit Care Clin. 2017;33(1):167-91.

28. Shepherd JM, Cole E, Brohi K. Contemporary Patterns of Multiple Organ Dysfunction in Trauma. Shock. 2017;47(4):429-35.

29. Ozanne J, Prescott AR, Clark K. The clinically approved drugs dasatinib and bosutinib induce anti-inflammatory macrophages by inhibiting the salt-inducible kinases. Biochem J. 2015;465(2):271-9.

30. Gonzalez Rodriguez E, Ostrowski SR, Cardenas JC, Baer LA, Tomasek JS, Henriksen HH, et al. Syndecan-1: A Quantitative Marker for the Endotheliopathy of Trauma. J Am Coll Surg. 2017;225(3):419-27.

31. Johansson PI, Henriksen HH, Stensballe J, Gybel-Brask M, Cardenas JC, Baer LA, et al. Traumatic Endotheliopathy: A Prospective Observational Study of 424 Severely Injured Patients. Ann Surg. 2017;265(3):597-603.

32. Hsyu P-H, Pignataro DS, Matschke K. Absolute Bioavailability of Bosutinib in Healthy Subjects From an Open-Label, Randomized, 2-Period Crossover Study. Clinical Pharmacology in Drug Development. 2018;7(4):373-81.

33. Kuo CY, Wang PN, Hwang WL, Tzeng CH, Bai LY, Tang JL, et al. Safety and efficacy of nilotinib in routine clinical practice in patients with chronic myeloid leukemia in chronic or accelerated phase with resistance or intolerance to imatinib: results from the NOVEL study. Ther Adv Hematol. 2018;9(3):65-78.

34. Lin Z, Yang Y, Huang Y, Liang J, Lu F, Lao X. Vascular endothelial growth factor receptor tyrosine kinase inhibitors versus bevacizumab in metastatic colorectal cancer: A systematic review and meta-analysis. Mol Clin Oncol. 2015;3(4):959-67.

35. Darlington DN, Craig T, Gonzales MD, Schwacha MG, Cap AP, Dubick MA. Acute coagulopathy of trauma in the rat. Shock. 2013;39(5):440-6.

36. Darlington DN, Wu X, Keesee JD, Cap AP. Severe Trauma and Hemorrhage Leads to Platelet Dysfunction and Changes in Cyclic Nucleotides In The Rat. Shock. 2019.

6

SUPPLEMENTAL INFORMATION

Supplemental table 1: Organ failure assessment scores

Lung injury was scored as follows:
• Lung edema
• Interstitial inflammatory cell infiltration
• Endothelialitis
• Hemorrhage

The severity of liver injury was scored as follows:
• Loss of intercellular borders
• Necrosis
• Hemorrhage
• Portal inflammation
• Neutrophil infiltration

The severity of spleen injury was scored as follows:
• Neutrophil infiltration
• Necrosis
• Congestion

| The severity of kidney injury was scored as follows: |
| --- |
| • Tubules in the cortex or the outer medulla that showed epithelial necrosis or had luminal necrotic debris |
| • Tubular dilation |
| • Neutrophil extravasation |
| • Interstitial changes |
| • Hemorrhage |

The severity of small intestine injury was scored as follows:
• Focal epithelial edema
• Diffuse swelling of the villi
• Neutrophil infiltration in the submucosa
• Necrosis
• Hemorrhage

Supplemental table 1: All evaluations were made on five fields per section and five sections per organ. Severity was assessed based on a scale from 0-3 (0, absent; 1, mild; 2, moderate; 3, severe).
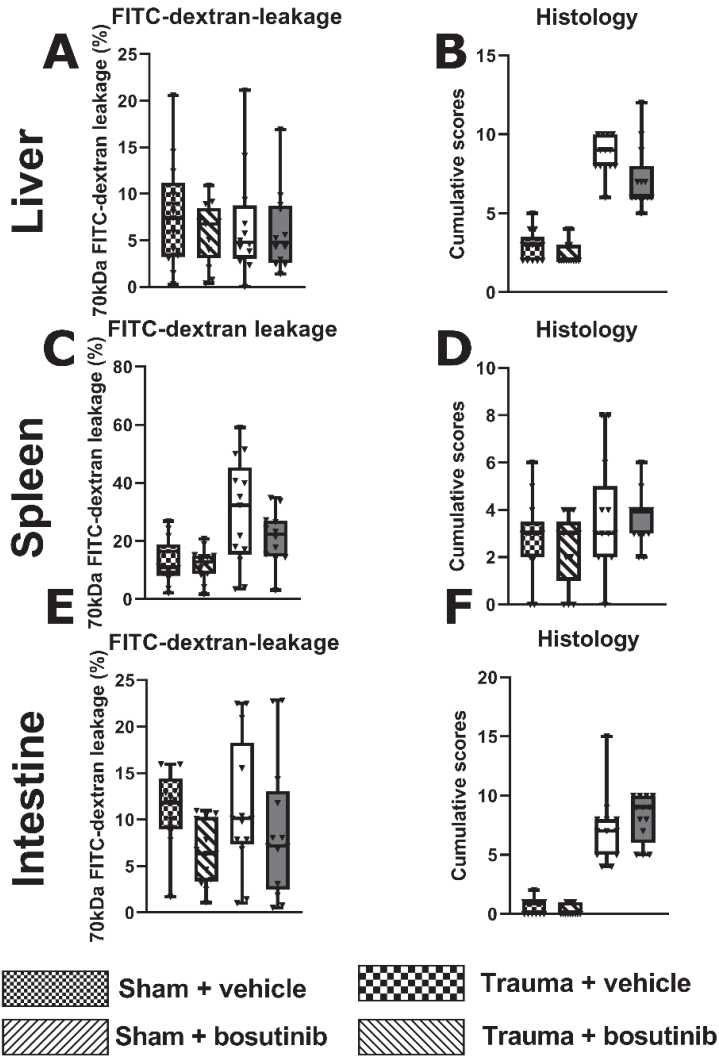
Supplemental figure 1
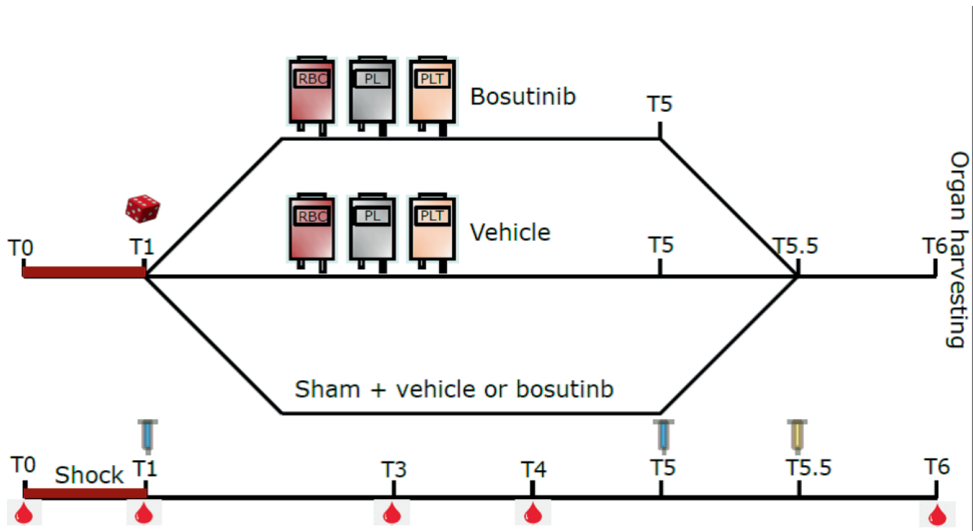
Supplemental figure 1: Schematic overview of the trauma transfusion model. T0 = baseline sample, T1 = 1 hour after injury and end of shock period, moment of randomization, initiation of treatment strategy, T3 = post-transfusion sample, T4 = additional blood gas sample to adjust ventilation if necessary, T5 = extra dose of bosutinib or vehicle if randomized to one of these groups, T5.5 administration of 70kDa FITC-labelled dextran, and T6 = 6h after injury, termination of the animal by blood draws and harvesting of different organs. RBC = red blood cell, PL = plasma product, PLT = platelet product, RL = Ringer's Lactate (crystalloid).

6

Supplemental table 2: Quality assessment of blood products

| Parameter	Red blood cell product		Plasma product		Platelet product	
	Trauma + vehicle	Trauma + bosutinib	Trauma + vehicle	Trauma + bosutinib	Trauma + vehicle	Trauma + bosutinib
pH	7.0 (7.0 – 7.1)	7.1 (7.0 – 7.2)	7.2 (7.1 – 7.2)	7.2 (7.1 – 7.2)	7.1 (7.0 – 7.1)	7.1 (7.0 – 7.1)
Lactate (mmol/L)	1.5 (1.3 – 2.4)	1.4 (1.0 – 1.6)	1.7 (1.2 – 2.2)	1.3 (1.1 – 2.3)	2.5 (1.9 – 2.7)	2.5 (2.0 – 3.2)
Hb (mmol/L)	12.3 (10.4 – 12.7)	12.2 (10.1 – 12.9)	NA	NA	NA	NA
K^+ (mmol/L)	1.5 (1.3 – 2.9)	1.6 (1.1 - 1.6)	3.1 (3.1 – 3.2)	3.1 (2.9 – 3.2)	3.3 (3.2 – 3.5)	3.2 (3.2 – 3.4)
Platelets ($*10^9$/L)	ND	ND	<100	<100	1184 (1112 – 1496)	1092 (1071 – 1496)
Leukocytes ($*10^9$/L)	1.6 (1.6 – 2.7)	1.8 (1.4 – 2.5)	NA	NA	NA	NA

Supplemental table 2: In total 13 different red blood cell, plasma products and platelet products were made. Measurements are on the day of transfusion. Some measurements had missing values due to technical errors in the blood gas analysis equipment or cell coulter. Maximum missing values were 6/13 products. ND=not determined. NA=not applicable.

Supplemental figure 2

Supplemental figure 2: Bosutinib has limited effects on injury of the splanchnic organs
Data are median (IQR) or boxplot with range. A – B: Liver FITC-70kDa dextran leakage and liver score. C – D Spleen FITC-70kDa dextran leakage and spleen score. E – F Small intestine FITC -70kDa dextran leakage and small intestine score.

Supplemental figure 3
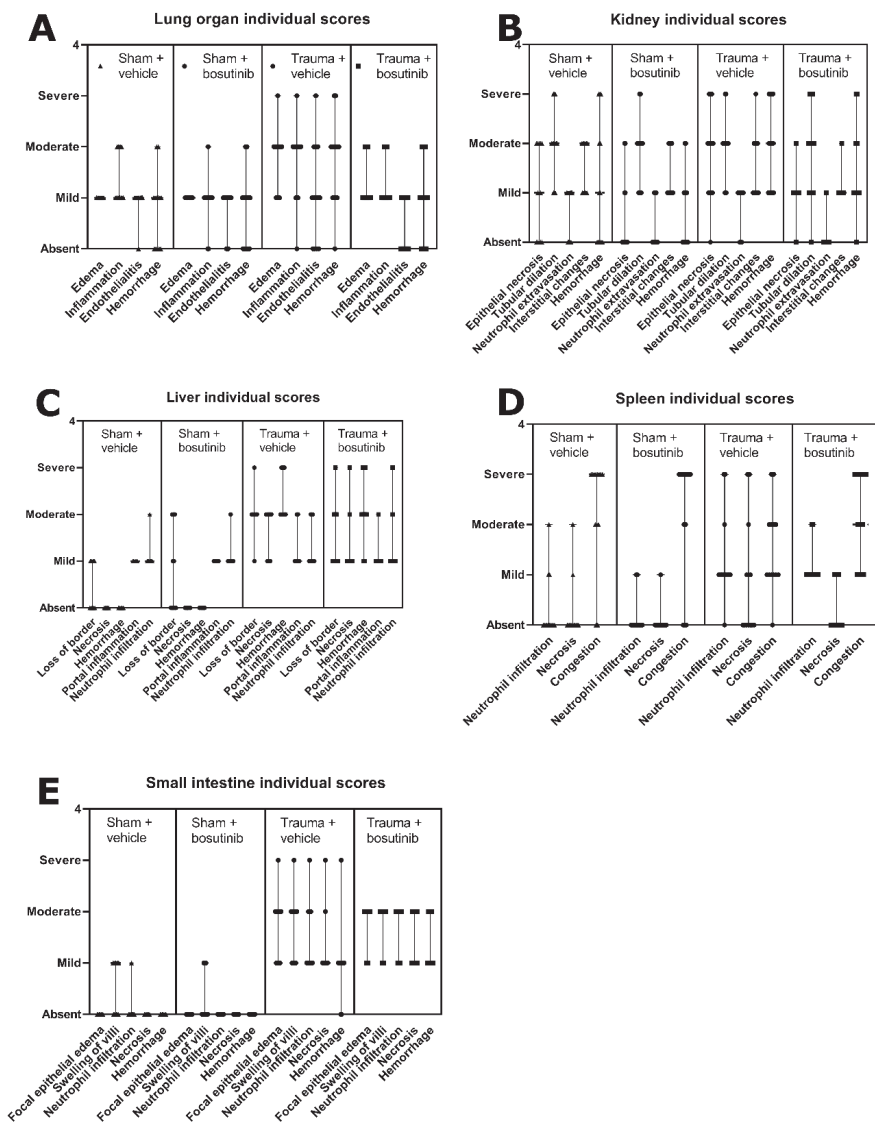
Supplemental figure 3: Individual organ scores. Data are median with range (all points are shown).
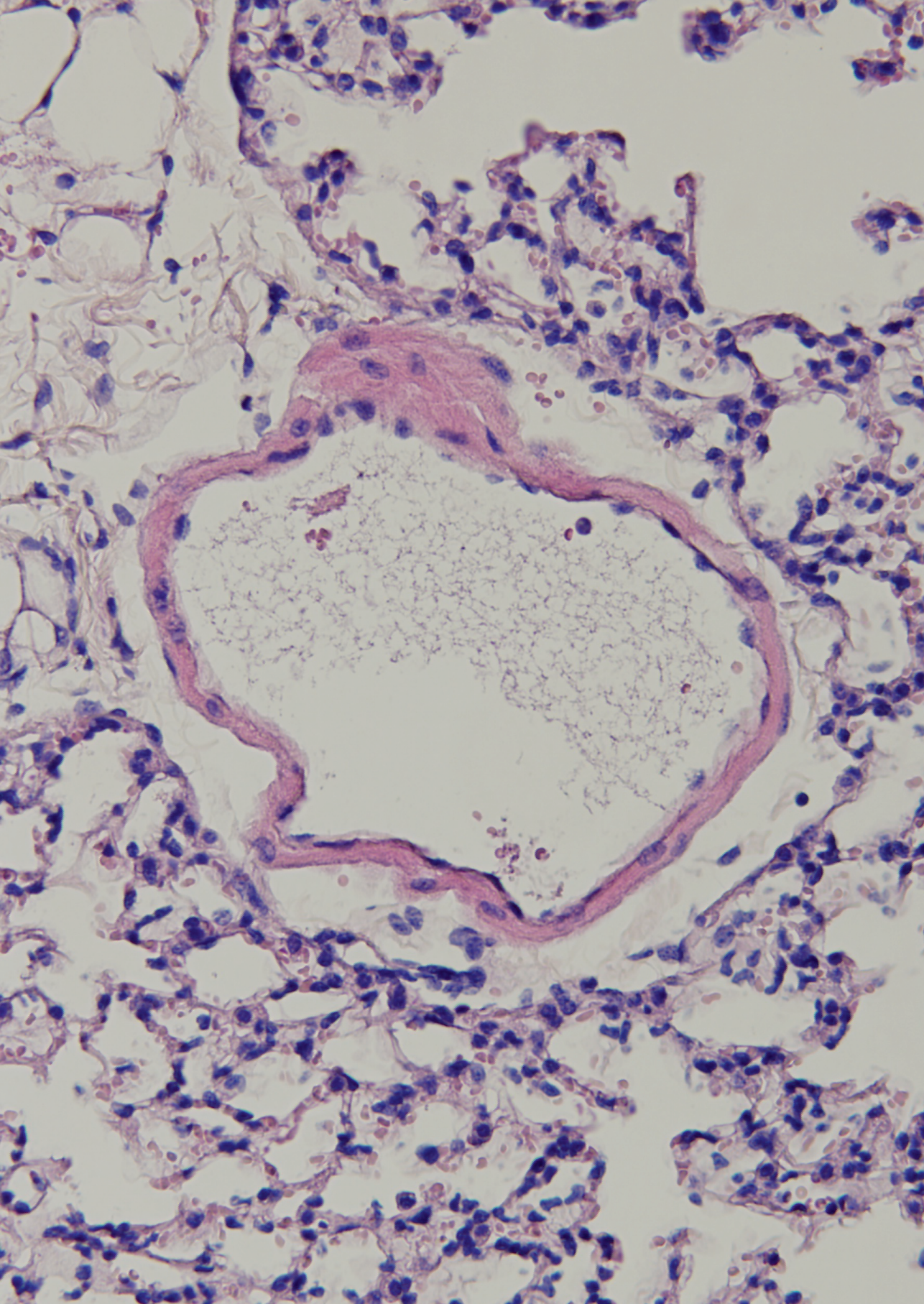
7

Imatinib in patients with severe COVID-19: a randomised, double-blind, placebo-controlled, clinical trial

Jurjan Aman, Erik Duijvelaar, Liza Botros*, Azar Kianzad*, Job R. Schippers*, Patrick J. Smeele*, Sara Azhang, Imke H. Bartelink, Ahmed Bayoumy, Pierre M. Bet, Wim Boersma, Peter I. Bonta, Karin A.T. Boomars, Lieuwe D.J. Bos, Job J.M.H van Bragt, Gert-Jan Braunstahl, Lucas R. Celant, Katrien A.B. Eger, Miranda Geelhoed, Yurika L.E. van Glabbeek, Hans P. Grotjohan, Laura A. Hagens, Chris M. Happe, Boaz Hazes, Leo M.A. Heunks, Michiel van den Heuvel, Wouter Hoefsloot, Rianne J.A. Hoek, Romke Hoekstra, Herman M.A. Hofstee, Nicolle P. Juffermans, Marleen Kemper, Renate Kos, Peter W.A. Kunst, Ivo van der Lee, Laurien van der Lee, Anke-Hilse Maitland-Van der Zee, Pearl F.M. Mau Asam, Adinda Mieras, Mirthe Muller, Liesbeth Neefjes, Esther J. Nossent, Laurien M.A. Oswald, Maria Overbeek, C. Pamplona, N. Paternotte, N. Pronk, Michiel A. de Raaf, Bas van Raaij, Merlijn Reijrink, Marcus J. Schultz, Ary Serpa Neto, Elise M. Slob, Frank Smeenk, Marieke R. Smit, Josien Smits, Janneke E. Stalenhoef, Pieter R. Tuinman, Arthur L.E.M. Vanhove, Jeroen Wessels, Jessie van Wezenbeek, Anton Vonk Noordegraaf, Frances S. Handoko-de Man, H.J. Bogaard.

*Equal contribution

Abstract

Background: The major complication of COVID-19 is hypoxaemic respiratory failure from capillary leak and alveolar oedema. Experimental and early clinical data suggest that the tyrosine-kinase inhibitor imatinib reverses pulmonary capillary leak.

Methods: This randomised, double-blind, placebo-controlled, clinical trial was done at 13 academic and non-academic teaching hospitals in the Netherlands. Hospitalised patients (aged ≥18 years) with COVID-19, as confirmed by an RT-PCR test for SARS-CoV-2, requiring supplemental oxygen to maintain a peripheral oxygen saturation of greater than 94% were eligible. Patients were excluded if they had severe pre-existing pulmonary disease, had pre-existing heart failure, had undergone active treatment of a haematological or non-haematological malignancy in the previous 12 months, had cytopenia, or were receiving concomitant treatment with medication known to strongly interact with imatinib. Patients were randomly assigned (1:1) to receive either oral imatinib, given as a loading dose of 800 mg on day 0 followed by 400 mg daily on days 1–9, or placebo. Randomisation was done with a computer-based clinical data management platform with variable block sizes (containing two, four, or six patients), stratified by study site. The primary outcome was time to discontinuation of mechanical ventilation and supplemental oxygen for more than 48 consecutive hours, while being alive during a 28-day period. Secondary outcomes included safety, mortality at 28 days, and the need for invasive mechanical ventilation. All efficacy and safety analyses were done in all randomised patients who had received at least one dose of study medication (modified intention-to-treat population). This study is registered with the EU Clinical Trials Register (EudraCT 2020–001236–10).

Findings: Between March 31, 2020, and Jan 4, 2021, 805 patients were screened, of whom 400 were eligible and randomly assigned to the imatinib group (n=204) or the placebo group (n=196). A total of 385 (96%) patients (median age 64 years [IQR 56–73]) received at least one dose of study medication and were included in the modified intention-to-treat population. Time to discontinuation of ventilation and supplemental oxygen for more than 48 h was not significantly different between the two groups (unadjusted hazard ratio [HR] 0·95 [95% CI 0·76–1·20]). At day 28, 15 (8%) of 197 patients had died in the imatinib group compared with 27 (14%) of 188 patients in the placebo group (unadjusted HR 0·51 [0·27–0·95]). After adjusting for baseline imbalances between the two groups (sex, obesity, diabetes, and cardiovascular disease) the HR for mortality was 0·52 (95% CI 0·26–1·05). The HR for mechanical ventilation in the imatinib group compared with the placebo group was 1·07 (0·63–1·80; p=0·81). The median duration of invasive mechanical ventilation was 7 days (IQR 3–13) in the imatinib group compared with 12 days (6–20) in the placebo group (p=0·0080). 91 (46%) of 197 patients in the imatinib group and 82 (44%) of 188 patients in the placebo group had at least one grade 3 or higher adverse event. The safety evaluation revealed no imatinib-associated adverse events.

Interpretation: The study failed to meet its primary outcome, as imatinib did not reduce the time to discontinuation of ventilation and supplemental oxygen for more than 48 consecutive hours in patients with COVID-19 requiring supplemental oxygen. The observed effects on survival (although attenuated after adjustment for baseline imbalances) and duration of mechanical ventilation suggest that imatinib might confer clinical benefit in hospitalised patients with COVID-19, but further studies are required to validate these findings.

7

Introduction

A major complication of SARS-CoV2 infection is hypoxemic respiratory failure, responsible for the majority of hospitalisations, intubations and mortality in coronavirus disease 2019 (COVID-19) (1). The clinical manifestation of lung involvement in COVID-19 is pneumonitis, often progressing to acute respiratory distress syndrome (ARDS). Radiological investigations typically reveal extensive bilateral ground glass opacities and consolidations suggestive of diffuse pulmonary oedema. Post-mortem studies have demonstrated that endothelial injury is a key feature of COVID-19 and results from direct infection of pulmonary endothelial cells (2,3), disruption of the endothelial barrier and widespread endothelial apoptosis (3).

Therapeutic strategies evaluated in COVID-19 include antiviral treatment and immunomodulatory drugs. Remdesivir shortened the time to recovery in patients hospitalised with COVID-19 in the ACTT-1 trial (4), but this finding was not replicated in the World Health Organisation (WHO) Solidarity study (5). Neither study demonstrated a survival benefit from remdesivir. Other antiviral interventions, including (hydroxy)chloroquine (5,6), interferon (5) and lopinavir–ritonavir (5-7), also failed to show clinical benefit. As an alternative to antiviral treatment, and based on the recognition of a marked hyperinflammatory pattern in patients with a worse outcome, other investigators aimed to modulate the immune response. Dexamethasone reduced COVID-19 mortality from 24 to 20% in hospitalised patients and from 40 to 30% in those in the intensive care unit (ICU) (8). Most recent data from REMAP (Randomised, Embedded, Multifactorial, Adaptive Platform) indicates that monoclonal antibody-mediated blockage of Interleukin-6 (IL-6) with tocilizumab or sarilumab also reduces mortality in ICU patients (9).

Despite the direct contribution of alveolar oedema to hypoxemia and adverse outcomes like intubation or death in COVID-19, treatment strategies attenuating or reversing this type of lung damage have so far not been evaluated. One of the suggested approaches to accomplish this is treatment with the anti-neoplastic agent imatinib (1). The Abl kinase inhibitor imatinib protects against capillary leak and alveolar oedema caused by inflammatory stimuli. After a first observation in 2008 of a patient recovering from respiratory failure from pulmonary veno-occlusive disease after imatinib treatment (10), subsequent *in vitro* and *in vivo* studies revealed that imatinib protects the endothelial barrier under inflammatory conditions (11-15). Later case reports confirmed the protective effect of imatinib in other conditions characterised by alveolar oedema (16-18) including COVID-19 (19).

Here, we describe the results of a randomised, placebo-controlled clinical trial investigating the efficacy and safety of oral imatinib in hospitalised patients with polymerase chain reaction (PCR)-proven SARS-CoV2 infection who required supplemental administration of oxygen.

Methods

Study design and patients

This randomised, double-blind and placebo-controlled, clinical trial was done at 13 large academic and non-academic teaching hospitals in the Netherlands. Patients were eligible for inclusion if they were aged 18 years or older, had been admitted to hospital with SARS-CoV-2 infections (confirmed with an RT-PCR test), and required supplemental oxygen to maintain a peripheral oxygen saturation of greater than 94%. Exclusion criteria included, but were not limited to, pre-existing pulmonary disease, pre-existing heart failure (left ventricular ejection fraction <40%), active treatment of an haematological or non-haematological malignancy in the 12 months before enrolment, the presence of cytopenia, and concomitant treatment with medication known to strongly interact with imatinib. Full details on exclusion criteria are provided in the study protocol (supplemental data appendix). Women of childbearing age were asked to undergo pregnancy testing before enrolment.

The trial was approved by the Medical Ethics Committee of the Amsterdam UMC, location VUMC, and was done in accordance with Good Clinical Practice and the Declaration of Helsinki. All patients provided written informed consent before randomisation.

Randomisation and masking

Patients were enrolled by study investigators and randomly assigned (1:1) to either the placebo group or the imatinib group. Randomisation was done with the Castor Electronic Data Capturing System (Castor EDC; Amsterdam, Netherlands) using variable block sizes (two, four, or six patients), stratified by study site. Allocation to study groups was done by Castor, and was not accessible to study investigators. After randomisation, patients received oral imatinib (as 400 mg tablets) or non-identical placebo tablets, which were dispensed by the hospital pharmacy and distributed in sealed containers. Medical staff and investigators were not involved in the dispensing of the study drugs. Patients, medical staff, and investigators were masked to group assignment.

Procedures

After randomisation, patients in the imatinib group received a loading dose of 800 mg imatinib on day 0, followed by 400 mg once daily on days 1–9. Patients in the placebo group received placebo tablets in a similar dosing scheme. For evaluation of efficacy, the clinical status of patients (ie, whether they had been discharged, admitted to a hospital ward, admitted to the ICU, or had died) and whether they were receiving ventilatory or oxygen support (ie, receiving oxygen supplementation, high-flow nasal oxygen, non-invasive ventilation, mechanical ventilation, or extracorporeal membrane oxygenation) were recorded daily on days 0–9 and on day 28. If patients were discharged from the hospital before day 9, their clinical status was ascertained by a telephone call on days 9 and 28.

Safety evaluations included clinical laboratory testing at baseline (day 0) and on days 1, 2, 3, 5, 7, and 9, consisting of a blood cell count, and assessment of electrolytes, renal function, and liver enzymes. An electrocardiogram (ECG) was used to monitor corrected QT (QTc) intervals at baseline and on days 1, 3, 5, and 9. Stopping criteria included a reduction in haemoglobin of more than 30% relative to the baseline measurement before the loading dose was given; an absolute leukocyte count of less than $2 \cdot 5 \times 10^9$ cells per L; an absolute thrombocyte count of less than 100×10^9 cells per L; an increase in aminotransferase concentrations to more than three times the upper limit of normal if aspartate aminotransferase (AST) and alanine aminotransferase (ALT) concentrations were within reference values at baseline, or increased AST and ALT concentrations to more than three times the value at baseline if concentrations were higher than reference values at baseline; an increase in bilirubin concentrations of more than $1 \cdot 5$ times the upper limit of normal if bilirubin concentrations were within the normal range at baseline, or an increase in bilirubin concentrations of more than $1 \cdot 5$ times the baseline value if concentrations were higher than reference values at baseline; or an increase in QTc of more than 100 msec relative to baseline. In patients discharged from hospital before day 9, clinical laboratory testing and ECG measurements were suspended, according to guidelines for imatinib treatment of chronic myeloid leukaemia in an outpatient setting (20). Adverse events and severe adverse events, graded by use of the Common Terminology Criteria for Adverse Events version 5.0 (November, 2017), were recorded on a daily basis. All grade 3 or higher adverse events reported at any time during the 28-day study period by the patient or observed by the investigator or the medical staff were recorded. The investigators assessed whether an adverse event was related to treatment, and they consulted medical staff if the potential association was not clear.

Outcome parameters

The primary outcome was the time to discontinuation from ventilation and supplemental oxygen for more than 48 hours, while being alive, during a 28-day period after randomisation. Secondary efficacy parameters included: 28-day mortality, the number of ICU admissions, the length of ICU admission, the need for mechanical ventilation, the duration of mechanical ventilation, the duration of oxygen suppletion, the duration of hospital admission and the clinical status at day 9 and day 28, as assed by use of the WHO ordinal scale for clinical improvement (with 1 indicating discharge with full recovery [with no home oxygen use]; 2 indicating discharge without full recovery [with actual home oxygen use]; 3 indicating admission to a non-ICU ward and not receiving supplemental oxygen; 4 indicating admission to a non-ICU hospital ward and receiving supplemental oxygen; 5 indicating admission to a medium care unit [MCU] or an ICU without mechanical ventilation; 6 indicating admission to an MCU or ICU with mechanical ventilation; and 7 indicating death). The number of ventilator-free days was defined as the number of days alive and free from mechanical ventilation. Patients were only considered free from mechanical ventilation when they had a successful extubation, defined as being free from mechanical ventilation for

at least 48 consecutive hours. Non-survivors were considered to have no ventilator free days. Secondary safety outcomes were incidence of grade 3 and 4 adverse and severe adverse events, blood cell count, kidney function, liver enzymes, N-terminal-pro-B natriuretic peptide (NTproBNP) concentrations (all measured on days 0, 1, 2, 3, 5, 7, and 9), and QTc intervals (measured on days 0, 1, 3, 5, and 9). Pharmacokinetic and biomarker analyses, as defined in the study protocol, are currently being done and the results will be published separately.

Statistical Analysis

Based on an anticipated hazard ratio (HR) of 1·39 for the primary outcome (imatinib group vs the placebo group), a one-sided α level of 0·025 for superiority of the intervention and a β level of 0·20, the sample size was set at 193 patients per group. Analyses for primary and secondary outcomes were done in all patients who underwent randomisation and had received at least one dose of study medication (the modified intention-totreat population). All statistical analyses were predefined in the study protocol and the statistical analysis plan. No data were missing for the primary and secondary outcome analyses. No data imputation was done to account for missing data.

Baseline demographic variables are reported as absolute numbers (proportions) for categorical data, or as means (SDs) or medians (IQRs) for continuous variables. Categorical variables were analysed by use of the χ² test or Fisher's exact test. Continuous variables were analysed with a Wilcoxon rank-sum test. Imbalances at baseline (p<0·10) were carried forward as adjustment factors in regression analyses for the primary and secondary outcomes.

The primary outcome and the secondary outcomes of mortality at day 28 and the need for mechanical ventilation were analysed with Kaplan-Meier curves to plot event rates over time; between-group differences were expressed as HRs with 95% CIs, calculated as regression analyses. Kaplan-Meier and Cox regression analyses were done for time-to-event analyses of secondary outcomes. The assumption of proportional hazards was tested by examination of Schoenfeld residuals. Two-sided p values are provided for all tests.

All data were recorded in Castor EDC. The Clinical Research Office, an independent contract research organisation of the Amsterdam UMC, was responsible for data monitoring. The safety of patients was monitored by a Data Safety Monitoring Board (DSMB), which convened after enrolment of 30 patients (April 23, 2020) and 60 patients (May 7, 2020). During these meetings, patient safety was assessed on the basis of an unblinded line listing of severe adverse events. A severe adverse event was defined as any untoward medical event that occurred during the study period that (1) resulted in death; (2) was life-threatening; (3) required inpatient hospitalisation or led to an increased duration of hospitalisation; (4) resulted in persistent or significant disability; or (5) required intervention to prevent permanent impairment or damage. The DSMB subsequently convened after enrolment of 100 patients (Oct 22, 2020) and 200 patients (Dec 14, 2020), and patient safety

7

was assessed on the basis of an unblinded line listing of severe adverse events, and futility was assessed on the basis of predefined analyses of efficacy outcomes. All statistical analyses were done in RStudio, version 1.3.1073. This study is registered with the EU Clinical Trials Register (EudraCT 2020–001236–10).

Role of the funding source

The funders of the study had no role in study design, data collection, data analysis, data interpretation, or writing of the report.

Results

Between March 31st, 2020 and Jan 04th, 2021, 805 patients in 13 participating hospitals were screened (supplemental data appendix). Of these patients, 400 (50%) were enrolled and randomly assigned to the placebo group (n=196) or the imatinib group (n=204). A total of 11 (3%) patients withdrew consent before receiving the first dose of study medication (figure 1). During the peaks of the pandemic, two (1%) patients withdrew from the study before receiving their first dose of study medication, as they were relocated to non-participating hospitals with fewer COVID-19 admissions. The final analysis population included 197 patients in the imatinib group and 188 patients in the placebo group (figure 1).

The baseline characteristics of patients are shown in table 1. The median age of patients was 64 years (IQR 56–73; range 28–93). 264 (69%) of 385 patients were men, and the median body-mass index of patients at enrolment was 28·5 kg/m² (IQR 25·5–32·4). Clinical presentations at baseline included chest pain, dyspnoea, cough, and fever. The median duration from onset of symptoms to randomisation was 10 days (IQR 8–12) in the imatinib group and 10 days (8–12) in the placebo group.

Table 1: Baseline characteristics and demographic variables.

	Imatinib (n=197)	Placebo (n=188)
Age - median [IQR]	64 [57-73]	64 [55-74]
BMI - median [IQR]	27·5 [25·3-31·1]	29·7 [25·6-32·9]
Males - no· (%)	146 (74)	118 (63)
Co-morbidities * (%)		
Current/former smoker	77 (39)	76 (40)
BMI>30	53 (29)	83 (47)
Diabetes	41 (21)	54 (29)
Cardiovascular disease**	35 (18)	48 (26)
Hypertension	69 (35)	76 (40)
COPD/Asthma	38 (19)	33 (18)
Venous thromboembolism	5 (3)	5 (3)
Renal failure	7 (4)	7 (4)
Hepatic disease	1 (1)	1 (1)
Rheumatic disease	11 (6)	18 (10)
Heart failure	8 (4)	4 (2)
Medical treatment † (%)		
Glucose lowering drugs	40 (20)	54 (29)
Antihypertensive treatment	91 (46)	102 (54)
ACE/ARB	51 (26)	70 (37)
Statins	62 (32)	65 (35)
Platelet inhibitors	42 (21)	40 (21)
Oral anticoagulants	17 (9)	21 (11)
Clinical presentation (%)		
Atypical	24 (12)	32 (17)
Chest pain	34 (17)	27 (14)
Cough	151 (77)	141 (75)
Dyspnoea	160 (81)	158 (84)
Fever	133 (68)	112 (60)
Other flu-like symptoms	82 (42)	78 (42)
Days from symptom onset – median [IQR]	8 [10-12]	8 [10-12]
SpO2/FiO2 – median [IQR]	321 [265-380]	323 [238-377]
Laboratory values at admission		
Haemoglobin - g/dL	13·5 [12·6-14·7]	13·7 [12·6-14·7]
C-reactive protein - mg/L	102 [47·8-157·5]	95 [45 -149]
NTproBNP - ng/L	147 [49-411]	132 [50-352]
LDH - U/L	365 [279-445]	366 [293-496]
Lymphocytes - 10^9/L	0·90 [0·60-1·19]	0·94 [0·68-1·28]
Neutrophils - 10^9/L	6·00 [4·10-8·56]	5·94 [4·40-8·29]
Leukocytes - 10^9/L	7·60 [5·60-10·40]	7·60 [5·77-10·00]

7

Thrombocytes - 10^9/L	248 [184-323]	236 [190-310]
Medication initiated at admission (%)		
Low-molecular heparin	167 (85)	150 (80)
Oral anticoagulants	6 (3)	8 (4)
Antibiotics	85 (43)	77 (41)
Dexamethasone	143 (73)	133 (71)
Remdesivir	40 (20)	40 (21)
(Hydroxy)chloroquine	15 (8)	17 (9)

Table 1: Data are median (IQR) or n (%). BMI=body-mass index. COPD=chronic obstructive pulmonary disease. ACE=angiotensin-converting enzyme. ARB=angiotensin receptor blocker. SpO2=oxygen saturation. FiO2=fractional concentration of oxygen in inspired air. NTproBNP=N-terminal-pro-B natriuretic peptide. *Comorbidities as reported at admission or present in the patient's medical record. †Cardiovascular diseases included arrythmias (predominantly atrial fibrillation), valvular disease, coronary artery disease, and conduction disorders. ‡Medical treatment (or home medication) as reported at admission or present in the patient's medical record.
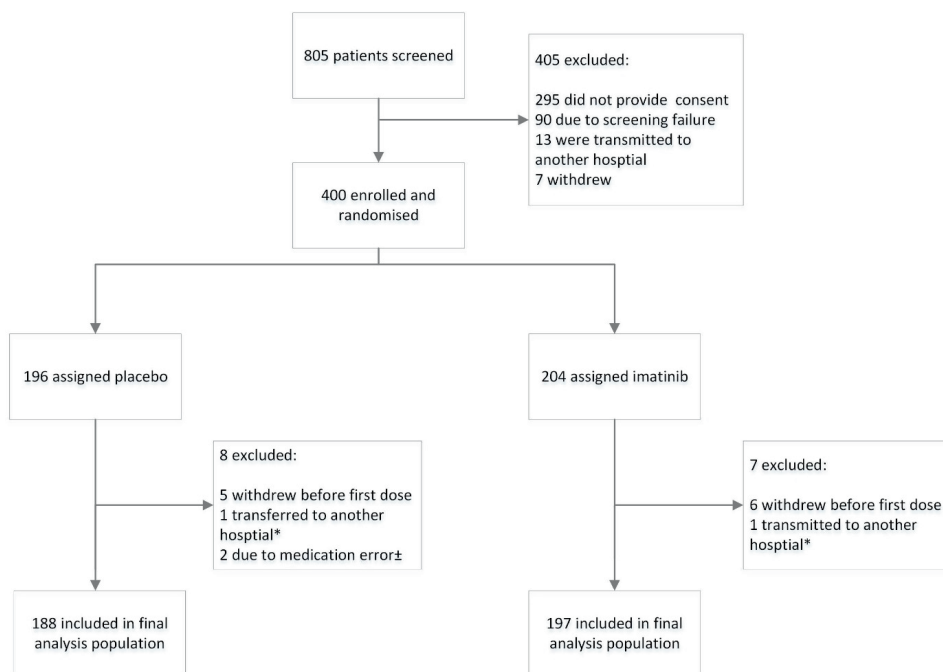
Figure 1

Figure 1: Trial profile. *Patients lost to follow-up due to transfer to another hospital before the first dose of study medication could be administered. ±Study medication was dispensed to the wrong patients and they were withdrawn from the study. Errors were detected before the first dose of study medication was given.

Common risk factors for a poor outcome and comorbidities included smoking (153 [40%] of 385 patients), obesity (136 [38%]), diabetes (95 [25%]), cardiovascular disease (83 [22%]), and chronic obstructive pulmonary disease or asthma (71 [18%]). Despite randomisation, sex, obesity, diabetes, and cardiovascular disease were slightly unbalanced between the two groups. No differences in baseline laboratory measurements were observed between the two groups, suggesting similar disease severity at presentation. Medications started at admission included low-molecular-weight heparin, oral anticoagulants, and antibiotics (table 1). Dexamethasone was started at admission in 276 (72%) patients and remdesivir was started in 80 (21%) patients. Most patients (276 [72%] of 385) received dexamethasone on admission to emergency care units before receiving study medication. As participation in other interventional studies was not allowed at enrolment, and because tocilizumab, anakinra, lopinavir–ritonavir, and convalescent plasma were not routinely administered to patients with COVID-19 in the Netherlands at the time the study was done, no patients received these treatments during the trial.

Table 2: Clinical outcomes in the final population

	HR	95% CI	p-value
Primary endpoint			
Imatinib	0·95	0·76-1·20	0·69
Imatinib corrected for sex	1·01	0·81-1·28	0·90
Imatinib corrected for obesity	0·99	0·78-1·26	0·92
Imatinib corrected for diabetes	0·96	0·76-1·20	0·69
Imatinib corrected for cardiovascular disease	0·94	0·75-1·18	0·59
Imatinib corrected for all of the above	1·07	0·62-1·84	0·82
Secondary endpoint: Mortality			
Imatinib	0·51	0·27-0·95	0·034
Imatinib corrected for sex	0·47	0·25-0·89	0·019
Imatinib corrected for obesity	0·46	0·23-0·92	0·029
Imatinib corrected for diabetes	0·54	0·29-1·02	0·057
Imatinib corrected for cardiovascular disease	0·54	0·29-1·01	0·055
Imatinib corrected for all of the above	0·52	0·26-1·05	0·068
Secondary endpoint: Need for mechanical ventilation			
Imatinib	1·07	0·63-1·80	0·81
Imatinib corrected for sex	0·98	0·58-1·67	0·95
Imatinib corrected for obesity	1·08	0·63-1·86	0·77
Imatinib corrected for diabetes	1·13	0·66-1·91	0·66
Imatinib corrected for cardiovascular disease	1·06	0·62-1·79	0·84
Imatinib corrected for all of the above	1·02	0·80-1·30	0·87

Table 2: All HRs are for the imatinib group versus the placebo group. The final analysis population consisted of 188 patients in the placebo group and 197 patients in the imatinib group. HRs and 95% CIs were calculated by use of Cox regression analysis and adjusted for sex and the indicated comorbidities. HR=hazard ratio.

7

Figure 2

A   Primary endpoint: 48h oxygen liberation and alive

Treatment period
— Placebo
— Imatinib

Cumulative incidence

HR: 0.95, 95%CI: 0.76-1.20, p=0.69

Time [days]

Number at risk (number censored)

	0	2	4	6	8	10	12	14	16	18	20	22	24	26	28
Placebo	188 (0)	187 (3)	155 (12)	116 (13)	90 (16)	71 (19)	52 (19)	44 (19)	36 (21)	33 (21)	32 (23)	27 (25)	24 (26)	22 (26)	20 (45)
Imatinib	197 (0)	196 (1)	171 (4)	140 (6)	108 (7)	89 (7)	65 (9)	56 (10)	48 (10)	41 (11)	34 (11)	32 (11)	28 (13)	27 (14)	24 (37)

Time [days]

B   Secondary endpoint: mortality

Treatment period
— Placebo
— Imatinib

Cumulative mortality

HR: 0.51, 95%CI: 0.27-0.95, p=0.03

Time [days]

Number at risk (number censored)

	0	4	8	12	16	20	24	28
Placebo	188 (0)	179 (0)	172 (0)	169 (0)	168 (0)	166 (0)	161 (0)	161 (161)
Imatinib	197 (0)	195 (0)	190 (0)	189 (0)	187 (0)	186 (0)	184 (0)	182 (182)

Time [days]

C   Secondary endpoint: intubation

Treatment period
— Placebo
— Imatinib

Cumulative incidence

HR: 1.07, 95%CI: 0.63-1.80, p=0.81

Time [days]

Number at risk (number censored)

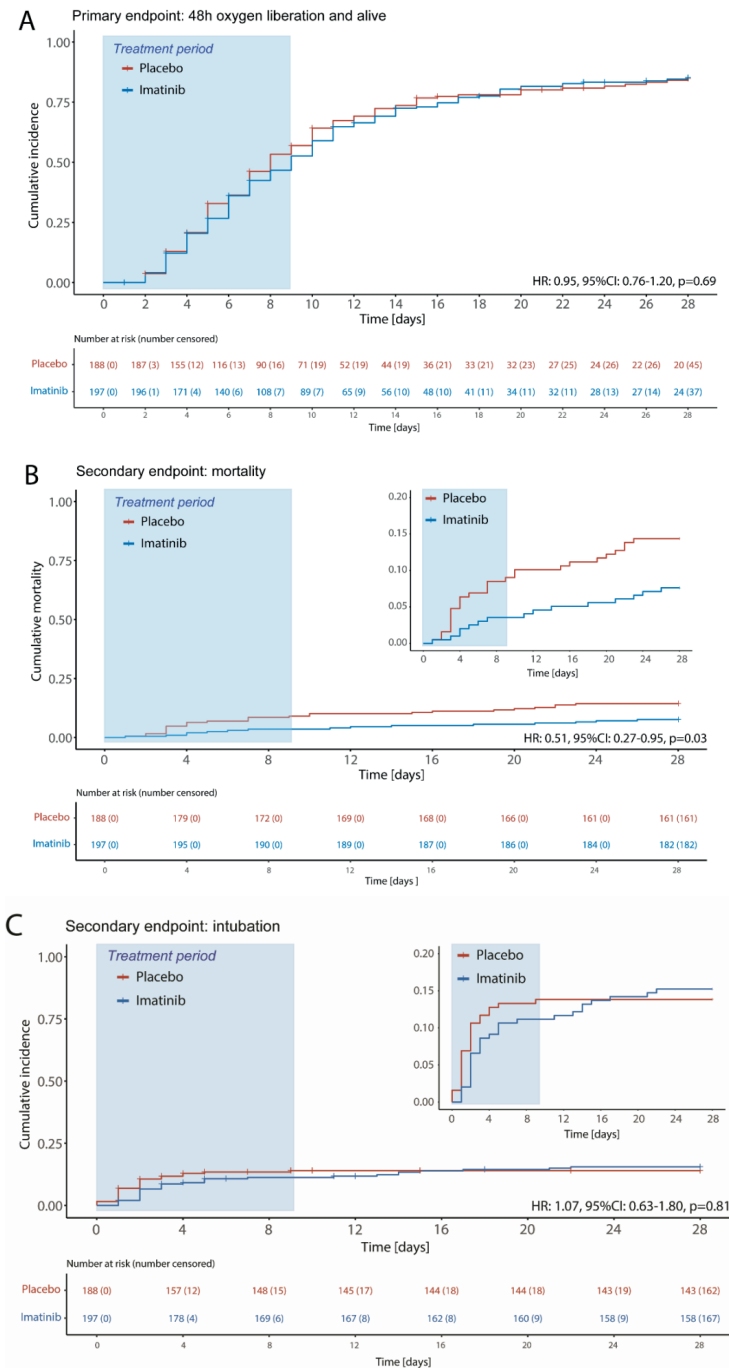|	0	4	8	12	16	20	24	28
Placebo	188 (0)	157 (12)	148 (15)	145 (17)	144 (18)	144 (18)	143 (19)	143 (162)
Imatinib	197 (0)	178 (4)	169 (6)	167 (8)	162 (8)	160 (9)	158 (9)	158 (167)

Time [days]

Figure 2: Kaplan-Meier analysis of primary and secondary outcomes Kaplan-Meier curves showing time-to-event analyses for time to discontinuation of ventilation and supplemental oxygen for more than 48 consecutive hours, while being alive during the 28-day study period as the primary outcome (A), mortality at 28 days as a secondary outcome (B), and time to invasive mechanical ventilation during the 28-day study period as a secondary outcome (C). Unadjusted HRs with 95% CIs were calculated by Cox regression analyses. HR=hazard ratio.

During the 28-day study period, 303 (79%) patients discontinued supplemental oxygen and mechanical ventilation for more than 48 consecutive hours, including 160 (81%) of 197 patients in the imatinib group and 143 (76%) of 188 patients in the placebo group. For the primary outcome, time to discontinuation of supplemental oxygen and mechanical ventilation was not significantly different between the two groups (unadjusted HR 0·95 [95% CI 0·76–1·20], p=0·69; figure 2A). This difference remained non-significant after adjusting for each baseline imbalance (sex, obesity, diabetes, and cardiovascular disease) separately and combined (table 2).

The Kaplan-Meier curves for mortality are shown in figure 2B. At day 28, 15 (8%) of 197 patients had died in the imatinib group compared with 27 (14%) of 188 patients in the placebo group. The unadjusted HR for mortality in the imatinib group versus the placebo group was 0·51 (95% CI 0·27–0·95; p=0·034). The HRs for mortality were attenuated, and for some of the adjusted analyses became non-significant after adjusting for imbalances in the baseline characteristics (table 2), as the number of men outnumbered the number of women in the imatinib group, and a higher proportion of patients in the placebo group had diabetes, cardiovascular disease, or both than in the imatinib group. After adjusting for all imbalances, the HR for mortality was 0·52 (95% CI 0·26–1·05; p=0·068; table 2). Logistic regression analysis yielded an odds ratio for mortality at 28 days in the imatinib group versus the placebo group of 0·49 (95% CI 0·25–0·96).

During the 28-day study period, 39 (20%) of 197 patients in the imatinib group and 33 (18%) of 188 patients in the placebo group were admitted to the ICU. Patients in the ICU in the two treatment groups were balanced in terms of baseline characteristics (data not shown). Of these patients, 30 (77%) in the imatinib group and 26 (79%) in the placebo group were intubated and mechanically ventilated (figure 2C). The unadjusted HR for mechanical ventilation in the imatinib group versus the placebo group was 1·07 (95% CI 0·63–1·80; p=0·814; figure 2C, table 2), and this difference between the groups remained insignificant when adjusting for sex, obesity, diabetes, and cardiovascular disease (figure 2C, table 2). The median duration of mechanical ventilation was 7 days (IQR 3–13) in the imatinib group and 12 days (6–20) in the placebo group (p=0·0080; table 3). In post-hoc analyses, we restricted the analysis to survivors only, and observed that the median duration of mechanical ventilation in the imatinib group was 7 days (3–12) compared with 12 days (6–25) in the placebo group (p=0·023). In patients admitted to the ICU, the number of ventilator-free days

7

was 22 (14–26) in the imatinib group versus 9 days (0–23) in the placebo group (p=0·018; table 3).

The median duration of hospital admission was 7 days (IQR 4–11) in the imatinib group and 6 days (3–11) in the placebo group (p=0·51). The median duration of oxygen supplementation was 7 days (3–12) in the imatinib group and 5 days (3–11) in the placebo group (p=0·23; table 3). The median duration of ICU stay was 8 days (5–13) in the imatinib group and 15 days (7–21) in the placebo group (p=0·025). The proportions of patients at different stages of clinical recovery, classified as per the WHO ordinal scale for clinical recovery, at day 9 and day 28 of the study period are shown in figure 3. Compared with placebo, imatinib use was associated with fewer patients classified as having high disease severity on day 9 and day 28 (figure 3).

Table 3: Duration of respiratory support and care in the final analysis population

	N	Median	p-value
Total days of oxygen supplementation			
Imatinib	197 (100%)	7 [3-12]	
Placebo	188 (100%)	5 [3-11]	0·23
Duration of mechanical ventilation			
Imatinib	30 (15%)	7 [3-13]	
Placebo	26 (14%)	12 [6-20]	0·008
Days at ICU			
Imatinib	39 (20%)	8 [5-13]	
Placebo	33 (18%)	15 [7-21]	0·025

Table 3: Data are median (IQR). *Measured in 30 (15%) participants in the imatinib group and 26 (14%) patients in the placebo group. †Measured in 24 (12%) patients in the imatinib group and 18 (10%) patients in the placebo group. ‡Measured in 39 (20%) patients in the imatinib group and 33 (18%) patients in the placebo group. §Measured in 39 (20%) patients in the imatinib group and 33 (18%) patients in the placebo group.
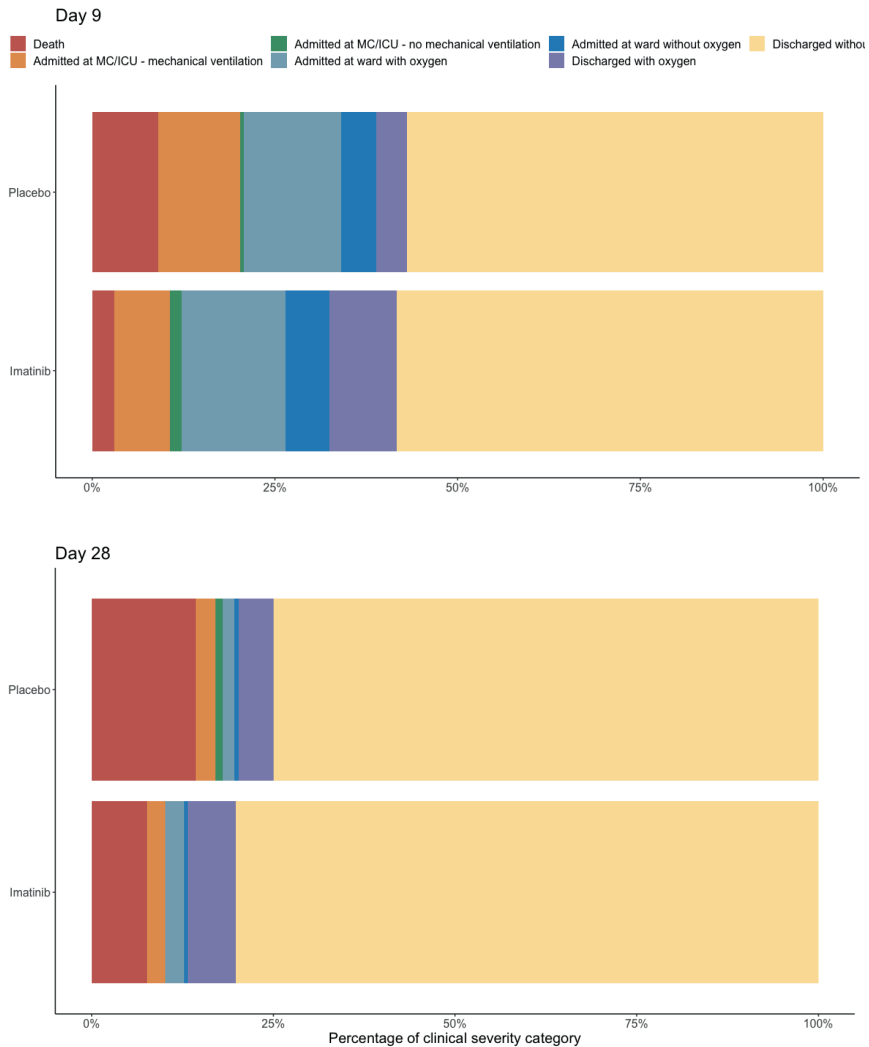
Figure 3

Day 9

Legend:
- Death
- Admitted at MC/ICU - mechanical ventilation
- Admitted at MC/ICU - no mechanical ventilation
- Admitted at ward with oxygen
- Admitted at ward without oxygen
- Discharged with oxygen
- Discharged without

Day 28

Percentage of clinical severity category

Figure 3: Clinical status at day 9 (A) and day 28 (B) Classification of patients in the imatinib group versus the placebo group according to the WHO seven-point ordinal scale for clinical improvement at day 9 and day 28 of the study period. MCU=medium care unit. ICU=intensive care unit.

Of all 385 patients, 231 (60%) received the complete 10-day course of study medication; 77 (38%) of 197 patients in the imatinib group and 77 (41%) of 188 patients in the placebo group did not receive the complete course of study medication. The mean duration of study drug use was 7·6 days (SD 3·4) in the imatinib group and 7·7 days (3·2) in the placebo group. Frequent reasons for not completing the full course included requesting to stop treatment

(44 [11%] of 385 patients), discontinuation due to discharge or transfer to another hospital (37 [10%]), and discontinuation based on stopping criteria (34 [9%]). 30 (15%) patients in the imatinib group and 14 (7%) patients in the placebo group requested to discontinue the study medication (supplemental data appendix). The most frequent reasons for discontinuation of study medication reported by patients included grade 1 or 2 gastrointestinal discomfort (supplemental data appendix). 11 (6%) patients in the imatinib group and 23 (12%) patients in the placebo group discontinued treatment because they met predefined stopping criteria (supplemental data).

Test results for kidney function, liver and cardiac enzymes, and QTc intervals on days 0–5 are provided in the appendix (pp 3–4). Creatinine concentrations on day 1 were slightly higher in the imatinib group than in the placebo group, but no differences were observed on subsequent days. Additionally, no differences in liver enzymes, NTproBNP concentrations, or QTc intervals were observed between the two groups.

During the study, grade 3, 4, and 5 adverse events were recorded. A total of 188 grade 3 or 4 adverse events were reported in patients in the imatinib group and 260 events were reported in the placebo group. 91 (46%) of 197 patients in the imatinib group and 82 (44%) of 188 patients in the placebo group had at least one grade 3 or higher adverse event. The most frequent grade 3 adverse events included thromboembolic events, decreased lymphocyte counts, alkalosis, and hyperglycaemia (table 4). The most frequent grade 4 adverse event was ARDS. No specific adverse events were attributed to imatinib treatment. Two (1%) patients in the placebo group had acute renal failure compared with none of the patients in the imatinib group. Most grade 5 adverse events were ARDS, which occurred in 12 (6%) patients in the imatinib group and in 35 (12%) patients in the placebo group (supplemental data). Haemorrhagic stroke was observed in one (1%) patient in the imatinib group and in one (1%) patient in the placebo group, both of which occurred after extended anticoagulation treatment for extracorporeal membrane oxygenation.

Table 4: Adverse events in the safety population.

	Total	Imatinib	Placebo
Total Adverse events – No. (%)			
Grade 3 or 4 - All	448 (116)	188 (95)	260 (138)
Grade 3 - All	374 (97)	156 (79)	218 (116)
Grade 4 - All	74 (19)	32 (16)	42 (22)
Number of participants with >1 adverse event (Grade 3 or higher)	173 (45)	91 (46)	82 (44)
Blood and lymphatic system disorders – No. (%)			
Grade 3 - Anaemia	10 (3)	3 (2)	7 (4)
Cardiac disorders – No. (%)			
Grade 3 - Atrioventricular block complete	1 (0)	0 (0)	1 (1)
Grade 3 - Myocardial infarction	1 (0)	0 (0)	1 (1)
Grade 3 - Rhythm disorder (Atrial fibrillation/flutter)	8 (2)	4 (2)	4 (2)
Grade 3 - Sinus bradycardia	1 (0)	0 (0)	1 (1)
Grade 4 - Rhythm disorder (Atrial fibrillation/flutter)	2 (1)	0 (0)	2 (1)
Grade 4 - Sinus bradycardia	1 (0)	0 (0)	1 (1)
Ear and labyrinth disorders – No. (%)			
Grade 3 - Other - Myringitis with bloody otorrhea	1 (0)	0 (0)	1 (1)
Endocrine disorders – No. (%)			
Grade 3 - Adrenal insufficiency	2 (1)	0 (0)	2 (1)
Eye disorders – No. (%)			
Grade 3 - Conjunctivitis	1 (0)	0 (0)	1 (01)
Grade 4 - Other**	1 (0)	1 (1)	0 (0)
Gastrointestinal disorders – No. (%)			
Grade 3 - Diarrhoea	1 (0)	1 (1)	0 (0)
Grade 3 - Ileus	1 (0)	0 (0)	1 (1)
Grade 3 - Rectal haemorrhage	1 (0)	0 (0)	1 (1)
Grade 3 - Vomiting	1 (0)	0 (0)	1 (1)
Grade 4 - Gastric ulcer	1 (0)	1 (1)	0 (0)
Grade 4 - Rectal haemorrhage	1 (0)	0 (0)	1 (1)
General disorders and administration site conditions – No. (%)			
Grade 3 - Fever	4 (1)	1 (1)	3 (2)
Grade 4 - Multi-organ failure	1 (0)	0 (0)	1 (1)
Infections and infestations – No. (%)			
Grade 3 - Lip infection	2 (1)	0 (0)	2 (1)
Grade 3 - Lung infection (non-COVID-19)	17 (4)	7 (4)	10 (5)
Grade 3 - Other**	9 (2)	5 (3)	4 (2)
Grade 3 - Sepsis	3 (1)	1 (1)	2 (1)
Investigations – No. (%)			

7

Grade 3 - Blood ALT/AST increased	11 (3)	6 (3)	5 (3)
Grade 3 - Blood Bilirubin Increased	3 (1)	1 (1)	2 (1)
Grade 3 - Blood Creatinine increased	3 (1)	2 (1)	1 (1)
Grade 3 - Blood Gamma-GT increased	3 (1)	0 (0)	3 (2)
Grade 3 – Prolonged QT corrected interval	22 (6)	8 (4)	14 (7)
Grade 3 - Lymphocyte count decreased	35 (9)	20 (10)	15 (8)
Grade 3 - White blood cell decreased	1 (0)	0 (0)	1 (1)
Grade 4 - Creatinine increased	1 (0)	0 (0)	1 (1)
Grade 4 - Platelet count decreased	2 (1)	1 (1)	1 (1)
Metabolism and nutrition disorders - No· (%)			
Grade 3 - Acidosis	18 (5)	10 (5)	8 (4)
Grade 3 - Alkalosis	41 (11)	21 (11)	20 (11)
Grade 3 - Anorexia	1 (0)	1 (1)	0 (0)
Grade 3 - Hyperglycaemia	59 (15)	22 (11)	37 (20)
Grade 3 - Hyperkalaemia	7 (2)	1 (1)	6 (3)
Grade 3 - Hypernatremia	5 (1)	1 (1)	4 (2)
Grade 3 - Hypoalbuminemia	7 (2)	2 (1)	5 (3)
Grade 3 - Hypokalaemia	5 (1)	2 (1)	3 (2)
Grade 3 - Hyponatremia	4 (1)	1 (1)	3 (2)
Grade 4 - Acidosis	6 (2)	1 (1)	5 (3)
Grade 4 - Hypernatremia	1 (0)	0 (0)	1 (1)
Grade 4 - Hypokalaemia	1 (0)	1 (1)	0 (0)
Neoplasms benign malignant and unspecified – No. (%)			
Grade 4 - Other****	1 (0)	0 (0)	1 (1)
Nervous system disorders – No. (%)			
Grade 3 - Peripheral motor neuropathy	2 (1)	0 (0)	2 (1)
Grade 3 - Stroke - ischemic	2 (1)	0 (0)	2 (1)
Psychiatric disorders – No. (%)			
Grade 3 - Delirium	14 (4)	2 (1)	12 (6)
Grade 4 - Delirium	1 (0)	0 (0)	1 (1)
Renal and urinary disorders – No. (%)			
Grade 3 - Hematuria	3 (1)	1 (1)	2 (1)
Grade 4 - Acute kidney injury	2 (1)	0 (0)	2 (1)
Respiratory thoracic and mediastinal disorders – No. (%)			
Grade 3 - Adult respiratory distress syndrome	15 (4)	9 (5)	6 (3)
Grade 3 - Pneumothorax	1 (0)	1 (1)	0 (0)
Grade 3 - Pulmonary fibrosis	1 (0)	1 (1)	0 (0)
Grade 3 - Other****	6 (2)	4 (2)	2 (1)
Grade 4 - Adult respiratory distress syndrome	46 (12)	26 (13)	20 (11)
Grade 4 - Aspiration	1 (0)	0 (0)	1 (1)
Grade 4 - Pneumothorax	1 (0)	1 (1)	0 (0)
Grade 4 - Other*****	1 (0)	1 (1)	0 (0)

Skin and subcutaneous tissue disorders – No. (%)			
Grade 3 - Rash maculo-papular	1 (0)	1 (1)	0 (0)
Grade 3 - Other ******	1 (0)	1 (1)	0 (0)
Vascular disorders – No. (%)			
Grade 3 - Hypotension	8 (2)	1 (1)	7 (4)
Grade 3 - Thromboembolic event	3 (8)	18 (9)	14 (7)
Grade 4 - Hypotension	1 (0)	0 (0)	1 (1)
Grade 4 - Thromboembolic event	1 (0)	1 (1)	0 (0)

Table 4: * The incidence and severity of adverse events was determined and displayed according to the Common Terminology Criteria for Adverse Events (CTCAE), version 5.0. All patients who received at least one dose were included in the safety population. COVID-19 = COronaVIrus Disease 2019, ALT = ALanine AminoTransferase, AST = ASpartate aminotransferase. ** One patient developed a conjunctivitis with a hematoma in both of the eyes. The patient was unblinded and treatment was discontinued. Shortly thereafter symptoms resolved. *** Positive throat swab culture that resulted in the start of intravenous antibiotic, antifungal or antiviral intervention. **** One patient was diagnosed with a malignancy. ***** Four patients were readmitted due to complaints of dyspnoea, one patient because of a Non-COVID-19 pneumonia, one patient because of a COPD exacerbation. ****** One patient was diagnosed with a leukocytoclastic vasculitis confirmed by a skin biopsy.

Discussion

Treatment of hospitalised, hypoxaemic patients with COVID-19 pneumonitis with imatinib did not change the time to discontinuation of supplemental oxygen and ventilation when compared with placebo (primary outcome). However, the analysis of secondary outcomes indicated that mortality at 28 days was lower in the imatinib group than in the placebo group, which paralleled reductions in the duration of mechanical ventilation and length of ICU stay. Of note, the statistical significance of the change in mortality was somewhat attenuated after adjustment for baseline imbalances. In terms of safety, no imatinib-related adverse events (grade 3 or higher) were observed.

To our knowledge, this is the first clinical trial to evaluate imatinib in patients with COVID-19. The rationale behind the use of imatinib treatment was to mitigate pulmonary capillary leak and alveolar oedema in these patients, as experimental and early clinical evidence suggests that imatinib protects the integrity of the vascular barrier in a wide array of inflammatory conditions (11-15). Contrary to our expectations, and despite reductions in mortality and duration of mechanical ventilation, imatinib did not reduce the time to discontinuation of respiratory support, as measured by the combined endpoint of use of supplemental oxygen and mechanical ventilation. This primary outcome was chosen on the premise that imatinib would accelerate recovery in all patients. Of all 385 patients included in the final analysis, 303 (79%) discontinued supplemental oxygen and mechanical ventilation for more than 48 consecutive hours, indicating a mild disease course in most patients. Although this study does not provide evidence of clinical benefit in patients with a mild disease course, our data do suggest that imatinib might confer benefit specifically in patients with severe COVID-19.

7

Imatinib did not prevent the need for mechanical ventilation, but did reduce its duration. These findings suggest that imatinib might have altered the disease course, specifically in patients with severe COVID-19; from critically ill to a less severe state of disease, with a long-term need for oxygen supplementation. Independent validation of this clinical benefit from imatinib in patients with severe forms of COVID-19 is required. Trials of oral imatinib in hospitalised patients with COVID-19 are currently recruiting patients in Spain (NCT04346147) and in the USA (NCT04394416).

Although the rationale behind imatinib treatment was to mitigate pulmonary capillary leak, the question of why clinical benefit was predominantly observed in patients with COVID-19-associated ARDS remains. One explanation might be that the relative contribution of pulmonary capillary leak is larger in patients with COVID-19-associated ARDS than in less severe forms of COVID-19. This hypothesis is supported by plasma studies, which have linked circulating markers of vascular injury, such as angiopoietin-2, von Willebrand factor, and E-selectin, to clinical severity in patients with COVID-19 (21). Concentrations of circulating angiopoietin-2 and E-selectin were higher in patients requiring ICU admission (22) and high concentrations at presentation (23) or increasing concentrations during admission were predictors of mortality (24). Similar findings were observed in patients with ARDS unrelated to COVID-19, in which increasing concentrations of angiopoietin-2 and von Willebrand factor were associated with pulmonary vascular leak and increased ARDS severity (25). The results of these biomarker studies together with our clinical observations could indicate that pulmonary capillary leak underlies the transition to a clinical ARDS phenotype, which can be targeted by imatinib. Alternatively, imatinib could target pathways other than alveolocapillary integrity. Imatinib exerts a vasculoprotective effect via inhibition of the ABL2 tyrosine kinase (12,26). ABL2 is an important regulator of the cytoskeleton, and, as such, has also been shown to mediate endosomal trafficking of SARS-CoV and MERS-CoV viral particles (27). Imatinib has shown antiviral activity against SARS-CoV27 and SARS-CoV-2 *in vitro* (28). However, another study found no evidence that viral replication or cell entry of SARS-CoV-2 was inhibited at clinically achievable concentrations (29). Whether there are direct antiviral effects of ABL tyrosine-kinase inhibitors against SARS-CoV-2 therefore remains controversial.

This trial has some limitations. First, 14 (7%) of 188 patients in the placebo group and nine (5%) of 197 patients in the imatinib group were lost to follow-up or withdrew consent between randomisation and the first dose of study medication. This attrition was partly explained by the fact that, during the pandemic, high numbers of admissions in particular regions in the Netherlands forced hospitals to relocate their patients to hospitals in other regions. Second, despite randomisation, there were imbalances in several baseline variables between the two groups (including sex and comorbidities). We corrected for these imbalances by calculating adjusted HRs. Third, hospital discharge policies changed over the course of the pandemic, with early home or nursing home discharge on continued oxygen treatment (30) only possible from the second half of the year. These policy changes could have affected measurement of the primary outcome. Fourth, although a significant

difference in mortality at 28 days was observed between the imatinib group and the placebo group, the study was not powered to detect significant differences in mortality, precluding robust conclusions from these analyses. Adjustment for baseline imbalances also yielded a non-significant result; however, the HR for mortality at 28 days remained mostly unchanged, indicating that it shows little residual confounding. Finally, the study period of 28 days might be short relative to other trials of treatments for COVID-19, given the high frequency of readmissions due to COVID-19 and that several patients have an extended recovery period. Follow-up for 3 or 6 months, as has been done in most studies of long-term COVID-19 sequelae, could provide relevant information about the effects of imatinib on the long-term outcomes and functional status of patients.

The major strengths of our trial are its randomised, placebo-controlled, double-blind design, and the fact that it was done in a day-to-day health-care setting. All hospitalised patients aged 18 years or older were eligible, including patients aged older than 85 years and patients with a do-not-resuscitate order. In addition, 72% of patients received dexamethasone as a co-treatment, indicating that the possible benefits of imatinib treatment have an additive effect to standard care. Finally, although imatinib was originally developed as an outpatient therapy for chronic myeloid leukaemia (31), this study provides extensive safety data on imatinib in a severe, critically ill population. An extensive safety analysis, which included laboratory and ECG tests, as well extensive adverse event reporting, revealed that imatinib was well tolerated and safe in patients with moderate to severe COVID-19. In fact, only a few adverse events were observed, and no renal, hepatic, or cardiac toxicity was reported.

The observed reductions in mortality and duration of mechanical ventilation in patients given imatinib are of direct relevance. First, as our study suggests that imatinib predominantly benefits patients with severe course of COVID-19, future trials are needed in selected patients with COVID-19-associated ARDS or in larger study populations, thus allowing stratification by disease severity. Of note, one trial of intravenous imatinib in patients with COVID-19 on mechanical ventilation started patient recruitment in March, 2021 (NCT04794088). Second, a treatment period of 10 days, as used in our study, might need to be reconsidered. We based our choice of treatment duration on early observations that respiratory deterioration in COVID-19 occurs within the first 10 days after onset of symptoms (32). Time-to-event analyses, however, showed that the Kaplan-Meier curves for mechanical ventilation in the imatinib and placebo groups crossed after day 9 (figure 2C), which could indicate a catch-up phenomenon after the final day of study medication. The proportional hazards assumption was violated for the secondary outcome of the need for mechanical ventilation. This violation could have resulted in an underestimation of the treatment effect and advocates for increasing the treatment duration.

In conclusion, this randomised, placebo-controlled trial showed that imatinib does not reduce the time to discontinuation of supplemental oxygen and mechanical ventilation in hospitalised patients with COVID-19. However, the reduction in mortality (even if attenuated

after correction for baseline imbalances) and duration of mechanical ventilation indicates that imatinib might confer clinical benefit in patients with COVID-19, and provide a rationale for further studies.

References

1. Wiersinga WJ, Rhodes A, Cheng AC, Peacock SJ, Prescott HC. Pathophysiology, Transmission, Diagnosis, and Treatment of Coronavirus Disease 2019 (COVID-19): A Review. JAMA. 2020;324(8):782-793.

2. Varga Z, Flammer AJ, Steiger P, et al. Endothelial cell infection and endotheliitis in COVID-19. Lancet. 2020;395(10234):1417-1418.

3. Ackermann M, Verleden SE, Kuehnel M, et al. Pulmonary Vascular Endothelialitis, Thrombosis, and Angiogenesis in Covid-19. N Engl J Med. 2020;383(2):120-128.

4. Beigel JH, Tomashek KM, Dodd LE, et al. Remdesivir for the Treatment of Covid-19 - Final Report. N Engl J Med. 2020;383(19):1813-1826.

5. WHO Solidarity Trial Consortium, Pan H, Peto R, et al. Repurposed Antiviral Drugs for Covid-19 - Interim WHO Solidarity Trial Results. N Engl J Med. 2021;384(6):497-511.

6. RECOVERY Collaborative Group, Horby P, Mafham M, et al. Effect of Hydroxychloroquine in Hospitalized Patients with Covid-19. N Engl J Med. 2020;383(21):2030-2040.

7. Cao B, Wang Y, Wen D, et al. A Trial of Lopinavir-Ritonavir in Adults Hospitalized with Severe Covid-19. N Engl J Med. 2020;382(19):1787-1799.

8. RECOVERY Collaborative Group, Horby P, Lim WS, et al. Dexamethasone in Hospitalized Patients with Covid-19 - Preliminary Report. N Engl J Med. 2020:NEJMoa2021436.

9. REMAP-CAP Investigators, Gordon AC, Mouncey PR, et al. Interleukin-6 Receptor Antagonists in Critically Ill Patients with Covid-19. N Engl J Med. 2021 Feb 25:NEJMoa2100433.

10. Overbeek MJ, van Nieuw Amerongen GP, Boonstra A, Smit EF, Vonk-Noordegraaf A.

11. Possible role of imatinib in clinical pulmonary veno-occlusive disease. Eur Respir J. 2008;32(1):232–235.

12. Su EJ, Fredriksson L, Geyer M, et al. Activation of PDGF-CC by tissue plasminogen activator impairs blood-brain barrier integrity during ischemic stroke. Nat Med. 2008;14(7):731-7.

13. Aman J, van Bezu J, Damanafshan A, et al. Effective treatment of edema and endothelial barrier dysfunction with imatinib. Circulation. 2012;126(23):2728-38.

14. Chislock EM, Pendergast AM. Abl family kinases regulate endothelial barrier function in vitro and in mice. PLoS One. 2013;8(12):e85231.

15. Letsiou E, Rizzo AN, Sammani S, et al. Differential and opposing effects of imatinib on LPS- and ventilator-induced lung injury. Am. J. Physiol. Lung Cell Mol. Physiol. 2015;308: L259–269.

16. Langer V, Vivi E, Regensburger D, et al. IFN-γ drives inflammatory bowel disease pathogenesis through VE-cadherin-directed vascular barrier disruption. J Clin Invest. 2019;129(11):4691-4707.

17. Carnevale-Schianca F, Gallo S, Rota-Scalabrini D, et al. Complete resolution of life-threatening bleomycin-induced pneumonitis after treatment with imatinib mesylate in a patient with Hodgkin's lymphoma: hope for severe chemotherapy-induced toxicity? J Clin Oncol. 2011;29(24):e691-3.

18. Aman J, Peters MJ, Weenink C, van Nieuw Amerongen GP, Vonk Noordegraaf A. Reversal of vascular leak with imatinib. Am J Respir Crit Care Med. 2013;188(9):1171-3.

19. Langberg MK, Berglund-Nord C, Cohn-Cedermark G, Haugnes HS, Tandstad T, Langberg CW. Imatinib may reduce chemotherapy-induced pneumonitis. A report on four cases from the SWENOTECA. Acta Oncol. 2018;57(10):1401–1406.

20. Morales-Ortega A, Bernal-Bello D, Llarena-Barroso C, et al. Imatinib for COVID-19: A case report. Clin Immunol. 2020;218:108518.

21. Hochhaus A, Saussele S, Rosti G, et al; ESMO Guidelines Committee. Chronic myeloid leukaemia: ESMO Clinical Practice Guidelines for diagnosis, treatment and follow-up. Ann Oncol. 2017;28(suppl_4):iv41-iv51.

22. Abou-Arab O, Bennis Y, Gauthier P, et al. Association between inflammation, angiopoietins, and disease severity in critically ill COVID-19 patients: a prospective study. Br J Anaesth. 2020:S0007-0912(20)31006-0.

7

23. Smadja DM, Guerin CL, Chocron R, et al. Angiopoietin-2 as a marker of endothelial activation is a good predictor factor for intensive care unit admission of COVID-19 patients. Angiogenesis. 2020;23(4):611-620.

24. Vassiliou AG, Keskinidou C, Jahaj E, et al. ICU Admission Levels of Endothelial Biomarkers as Predictors of Mortality in Critically Ill COVID-19 Patients. Cells. 2021 Jan 19;10(1):186.

25. Villa E, Critelli R, Lasagni S, et al. Dynamic angiopoietin-2 assessment predicts survival and chronic course in hospitalized patients with COVID-19. Blood Adv. 2021 9;5(3):662-673.

26. van der Heijden M, van Nieuw Amerongen GP, Koolwijk P, van Hinsbergh VW, Groeneveld AB. Angiopoietin-2, permeability oedema, occurrence and severity of ALI/ARDS in septic and non- septic critically ill patients. Thorax. 2008;63(10):903-9.

27. Amado-Azevedo J, van Stalborch AD, Valent ET, et al. Depletion of Arg/Abl2 improves endothelial cell adhesion and prevents vascular leak during inflammation. Angiogenesis. 2021 Mar 26:1–17.

28. Coleman CM, Sisk JM, Mingo RM, et al. Abelson Kinase Inhibitors Are Potent Inhibitors of Severe Acute Respiratory Syndrome Coronavirus and Middle East Respiratory Syndrome Coronavirus Fusion. J Virol. 2016;90:8924-33.

29. Han Y, Duan X, Yang L, et al. Identification of SARS-CoV-2 inhibitors using lung and colonic organoids. Nature. 2021;589(7841):270-275.

30. Zhao H, Mendenhall M, Deininger MW. Imatinib is not a potent anti-SARS-CoV-2 drug. Leukemia. 2020;34(11):3085-3087.

31. Nederlands Huisartsen Genootschap. "Leidraad zuurstofgebruik THUIS bij (verdenking op / bewezen) COVID-19". Nhg.org, 2020 Apr. Available from: https://www.nhg.org/sites/default/files/content/nhg_org/uploads/050620_zuurstof_thuis_ten_tijde_van_corona_definitieve_versie_1.1_nvalt-nhg-pznl.pdf

32. Druker BJ, Talpaz M, Resta DJ, et al. Efficacy and safety of a specific inhibitor of the BCR-ABL tyrosine kinase in chronic myeloid leukemia. N Engl J Med. 2001;344(14):1031-7.

33. Huang C, Wang Y, Li X, et al. Clinical features of patients infected with 2019 novel coronavirus in Wuhan, China. Lancet. 2020;395(10223):497-506.
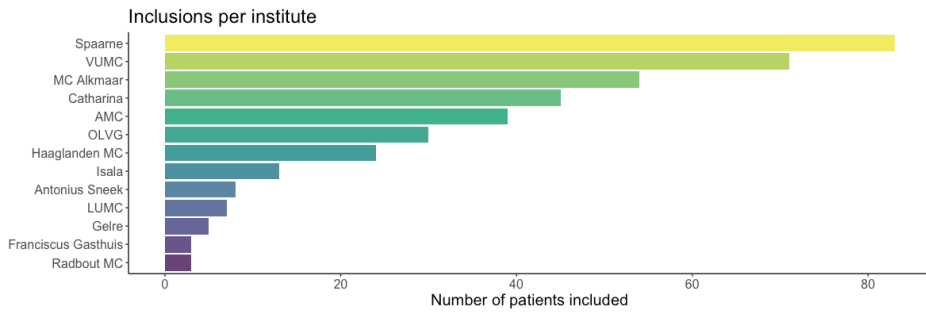
SUPPLEMENTAL INFORMATION

Supplemental figure 1

A
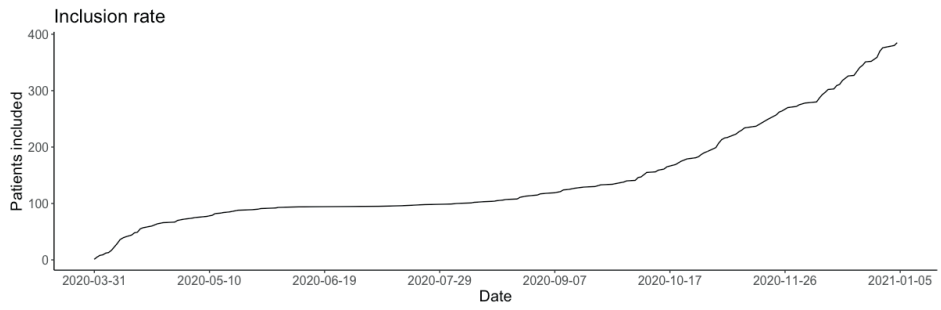
B

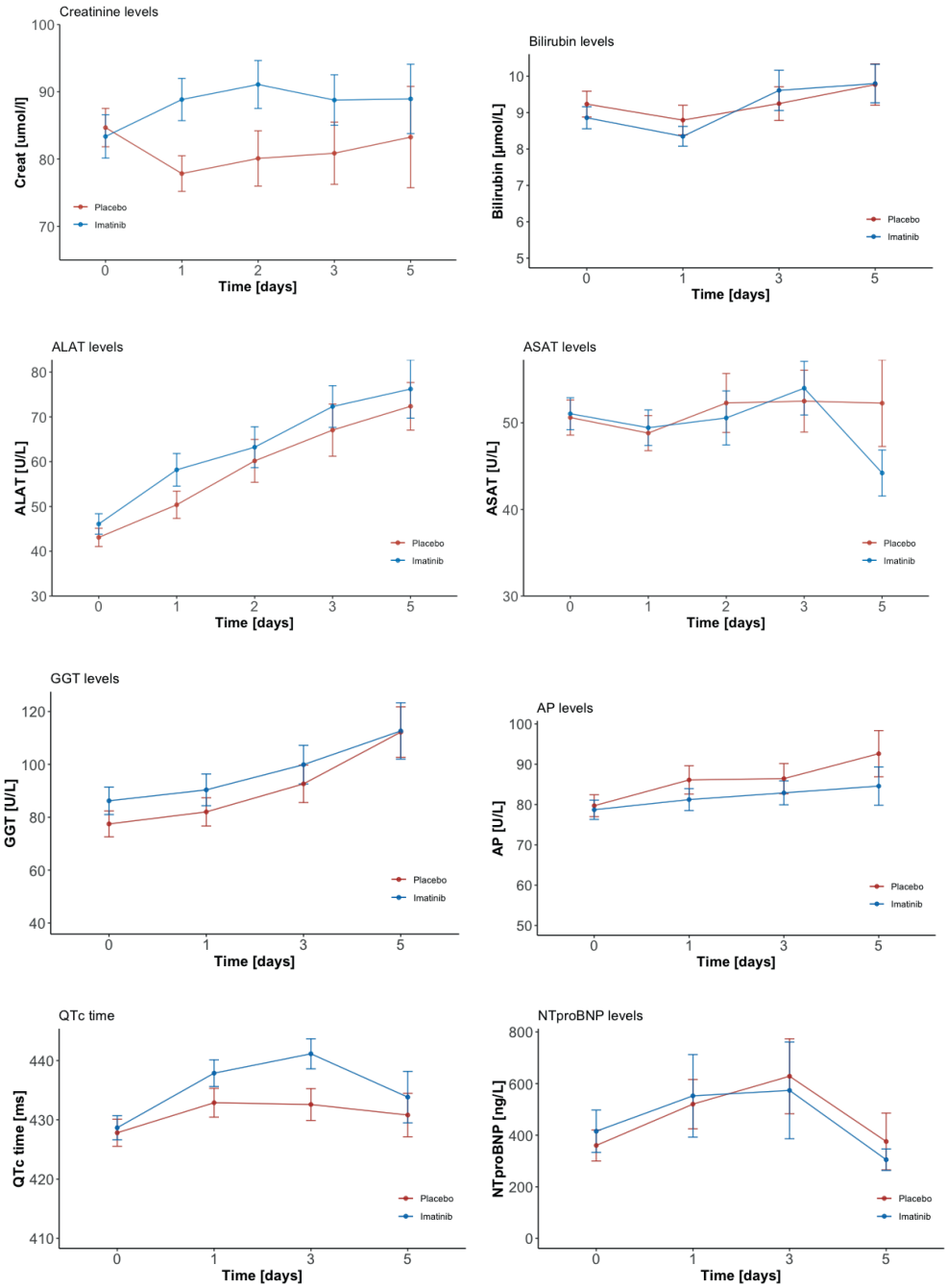
Supplemental figure 1: A) Inclusion rates over time. B) Number of inclusions per participating centre.

Supplemental figure 2

Figure S2: Blood biochemistry values during the first 5 days of treatment, representing kidney function, liver enzymes and cardiac enzymes, as well as electrocardiogram data and corrected QT (QTc) intervals. The number of missing values increases over time, due to patient discharge or death. ALT = alanine amino transferase, AP = alkaline phosphatase, AST = aspartate amino transferase, Creat = creatinine, GGT = gamma-glutamyltransferase, NT-proBNP = N-terminal prohormone of Brain Natriuretic Peptide.

Supplemental table 1: Regression analyses with adjustment for baseline parameters

	HR	95% CI	p-value
Primary endpoint			
Imatinib	0·95	0·76-1·20	0·689
Imatinib corrected for sex	1·01	0·81-1·28	0·900
Imatinib corrected for obesity	0·99	0·78-1·26	0·919
Imatinib corrected for diabetes	0·96	0·76-1·20	0·690
Imatinib corrected for cardiovascular disease	0·94	0·75-1·18	0·591
Secondary endpoint: Mortality			
Imatinib	0·51	0·27-0·95	0·034
Imatinib corrected for sex	0·47	0·25-0·89	0·019
Imatinib corrected for obesity	0·46	0·23-0·92	0·029
Imatinib corrected for diabetes	0·54	0·29-1·02	0·057
Imatinib corrected for cardiovascular disease	0·54	0·29-1·01	0·055
Secondary endpoint: Need for mechanical ventilation			
Imatinib	1·07	0·63-1·80	0·814
Imatinib corrected for sex	0·98	0·58-1·67	0·953
Imatinib corrected for obesity	1·08	0·63-1·86	0·772
Imatinib corrected for diabetes	1·13	0·66-1·91	0·657
Imatinib corrected for cardiovascular disease	1·06	0·62-1·79	0·842

Supplemental table 1: CI = confidence interval, HR = hazard ratio. The final analysis was done on 188 patients in the placebo group and 197 patients in the imatinib group. Hazard ratios and 95% confidence intervals were calculated using Cox regression analysis, adjusted for indicated factors.

Supplemental table 2: Reasons for incomplete study dose

	All patients No. (%)	Imatinib No. (%)	Placebo No. (%)
Total number of participants that did not complete the full trial regimen	154 (40)	77 (39)	77 (41)
Upon request of either patient or treating physician	44 (11)	30 (15)	14 (7·4)
Upon request of patient	41 (11)	29 (15)	12 (6·4)
Upon request of treating physician	3 (0·8)	1 (0·5)	2 (1·1)
discontinuation due to discharge or transfer to another hospital	37 (9·6)	20 (10·2)	17 (9·0)
Transfer to non-participating hospital	10 (2·6)	5 (2·5)	5 (2·7)
Not given to patient upon discharge/transfer	27 (7·0)	15 (7·6)	12 (6·4)
Some missed	16 (4·2)	8 (4·1)	8 (4·3)
Container lost	2 (0·5)	0 (0)	2 (1·1)
Discontinuation after meeting predefined stop criteria	34 (8·8)	11 (5·6)	23 (12)
Increased ALT/AST/bilirubin*	28 (7·3)	10 (5·1)	18 (9·6)
Haemoglobin drop**	1 (0·3)	0 (0)	1 (0·5)
Leukopenia***	1 (0·3)	0 (0)	1 (0·5)
Thrombocytes****	2 (0·5)	1 (0·5)	1 (0·5)
QT corrected interval prolongation****	2 (0·5)	0 (0)	2 (1·1)
Deceased before end of course	21 (5·5)	8 (4·1)	13 (6·9)

Supplemental table 2: *ALT/AST: elevation of >3x ULN in case of AST/ALT within reference values at baseline/inclusion or an elevation of >3x baseline in case of elevated AST/ALT at baseline/inclusion; bilirubin: elevation of >1.5x ULN in case of bilirubin levels within reference values at baseline/inclusion or an elevation of >1.5x baseline in case of elevated bilirubin levels at baseline/inclusion. ** >30% as compared to baseline. *** <2.5 x 10^9/L. ****<100 x 10^9/L. *****>100ms as compared to baseline. ALT = ALanine aminoTransferase, AST = ASpartate aminoTransferase, ULN = Upper Limit of Normal, L = Liter, ms = millisecond.

7

Supplemental table 3: Reasons for patients' request to discontinue study medication

	All patients No. (%)	Imatinib No. (%)	Placebo No. (%)
Number of patient requests for stopping trial regimen	41 (11)	29 (15)	12 (6·4)
Vomiting	10 (2·6)	8 (4·1)	2 (1·1)
No specific reason given	12 (3·1)	7 (3·6)	5 (2·7)
Skin reaction, suspicion of allergic reaction	1 (0·3)	1 (0·5)	0 (0·0)
Diarrhoea	8 (2·1)	7 (3·6)	1 (0·5)
Nausea without vomiting	6 (1·6)	4 (2·0)	2 (1·1)
Conjictual hemorrhage	1 (0·3)	1 (0·5)	0 (0·0)
Pills are too large to swallow	1 (0·3)	1 (0·5)	0 (0·0)
Feels to weak to take any medication at all	2 (0·5)	0 (0)	2 (1·1)

Supplemental table 4: Grade 5 adverse events

		All patients No. (%)	**Imatinib No. (%)**	**Placebo No. (%)**
Total deaths	All	42 (11)	15 (7·6)	27 (14)
Respiratory, thoracic and mediastinal disorders	Adult respiratory distress syndrome	37 (9·6)	12 (5·9)	25 (12)
Nervous system disorders	Stroke - haemorrhagic*	2 (0·5)	1 (0·5)	1 (0·5)
Cardiac disorders	Myocardial infarction	1 (0·3)	1 (0·5)	0 (0)
Vascular disorders	Arterial thromboembolism	1 (0·3)	1 (0·5)	0 (0)
Infections and infestations	Sepsis	1 (0·3)	0 (0)	1 (0·5)

Supplemental table 4 : The incidence of death was determined and displayed according to the Common Terminology Criteria for Adverse Events (CTCAE), version 5.0. All patients who received at least one dose were included in the safety population. *Two patients died as a result of a large cerebral haemorrhage that occurred shortly after the start of extracorporeal membrane oxygenation (ECMO). It is presumed that this hemorrhage is a result of the systemic anticoagulation used during ECMO.

8

Conclusions and future perspectives

Liza Botros

In this thesis we investigated the pulmonary vasculature through both pre-clinical and clinical studies. We investigated novel methods for early detection, monitoring and treatment for PAH. We sought for blood- and urine biomarkers and identified several easily accessible and inexpensive circulating markers. However, none of them was specific for PAH and external validation is necessary to evaluate the possibility to use these biomarkers in daily practice. Second, we tried to measure lung vascular proliferation by ^{18}FLT phosphorylation using PET scanning, however also this technique failed to outweigh current diagnostic procedures. Third, we tested an anti-proliferative treatment as therapy for PAH. We conclude that treatment with mercaptopurine against PAH was effective but not safe as it reduced pulmonary vascular resistance, but with an unfavorable benefit-to-risk ratio in this dosing scheme. In part II of this thesis, we have recognized important players in endothelial stability and vascular leakage using TKIs. We identified MAP4K4 as an important novel player in endothelial barrier regulation. In both *in vitro* and *in vivo* models, combined inhibition of Arg and MAP4K4 restored endothelial barrier dysfunction and vascular leakage during inflammation and trauma. In hypoxemic hospitalized COVID-19 pneumonia patients, a direct infection of pulmonary endothelial cells (1, 2) disrupts the endothelial barrier leading to severe acute respiratory distress syndrome with high morbidity and mortality. We performed a randomized, placebo-controlled clinical trial investigating the efficacy and safety of imatinib in COVID-19 patients who required supplemental oxygen administration. Imatinib did not change the time to liberation from supplemental oxygen and ventilation. However we did find a reduction in 28-day mortality paralleled with reductions in duration of mechanical ventilation and length of ICU stay. In conclusion, both vascular leakage disorders and pulmonary arterial hypertension are a problem based on damage and dysfunction of endothelial cell function, amplified by inflammatory stimuli, which puts the endothelium in the center of vascular disorders (Figure 1).

Homeostasis
- Vasomotor tone
- Metabolism
- Exchange of gasses and nutrients
- Immunity

Vascular remodeling
- Endothelial proliferation
- Apoptosis resistance
- Sustained vasoconstriction
- BMPR2 mutations

Dysfunctional barrier
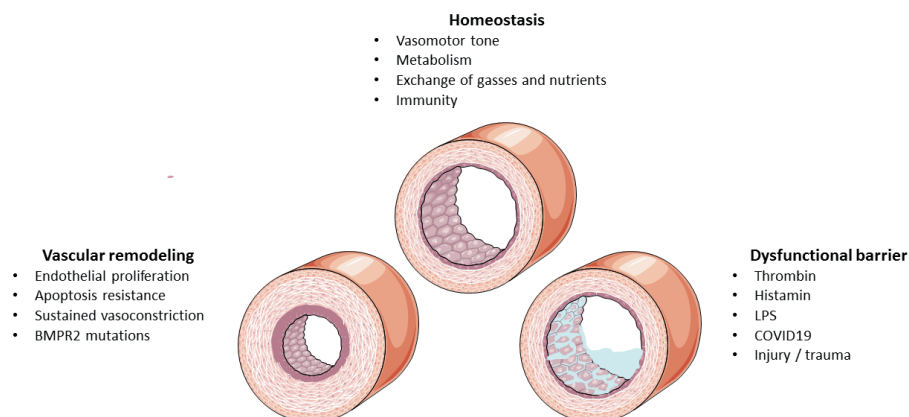- Thrombin
- Histamin
- LPS
- COVID19
- Injury / trauma

Figure 1: The endothelium as central orchestrator of pulmonary vascular remodeling and integrity. In a healthy state, there is a balanced homeostasis of vasomotor tone, metabolism, exchange of gases and nutrients and transport of immune cells. Both in pulmonary vascular remodeling and leakage, the endothelium plays a central dysfunctional role.

Part I - Assessing cell proliferation in PAH

Once considered a consequence of abnormal pulmonary vasoconstriction, the general hypothesis is now that PAH is mainly caused by pulmonary vascular remodeling due to proliferation of endothelial cells and vascular smooth muscle cells (3). As screening and monitoring of disease progression rely on indicators of right ventricular dysfunction (4) and no biomarkers of pulmonary vascular remodeling in PAH are available, there is an urgent need for a quantitative measure of vascular remodeling in patients with PAH. As an alternative approach, we tried to measure lung vascular proliferation by [18]FLT phosphorylation using PET scanning. The [18]FLT tracer is routinely used in oncology as it correlates with histological proliferation markers Ki-67 and proliferating cell nuclear antigen (PCNA) (5). We observed no differences in [18]FLT phosphorylation between PAH patients, unaffected BMPR2 mutation carriers and healthy controls. In fact, whether [18]FLT-PET scanning is a suitable technique to detect changes in the microvasculature remains debatable. This is a problem that is observed in other imaging techniques as well, as shown by a study of Kofoed et al. that observed that one third of patients with acute ischemic coronary artery syndrome did not show obstruction in angiography (6) but probably had abnormalities in the microvasculature, which cannot be detected by imaging. Besides the high costs of PET scanning and difficulties in interpretation of the data, our sequential [18]FLT-PET scanning in three PAH patients during their follow up did not match with the patients' hemodynamic or clinical course, making it difficult to monitor disease progression or to screen for subjects at risk. This underscores the poor intraclass correlation of [18]FLT-PET (7). Disease heterogeneity is a fact and not all regions of the lung are in an active proliferative state. Therefore, measuring an average phosphorylation might not be appropriate. It is challenging to interpret proliferation rates inside the lung as we are limited to directly correlate the [18]FLT signal with pulmonary pathology in the same subject. Nonetheless, the natural history of the pulmonary pathology following clinical presentation is unknown. Proliferation may be episodic or activated at initiation of the disease whereas fibrosis and cellular senescence may play a role in the later phase of the disease. Expression of p16 and p21, important in cell cycle arrest, were increased in end-stage PAH rat-and human lungs (8).

Another method to asses proliferation in the lung vasculature in PAH, is measuring BMPR2 expression. Impaired BMP signaling is observed in both HPAH and IPAH lungs and in animal models and pulmonary vascular remodeling can be attenuated by enhancing BMPR2 activity (9, 10). Cumulative evidence shows a link between the BMP pathway and proliferation as decreased expression of BMPR2 in PAH microvascular endothelial cells compromises the genomic stability via increased sensitivity to DNA damage in ECs (11, 12). Although we observed an increased BMPR2 mRNA expression after mercaptopurine treatment, this was only measured in PBMCs as surrogate of lung microvascular cells. Measuring and targeting the BMPR2 pathway using PBMCs was done before (13), although it remains an ongoing debate how representative these cells are as the use of PBMCs neglects the considerable influence of lung microenvironment. The number of PBMCs, or its subfraction endothelial

8

colony forming cells (ECFCs) is estimated at 0.001 – 0.007 per 1 million cells/mL of blood. These precursor cells have high proliferative ability and express endothelial-specific markers such as CD31, VEGFR and CD144 (14). ECFCs depict functional incompetence and may be involved in vascular remodeling, although the precise mechanism is still under debate (14). Unsurprisingly, outgrowth and phenotype of endothelial colony forming cells (ECFCs) in PAH had a broad inter-patient variability. Along with the low sensitivity and specificity of these cells, the paucity and high work effort to grow and stain these cells for analysis, makes them not appropriate as read-out for BMPR2 expression or to asses proliferation in daily clinical practice. What other options for measuring lung vascular proliferation do we have then?

Various growth factors have been found to be important in the proliferation of lung vascular cells. Besides a mitogenic signal, growth factors are involved in cellular migration, differentiation and apoptosis. Abnormalities in growth factor production and receptor expression have been found in experimental models of PAH (15). However, robust evidence for a causative role for growth factors in PAH in a clinical setting is lacking. For example, platelet derived growth factor (PDGF) mRNA was increased in dissected arteries from IPAH patients compared to controls (16) however a limitation of this tissue analysis is that it represents end-stage disease obtained at the time of lung transplantation. In addition, circulating plasma fibroblast growth factor (FGF) was increased in primary pulmonary hypertension patients (17), however considering an observed difference of 1 pg/mL, this might be statistically different but the clinical relevance is debatable. Moreover, primary PH-conditioned medium increased FGF production and proliferation of smooth muscle cells (18), although no patient material was used and proof of structurally altered growth factor receptors is still lacking. This might be the reason why clinical trials with growth factor inhibitors such as tyrosine kinase inhibitors (3, 19, 20) or tacrolimus (21) have not yet shown an overall clinical benefit. Recently, the sotatercept trail (22) showed a decrease in PVR of $-239,5$ dyn·sec·cm^{-5}, together with an improved 6 minute walking distance and NT-proBNP levels. Preclinical evidence suggested that sotatercept has a direct effect on pulmonary vascular remodelling by sequestering ActRIIA ligands, thereby reducing ActRIIA–Smad2/3 signaling and reducing the proproliferative signal (23). However, the clinical sotenercept trail did not show evidence of increased BMP signalling, nor of decreased growth factor signaling in the patient. Taken all together, the general consensus of sustained proliferative signalling and sustained growth factor signalling in the PAH lung might be more nuanced and complex.

Perhaps the answer can be found in another organ. Prior work showed that the bone marrow of PAH patients displays abnormalities and is involved in the susceptibility to PAH (24, 25). Additionally, bone marrow transplantation can prevent the development of PAH in BMPR2-mutated mice (24, 25). Interestingly, we observed a high rate of bone marrow depression after mercaptopurine treatment in our PAH population compared to reports of other diseased patients (i.e. Crohns disease). Incidence rates for mild leukopenia (3-4 *109/L) in thiopurine-treated inflammatory bowel disease vary between 5-25%, and for severe leukopenia ($<3*10^9$/L) around 4% (26). We observed a higher frequency and severity

of leukopenia than expected, which led to a high drop-out rate. We confirmed the immunosuppressive effects of mercaptopurine by showing a reduced number of circulating PBMCs and a decrease in monocyte number. This might be a consequence of reduced proliferation and increased apoptosis of endothelial cells through blocking Rac1 activation by mercaptopurine (27). Plexiform lesions in IPAH were found to be monoclonal in nature which also strongly suggests that progenitor-like cells have a mutational advantage for growth (either increased cell proliferation or decreased cell death) and were genetically unstable to favor their long term survival (28). Techniques that evaluate bone marrow activity, for example through imaging techniques or by measuring cell number and activity from (invasive) bone marrow aspiration, could give new leads in the development and monitoring of disease.

From clinical endpoints to biological endpoints

There is an increased understanding of the molecular and cellular processes that participate in the pathogenesis of PAH, including the role of genes, metabolism, inflammation and autoimmunity. Unfortunately, until now no clinical trial has succeeded to reverse pulmonary vascular remodeling, including those based on hyperproliferation. Preclinical studies generally focus on one player or pathway in cell culture or in an animal model, which is an oversimplification of the clinical course and does not take into account the spatial-temporal changes in affected tissues over time (28). On the other hand, clinical studies use pulmonary artery pressures, markers of right ventricular function and functional capacity as endpoints, which are not representative for (early) microvascular changes. Considering this, it is no surprise that there exists a large translational gap from bench to bed, leading to failure of clinical trials. As next step to clinical translation, an integral assessment of the ever-growing list of molecular and signaling pathways has to be combined with insights on how these multiple pathways are orchestrated at disease initiation and during disease course. The use of omics approach (genomics, transcriptomics, proteomics and metabolomics), which is increasingly used to address the complexity in PAH, could generate several PAH-signatures to stratify patient subgroups into high/low inflammatory, high/low proliferative or genetic clusters (29). Recently, several novel mutations in genes have been identified in PAH such as BMP10, Sox17 and KDR (VEGFR2) (30-33). The evidence of causality between these mutations and disease phenotype has to be robust in order to use these genes in a clinical (screening) setting. Perhaps implementation of a quantitative risk-assessment using a high-throughput multiplex panel of circulating biomarkers combined with genetic testing and current imaging techniques, will give rise to an integrated-and unbiased method to screen for PAH. Swarm classification of platelet RNA profiles is under current investigation as alternative strategy to detect and classify PAH.

8

Part II - Novel approaches against vascular leak

We focused on the regulatory mechanisms that underlie vascular leak and identified MAP4K4 as important regulator of endothelial barrier function. The physiological importance of MAP4K4 is evident as both MAP4K4 whole-body knock out and endothelial-specific conditional knock out are both lethal due to defective vascular development (34, 35). Studies using a wide range of cancer cell lines suggested that MAP4K4 promotes cell migration (34) and, importantly, MAP4K4 inhibition has no impact on cell survival (36). Amongst a CRISPR-Cas9 loss-of-function screen including 4574 genes that facilitate cell invasion, MAP4K4 was identified as strongest regulator (36). In addition, the importance of MAP4K4 in the endothelium is shown by its activation during inflammation. For example, MAP4K4 activation by TNFα regulates cytokine production and atherosclerosis (37, 38). MAP4K4 depletion increased basal barrier resistance through focal adhesion stabilization in our study, and through Rap2 in the study of Pannekoek et al (39). While others have debated that basal and inflamed endothelium is regulated by different systems, we propose that MAP4K4 is important in both resting and inflamed endothelium. The involvement of MAP4K4 in FA and integrinβ1 regulation is already confirmed in the context of cancer cell migration and adhesion (40). As integrins at FA sites can signal bidirectionally, targeting FA is an attractive treatment strategy for vascular disorders such as vascular leakage syndromes. Promisingly, the function of FAs has been targeted biochemically using agents that specifically and competitively inhibit ATP-binding of MAP4K4 by PF-6260933 (41).

Use of tyrosine kinase inhibitors in vascular disorders

In the past decade, it has been shown that TKIs are both protective in endothelial barrier function (42, 43), but also cause pulmonary vascular damage (44). Imatinib has shown beneficial effects on endothelial barrier function in models of acute lung injury (45, 46) and in a cardiopulmonary bypass model (47). In addition, imatinib reduced vascular leak in a patient with pulmonary edema (43). On the other hand, dasatinib increased *in vivo* and *in vitro* endothelial permeability independent of its inhibition of the Src family kinase Lyn (48). Tyrosine kinases of the Src family play a significant role in regulation of vital cellular processes including proliferation, adhesion, motility, differentiation and survival (49). Abl family kinases (AKIs) are important modulators of vascular permeability due to their role in regulation of the actin cytoskeleton, adherens junctions and matrix binding (50). AKIs are non-receptor tyrosine kinases that phosphorylate their tyrosine residue through several membrane receptors including receptor tyrosine kinases and integrins (51). Activity of the receptor tyrosine kinase leads to receptor dimerization and phosphorylation of multiple serine / threonine residues within the structure of the receptor itself as well as in the structure of multiple substrates for the receptor (51). As MAP4K4 is a serine/threonine kinase, its inhibition by bosutinib, a tyrosine kinase inhibitor, appears to be an off-target effect. Nonetheless, we propose that the established effects on cell spreading, migration, and stabilized cell-to-cell adhesions (52), are due to MAP4K4 inhibition by bosutinib. As

tyrosine kinases phosphorylate a large number of different substrates, TKI selectivity is often a critical issue and further studies are needed to identify which potential protein tyrosine kinases are targeted by bosutinib and imatinib and which kinases, both barrier protective and disruptive, are specifically involved. It is not only important to thoroughly characterize the target inhibition of every TKI, but also to evaluate additional off-targets effect for repurposing drugs and in explaining undesired side effects (53).

Protect the endothelium in COVID-19

Despite the undoubted progress achieved with the first vaccines against SARS-CoV-2 infection, the COVID-19 pandemic continues to affect thousands of people across the globe, particularly in those countries where vaccination is still incipient or the resources available to deal with the virus are scarce (54). To manage these patients, therapies with an antiviral activity or anti-inflammatory mechanism are tested in clinical trials, although without an overall benefit so far (55, 56). Immunomodulatory drugs such as dexamethasone (57) and interleukin blockers (58, 59) have shown to mitigate the excessive inflammatory state, but further validation of these drugs in COVID19 is needed. We describe the effects of oral imatinib in hospitalised patients with polymerase chain reaction (PCR)-proven SARS-CoV2 infection who required supplemental administration of oxygen. Despite reductions in mortality and duration of mechanical ventilation, imatinib did not reduce the time to liberation of supplemental oxygen use. As imatinib did not prevent the need for mechanical ventilation, but reduced its duration, we propose that imatinib may specifically be beneficial in patients with severe COVID19. Importantly, no renal, hepatic or cardiac toxicity was reported with imatinib treatment. The cardiovascular safety profiles of TKIs are studied extensively (60) and although imatinib may cause cardiac adverse events such as QTc-prolongation, we did not observe serious cardiac side effects in our study. We propose that the use of TKIs in vascular leakage disorders looks promising, but our clinical study was not powered to detect differences in mortality. Therefore optimization studies in larger cohorts are needed for imatinib, and potentially also bosutinib. Still our data give reason for hope, as they point to a broadening of the therapeutic arsenal against COVID-19 (54). Currently, oral imatinib in hospitalised patients are recruiting in clinical trails in Spain (NCT04346147), in the United States (NCT04394416), and intravenous imatinib in the ICU is under current investigation within our department.

8

References

1. Varga Z, Flammer AJ, Steiger P, Haberecker M, Andermatt R, Zinkernagel AS, et al. Endothelial cell infection and endotheliitis in COVID-19. Lancet. 2020;395(10234):1417-8.

2. Ackermann M, Verleden SE, Kuehnel M, Haverich A, Welte T, Laenger F, et al. Pulmonary Vascular Endothelialitis, Thrombosis, and Angiogenesis in Covid-19. N Engl J Med. 2020.

3. Hoeper MM, Barst RJ, Bourge RC, Feldman J, Frost AE, Galie N, et al. Imatinib mesylate as add-on therapy for pulmonary arterial hypertension: results of the randomized IMPRES study. Circulation. 2013;127(10):1128-38.

4. Galie N, Humbert M, Vachiery JL, Gibbs S, Lang I, Torbicki A, et al. 2015 ESC/ERS Guidelines for the diagnosis and treatment of pulmonary hypertension: The Joint Task Force for the Diagnosis and Treatment of Pulmonary Hypertension of the European Society of Cardiology (ESC) and the European Respiratory Society (ERS): Endorsed by: Association for European Paediatric and Congenital Cardiology (AEPC), International Society for Heart and Lung Transplantation (ISHLT). Eur Heart J. 2016;37(1):67-119.

5. Salskov A, Tammisetti VS, Grierson J, Vesselle H. FLT: measuring tumor cell proliferation in vivo with positron emission tomography and 3'-deoxy-3'-[18F]fluorothymidine. Semin Nucl Med. 2007;37(6):429-39.

6. Kofoed KF, Kelbaek H, Hansen PR, Torp-Pedersen C, Hofsten D, Klovgaard L, et al. Early Versus Standard Care Invasive Examination and Treatment of Patients With Non-ST-Segment Elevation Acute Coronary Syndrome. Circulation. 2018;138(24):2741-50.

7. de Langen AJ, Klabbers B, Lubberink M, Boellaard R, Spreeuwenberg MD, Slotman BJ, et al. Reproducibility of quantitative 18F-3'-deoxy-3'-fluorothymidine measurements using positron emission tomography. Eur J Nucl Med Mol Imaging. 2009;36(3):389-95.

8. van der Feen DE, Bossers GPL, Hagdorn QAJ, Moonen JR, Kurakula K, Szulcek R, et al. Cellular senescence impairs the reversibility of pulmonary arterial hypertension. Sci Transl Med. 2020;12(554).

9. Long L, Ormiston ML, Yang X, Southwood M, Graf S, Machado RD, et al. Selective enhancement of endothelial BMPR-II with BMP9 reverses pulmonary arterial hypertension. Nat Med. 2015;21(7):777-85.

10. Long L, Yang X, Southwood M, Lu J, Marciniak SJ, Dunmore BJ, et al. Chloroquine prevents progression of experimental pulmonary hypertension via inhibition of autophagy and lysosomal bone morphogenetic protein type II receptor degradation. Circ Res. 2013;112(8):1159-70.

11. Hurst LA, Dunmore BJ, Long L, Crosby A, Al-Lamki R, Deighton J, et al. TNFalpha drives pulmonary arterial hypertension by suppressing the BMP type-II receptor and altering NOTCH signalling. Nat Commun. 2017;8:14079.

12. Vattulainen-Collanus S, Southwood M, Yang XD, Moore S, Ghatpande P, Morrell NW, et al. Bone morphogenetic protein signaling is required for RAD51-mediated maintenance of genome integrity in vascular endothelial cells. Commun Biol. 2018;1:149.

13. Spiekerkoetter E, Sung YK, Sudheendra D, Bill M, Aldred MA, van de Veerdonk MC, et al. Low-Dose FK506 (Tacrolimus) in End-Stage Pulmonary Arterial Hypertension. Am J Respir Crit Care Med. 2015;192(2):254-7.

14. Smits J, Tasev D, Andersen S, Szulcek R, Botros L, Ringgaard S, et al. Blood Outgrowth and Proliferation of Endothelial Colony Forming Cells are Related to Markers of Disease Severity in Patients with Pulmonary Arterial Hypertension. Int J Mol Sci. 2018;19(12).

15. Godinas L, Guignabert C, Seferian A, Perros F, Bergot E, Sibille Y, et al. Tyrosine kinase inhibitors in pulmonary arterial hypertension: a double-edge sword? Semin Respir Crit Care Med. 2013;34(5):714-24.

16. Perros F, Montani D, Dorfmuller P, Durand-Gasselin I, Tcherakian C, Le Pavec J, et al. Platelet-derived growth factor expression and function in idiopathic pulmonary arterial

hypertension. Am J Respir Crit Care Med. 2008;178(1):81-8.

17. Benisty JI, McLaughlin VV, Landzberg MJ, Rich JD, Newburger JW, Rich S, et al. Elevated basic fibroblast growth factor levels in patients with pulmonary arterial hypertension. Chest. 2004;126(4):1255-61.

18. Izikki M, Guignabert C, Fadel E, Humbert M, Tu L, Zadigue P, et al. Endothelial-derived FGF2 contributes to the progression of pulmonary hypertension in humans and rodents. J Clin Invest. 2009;119(3):512-23.

19. Rol N, de Raaf MA, Sun XQ, Kuiper VP, da Silva Goncalves Bos D, Happe C, et al. Nintedanib improves cardiac fibrosis but leaves pulmonary vascular remodelling unaltered in experimental pulmonary hypertension. Cardiovasc Res. 2019;115(2):432-9.

20. Montani D, Bergot E, Gunther S, Savale L, Bergeron A, Bourdin A, et al. Pulmonary arterial hypertension in patients treated by dasatinib. Circulation. 2012;125(17):2128-37.

21. Spiekerkoetter E, Sung YK, Sudheendra D, Scott V, Del Rosario P, Bill M, et al. Randomised placebo-controlled safety and tolerability trial of FK506 (tacrolimus) for pulmonary arterial hypertension. Eur Respir J. 2017;50(3).

22. Humbert M, McLaughlin V, Gibbs JSR, Gomberg-Maitland M, Hoeper MM, Preston IR, et al. Sotatercept for the Treatment of Pulmonary Arterial Hypertension. N Engl J Med. 2021;384(13):1204-15.

23. Yung LM, Yang P, Joshi S, Augur ZM, Kim SSJ, Bocobo GA, et al. ACTRIIA-Fc rebalances activin/GDF versus BMP signaling in pulmonary hypertension. Sci Transl Med. 2020;12(543).

24. Farha S, Asosingh K, Xu W, Sharp J, George D, Comhair S, et al. Hypoxia-inducible factors in human pulmonary arterial hypertension: a link to the intrinsic myeloid abnormalities. Blood. 2011;117(13):3485-93.

25. Crosby A, Toshner MR, Southwood MR, Soon E, Dunmore BJ, Groves E, et al. Hematopoietic stem cell transplantation alters susceptibility to pulmonary hypertension in Bmpr2-deficient mice. Pulm Circ. 2018;8(4):2045894018801642.

26. van Gennep S, Konte K, Meijer B, Heymans MW, D'Haens GR, Lowenberg M, et al. Systematic review with meta-analysis: risk factors for thiopurine-induced leukopenia in IBD. Aliment Pharmacol Ther. 2019;50(5):484-506.

27. Marinkovic G, Kroon J, Hoogenboezem M, Hoeben KA, Ruiter MS, Kurakula K, et al. Inhibition of GTPase Rac1 in endothelium by 6-mercaptopurine results in immunosuppression in nonimmune cells: new target for an old drug. J Immunol. 2014;192(9):4370-8.

28. Tuder RM, Stenmark KR. Perspective: pathobiological paradigms in pulmonary hypertension, time for reappraisal. Am J Physiol Lung Cell Mol Physiol. 2020;318(6):L1131-L7.

29. Hemnes A, Rothman AMK, Swift AJ, Zisman LS. Role of biomarkers in evaluation, treatment and clinical studies of pulmonary arterial hypertension. Pulm Circ. 2020;10(4):2045894020957234.

30. Eyries M, Montani D, Girerd B, Favrolt N, Riou M, Faivre L, et al. Familial pulmonary arterial hypertension by KDR heterozygous loss of function. Eur Respir J. 2020.

31. Hodgson J, Swietlik EM, Salmon RM, Hadinnapola C, Nikolic I, Wharton J, et al. Characterization of GDF2 Mutations and Levels of BMP9 and BMP10 in Pulmonary Arterial Hypertension. Am J Respir Crit Care Med. 2019.

32. Botros L, Vonk Noordegraaf A, Aman J. Vanishing vessels aboding pulmonary disease: a role for VEGFR2. Eur Respir J. 2020;55(4).

33. Graf S, Haimel M, Bleda M, Hadinnapola C, Southgate L, Li W, et al. Identification of rare sequence variation underlying heritable pulmonary arterial hypertension. Nat Commun. 2018;9(1):1416.

34. Chuang HC, Wang X, Tan TH. MAP4K Family Kinases in Immunity and Inflammation. Adv Immunol. 2016;129:277-314.

35. Vitorino P, Yeung S, Crow A, Bakke J, Smyczek T, West K, et al. MAP4K4 regulates integrin-FERM binding to control endothelial cell motility. Nature. 2015;519(7544):425-30.

36. Prolo LM, Li A, Owen SF, Parker JJ, Foshay K, Nitta RT, et al. Targeted genomic CRISPR-Cas9 screen identifies MAP4K4 as

8

essential for glioblastoma invasion. Sci Rep. 2019;9(1):14020.

37.   Huang H, Tang Q, Chu H, Jiang J, Zhang H, Hao W, et al. MAP4K4 deletion inhibits proliferation and activation of CD4(+) T cell and promotes T regulatory cell generation in vitro. Cell Immunol. 2014;289(1-2):15-20.

38.   Roth Flach RJ, Skoura A, Matevossian A, Danai LV, Zheng W, Cortes C, et al. Endothelial protein kinase MAP4K4 promotes vascular inflammation and atherosclerosis. Nat Commun. 2015;6:8995.

39.   Pannekoek WJ, Linnemann JR, Brouwer PM, Bos JL, Rehmann H. Rap1 and Rap2 antagonistically control endothelial barrier resistance. PLoS One. 2013;8(2):e57903.

40.   Tripolitsioti D, Kumar KS, Neve A, Migliavacca J, Capdeville C, Rushing EJ, et al. MAP4K4 controlled integrin beta1 activation and c-Met endocytosis are associated with invasive behavior of medulloblastoma cells. Oncotarget. 2018;9(33):23220-36.

41.   Ammirati M, Bagley SW, Bhattacharya SK, Buckbinder L, Carlo AA, Conrad R, et al. Discovery of an in Vivo Tool to Establish Proof-of-Concept for MAP4K4-Based Antidiabetic Treatment. ACS Med Chem Lett. 2015;6(11):1128-33.

42.   Aman J, van Bezu J, Damanafshan A, Huveneers S, Eringa EC, Vogel SM, et al. Effective treatment of edema and endothelial barrier dysfunction with imatinib. Circulation. 2012;126(23):2728-38.

43.   Aman J, Peters MJ, Weenink C, van Nieuw Amerongen GP, Vonk Noordegraaf A. Reversal of vascular leak with imatinib. Am J Respir Crit Care Med. 2013;188(9):1171-3.

44.   Guignabert C, Phan C, Seferian A, Huertas A, Tu L, Thuillet R, et al. Dasatinib induces lung vascular toxicity and predisposes to pulmonary hypertension. J Clin Invest. 2016;126(9):3207-18.

45.   Rizzo AN, Sammani S, Esquinca AE, Jacobson JR, Garcia JG, Letsiou E, et al. Imatinib attenuates inflammation and vascular leak in a clinically relevant two-hit model of acute lung injury. Am J Physiol Lung Cell Mol Physiol. 2015;309(11):L1294-304.

46.   Letsiou E, Rizzo AN, Sammani S, Naureckas P, Jacobson JR, Garcia JG, et al. Differential and opposing effects of imatinib on LPS- and ventilator-induced lung injury. Am J Physiol Lung Cell Mol Physiol. 2015;308(3):L259-69.

47.   Koning NJ, de Lange F, van Meurs M, Jongman RM, Ahmed Y, Schwarte LA, et al. Reduction of vascular leakage by imatinib is associated with preserved microcirculatory perfusion and reduced renal injury markers in a rat model of cardiopulmonary bypass. Br J Anaesth. 2018;120(6):1165-75.

48.   Phan C, Jutant EM, Tu L, Thuillet R, Seferian A, Montani D, et al. Dasatinib increases endothelial permeability leading to pleural effusion. Eur Respir J. 2018;51(1).

49.   Guignabert C, Montani D. Key roles of Src family tyrosine kinases in the integrity of the pulmonary vascular bed. Eur Respir J. 2013;41(1):3-4.

50.   Rizzo AN, Aman J, van Nieuw Amerongen GP, Dudek SM. Targeting Abl kinases to regulate vascular leak during sepsis and acute respiratory distress syndrome. Arterioscler Thromb Vasc Biol. 2015;35(5):1071-9.

51.   Bogatcheva NV, Garcia JG, Verin AD. Role of tyrosine kinase signaling in endothelial cell barrier regulation. Vascul Pharmacol. 2002;39(4-5):201-12.

52.   Vultur A, Buettner R, Kowolik C, Liang W, Smith D, Boschelli F, et al. SKI-606 (bosutinib), a novel Src kinase inhibitor, suppresses migration and invasion of human breast cancer cells. Mol Cancer Ther. 2008;7(5):1185-94.

53.   Klaeger S, Heinzlmeir S, Wilhelm M, Polzer H, Vick B, Koenig PA, et al. The target landscape of clinical kinase drugs. Science. 2017;358(6367).

54.   Bernal-Bello D, Morales-Ortega A, Isabel Farfan-Sedano A, de Tena JG, Martin-Lopez JVS. Imatinib in COVID-19: hope and caution. Lancet Respir Med. 2021.

55.   Beigel JH, Tomashek KM, Dodd LE, Mehta AK, Zingman BS, Kalil AC, et al. Remdesivir for the Treatment of Covid-19 - Final Report. N Engl J Med. 2020;383(19):1813-26.

56.   Group RC, Horby P, Mafham M, Linsell L, Bell JL, Staplin N, et al. Effect of Hydroxychloroquine in Hospitalized Patients with Covid-19. N Engl J Med. 2020;383(21):2030-40.

57.   Group RC, Horby P, Lim WS, Emberson JR, Mafham M, Bell JL, et al. Dexamethasone in Hospitalized Patients with Covid-19 - Preliminary Report. N Engl J Med. 2020.

58.   The REMAP-CAP Investigators VOPCG, Paul R. Mouncey, Farah Al-Beidh, Kathryn M. Rowan, Alistair D. Nichol, Yaseen M. Arabi, Djillali Annane, Abi Beane, Wilma van Bentum-Puijk, Lindsay R. Berry, Zahra Bhimani, Marc J.M. Bonten, Charlotte A. Bradbury, Frank M. Brunkhorst, Adrian Buzgau, Allen C. Cheng, Michelle A. Detry, Eamon J. Duffy, Lise J. Estcourt, Mark Fitzgerald, Herman Goossens, Rashan Haniffa, Alisa M. Higgins, Thomas E. Hills, Christopher M. Horvat, Francois Lamontagne, Patrick R. Lawler, Helen L. Leavis, Kelsey M. Linstrum, Edward Litton, Elizabeth Lorenzi, John C. Marshall, Florian B. Mayr, Danny McAuley, Anna McGlothlin, Shay P McGuinness, Bryan J. McVerry, Stephanie K. Montgomery, Susan C. Morpeth, Srinivas Murthy, Katrina Orr, Rachael L. Parke, Jane C. Parker, Asad E. Patanwala, Ville Pettilä, Emma Rademaker, Marlene S. Santos, Christina T. Saunders, Christopher W. Seymour, Manu Shankar-Hari, Wendy I. Sligl, Alexis F. Turgeon, Anne M. Turner, Frank L. van de Veerdonk, Ryan Zarychanski, Cameron Green, Roger J. Lewis, Derek C. Angus, Colin J. McArthur, Scott Berry, Steve A. Webb, Lennie P.G. Derde. Interleukin-6 Receptor Antagonists in Critically Ill Patients with Covid-19 – Preliminary report.

59.   Salama C, Han J, Yau L, Reiss WG, Kramer B, Neidhart JD, et al. Tocilizumab in Patients Hospitalized with Covid-19 Pneumonia. N Engl J Med. 2021;384(1):20-30.

60.   Aghel N, Delgado DH, Lipton JH. Cardiovascular toxicities of BCR-ABL tyrosine kinase inhibitors in chronic myeloid leukemia: preventive strategies and cardiovascular surveillance. Vasc Health Risk Manag. 2017;13:293-303.

8

Appendices

Nederlandse samenvatting

Een bloedvat of vas sanguineum, in de volksmond ader genoemd, maakt deel uit van de bloedsomloop. De totale lengte van alle bloedvaten in het menselijk lichaam bedraagt ongeveer 100.000 kilometer, dat is 2.5x de omtrek van de aarde. Bloedvaten zijn verantwoordelijk voor het uitwisselen van gassen zoals zuurstof en koolstofdioxide, en voedingsstoffen zoals suikers, eiwitten en vetten naar de weefsels en organen. De binnenbekleding van elk bloedvat bestaat uit endotheelcellen. Dit zijn bakstenen die als een strakke keten tegen elkaar aan liggen zodat er geen vocht uit de bloedvaten kan weglekken en zodat de bloeddruk wordt gereguleerd. Dit proefschrift focust zich op het endotheel in de longen.

In **hoofdstuk 2, 3 en 4** onderzoeken wij pulmonale arteriële hypertensie (PAH). Dit is een ziekte van de long slagaderwand. Deze wand wordt dikker en stijver waardoor de bloeddruk in de longen te hoog wordt. Het ontstaan van deze ziekte is nog steeds niet helemaal duidelijk, maar het verlies en beschadigen van bloedvaten staat centraal. Het ontdekken, ook wel diagnosticeren van de ziekte is erg moeilijk omdat patiënten vaak aspecifieke klachten hebben zoals benauwdheid en zich minder goed kunnen inspannen, iets wat ook door heel veel andere oorzaken kan komen. Op dit moment zijn er heel veel onderzoeken nodig om PAH te kunnen vaststellen. Het belangrijkste onderzoek is de rechter hartkatheterisatie. Hierbij wordt er, via de halsader een ballonnetje opgeblazen in de rechter kant van het hart, om de druk in de longslagader te meten. Dit is een ingewikkeld, invasief onderzoek dat alleen in een academisch ziekenhuis kan plaatsvinden. Het zou daarom erg handig zijn als we met een simpel buisje bloed bij de huisarts kunnen vaststellen wie de ziekte heeft en wie niet. In **hoofdstuk 2** proberen wij stofjes in het bloed te vinden, zogenaamde biomarkers, die specifiek zijn voor PAH. Helaas blijken er op dit moment nog geen stofjes in de bloedbaan te circuleren die specifiek zijn voor PAH, met name omdat deze stofjes ook vaak verhoogd zijn bij mensen met een hartziekte zoals hartfalen. Daarom hebben we nog geen snelle én specifieke bloedtest die we in de praktijk kunnen gebruiken om PAH patiënten te diagnosticeren.

In **hoofdstuk 3** proberen wij een andere methode om patiënten met PAH te detecteren. Door middel van een scan met een radioactieve stof (PET-scan) onderzochten wij of scans van gezonde vrijwilligers en gezonde familieleden verschilden van scans van PAH patiënten. Helaas bleek ook deze methode niet effectief in het diagnosticeren van PAH.

In **hoofdstuk 4** behandelen wij 15 patiënten met een experimenteel geneesmiddel dat mercaptopurine heet, gedurende 4 maanden. De onderzoeksvraag was, of de druk in de longslagaders zou dalen na behandeling. Wij vonden inderdaad een daling in de bloeddruk van de longen na therapie, maar er waren ook erg veel bijwerkingen. Daarom blijkt dit geneesmiddel wel effectief, maar niet veilig voor dagelijks gebruik.

In het tweede gedeelte van dit proefschrift onderzoeken wij een ander probleem van de bloedvaten in de longen. Als er vocht uit de bloedvaten in de longen weglekt, kan er niet genoeg gasuitwisseling plaatsvinden en worden patiënten erg benauwd. Soms wordt dit 'vocht achter de longen' genoemd, maar eigenlijk zit dit vocht dus ín de longen. Om meer inzicht te krijgen in het ontstaan van lekkende bloedvaten in de longen kijken wij in **hoofdstuk 5 en 6** naar de effecten van een geneesmiddel met de naam bosutinib, op het endotheel. Wij zagen dat de verbindingen tussen de endotheelcellen verder versterkt was na behandeling met bosutinib. Zoals hierboven aangegeven werd dus als het ware het cement tussen de bakstenen verstevigd.

Ten tweede testten wij bosutinib in een muis met een longinfectie waardoor er vocht weglekt in de longen. Wij zagen na 6 uur behandeling met bosutinib al een sterk beschermend effect op het endotheel, en daarmee een duidelijke vermindering in de lekkage van de longbloedvaten. Als laatste testten wij bosutinib in een rat waarbij we kunstmatig een ongeluk, ook wel 'trauma', hebben nagedaan. Vervolgens kregen deze dieren een bloedtransfusie. Zowel een trauma als een bloedtransfusie kan namelijk ook aanleiding geven tot lekkende bloedvaten in verschillende organen. Door middel van kleurstoffen die wij in de bloedsomloop hadden gespoten, zagen wij dat er veel minder kleurstof in de longen was weggelekt. Hieruit concluderen wij dus dat bosutinib een potentiele nieuwe behandeling is voor patiënten met vaatlekkage.

Toen er in 2019 het SARS-CoV-2 virus oprukte over de wereld, werden veel mensen met het Corona virus disease 2019 (COVID-19) opgenomen. Opmerkelijk veel patiënten hadden vocht in de longen door lekkende bloedvaten. In **hoofdstuk 7** hebben wij imatinib, een geneesmiddel tegen leukemie, bij ongeveer 400 patiënten getest. De helft van de patiënten kreeg imatinib, de andere helft kreeg een placebo. Wij zagen geen verbetering in de zuurstofbehoefte van de patiënten, maar wel een vermindering van aantal overlijden en een kortere intensive care (IC) opname. Dit is belangrijk omdat hiermee de druk op de IC's in Nederland kan worden verminderd.

A

English summary

A blood vessel or vas sanguineum, is part of the circulatory system. The total length of all blood vessels in the human body is approximately 100.000 kilometers, which is 2.5 times the circumference of the Earth. Blood vessels are responsible for exchanging gases such as oxygen and carbon dioxide, and nutrients such as sugars, proteins and lipids to the tissues and organs. The inner lining of each blood vessel is made up of endothelial cells. These are bricks that lie next to each other like a tight chain to enable no fluid leakage out of the blood vessels into the tissues and to regulate blood pressure. This thesis focuses on the endothelium in the lungs.

In **chapter 2, 3 and** 4 we investigate pulmonary arterial hypertension (PAH). This is a disease of the vascular wall of lung arteries and the lung microvasculature. This wall becomes thicker and stiffer, causing the blood pressure in the lungs to increase. The origin of this disease is still not completely clear, but the loss and damage of blood vessels is a crucial hallmark. Diagnosing this disease is very difficult because patients often have non-specific complaints such as shortness of breath and dyspnea on exertion, symptoms that can also be caused by many other diseases. Currently, the diagnostic process of PAH is very complex, invasive and time consuming. The most important examination is the right heart catheterization where a balloon is inflated in the right side of the heart via the jugular vein to measure the pressure in the right ventricle and pulmonary artery. This is a complicated, invasive procedure that can only take place in an academic teaching hospital. It would therefore be very useful if we could use a simple blood test to discriminate patients. In **chapter 2** we try to find substances in the blood, so-called biomarkers, that are specific for PAH. Unfortunately, there are currently no biomarkers in the bloodstream that are specific for PAH, mainly because most biomarkers are non-specific and often increased in people with another heart disease such as heart failure. This is why we do not yet have a quick and specific blood test to use in daily clinical practice to diagnose PAH patients.

In **chapter 3** we try another method to detect patients with PAH. By means of a scan with a radioactive substance (PET scan), we compared healthy volunteers and healthy family members with PAH patients. Unfortunately, this method also proved not sensitive enough to diagnose PAH.

In **chapter 4**, we treated 15 patients with an mercaptopurine for four months. The research question was, if the blood pressure in the pulmonary artery would decrease after treatment. We indeed found a lower lung blood pressure after therapy, but there were also a lot of side effects. Therefore, this medicine appears to be effective, but not safe for daily use.

In the second part of this thesis, we focus on fluid leakage from the blood vessels into the lung tissue. This hampers gas exchange and patients become very short of breath. To gain more insight into the origin of leaky blood vessels in the lungs, we focused on the effects of a drug called bosutinib on the endothelium in **chapters 5 and 6.** We noticed that the

connections between the endothelial cells were reinforced after treatment with bosutinib. As indicated above, the cement between the bricks was strengthened. Second, we tested bosutinib in a mouse with a lung infection that causes fluid to leak into the lungs. We observed a strong protective effect on the endothelium already after 6 hours of treatment with bosutinib, and thus a clear reduction in the leakage of the pulmonary blood vessels. Finally, we tested bosutinib in a rat with a trauma, which we then gave a blood transfusion. Both a trauma and a blood transfusion can also lead to leaky vessels in various organs. By means of dyes that we injected into the bloodstream, we could measure the pulmonary vascular leakage. We therefore conclude that bosutinib is a potential new treatment for patients with vascular leakage syndromes.

When the SARS-CoV-2 virus spread across the world in 2019, many people with the Corona virus disease 2019 (COVID-19) were admitted. Remarkably many patients had fluid in the lungs due to leaky vessels. In **chapter 7** we tested imatinib, a drug used for leukemia patients, in approximately 400 patients. Half of the patients received imatinib, the other half received a placebo. We did not see an improvement in the oxygen demand of the patients, but we did see a reduction in death and a shorter intensive care (ICU) admission.

A

List of publications

Jurjan Aman, Erik Duijvelaar, **Liza Botros***, Azar Kianzad*, Job R. Schippers*, Patrick J. Smeele*, (…), Anton Vonk Noordegraaf, Frances S. Handoko-de Man, H.J. Bogaard. *equal contribution. A randomised, double-blind, placebo controlled, clinical trial evaluating imatinib in patients with severe COVID-19. *equal contribution
Lancet Respiratory Medicine September 2021

Liza Botros*, Samara M.A. Jansen*, Ali Ashek, Onno A. Spruijt, Jelco Tramper, Anton Vonk Noordegraaf, Jurjan Aman, Hans Harms, Frances S. de man, Marc C. Huisman, Lan Zhao, Harm Jan Bogaard. [18F]FLT-PET in Pulmonary Arterial Hypertension (PAH): A clinical study in PAH patients and unaffected BMPR2 mutation carriers. *equal contribution
Pulmonary Circulation June 2021

Derek J.B. Kleinveld, **Liza Botros**, Adrie Maas, Jesper Kers, Jurjan Aman, Markus W. Hollmann, Nicole P. Juffermans. Bosutinib reduces endothelial permeability and organ failure in a rat polytrauma transfusion model.
British Journal of Anaesthesia May 2021

Max C.H. Cheng, Kevin K.H. Cheng, Anton Vonk Noordegraaf, **Liza Botros**
The role of endotheliopathy in the pathogenesis of Covid-19: A narrative review
Amsterdam Medical Student Journal February 2021

Abhilash S. Kizhakke Puliyakote, Sebastiaan Holverda, Rui C. Sá, Tatsuya J. Arai, Rebecca J. Theilmann, **Liza Botros,** Harm Jan Bogaard, G. Kim Prisk, Susan R. Hopkins. Prone positioning redistributes gravitational stress in the lung under normal conditions and in simulations of edema
Experimental Physiology December 2020

Liza Botros, Robert Szulcek, Samara M.A. Jansen, Kondababu Kurakula, Marie-Jose T. H. Goumans, Andre B.P. van Kuilenburg, Anton Vonk Noordegraaf, Frances S. de Man, Jurjan Aman, Harm Jan Bogaard. The Effects of Mercaptopurine on Pulmonary Vascular Resistance and BMPR2 Expression in Pulmonary Arterial Hypertension.
American Journal of Respiratory and Critical Care Medicine April 2020

Liza Botros, Anton Vonk Noordegraaf, Jurjan Aman. Vanishing vessels aboding pulmonary disease: a role for VEGFR2.
European Respiratory Journal April 2020

Liza Botros, Manon C.A. Pronk, Jenny Juschten, John Liddle, Sofia K.H. Morsing, Jaap D. van Buul, Robert H. Bates, Pieter Roel Tuinman, Jan S.M. van Bezu, Stephan Huveneers, Harm Jan

Bogaard, Victor W.M. van Hinsbergh, Peter L. Hordijk, Jurjanb Aman. Bosutinib prevents vascular leakage by reducing focal adhesion turnover and reinforcing junctional integrity.
Journal of Cell Science March 2020

A. Josien Smits, Dimitar Tasev, Stine Andersen, Robert Szulcek, **Liza Botros**, Steffen Ringaard, Asger Andersen, Anton Vonk Noordegraaf, Pieter Koolwijk, Harm Jan Bogaard. Blood outgrowth and proliferation of Endothelial Colony Forming Cells are related to Markers of disease severity in Patients with Pulmonary Arterial Hypertension.
International Journal of Molecular Sciences November 2018

Ali Ashek, Onno A. Spruijt, Hendrik J. Harms, Adriaan A. Lammertsma, John Cupitt, Olivier Dubois, John Wharton, Swati Dabral, Soni Savai Pullamsetti, Marc C. Huisman, Virginie Frings, Ronald Boellaard, Frances S. de Man, **Liza Botros**, Samara Jansen, Anton Vonk Noordegraaf, Martin R. Wilkins, Harm Jan Bogaard, Lan Zhao. 3'-Deoxy-3'-[18F]Fluorothymidine Positron Emission Tomography Depicts Heterogeneous Proliferation Pathology in Idiopathic Pulmonary Arterial Hypertension Patient Lung.
Circulation Cardiovascular Imaging August 2018

Liza Botros, Jurjan Aman, Harm Jan Bogaard, Anton Vonk Noordegraaf. Pulmonary Hypertension with warm hands.
Thorax December 2017

Liza Botros, Geerten P Van Nieuw Amerongen, Anton Vonk Noordegraaf, Harm Jan Bogaard. Recovery from Mitomycin-induced Pulmonary Arterial Hypertension.
Annals of the American Thoracic Society March 2014

Submitted manuscripts:

A. Josien Smits, **Liza Botros**, Mariska Mol, Kirsten A. Ziesemer, Martin R. Wilkins, Anton Vonk Noordegraaf, Harm Jan Bogaard & Jurjan Aman
Blood biomarkers for the detection of idiopathic and hereditary pulmonary arterial hypertension; a meta-analysis.

A. Josien Smits, Mohammad Arkani, Sjors G.J.G. In ´t Veld, Anna E. Huis in 't Veld, Nik Sol, Suengcham Kim, Gil Speyer, Joanne A. Groeneveldt, **Liza Botros**, …, Tom Wurdinger, Harm Jan Bogaard. A distinctive platelet RNAseq signature and swarm intelligence-mediated detection of Pulmonary Hypertension

A

Bookchapter

"The Right Heart", Second Edition Gaine S. Naeije R,Peacock A.
Chapter: Treating the Right Ventricle Directly in Pulmonary Hypertension. Norbert F. Voelkel, Dietmar Schranz, **Liza Botros**, Harm Jan Bogaard. Springer Nature 2021

International abstract presentations

 [^{18}F]FLT-PET is not a sensitive method for detecting Pulmonary Arterial Hypertension. Pulmonary Vascular Research Institute online event Dec 2020

The Effects of Mercaptopurine on Pulmonary Vascular Resistance and BMPR2 Expression in Pulmonary Arterial Hypertension. Oral presentation.
American Thoracic Society International Conference, online event December 2020
Best abstract Award

Bosutinib Protects Against Endothelial Vascular Leakage By Reinforcing Junctions and Stabilizing Focal Adhesions. Poster.
European Respiratory Society, International Conference, Madrid Spain September 2019

Bosutinib Protects Against Endothelial Vascular Leakage By Reinforcing Junctions and Stabilizing Focal Adhesions., Oral Presentation.
European Society for Microcirculation & European Vascular Biology Organization, International Conference, Maastricht, The Netherlands April 2019

Bosutinib Protects Against Endothelial Vascular Leakage By Preventing Focal Adhesion Disassembly. Poster.
American Thoracic Society International Conference, San Diego USA May 2018

Pulmonary arterial hypertension reversal in clusters of patients with pro-proliferative signatures: 6-MercaptoPurine Proof-of-Concept Trial. Poster. GlaxoSmithKine, Leuven Belgium December 2017

Progressive right ventricular dysfunction in PAH despite responding to targeted therapy. Oral presentation.
AOP Focus on Orphan diseases, Vienna Austria November 2017

National abstract publications

Anti-proliferative therapy with 6-mercaptopurine in Pulmonary Arterial Hypertension: Hemodynamic improvement at the cost of serious side effects. Poster.
Science Exchange day Amsterdam UMC, September 2019

Bosutinib Protects Against Endothelial Vascular Leakage By Preventing Focal Adhesion Disassembly. Poster.
Amsterdam Cardiovascular Sciences Annual Meeting June 2018

Pulmonary arterial hypertension reversal in clusters of patients with pro-proliferative signatures. Oral presentation.
Netherlands Respiratory Society Annual Meeting, Amsterdam November 2017

Pulmonary hypertension in pregnancy; No way or no problem? Oral presentation.
Amsterdam Cardiovascular Sciences Pulmonary Hypertension meeting June 2017

A

Curriculum Vitae

Liza Botros was born on February 25th 1991 in Amsterdam, The Netherlands. After obtaining her Bachelor's degree in Biomedical Sciences at the University of Amsterdam in 2012, she continued with a Graduate Medical Master's program (ZIGMA) at the VU University of Amsterdam. This is a four year graduate entry program to obtain a selective honors medical Master's degree. She chose to perform her scientific internship at the department of Pulmonology and Physiology with Prof. Dr. Harm Jan Bogaard. After an international surgical rotation in South-Africa and her graduate internship at the critical Intensive Care Unit in Hilversum, she graduated as medical doctor (MD) in 2016.

Her combined background in biomedical sciences and medicine made her a highly translationally orientated researcher. This is why she decided to continue working with Prof. Bogaard on pulmonary vascular diseases including Pulmonary Arterial Hypertension (PAH) and pulmonary vascular leakage syndromes. She acquired a broad spectrum of skills, including molecular and cell biological techniques focusing on pulmonary endothelial vascular biology, combined with the coordination of two therapeutic clinical trials. Meanwhile, she worked as a clinical resident not-in-training (ANIOS) at the pulmonary ward in 2018. In parallel with finalizing her thesis, she decided to move to the United States with her husband and three children whilst exploring new opportunities in both research and medical education abroad.

A

Dankwoord

In de jaren als promovendus ben ik vrijwel elke dag met plezier naar mijn werk gegaan en dat komt vooral omdat ik zo veel leuke collega's om mij heen had die allemaal als team hebben bijgedragen aan de totstandkoming van dit proefschrift. De zelfstandigheid en flexibiliteit van het werk, de binnen- en buitenlandse congressen met bijbehorende reisjes en borrels, het samenwerken met verschillende onderzoeksgroepen en verschillende disciplines vond ik geweldig! Ik heb ontzettend veel verschillende technieken mogen leren, waaronder diverse cel -en moleculair biologische procedures, verschillende diermodellen en dierproeven, klinische data analyse en verschillende soorten immuunofluoriscentie en klinische imaging. Er zijn maar weinig afdelingen bij wie ik dit grote scala aan technieken mijzelf eigen had kunnen maken als bij de longziekten in het VUmc.

Graag wil ik mijn promotie team bedanken:

Allereerst mijn promotor Harm Jan bij wie de kennismaking met de wetenschap is begonnen. Na enige twijfel om eerst als ANIOS op de IC aan de slag te gaan, na een niet zo succesvolle master stage, heb jij mij toch kunnen overtuigen te starten met een promotietraject bij de longziekten. Er was geen plan of project waarop ik werd aangenomen, waardoor ik in eerste instantie niet goed wist wat ik moest doen, maar hierdoor heb je mij tegelijkertijd de vrijheid gegeven om van alles op te pakken gedurende de jaren waar ik zelf interesse in had. Je gaf me de ruimte om er halverwege tussenuit gaan om het werk als ANIOS longziekten te ervaren. Het is ontzettend knap en uniek hoe jij het huidige translationele Phenix lab hebt kunnen opzetten, zeker met jouw, slechts beperkte, lab-expertise. Daarom verkocht jij elk experiment als: 'dat doen we even', en voor ik het wist waren we drie jaar verder. Het is zeker ook dit optimisme dat de wetenschap verder brengt. Groots denken, enthousiaste discussies en altijd toegankelijk zijn voor al je PhD's en collega's terwijl je mega druk bent is bewonderenswaardig.

Beste Peter, ik kwam compleet groen binnen op het lab, maar jij hebt mij vele biochemische en celbiologische lessen geleerd. Jouw deur in het O2 staat altijd open. Ik vond de meetings over mijn projecten vaak erg leerzaam omdat jij als biochemicus weer problemen vanuit een heel andere kant aanvliegt dan de clinici die ik wekelijks sprak. Bovendien ben je ook persoonlijk betrokken bij je collega's, doe je mee aan de borrels en stuur je zelfs kraam kadootjes. Bedankt voor je input en steun de afgelopen jaren.

Beste Jurjan, voor onze eerste kennismaking was ik enigszins zenuwachtig en ik had mij voorbereid om mijn motivatie speech te houden waarom ik graag wilde promoveren. Maar jij viel direct met de deur in huis: of ik onderzoek wilde doen om in opleiding tot longarts te komen of omdat ik het ook echt leuk vind? Gelukkig was dit laatste de waarheid, want onze passie voor de wetenschap is zeker een match. Zelden heb ik zo een integer, oprecht persoon leren kennen die betrokken is met mij als onderzoeker, maar ook als persoon. Jij legt de lat hoog en ik had geen enkele mogelijkheid mij door een antwoord heen te bluffen

omdat jij elk detail van elk experiment had onthouden. Ook op afstand vanuit Londen bleef jij betrokken en mij begeleiden. Bedankt voor de leuke congressen in Maastricht en Madrid en voor jullie gastvrijheid thuis in Londen.

Anton, toen ik jou als student leerde kennen gaf jij mij gelijk het gevoel dat ook mijn onbenullige studenten projectje ertoe deed. Jouw passie voor het vak, inzet en betrokkenheid naar je studenten, PhD's en patiënten is bewonderingswaardig. Bedankt voor je bevlogenheid de afgelopen jaren.

Frances, als één van de weinige vrouwen houd jij je goed staande in het mannenbolwerk en daarin ben je voor mij een voorbeeld. Bedankt voor je openheid en betrokkenheid over het combineren van werk en privé en bedankt voor al je kritische vragen bij mijn presentaties.

Victor, uw kennis over de literatuur is indrukwekkend. Bij elk vraagstuk had u wel een artikel dat het antwoord gaf. U heeft mij geleerd altijd te beginnen en te eindigen met degelijk literatuuronderzoek en niet lukraak wat experimenten uit te voeren.

Dan de buddy's in het lab: The Finnish triangle: Jisca en Natalija. Jisca, je bent behoorlijk slim en had geduld voor al mijn vragen en knulligheden in het lab. Ik weet zeker dat je een uitstekend onderzoeker bent, en gaat worden, en ik ben benieuwd naar al je ontdekkingen. Natalija, the Sexy Serbian. You are one of the most social intelligent people I've ever met, and I love your personality analysis, intercollegial readings and I admire your autonomy and authenticity. I will never forget our trip to Helsinki and the parties and festivals with the three of us, thank you for all the fun and support (and unasked psycho-analysis).

Lieve Xue, ik heb jou pas in de tweede helft van mijn PhD heb leren kennen. Team jut-en-jul, maar wel met strakke data. Ik vind het echt jammer dat we de laatste maanden niet intensiever hebben kunnen samenwerken in het lab door COVID19, maar ik ben ervan overtuigd dat je een prachtig boekje zal neerzetten en ik ben benieuwd welk pad je kiest de komende jaren.

Dan de roomies aan de andere kant: Josien en Adinda a.k.a. fiets-schaats-hardloop-zwem-kite-klim vrouwen. Als niet-topsporter leken mijn twee uurtjes bodyshape per week erg amateuristisch. Ik heb genoten van ons geklaag over alles in het leven, mannen, sporten, het weekend, maar vooral over onze PhD's. Adinda, bedankt voor de trip naar Friesland maar ik ben nog steeds blij dat we niet konden gaan zeilen. Josien, gelukkig zijn we niet gearresteerd toen wij de Deense grens overstaken met een achterbak vol aan cellen in de stoof (lees: wietplantage). Ik wens jullie alle geluk toe in de nieuwe wegen die jullie zijn ingeslagen.

Alle collega's van 3F. Moeder Anna, de oudste en meest wijze van de groep. Jij bent een super betrouwbare collega en ik vond alle festivals en borrels altijd een genot. Joanne, altijd behulpzaam en collegiaal. Ik bewonder jouw geduld en empathie voor zowel collega's als patiënten en je wordt vast een super goede longarts. Natalia, spuitelf-zwemster. Tijdens onze memorabele Madrid trip heb ik dankzij jou met een mannenzwembroek op mijn hoofd

A

het Spaanse zwembadwater getrotseerd en de grootste kater uit mijn leven ervaren. Samara, bedankt voor het fijne samenwerken op de vreselijke PET studie en je betrokkenheid en interesse ook na mijn vertrek naar de States. Azar, bridezilla-buddy, bedankt voor ons heerlijke Arabisch-Perzische vrouwengeklets op de kamer en de samenwerking tijdens de counter-covid. Anna-Larissa, Jelco, Eveline, Nicole, Jessie, Jeroen, Erik, Cher, Patrick, Lucas en Job, bedankt voor de leuke tijd en de gezellige sinterklaas-en kerstvieringen.

Aida, Kim, Eva, Sun, Robert, Denielli, Taka, Fjodor, Pan, Ingrid en Rowan. Toen ik begon waren wij nog versnipperd over het fysiologie lab, maar de laatste 2 jaar zijn we écht een groep geworden in het Phenix lab. Ik heb de werksfeer altijd super gezellig ervaren en bedankt voor de leuke tijd en al jullie hulp in het lab.

To all the physiology O2 colleagues, thanks for the help and interesting research meetings. Thanks for two wonderfull TPO weekends. Phaedra colleagues, MJ and Babu, thanks for the help with the 6MP study and the input during the Friday morning meetings. Jan, jij gaf mij de vuurdoop in het HUVEC lab en hielp mij met alle berekeningen, waar was ik zonder jou. Bedankt voor je geduld met mijn kleine rekenknobbel.

Alle collega's van het klinische PH team, Frank, Iris, Martha, Esther, Anco, Fred, Jan en Tim. Bedankt voor alle hulp bij de inclusies van de studies en de leuke tijd op de behandelkamer.

Bedankt aan de collega's in het AMC. Stephan Huveneers, jij bent een super enthousiaste celbioloog met wie ik met plezier mooie filmpjes heb gemaakt. Bedankt voor je hulp met de FA-imaging. Ik vind het erg leuk om jou als opponent in mijn commissie te hebben. De promovendi van het LEICA: Derek en Jenny. Met jullie beiden heb ik ontzettend fijn samengewerkt en er zijn twee prachtige papers uit voortgekomen. Succes allebei met de opleiding tot anesthesioloog.

De vriendinnen van de strong nucleus en Sinterkerst wil ik bedanken voor al jullie support, etentjes, feestjes, wandelingen en gesprekken de afgelopen jaren. Iris en Dirk, het andere muzikale koppel en Natalia en Blas a.k.a. wintersport buddies, jullie kennen mij als één van de beste en ik waardeer ons contact met jullie ontzettend. Ik hoop dat jullie snel langskomen in de States! Tante Gradda en oom Franta, bedankt voor al jullie oppas hulp waardoor ik verder kon typen aan de manuscripten. Aziza en Marco, beste vriendin, mariska, mevrouw konijnenburg. Ik ben dankbaar dat jij mijn grote zus bent. Jij helpt helpt mij herinneren aan wat echt belangrijk in het leven is. Papa, ook al vraag jij al jaren: Ben je nou nog steeds bezig? Zie hier dan het resultaat van de afgelopen jaren. Ik weet zeker dat je nu zal zeggen: heb je daar zo lang over gedaan? En Patty, bedankt voor je geduld met mijn vader en dat je hem zo gelukkig maakt.

Mama, jij bent altijd empathisch en geïnteresseerd geweest in mijn onderzoek en het liefste wilde je elk experiment tot in detail weten en snappen. Ik denk dat ik mijn nieuwsgierigheid en enthousiasme over de wetenschap van jou heb. Bedankt voor al je positiviteit en

onvoorwaardelijke steun de afgelopen jaren. Nu ik zelf moeder ben geworden (en jij oma) is onze band nog hechter geworden. Ik realiseer me nu, meer dan ooit, hoe jij dat vroeger allemaal hebt gered. Diep respect en bewondering voor jou. En Guy, bedankt dat je mijn moeder zo gelukkig maakt.

Lieve Rich, jij steunt mij onvoorwaardelijk, welke keuze ik ook maak. Nu we in de VS wonen met drie kinderen staan ons weer allemaal nieuwe uitdagingen te wachten, ik kan niet wachten ze allemaal aan te gaan samen met jou.

A